

Some pages of this thesis may have been removed for copyright restrictions.

If you have discovered material in AURA which is unlawful e.g. breaches copyright, (either yours or that of a third party) or any other law, including but not limited to those relating to patent, trademark, confidentiality, data protection, obscenity, defamation, libel, then please read our [Takedown Policy](#) and [contact the service](#) immediately

A STUDY OF THERMODYNAMIC CHARACTERISTICS AND PREDICTIVE
COMPUTER MODELLING OF AN AIR TO WATER HEAT PUMP SYSTEM

A Thesis Submitted For The Degree Of
Doctor of Philosophy

by

RAMLI BIN ABU HASSAN

The University Of Aston In Birmingham

Department Of Physics

February 1984

ACKNOWLEDGEMENTS

I would like to thank the following:

Mr M.S. Wrenn for his supervision of the project.

Professor W.E.J. Neal, Mr C.G. Pearce and Dr P.N. Cooper for their guidance, encouragement and interest shown throughout the course of this project.

University of Teknologi of Malaysia for the financial support.

Finally my wife, Zaiton and sons Eswadi and Fitri for their support and patience throughout the last three years.

The University Of Aston In Birmingham
A STUDY OF THERMODYNAMIC CHARACTERISTICS AND PREDICTIVE
COMPUTER MODELLING OF AN AIR TO WATER HEAT PUMP SYSTEM

Ramli Bin Abu Hassan

Submitted For The Degree Of PhD

1984

SUMMARY

A study on heat pump thermodynamic characteristics has been made in the laboratory on a specially designed and instrumented air to water heat pump system. The design, using refrigerant R12, was based on the requirement to produce domestic hot water at a temperature of about 50 C and was assembled in the laboratory. All the experimental data were fed to a microcomputer and stored on disk automatically from appropriate transducers via amplifier and 16 channel analogue to digital converters. The measurements taken were R12 pressures and temperatures, water and R12 mass flow rates, air speed, fan and compressor input powers, water and air inlet and outlet temperatures, wet and dry bulb temperatures. The time interval between the observations could be varied.

The results showed, as expected, that the COP was higher at higher air inlet temperatures and at lower hot water output temperatures. The optimum air speed was found to be at a speed when the fan input power was about 4% of the condenser heat output. It was also found that the hot water can be produced at a temperature higher than the appropriate R12 condensing temperature corresponding to condensing pressure. This was achieved by condenser design to take advantage of discharge superheat and by further heating the water using heat recovery from the compressor. Of the input power to the compressor, typically about 85% was transferred to the refrigerant, 50% by the compression work and 35% due to the heating of the refrigerant by the cylinder wall, and the remaining 15% (of the input power) was rejected to the cooling medium. The evaporator effectiveness was found to be about 75% and sensitive to the air speed.

Using the data collected, a steady state computer model was developed. For given input conditions: air inlet temperature, air speed, the degree of suction superheat, water inlet and outlet temperatures; the model is capable of predicting the refrigerant cycle, compressor efficiency, evaporator effectiveness, condenser water flow rate and system Cop.

Key Words : Heat Pump , Computer Model , Heat Exchanger , Compressor

CONTENTS

i	: List of tables	viii
ii	: List of photographs	x
iii	::List of figures	xi
iv	: List of symbols	xix
v	: A summary of the aims, objectives and programmes of work	xxii
CHAPTER 1 : INTRODUCTION		1
CHAPTER 2 : THERMODYNAMICS OF A HEAT PUMP		7
2.1	: Introduction	7
2.2	: Heat pump cycle	8
1.	: Carnot cycle	8
2	: Rankine refrigerant cycle	12
3	: Practical heat pump cycle	14
2.3	: Heat pump performance	15
2.4	: Refrigerant choice	18
CHAPTER 3 : AN AIR TO WATER HEAT PUMP		27
3.1	: Compressor	27
1	: The Danfoss SC10H	28
2	: Reciprocating compressors.	28
3	: Compressor efficiency	33
4	: Compressor cooling	33
3.2	: Condenser	34
1	: Tube side by side condenser	34
2	: Thermal analysis of the condenser	35
3.3	: Evaporator	41
1	: An air source compact evaporator	41
2	: Thermal analysis of the evaporator	43
3.4	: Expansion Valve	45
1:	Thermostatic expansion valve	46

3.5 : Other components	47
1 : Fan	47
2 : Condenser's water flow regulator	49
3 : Filter drier	50
4 : Sight Glass	51
5 : The air heater	51
3.6 : The construction	53
 CHAPTER 4 : THE DIGITAL DATA ACQUISITION SYSTEM	 56
4.1 : The microcomputer	57
4.2 : Analogue to digital converter	58
4.3 : Instrumentation operational amplifier	59
4.4 : Frequency to voltage converter	63
4.5 : Temperature measurement	66
1 : Thermocouple	66
2 : The calibration	69
4.6 : Pressure measurement	70
1 : The strain gauge	70
2 : The calibration	71
4.7 : The compressor input power measurement	75
1 : The opto- switch	75
2 : The calibration	78
4.8 : The water flow rate measurement	79
1 : The water flow sensor	79
2 : The calibration	81
4.9 : The refrigerant flow rate measurement	83
1 : The flow sensor	83
2 : The calibration	84
4.10 : The air speed measurement	86
1 : The sensor	86
2 : The calibration	86

4.11 : The fan input power measurement	88
1 : The sensor	88
2 : The calibration	89
4.12 : The air relative humidity measurement	90
1 : The sensor	90
2 : The calculation of air relative humidity	90
4.13 : The computer program	92
 CHAPTER 5 : EXPERIMENTAL RESULTS	 95
5.1 : The expansion valve: Variation of suction superheat	95
5.2 : The evaporator	100
1 : Effect of air inlet temperature	100
2 : Effect of air speed	102
3 : Effect of relative humidity	104
4 : The heat transfer coefficient	106
5.3 : The compressor	107
1 : Variation of polytropic index with compression ratio.	107
2 : Variation of hot water temperature with compression ratio	107
3 : Variation in condensing and evaporating temperatures	112
4 : Compressor energy balance.	114
5.4 : The condenser	120
1 : Variation of hot water temperature	120
2 : Pressure drop across the condenser	120
3 : The water and freon temperature profiles	124
4 : The operation of the water flow regulator	129
5 : Effect of water inlet temperature	131

5.5 : Transient response: Decreasing and increasing air inlet temperature	133
CHAPTER 6 : THE COMPUTER MODEL	138
6.1 : Introduction	138
6.2 : The components model	139
1 : Compressor model	139
2 : Evaporator model	145
3 : Condenser model	149
6.3 : The heat pump model	150
6.4 : The detailed model of the condenser	156
CHAPTER 7 : THERMODYNAMIC CHARACTERISTICS OF AN AIR TO WATER HEAT PUMP DETERMINED FROM THE MODEL	171
7.1 : Air inlet temperature	171
7.2 : Air speed	172
7.3 : Suction superheat	173
7.4 : Hot water temperature	174
7.5 : Compressor characteristics and energy balance	176
7.6 : Evaporator effectiveness	182
CHAPTER 8 : CONCLUSION	207
8.1 : Main conclusions	207
8.2 : Suggestions for future work	210
APPENDIX:	
A : Thermodynamic properties of R12	213
B : Thermodynamic properties of water	216
C : Thermodynamic properties of air	217
D : Determination of polytropic index n	218
E : Computer program: calculates n from P1,T1,P5 and T5	221
F : Computer program: calculates T1 from n,P5,T5 and P1	222

G: Computer program: calculates R12 properties	223
H::Computer program: Heat pump model	224
I: Computer program: Condenser model	234
J: Computer program: Data acquisition system	245
K: Compressor Theory	250

REFERENCES	252
------------	-----

LIST OF TABLES

Table	Title	Page
1.1	The average number of days and nights per year when average temperatures drop to -1°C or less.	4
2.1	The commonly used refrigerants in refrigeration .	20
2.2	Some important properties of the refrigerant.	21
2.3	Comparision of R11, R12, R22 and R114 for heat pump application.	23
4.1	Comparision of equation (4.3) with values from the calibration table.	69
4.2	The accuracy of temperature measurement.	70
4.3	Pressure transducer calibration.	74
4.4	Calibration of the compressor input power.	78
4.5	The calibration of the water flow sensor.	83
4.6a	Data from the manufacturer's calibration certificate.	85
4.6b	The calibration of R12 flow sensor.	85
4.7	The evaporator air speeds at several fan frequencies.	87
4.8	The fan input power calibration.	89
5.1	The evaporating temperature as measured by the thermocouple and pressure transducer.	100
5.1a	The COP is higher at higher $T_a(i)$.	102

5.2	The effect of air speed on the system COP	104
5.3	Shows the effect of relative humidity and air speed on the heat pump performance.	105
5.4	Three set of results at $T_e = 5\text{ C}$	112
5.5	Three set of results at $T_c = 40\text{ C}$	113
5.6	The value of freon gas constant before and after the compression. If freon is considered as a perfect gas R is $68.77\text{ J kg}^{-1}\text{C}^{-1}$	116
5.7	The compressor energy balance	118
5.8	About 50% of the electrical input power is transferred to the freon gas by compression and about 35% by heating. The cooling water removed about 10% of the input power.	119
5.9	The compressor efficiencies η_i and η_v with $\frac{V_i}{V_s} = 95\%$	119
5.10	Comparison of the condenser with and without the subcooler.	129
5.11	The water flow rate is increasing with increasing T_e even though the discharge pressure P_1 is almost unchanged.	130
5.1		
5.12	INcreasing water inlet temperature will reduce the system COP.	132
6.1	Validation of equation (6.2). The polytropic index as a function of P_1 , P_5 and T_5 .	142
6.2	Validation of equation (6.8)	143

6.3	Validation of equation (6.9).	144
6.4	Validation of the evaporator model.	147
6.5	T_e (Eq) is from equation (6.32). T_e is adjusted in the model.	148
6.6	T_c (eq) is calculated from equation (6.36). T_c is adjusted in the model.	151
6.7	Validation of equation (6.35).	152
6.8 to 6.16	Validation of the heat pump model.	162-170
7.1	The compressor energy distribution.	181

LIST OF PHOTOGRAPHS

Photo	Title	Page
3.1	The position of the fan in the heat pump system.	48
3.2	The heat pump and digital data acquisition systems.	55
4.1	The amplifiers. At the top are the ATD converters.	67

LIST OF FIGURES

Figure	Title	Page
2.1	An air to water heat pump system	7
2.2	A schematic diagram of an air to water heat pump system showing the basic components and their arrangement.	9
2.3	Heat engine cycle; (a) on P-V diagram and (b) on T-S diagram.	10
2.4	Heat pump is a reversed heat engine.	11
2.5	The Rankine cycle can be plotted on (a) P- V diagram (b) T-S diagram and (c) P-h diagram. In process e-a refrigerant passed irreversibly through an expansion valve. This change is denoted by a hatched line and is isenthalpic.	13
2.6	An ideal (1345) and saturated (1345) heat pump cycle. The effect of superheating and the irreversible nature of the throttle expansion combine to reduce the coefficient of performance COP below that given by the Carnot theory.	15
2.7	Heat pump cycle on P-h diagram for R12 .	16
2.8	The various states of the heat pump working fluid.	16
2.9	A practical heat pump cycle (1345). The condensing temperature T_c is the temperature at 2, and the evaporating temperature T_e is the temperature at 4 .	17
2.10	Evaporating temperature versus coefficient of performance for the four refrigerants	24
2.11	Comparison of the four refrigerant swept volumes.	25

3.1	An air - water heat pump system showing the basic components.	27
3.2	The P-V diagram of the reciprocating compressor.	29
3.2a	A schematic diagram of reciprocating compressor.	30
3.3	The compressor, SC10H , characteristics .	33
3.4	A cross section of the condenser.	35
3.4a	The schematic diagram of the condenser.	36
3.5	The variation of R12 and water temperature in the condenser.	37
3.6	Heat is transferred from T1 to T2.	39
3.7	The cross section of the evaporator.	42
3.8	The throttling valve. Pressure and temperature at 1 is higher than at 2.	45
3.9	A schematic diagram of a thermostatic expansion valve.	47
3.10	The fan.	49
3.11	The c ondenser water flow regulator.	50
3.12	The air heater.	51
3.13	A block diagram of an air to water heat pump showing the size of the pipes used.	52
4.1	The digital. data acquisition system.	57
4.2	An analogue to digital converter.	59

4.3	Arrangement of transducers in the air to water heat pump system.	60
4.4	Block diagram of the transducers arrangement in the digital data acquisition system.	61
4.5	(a) Instrumentation operational amplifier circuit (b) RS 725 CN integrated circuit.	62
4.6	(a) RS 307-070, the frequency to voltage converter IC (b) The voltage limiting circuit.	63
4.7	A circuit diagram of frequency to voltage converter. The values of R1,R2,R3 and C1 depend on the application.	64
4.8	The output of the thermocouple is increased by the amplifier by 219 times.	66
4.8a	Connection of thermocouple to the R12 and water tubes.	68
4.9	(a) A schematic diagram of a pressure transducer gauge. (b) Strain gauge for tensile and compression strains.	71
4.10	A circuit diagram of the strain gauge for measuring pressure.	72
4.10a	The pressure transducer and the calibration certificate.	73
4.11	The RS opto-switch.	75
4.12	Circuit diagram for measuring compressor input power and air speed.	76
4.13	The opto-switch is made to count the lines on the watt hour meter disc.	77
4.14	(a) The water flow sensor. (b) A schematic diagram of the flow sensor showing the rotor and the sensing coil.	80

4.15	A circuit diagram for frequency to voltage converter for liquid flow sensor.	82
4.16	The opto switch is made to count the number of revolutions of the fan's shaft.	86
4.17	The evaporator face area is divided into 24 sections	87
4.18	Measuring the wet bulb temperature .	90
4.19	The flow chart for the data acquisition system.	93
4.20	Display on the computer screen during a typical experiment.	94
5.1	The variation of T_5 , T_e with suction superheat. The operating conditions are : $T_a(i)=23C$, $A_s=.1m^3s^{-1}$, $T_w(i)=12C$ and $T_w(o)=45C$.	96
5.2	The variation of freon and water mass flow rates with suction superheat. Operating condition as in fig(5.1).	97
5.3	The plot of COP against suction superheat. Operating condition as in fig (5.1) .	98
5.4	The variation of heat input and output with the suction superheat. Operating condition as in fig(5.1).	99
5.5	The evaporating temperature is increasing with the air inlet temperature. Operating condition are : $A_s=.1m^3s^{-1}$, $T_w(i)=12C$, $T_w(o)=45C$.	101
5.6	Increasing air speed will increase the evaporating temperature. $T_w(i)=12C$, $T_w(o)=45C$, $T_a(i)=15C$	102
5.7	Evaporator heat transfer coefficient at several evaporating temperatures.	108
5.8	Polytropic index versus Cr . $T_w(i)=12C$, $A_s=.1 m^3s^{-1}$	108

5.9	The compressor is cooled by water from the condenser.	109
5.10	The increment of water temperature after cooling the compressor.	110
5.11	Heat extracted by the cooling water from the compressor.	110
5.12	Water and freon mass flow rates change with the compression ratio.	111
5.13	The freon cycle with different T_c but constant T_e .	113
5.14	The cycles with different T_e but constant T_c .	113
5.15	The freon cycle with the symbols used.	115
5.16	The variation of the water flow rate and outlet temperature with T_c .	121
5.17	The condenser pressure drop. The pressure drop in the condensing region is about $2/3$ of the total pressure drop. The pressure drop at the condensing region is based on the pressure measurement at the accumulator.	122
5.17a	Condenser pressure plotted against the freon flow rate.	122
5.18	The condenser temperature profiles with and without pressure drop.	123
5.19	Condenser temperature profile at $T_c=30C, T_w(i)=12C, A_s=.1m^3s^{-1}, T_a(i)=15C$.	125
5.20	Condenser temperature profile at $T_c=40C$.	125
5.21	Condenser temperature profile at $T_c=45C$.	126
5.22	The freon cycle with and without subcooling.	127
5.23	Condenser temperature profile without the subcooling section. Operating at $T_w(i)=12.3C, A_s=.1m^3s^{-1}, T_a(i)=15C$.	128

5.24	(a) Three of the freon cycles chosen from the data in table (5.12) above. (b) The pressures involved in the water flow regulator	130
5.25	The air inlet temperature is allowed to drop from 25 C to 15 C in 30 minutes. $T_w(i)=12.5C, T_w(o)=45C,$ $A_s = .1m^3s^{-1}.$	135
5.26	The water and freon mass flow rates also decreasing with air inlet temperature.	135
5.27	The COP also decreasing with air temperature.	136
5.28	Air temperature is increased from about 14C to 25C in about 25 minutes.	136
5.29	The water and freon mass flow rates adjust themselves with the increasing air temperature.	137
5.30	The COP also increased with the air temperature.	137
6.1	The condenser can be divided into 3 regions; desuperheating, condensing and liquid cooling.	149
6.2	Flow chart of the heat pump model.	155
6.3	The condenser is divided into 15 sections, each of length 1 m.	156
6.4	Temperature profiles of freon and water in the condenser at $T_w(o)=51 C.$	160
6.5	Temperature profiles of freon and water in the condenser at $T_w(o)=45 C$	161
6.6 (a) to (i)	Validation of the heat pump model	170a-170c
7.1	T_e is increasing with $T_a(i).$ $A_s = .1 m^3 s^{-1}, T_w(i)=12 C$ and $T_w(o)=45 C.$	183

7.2	The variation of \dot{M}_r and \dot{M}_w with $T_a(i)$. A_s , $T_w(i)$ and $T_w(o)$ as in fig (7.1).	184
7.3	Heat input and output at several $T_a(i)$ s. A_s , $T_w(i)$ and $T_w(o)$ as in fig (7.1).	185
7.4	Cop versus $T_a(i)$. A_s , $T_w(i)$ and $T_w(o)$ as in fig(7.1)	186
7.5	T_e at several air speeds, A_s . $T_a(i)=15$ C, $T_w(i)=12$ C and $T_w(o)=45$ C .	187
7.6	The variation of \dot{M}_r and \dot{M}_w with A_s . Operating in the same condition as in fig (7.5).	188
7.7	Heat input and output at several A_s . Operating in the same condition as in fig (7.5).	189
7.8	COP versus air speed. Operating under the same condition as in fig (7.5) .	190
7.9	T_e at several suction superheat temperatures. $A_s=.1\text{m}^3\text{s}^{-1}$, $T_w(i)=12$ C and $T_w(o)=45$ C:	191
7.10	\dot{M}_r and \dot{M}_w against Sh . $T_a(i) =23$ C, $A_s=.1\text{m}^3\text{s}^{-1}$, $T_w(i)=12$ C and $T_w(o)=45$ C.	192
7.11	Heat output versus Sh . Same condition as in fig (7.10)	193
7.12	Variation of superheat with COP. Same condition as in figure(7.10) .	194
7.13	T_e at several $T_w(o)$ s . $T_a(i)=15$ C, $A_s=.1\text{m}^3\text{s}^{-1}$, $T_w(i)=12$ C	195
7.14	\dot{M}_r and \dot{M}_w versus $T_w(o)$. Same condition as in fig(7.13)	196
7.15	C_r versus $T_w(o)$. Same condition as in fig (7.13)	197
7.16	n versus $T_w(o)$. Same condition as in fig (7.13)	198
7.17	COP versus $T_w(o)$. Same condition as in fig (7.13)	199

7.18	n versus \dot{M}_r . $A_s = .1 \text{m}^3 \text{s}^{-1}$, $T_w(i) = 12\text{C}$, $T_w(o) = 45\text{C}$	200
7.19	Electrical power supplied to the compressor is a function of T_e and T_c . Air speed and water inlet temperature is constant.	201
7.20	Compressor frequency varies with air and hot water temperature.	202
7.21	The compressor efficiency for several C_r	203
7.22	Typical values of heat output and input and also isentropic work done.	204
7.23	Evaporator effectiveness at several air temperatures and speeds.	205
7.24	Evaporator HTC at several air speeds.	206

List Of Symbols

A	: Area (or total heat transfer area)	: m ²
A _f	: Fin heat transfer area	: m ²
A _r	: Inside R12 tube surface area	: m ²
A _o	: Evaporator frontal area	: m ²
A _s	: Air speed	: m ³ s ⁻¹
C	: Capacity rate (= Ḣ Cp)	: WK ⁻¹
C _f	: R12 capacity rate	: WK ⁻¹
C _r	: Compression ratio	
C _w	: Water capacity rate	: WK ⁻¹
C _p	: Specific heat	: Jkg ⁻¹ K ⁻¹
C _{pa}	: Air specific heat	: Jkg ⁻¹ K ⁻¹
C _{pw}	: Water specific heat	: Jkg ⁻¹ K ⁻¹
C _{pf}	: R12 specific heat	: Jkg ⁻¹ K ⁻¹
c	: Kinetic energy	: W
D	: Diameter (inside)	: m
D _o	: Diameter (outside)	: m
ε	: Effectiveness	
E _o	: Overall air side surface effectiveness	
F	: Friction factor	
F _c	: Frequency	: Hz
F _c '	: Colburn correlation	
F _s	: Stanton correlation	
G	: Mass velocity	: kgs ⁻¹ m ⁻²
H _c	: Heat transfer coefficient	: Wm ⁻² K ⁻¹
h _r	: R12 heat transfer coefficient	: Wm ⁻² K ⁻¹
h _e	: Effective heat transfer coefficient (air)	: Wm ⁻² K ⁻¹
h _a	: Heat transfer coefficient (air)	: Wm ⁻² K ⁻¹
h	: Enthalpy	: Jkg ⁻¹
k	: Thermal Conductivity	: Wm ⁻¹ K ⁻¹
k _f	: Conductivity of fin metal	: Wm ⁻¹ K ⁻¹

L	: Length	: m
l	: Fin length	: m
M	: Mass flow rate	: kg s^{-1}
\dot{M}_r	: R12 mass flow rate	: kg s^{-1}
\dot{M}_w	: Water mass flow rate	: kg s^{-1}
n	: Polytropic index	
η_f	: Fin efficiency	
η_i	: Isentropic efficiency	
η_m	: Mechanical efficiency	
η_o	: Overall isentropic efficiency	
η_v	: Volumetric efficiency	
Nu	: Nusselt number	
ΔP	: Pressure drop	
Pr	: Prandtl number	
Ps	: Saturation pressure	: bar
ρ	: Density	: kg m^{-3}
Q	: Heat or energy	: W
Rc	: Fin contact resistance	: $\text{W m}^{-2} \text{K}^{-1}$
RH	: Relative humidity	
Rt	: Inside the tube fouling resistance	: $\text{W m}^{-2} \text{K}^{-1}$
Ry	: Reynolds number	
Sh	: Suction superheat	: Deg K
ΔT	: Logmean (or effective) temperature difference	: Deg K
Te	: Evaporating temperature	: C
Tc	: Condensing temperature	: C
t	: Thickness	
Ta(i)	: Evaporator air inlet temperature	: C
Ta(o)	: Evaporator air outlet temperature	: C
Tw(i)	: Condenser water inlet temperature	: C
Tw(o)	: Condenser water outlet temperature	: C

tw : Tube wall thickness	: m
μ : Viscosity	: Nsm^{-2}
μ_B : Bulk viscosity	: Nsm^{-2}
μ_T : Viscosity at wall temperature	: Nsm^{-2}
V : Velocity	: ms^{-1}
V : Specific volume	: $\text{m}^3 \text{kg}^{-1}$
Vc : Clearance volume	: m^3
Vi : Induce volume	: m^3
Vs : Swept volume	: m^3
W : Work	: W
Wr : Work done by the reciprocating compressor	: W
Wc : Compression work	: W
α : Thermal diffusivity	: $\text{m}^2 \text{s}^{-1}$
X : Quality of R12 mixture (vapour and liquid)	
Xt : Lockhard and Martinelli parameter	

Subscript:

r : refrigerant (R12)
w : water
f : fin
a : air
l : liquid
v : vapour

A Summary Of The Aims, Objectives And Programme Of Work

1. To assemble an air to water heat pump system which can produce service hot water in the region of 50 C.
2. To evaluate the Danfoss SC10H compressor for a heat pump application in (1).
3. To study side by side tube condenser, where there exists the possibility that water can be produced at a higher temperature than the appropriate refrigerant condensing temperature; and also the effect of subcooling on the system COP.
4. To investigate the heat pump thermodynamic characteristics at different ambient air temperatures, air speed and suction superheat.
5. To develop a computer model which can be used to study the thermodynamic characteristics of the heat pump for a wide range of operating conditions; and to improve future design of similar systems.

To achieve the above aims and objectives, a heat pump system and the digital data acquisition system with some of the appropriate transducers were developed in the laboratory.

1. The heat pump system with access points for monitoring its thermodynamic parameters was constructed in the laboratory.
2. Instrumentation amplifiers for amplification of low level signals to improve the data handling system were also designed and built in the laboratory.
3. A technique for measuring air speed, compressor and fan input powers by utilising a frequency to voltage converter was developed in the present work.
4. A survey was conducted to find the suitable pressure and liquid flow sensors.
5. Computer programs for the data acquisition system and on line and off line analysis of the data were developed . Computer programs to facilitate the fitting of experimental data values to equations (polynomial, power and two variables regression) were also developed.
6. Based on the experimental data and theoretical principles a steady state computer model was developed.

CHAPTER 1

INTRODUCTION

Any process is never 100% efficient (1) ; and so it is with the process of producing hot water by heat pumping. In the wake of ever increasing energy costs, the current and future energy situations there is a challenge to produce service hot water using ambient energy. The questions of how to limit the use of fossil fuels, and how to make the most of ambient and alternative energy sources, are widely debated in the industrialised world. One of the answers and a very interesting one is the heat pump.

The heat pump concept is not new, it was first introduced by Lord Kelvin (2) in 1852. This idea lay dormant for nearly 80 years (3), mainly due to the energy situation at the time. The commercial application in the 1930's was principally for air conditioning in the USA. After the world energy crisis in the early 1970's , the heat pump became very attractive as a means of heating rather than cooling. Heat pump research and production increased rapidly. The International Energy Agency estimated total annual sales of 1.3 million units of all types in 1981/1982 , and forecast an increase to 2 and 3 million by the end of the 1990's (4).

In the United Kingdom , as in most European countries, heat pump development has been focussed on space and water heating units , usually substituting for the gas boiler and electric central heating system. At the moment the sales are estimated at around 4000

installations per year (5) . Hospitals , office blocks , schools , shops and supermarkets appear to take up most of the market . Industrial and commercial applications are currently mainly limited to low temperature drying processes (6) , dehumidification and heat recovery in swimming pools (7) . The only profitable market in the domestic sector is in houses without access to the gas grid; estimated to be several hundred installations per year. The slow response to the heat pump in the domestic market is certainly due to the initial capital cost. The lowest cost of a domestic heat pump is an air-air system at about £1200 for an output of 6kW (8) in 1981. Ambrose et al (5) suggested that this initial cost can be reduced by looking at four design aspects which could be improved :

1. Standardisation
2. Simplification
3. Improved performance
4. New or improved compressor

They estimated that after 15 to 20 years of development , design refinement of this kind would lead to a 25 to 50% reduction in initial cost . Clearly the basis for improvement is good understanding of the heat pump and its components . This is the main aim of the present study .

While the heat pump idea ^{for heating} lay dormant , the refrigeration industry grew steadily due to high demand for cold storage and air conditioning. When interest in the heat pump was renewed , it was not surprising to see that the refrigeration components were used , and in fact are still widely being used, in the heat pump system . Among the few specially designed heat pump components on the market is the Danfoss SC10H compressor. The manufacturer claims that the development of this heat pump

compressor has taken into account both economic and technical factors. It is one of the aims in the present work to study and evaluate this compressor for a heat pump application in supplying service hot water.

Commonly most of the water heating heat pumps utilize a shell and tube condenser, or immerse the refrigerant vapour line (at higher pressure) inside the hot water cylinder. In both cases, the final hot water temperature is lower than the refrigerant condensing temperature. Recently Carrington (9) has shown that hot water can be produced at a temperature higher than the condensing temperature and almost instantly (10) using a specially designed condenser. This is very interesting, since a lower condensing temperature means a higher coefficient of performance. It is one objective of the present work to study in detail this type of condenser. Another interesting aspect about this condenser is that it allows the subcooling of the liquid refrigerant, and so increases the heat output and the coefficient of performance. The effect of the subcooling on the heat pump system will be included in the study.

Apart from the equipment, the heat source is another factor which has enormous effect on the heat pump performance. Air appears to be very interesting heat source, because of its availability. Unlike earth (ground coil) and water (usually from well and river) heat sources , where their applications are limited, the air source heat pump can be installed anywhere; in factory, hospital, residential home, even a bungalow or a flat at the top of the building. The only disadvantage of the air source is that for space heating air temperatures are low when heating is most needed, and for water heating air temperatures

are low for about 30% of the year. In the United Kingdom the temperature for most of the days and nights in a year is higher than 0C. Table (1.1) shows the average of days and nights per year in the United Kingdom where the temperature is less than -1C. Higher air temperature means^a higher coefficient of performance . For an air temperature in the region of 0C, the coefficient of performance is between 2.5 to 3 when hot water at about 50C is produced,(see for example (11), (12), (13)) and this is good.

	London (Heathrow)	Birmingham (Elmdon)	Manchester (Ringway)	Glasgow (Abbotsinch)
Day	3.9	7.9	5.4	7.5
Night	6.7	12.5	8.4	12.5

Table (1.1) The average number of days and nights per year when average temperatures drop to -1C or less (source (14)).

It is quite true to say that an untreated air source is not the most attractive (15), since it is often too cold to achieve coefficient of performances greater than 3. Considering that solar energy technology is expanding rapidly, a solar assisted heat pump future looks very promising (16). Exhaust air from industrial processes is another source of warm air. In the supermarkets and big stores , heat rejected from the refrigeration system can be a very good heat source. Therefore it is very worthwhile to examine heat pump characteristics at various air inlet temperatures.

Another factor of interest is the effect of air speed on the heat pump system. Very low air speeds can cause frost formation on the evaporator surface. Very high air speeds means more power must be

given to the fan. To see how the air speed affects the system performance is another aim of the present work.

To facilitate the study and improve future designs, a predictive computer model is required. A model which would be able to predict, for a given operating condition, the refrigerant cycle on the P-h diagram, water and refrigerant flow rates, the compressor and system energy balances, some of the components efficiencies, and the overall coefficient of performance is essential for design purposes. The model developed in the study is based on theoretical concepts as much as possible. Where the theoretical concept is not applicable, empirical relations (developed from the experimental data obtained in the present study) are used.

In the laboratory a small air to water heat pump instrumented for research was designed and assembled. The heat output capacity is between 1 to 2 kW, while the compressor input power requirement is about 300 W. All the measurements are automatic and under computer control. This is considered to be very important so that large quantities of data can be collected in a short period with high accuracy. An instantaneous calculation of energy balance makes it possible to ensure the system is being monitored properly. Also an instantaneous print out of the coefficient of performance gives an idea of how the heat pump is responding to changes either in the heat source (air temperature, air speed) or in the refrigerant cycle (subcooling, superheating). All the data are stored on magnetic disks for fuller analysis later on.

All the experiments were carried out in the laboratory. The air relative humidity is not a controlled parameter , but it is measured at the inlet and outlet of the evaporator . The difference of air enthalpies at the outlet and inlet of the evaporator is taken as the energy absorbed by the evaporator into the system.

CHAPTER 2

THERMODYNAMICS OF A HEAT PUMP

2.1 Introduction

A heat pump is an apparatus for causing heat to flow from a low temperature heat source to a higher useable temperature heat sink. Some examples of natural heat sources are atmospheric air, water and earth. While the heat sink is a fluid, depending on the application of the heat pump. In space heating for example, the fluid can be air or water.

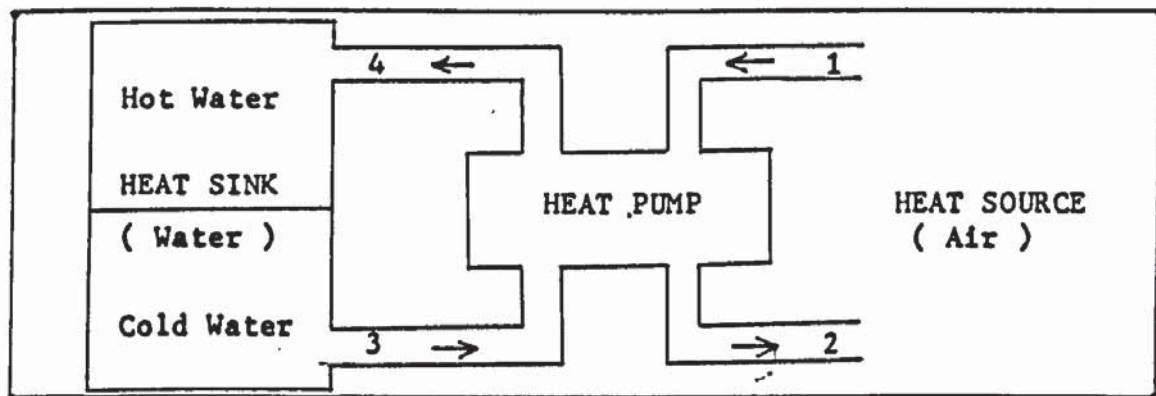


Fig (2.1) An air to water heat pump system.

The heat transfer medium of the heat source is passed through the heat pump, where heat is extracted, and then rejected back to the heat source at a lower temperature. In the case of earth normally a secondary fluid is used to extract heat from the earth and then transfer it to the heat pump. The heat is then upgraded by the heat pump and transferred to the heat sink. In figure (2.1), representing an air to water heat pump, the temperature of air at 1 is higher than at 2, and water temperature at 4 is higher than at 3.

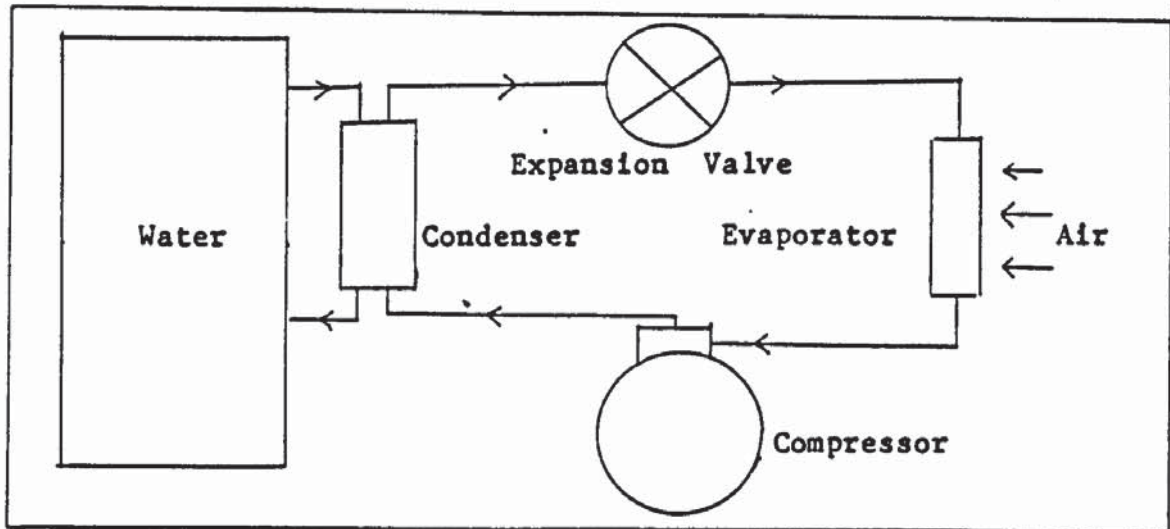
The fluid used in the heat pump to transport the heat extracted from heat source to heat sink is called the refrigerant. The refrigerant changes state from liquid to vapour while extracting heat from the heat source, and the heat exchanger where this process takes place is called the evaporator. The low pressure and temperature vapour is then compressed to a higher pressure and temperature by a compressor. This compressor requires external work for its operation. Heat is released by the refrigerant to the heat sink during condensation in another heat exchanger, the condenser. The liquid refrigerant then expands back to its original pressure and temperature as it returns to the evaporator via an expansion valve. Figure (2.2) is a schematic diagram showing the basic components of an air to water heat pump.

In thermodynamics, a process where the system reverts back to its original state is called a cycle. As has been discussed above the refrigerant is extracting and releasing heat repeatedly. The refrigerant is said to be working in a closed system.

2.2 Heat Pump Cycle

2.2.1 Carnot Cycle

Whenever a temperature difference exists, motive power can be produced. This statement is one form of the second law of thermodynamics, first reported by Carnot in 1824. A system that can produce motive power or work is known as heat engine. A heat engine cycle consists of a number of processes arranged to convert heat energy into work energy such that the system returns to its original state at the end of each cycle. The Carnot cycle for a heat engine is composed of reversible processes which give the maximum possible work when working between two fixed temperature limits, T_1 and T_2 . Figure(2.3) is a Carnot cycle for a heat engine



Fig(2.2) A schematic diagram of an air to water heat pump system showing the basic components and their arrangement.

with a gas as the working substance on P-V (pressure-volume) and T-S (temperature-entropy) diagrams. The cycle consists of four processes.

1. Process A-B : Heat energy is supplied to the system at constant temperature; an isothermal process.
2. Process B-C : Is an isentropic expansion of refrigerant, where no energy is transferred to or from the system.
3. Process C-D : Heat energy is rejected from the system at a constant lower temperature, an isothermal process.
4. Process D-A : Is an isentropic compression of the refrigerant, where no energy is transferred to or from the system as it returns to the initial state.

If Q_1 is heat supplied to the system, and Q_2 is heat rejected by the system,

The net work done = heat supplied - heat rejected

$$W = Q_1 - Q_2 \quad (2.1)$$

The efficiency is defined as,

$$\eta = \frac{Q_1 - Q_2}{Q_1} \quad (2.2)$$

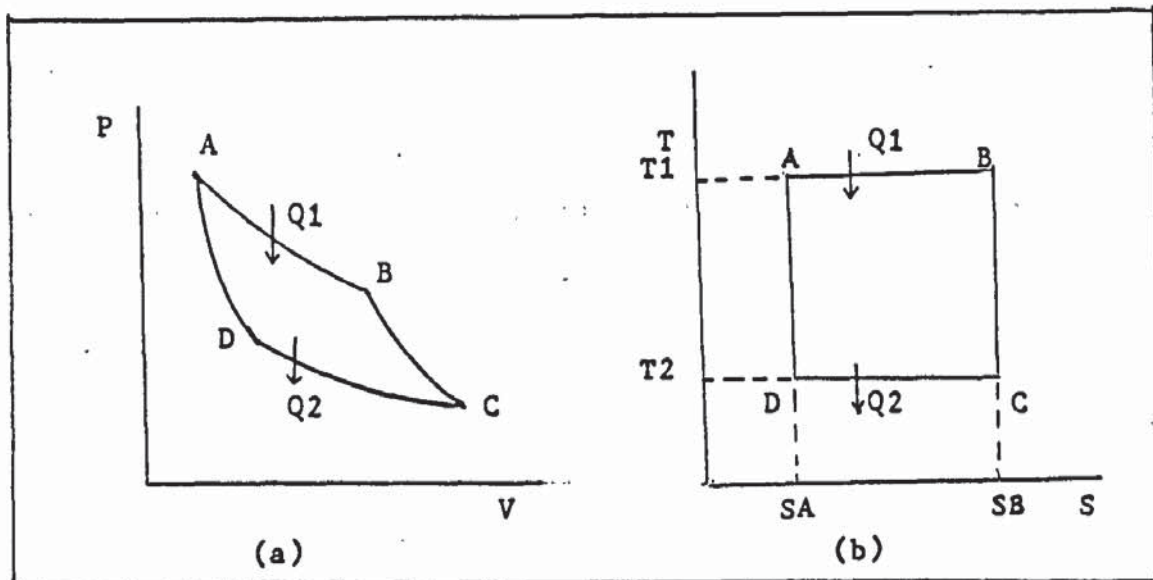


Fig (2.3) Heat engine cycle ; (a) on P - V diagram and (b) on T - S diagram

or
$$\eta = 1 - \frac{Q_2}{Q_1}$$

$$\eta = 1 - \frac{T_2(SB - SA)}{T_1(SB - SA)} \quad \text{since } Q = \int Tds \text{ for reversible process.}$$

$$\eta = 1 - \frac{T_2}{T_1}$$

or
$$\eta = \frac{T_1 - T_2}{T_1} \quad (2.3)$$

Equation (2.3) shows that the efficiency of Carnot heat engine can be expressed in terms of temperature only.

If this cycle is reversed, that is instead of ABCDA, the cycle is now operating from ADCBA, figure(2.3), this means that energy Q2 is absorbed into the system at T2 and energy Q1 is rejected at T1 from the system. The system following this cycle is known as a refrigerator or a heat pump, figure(2.4). If the application is for cooling it is called refrigerator (or air conditioning unit) and if for heating is a

heat pump.

For these devices a dimensionless quantity, the coefficient of performance, COP is introduced. The COP of the refrigerator for cooling is given by

$$\begin{aligned} \text{COP}(C) &= \frac{\text{Heat Extracted}}{\text{Work Done}} = \frac{Q_2}{W} \\ &= \frac{Q_2}{Q_1 - Q_2} = \frac{T_2}{T_1 - T_2} \end{aligned} \quad (2.4)$$

and for the heat pump, the COP for heating is

$$\begin{aligned} \text{COP}(H) &= \frac{\text{Heat Rejected}}{\text{Work Done}} = \frac{Q_1}{W} \\ &= \frac{Q_1}{Q_1 - Q_2} = \frac{T_1}{T_1 - T_2} \end{aligned} \quad (2.5)$$

The two are plainly simply related

$$\text{COP}(H) = 1 + \text{COP}(C) \quad (2.6a)$$

The COP for heating may also be written

$$\text{COP}(H) = \frac{W + Q_2}{W} = 1 + \frac{Q_2}{W} \quad (2.6b)$$

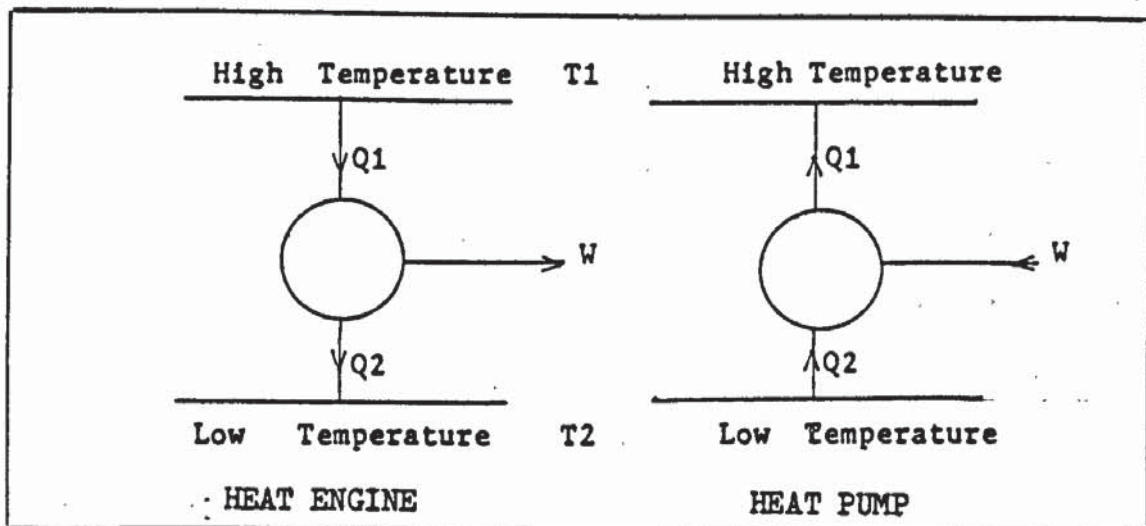


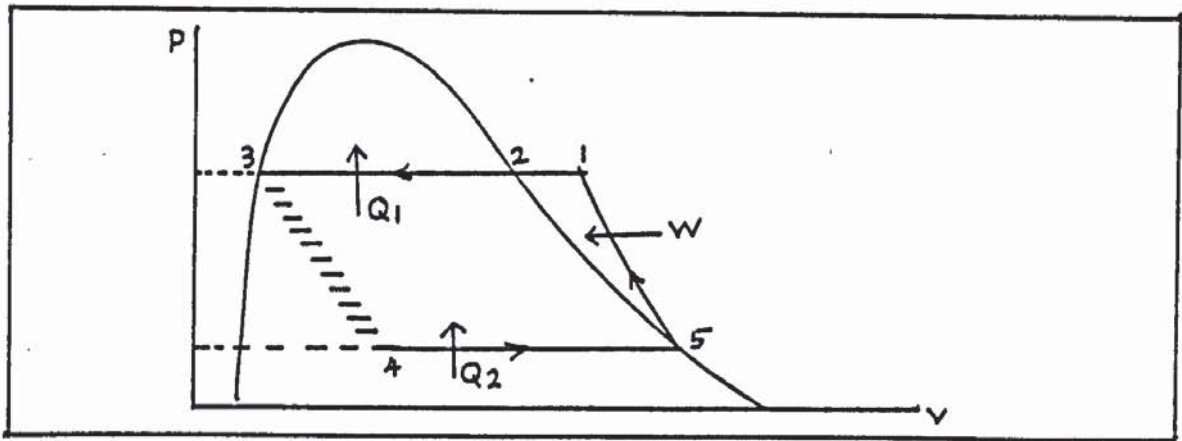
Fig (2.4) Heat pump is a reversed heat engine .

2.2.2 Rankine Refrigerant Cycle

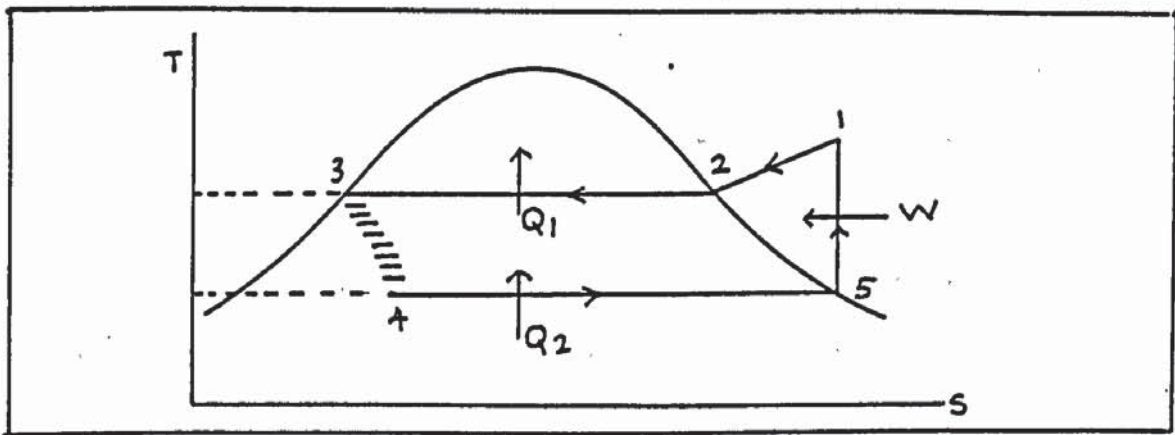
The Carnot cycle involves four processes, two adiabatics and two isothermals, while the rankine cycle has an extra process, the isobaric desuperheating of refrigerant vapour. In practice the heat pump cycle is more close to the Rankine cycle than the Carnot cycle. During the course of the Rankine cycle the refrigerant changes state several times, which can be followed in the phase diagram. The most suitable diagram for representing the processes of refrigeration and heat pump is the Mollier P-h chart. The vertical axis of this chart or diagram is pressure (P) and the horizontal axis is enthalpy (h). The curve on the left of the diagram is the boiling point pressure curve and on the right is the dew point curve. The two curves meet at the critical point. The area under the curve is the two phase region. To the left of this region is the liquid region and to the right is the vapour region.

Figure(2.5 c) shows the Rankine cycle drawn on a p-h chart of refrigerant 12 (or R12). The processes involved can be explained as follows,

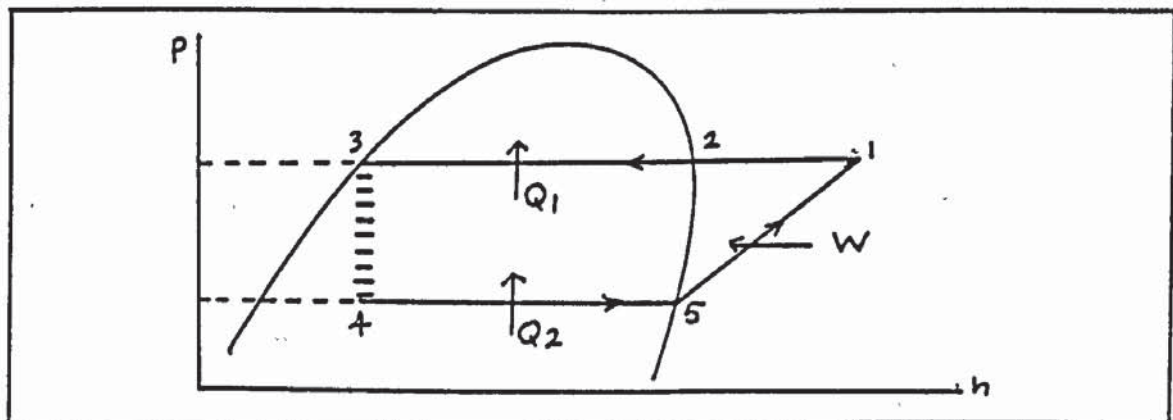
1. 5 - 1 : Isentropic compression of refrigerant vapour from low temperature and pressure to a higher temperature and pressure
2. 1 - 2 : Desuperheating of refrigerant vapour at constant pressure.
3. 2 - 3 : Heat rejected to the heat sink from the condensation of refrigerant at constant temperature and pressure.
4. 3 - 4 : Expansion of refrigerant at constant enthalpy. The pressure and temperature of refrigerant is lowered



(a)



(b)



(c)

Fig (2.5) The Rankine cycle can be plotted on (a) P-V diagram (b) T-S diagram and (c) P-h diagram. In process 3→4 refrigerant passes irreversibly through an expansion valve. This change is denoted by a hatched line and is isenthalpic.

to the evaporating pressure and temperature. Partial evaporation occurs in this process.

5. 4-5 : Heat is extracted from a heat source at constant temperature and pressure.

2.2.3 Practical Heat Pump Cycle

In practice, to ensure that no liquid enters the compressor, the saturated refrigerant vapour in the suction line (point 5 in figure (2.5c)) is further heated for a few degrees, normally between 5C to 10C. To increase the efficiency of the heat exchangers, liquid refrigerant is further cooled, for example in the present system between 10 and 20 degree C below ^{the} condensing temperature. The Rankine cycle in practice is now the cycle 1345 in figure (2.6). This cycle is known as an ideal heat pump cycle. For the cycle without suction superheat and liquid subcooling, cycle 1'2'4'5' is called a saturated cycle. These two additional processes are termed 'suction superheat' and 'subcooling'. The superheating of refrigerant vapour in the high pressure line (or condenser) is called 'discharge superheat' (or desuperheating).

The real heat pump cycle, must account for two more factors; the pressure losses in the heat exchangers, and that the compression is not isentropic, figure (2.9). The pressure drops in heat exchangers are due to the flow friction between the refrigerant and the tube, and for example, in the present heat pump system the pressure drops

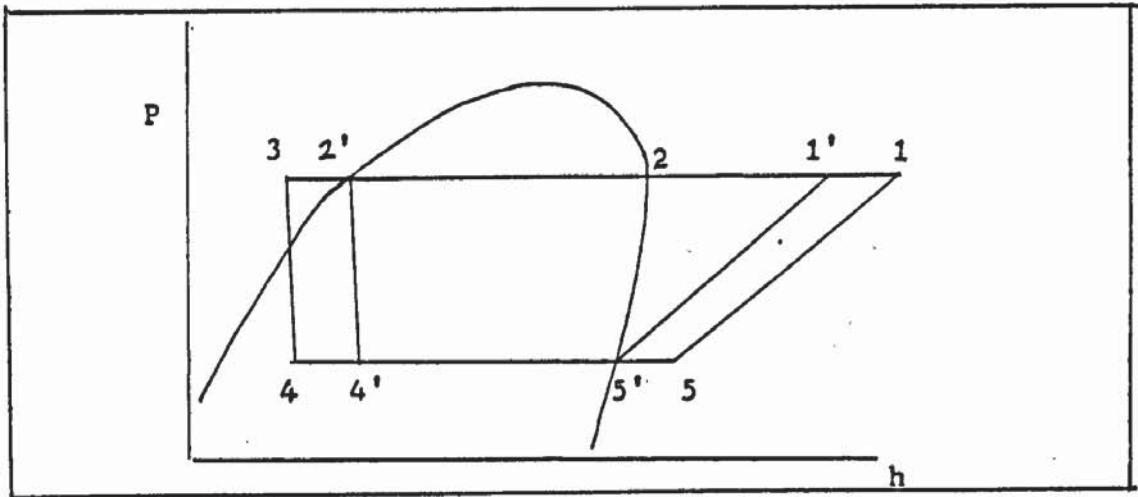


Fig (2.6) An ideal (1345) and saturated (1'2'4'5') heat pump cycle . The effect of superheating, and the irreversible nature of the throttle expansion combine to reduce the coefficient of performance COP below that given by Carnot theory.

are about .7 bar (10 psi) in the condenser and .14 (2psi) in the evaporator . The refrigerant also experiences pressure drops when entering and immediately after leaving the compressor's cylinder . In figure (2.9), 5 - 5' is suction pressure drop and 1-1' is discharge pressure drop. Pressure drops at the compressor mean the actual compression ratio is higher than the expected one. The heat exchangers efficiency will be reduced by the pressure drop, and the pressure drop in liquid line (point 3 in figure (2.9)) will reduce the expansion valve capacity.

2.3 Heat Pump Performance

The Carnot COP is the highest COP for a heat pump machine working between two fixed temperatures. It can be expressed using equation(2.5),

$$\text{COP (Carnot)} = \frac{T_c}{T_c - T_e} \quad (2.7)$$

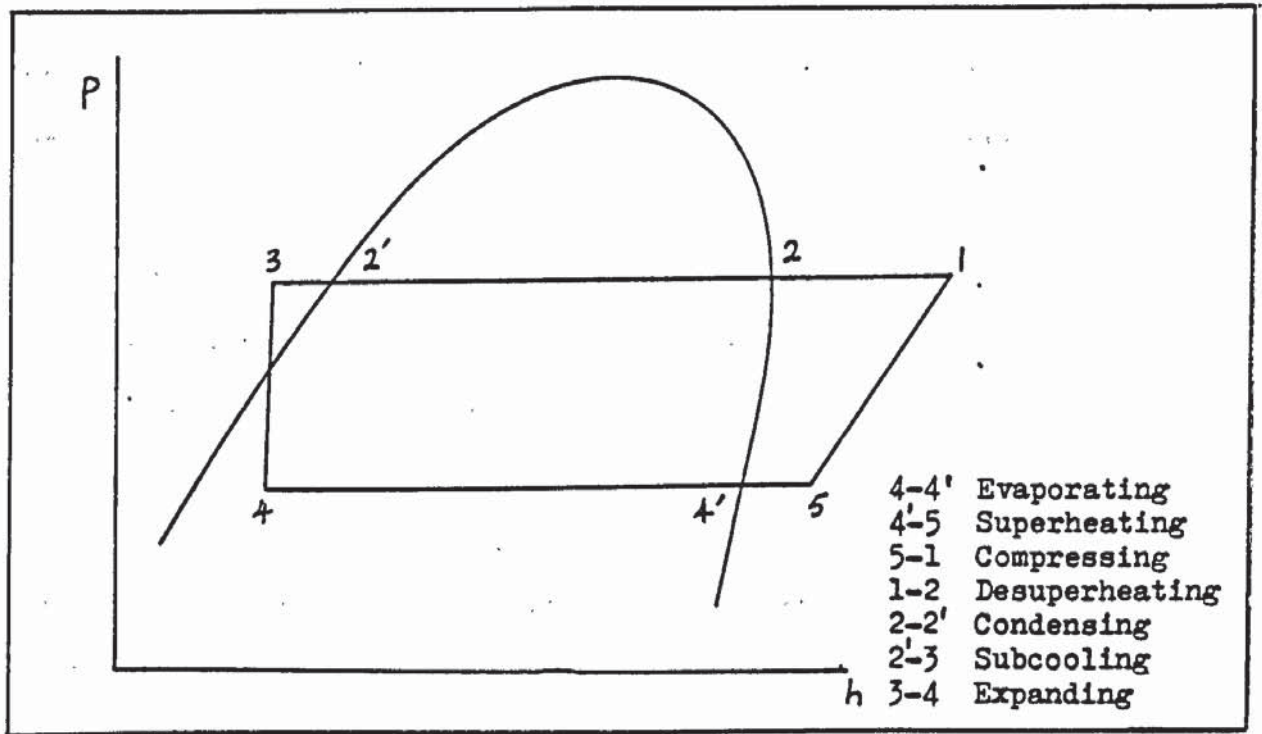


Fig (2.7) Heat pump cycle on P-h diagram for R12.

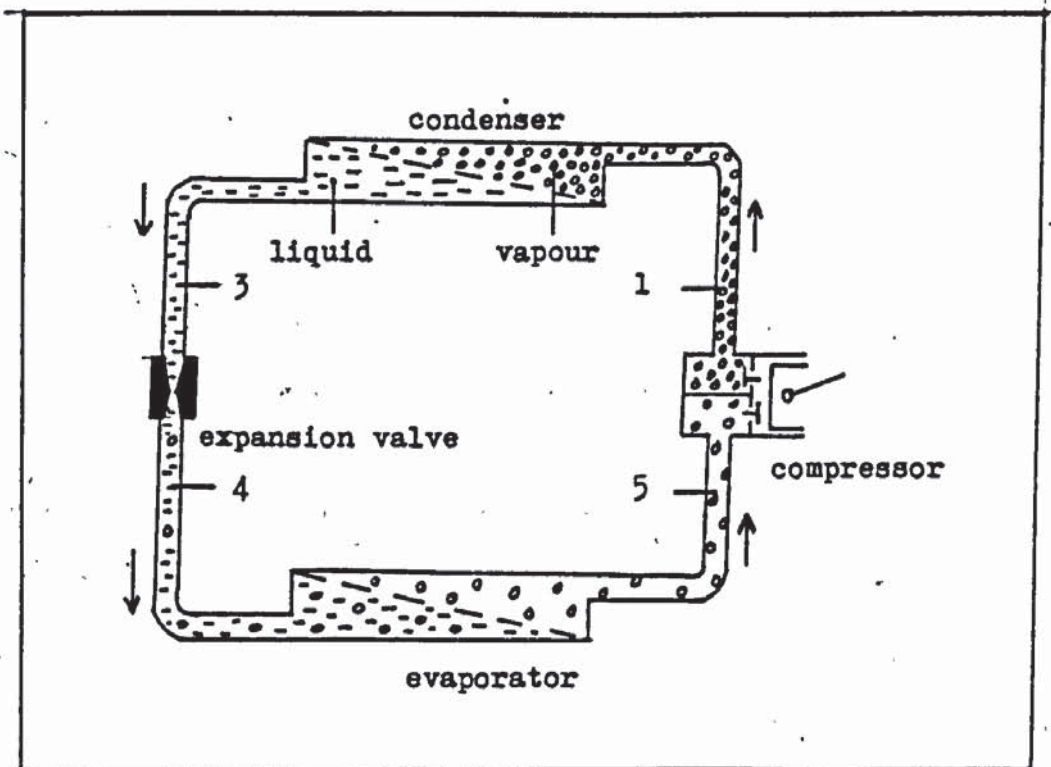


Fig (2.8) The various states of the heat pump working fluid.

where T_c and T_e are the condensing and evaporating temperatures in K respectively. The equation also ignores the discharge superheat.

Since during the isenthalpic throttling process no internal work is done and no heat is lost or gained, the work done by the compressor must equal the difference in heat output and input, $W = Q_1 - Q_2$ (1st law of thermodynamics). Since $Q_1 = h_1 - h_3$, $Q_2 = h_5 - h_4$ and $h_3 = h_4$ (see figure (2.6)),

$$W = h_1 - h_5 \quad (2.8)$$

Equation (2.5) can also be written in term of enthalpy differences, which is known as the Rankine COP.

$$\text{COP (Rankine)} = \frac{h_1 - h_3}{h_1 - h_5} \quad (2.9)$$

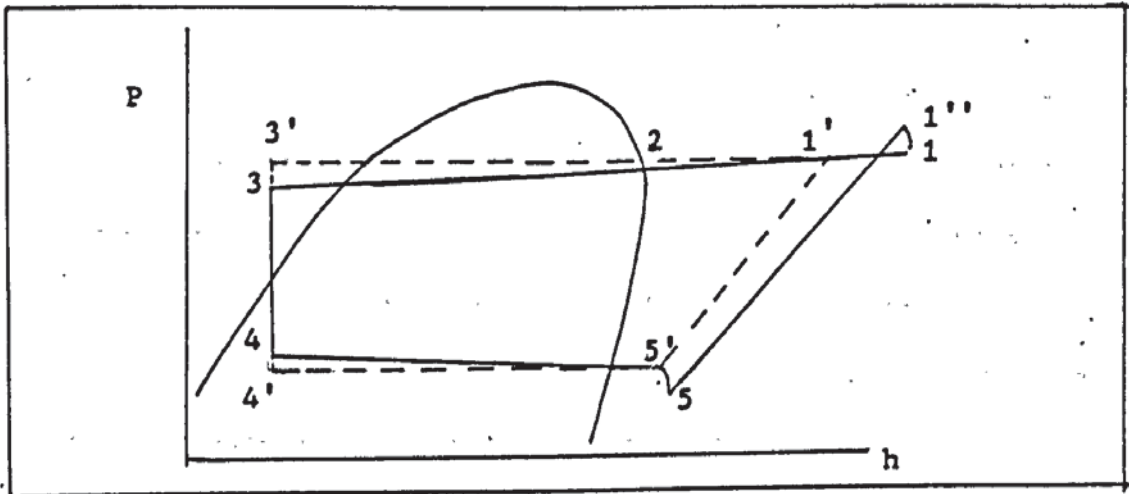


Fig (2.9) A practical heat pump cycle (1345). The condensing temperature T_c is the temperature at 2, and the evaporating temperature T_e is the temperature at 4.

In practice there are several factors which can reduce the COP. One of the biggest factors is compressor efficiency. Normally the efficiency of a reciprocating compressor is about 80 to 90 % (17). Usually other electrical appliances are needed in the operation. For example, in an air to water heat pump, a fan is needed to circulate air through the evaporator and water pump to circulate water through the condenser.

This will increase the total work input to the system, and so reducing the system COP.

2.4 Refrigerant Choice

In heat pump systems , refrigerants are the vital working fluids. Their function is to remove heat from the heat source and add it to the heat sink. Most mechanical compression heat pump systems use refrigerants that change phase during operation. Heat is removed from the heat source by evaporating the liquid refrigerant and transferred to the heat sink by condensing the refrigerant vapour. Systems that use gas , such as air (18), do not change phase during operation.

There are 23 refrigerants that are used in refrigeration (19) , as shown in tables (2.1) and (2.2) with some of their properties that are very important to the heat pump design. Basically there are five most important properties desirable for refrigerants.

1. The operating evaporator temperature should be well above the freezing temperature at the operating pressure. This is to ensure the smooth flow of refrigerant, without the possibility the line being blocked by the formation of solid refrigerant.
2. At the desired condenser temperature , the condensing pressure should be well below the critical pressure. When the condensing pressure is approaching the critical pressure, the latent heat of condensation is decreasing. This will reduce the amount of heat transferred to the heat sink.
3. The evaporating pressure should be higher than atmospheric pressure. This is because in the event of a leak, if the pressure

is lower than atmospheric, air will be sucked into the system. Some refrigerants react with air and the resulting chemicals may damage the system.

4. The refrigerant should be non toxic, non-flammable and non-corrosive.
5. The refrigerant should be easily obtainable at a low cost.

All refrigerants which contain carbon atoms or molecules are called organic refrigerants, known commercially as freons. These organic refrigerants are divided into two groups. One which contains one carbon atom in their molecular structure is known as methane based, the other with two carbon atoms is called ethane based. The mixture of two refrigerants is known as an azeotrope. Table (2.1) and (2.2) show 23 refrigerants with some of their properties.

In the United Kingdom, the required domestic hot water temperature is about 50C (20). For a heat pump to produce hot water at this temperature, it will require the condensing temperature also to be about 50C (assuming collection of energy in the discharge superheat vapour). If the ambient air is used as the heat source, the evaporating temperature is about -5C (for ambient air of about 0C). Therefore in order to comply with condition 1 and 2 to suit the application of a heat pump as domestic water heater, the refrigerants must have freezing temperature well below -5C and critical temperature should be higher than 50C.

Thermodynamically there are several refrigerants suitable for heat pump applications. Pabon-Diaz (21) and Ogbeide (22) evaluated and compared several refrigerants which are commonly used ⁱⁿ heat pumps.

	Name	Chemical Formula	Mol. Mass kg/K mol.
50	Methane	CH ₄	16.04
14	Tetrafluoromethane	CF ₄	88.01
1150	Ethylene	C ₂ H ₄	28.05
503	Azeotrope of R23 and R13		87.50
170	Ethane	C ₂ H ₆	30.07
23	Trifluoromethane	CHF ₃	70.02
13	Chlorotrifluoromethane	CClF ₃	104.47
744	Carbon Dioxide	CO ₂	44.01
13B1	Bromotrifluoromethane	CBrF ₃	148.93
1270	propylene	C ₃ H ₆	42.09
502	Azeotrope of R22 and R115		111.63
290	propane	C ₃ H ₈	44.10
22	Chlorodifluoromethane	CHClF ₂	86.48
717	Ammonia	NH ₃	17.03
500	Azeotrope of R12 and R152a		99.31
12	Dichlorodifluoromethane	CCl ₂ F ₂	120.93
152a	Difluoroethane	CH ₃ CHF ₂	66.05
600a	Isobutane	CH ₄ H ₁₀	58.13
142b	Chlorodifluoroethane	CH ₃ CClF ₂	170.94
600	Butane	C ₄ H ₁₀	137.38
114	Dichlorotetrafluoroethane	CClF ₂ CClF ₂	187.39
11	Trichlorofluoromethane	CCl ₃ F	100.5
113	Trichlorotrifluoroethane	CCl ₂ FCClF ₂	58.13

Table (2.1) The commonly used refrigerants in refrigeration

R	Boiling point at NBP* (c)	Freezing point (C)	Critical Temp (C)	Critical Pressure kPa
50	-161.5	-182.7	-82.5	4638
14	-127.9	-184.9	-45.7	3741
1150	-103.7	-169.0	9.3	5114
503	-88.7	-	19.5	4182
170	-88.8	-183	32.2	4891
23	-82.1	-155	25.6	4833
13	-81.4	-181	28.8	3865
744	-78.4	-56.6 ⁺	31.1	7372
13B1	-57.75	-168	67.0	3962
1270	-42.7	-185	91.8	4618
502	-45.4	-	82.2	4072
290	-42.07	-187.7	96.8	4254
22	-40.06	-160	96.0	4974
717	-33.3	-77.7	133.0	11417
500	-33.5	-159	105.5	4423
12	-29.57	-158	112.2	4113
152a	-25.0	-117	113.5	4492
600a	-11.73	-160	135.0	3645
142b	-9.8	-131	145.7	3259
600	-0.5	-138.5	198.0	4406
114	3.8	-94	214.1	3437
11	23.82	-111	137.1	4120
113	47.57	-35	152.0	3794
* At normal atmospheric pressure (101.3 kPa)				
+ At 527 kPa				

Table (2.2) Some important properties of the refrigerants

To show how the thermodynamic properties of the refrigerant can affect heat pump performance and system design, a comparison of four refrigerants is made here based on their cycles on P-h diagram. The four refrigerants chosen are;

R11 : Trichlorotrifluoromethane	(23)
R12 : Dichlorodifluoromethane	(24)
R22 : Chlorodifluoromethane	(25)
R114: Dichlorotetrafluoroethane	(26)

The references are where the application of the refrigerant are reported.

For this comparison, it is assumed that the evaporating temperature T_e is from -13°C to 27°C (260K to 300K) and condensing at $T_c=47^{\circ}\text{C}$ (320K). The suction superheat is taken as 5°C and liquid subcooling is assumed to be 20°C . All values of enthalpies and densities are taken from P-h diagrams as published by ASHREA (19). It is also assumed that the heat pump capacity is 1.2 kW (condenser output) , and the compression is isentropic. Table (2.3) shows the comparison of the four refrigerants.

From table (2.3), the evaporating pressure for R11 and R114 is seen to be low (very near to or below atmospheric pressure). This is not desirable for the reason already given. The evaporating pressures for R12 and R22 are about right, not too low. On the other hand, a low condensing pressure is also desirable. The condensing pressure of R22 is some what higher than R12. Higher condensing pressure means the condenser tube and other accessories must have the walls thick enough to withstand the pressure. This may be a set back for domestic heat pump because it may increase the cost and thus be uneconomic.

R	Condensing Pressure (MPa)	Evaporating Pressure (MPa)	Refrigerant Flow rate $\times 10^{-3} \text{ kgS}^{-1}$	Swept Volume $\times 10^{-3} \text{ m}^3 \text{ S}^{-1}$	COP
		T _c = 320 K T _e = 300 K			
R11	.23	.12	6.15	.991	21.67
R12	1.2	.7	7.79	.205	17.11
R22	1.58	1.1	6.0	.13	13.33
R114	.42	.22	8.82	.517	13.6
		T _c = 320 K T _e = 290 K			
R11	.23	.08	6.09	1.32	10.94
R12	1.2	.5	7.89	.282	12.67
R22	1.58	.8	6.06	.178	11.0
R114	.42	.15	9.23	.738	9.27
		T _c = 320 K T _e = 280 K			
R11	.23	.054	6.03	1.88	7.37
R12	1.2	.39	7.69	.366	7.8
R22	1.58	.62	5.83	.224	7.36
R114	.42	.12	9.09	1.01	7.33
		T _c = 320 K T _e = 270 K			
R11	.23	.034	5.98	2.83	6.12
R12	1.2	.26	7.5	.469	5.71
R22	1.58	.42	5.71	.317	5.68
R114	.42	.078	9.02	1.5	5.54
		T _c = 320 K T _e = 260 K			
R11	.23	.022	5.83	4.16	4.9
R12	1.2	.2	7.27	.559	4.46
R22	1.58	.31	5.5	.393	4.54
R114	.42	.04	8.82	2.205	4.0

Table (2.3) Comparison of R11, R12, R22 and R114 for heat pump application.

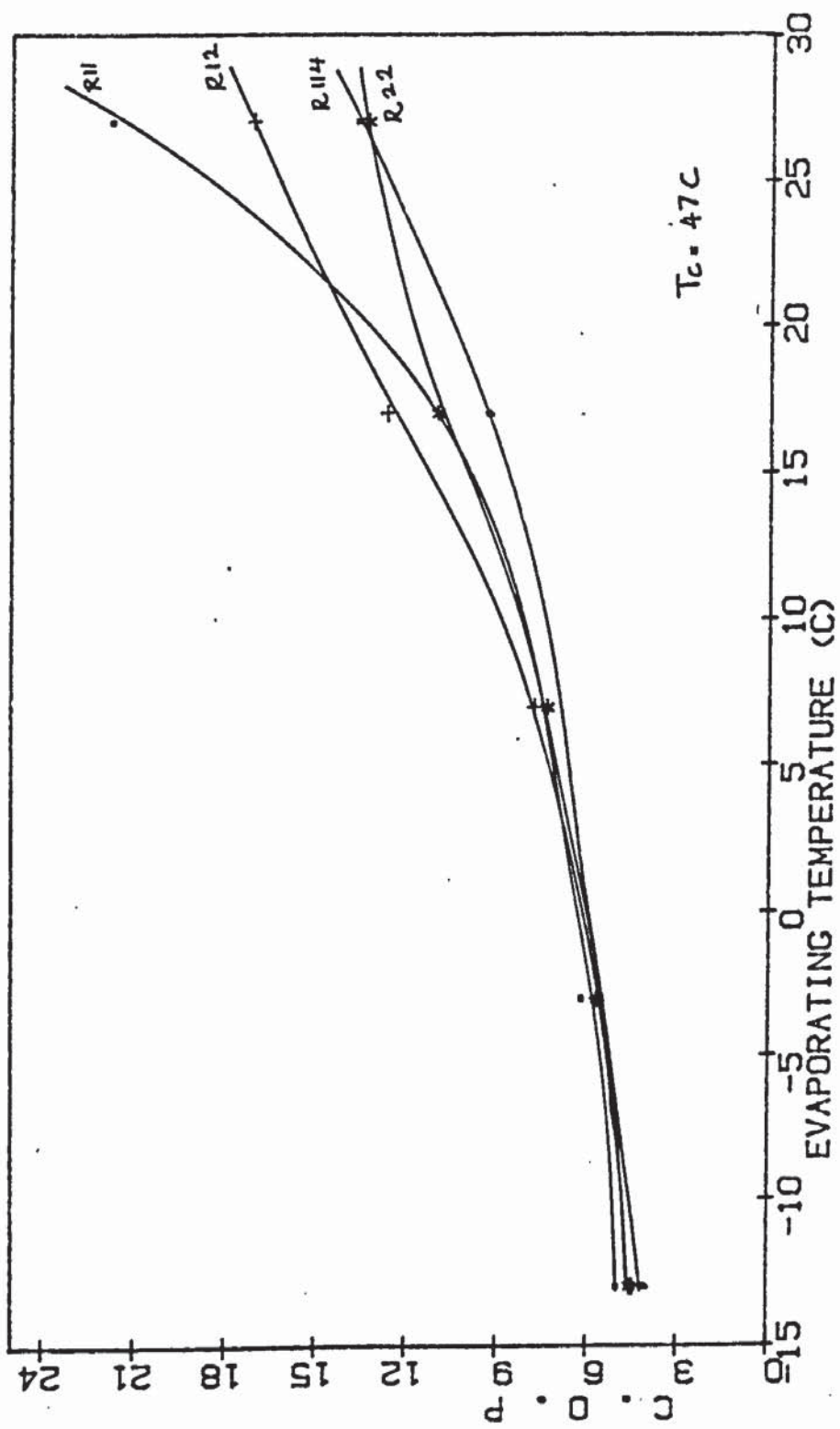


Fig (2.10) Evaporating temperature versus coefficient of performance for four refrigerants.

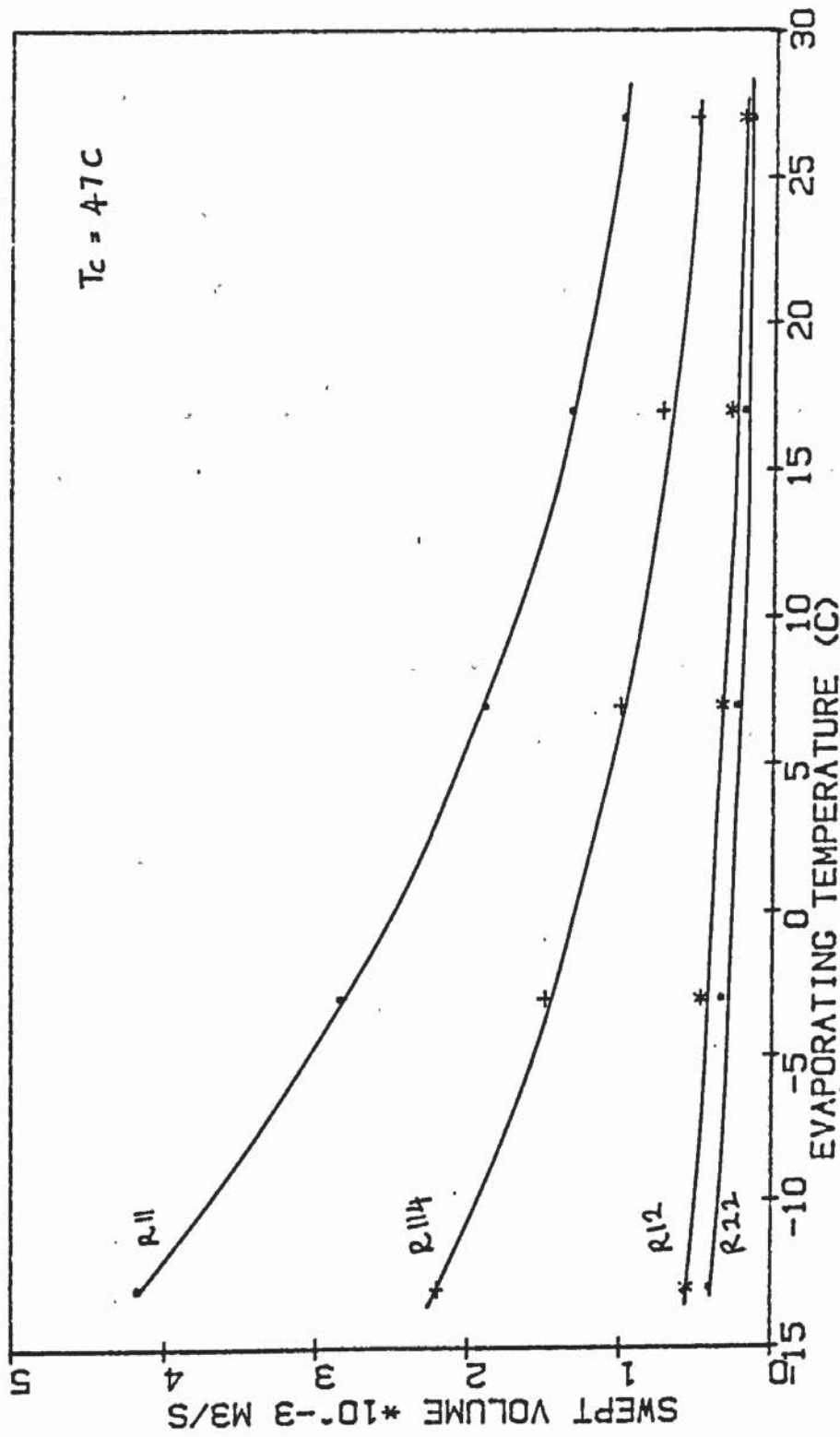


Fig (2.11) Comparison of the four refrigerant swept volumes.

Figure (2.11) and also table (2.3) show that for a heat output of 1.2kW the compressor requires higher swept volumes for R11 and R114 and in turn this means larger compressors. For domestic applications a small compressor is more attractive because of its lower cost and less space requirements.

Table (2.3) also shows R12 to give a greater COP than R22 for the operating conditions necessary for hot water production, except at $T_e = 260$ K.

Toxicity and flammability are other properties to look when choosing the refrigerant. Reference (19) shows that R12 is one of the most non-toxic and non-inflammable. The toxicity of R22 is higher than R12.

R12 is widely used in domestic refrigeration and air conditioning, so that it is easily obtainable, and at a low price.

For the above reasons, R12 appears to be the most suitable refrigerant for heat pump systems, especially for domestic application.

CHAPTER 3

AN AIR TO WATER HEAT PUMP

A small air-water heat pump with a heat output in the region of 1.2 kW was built in the laboratory. The schematic diagram of the unit is shown in figure (3.1). Four basic components of the unit are compressor, condenser, evaporator and expansion valve. Other accessories are the ^{sight} glass, filter drier, and condenser's water flow regulator and fan.

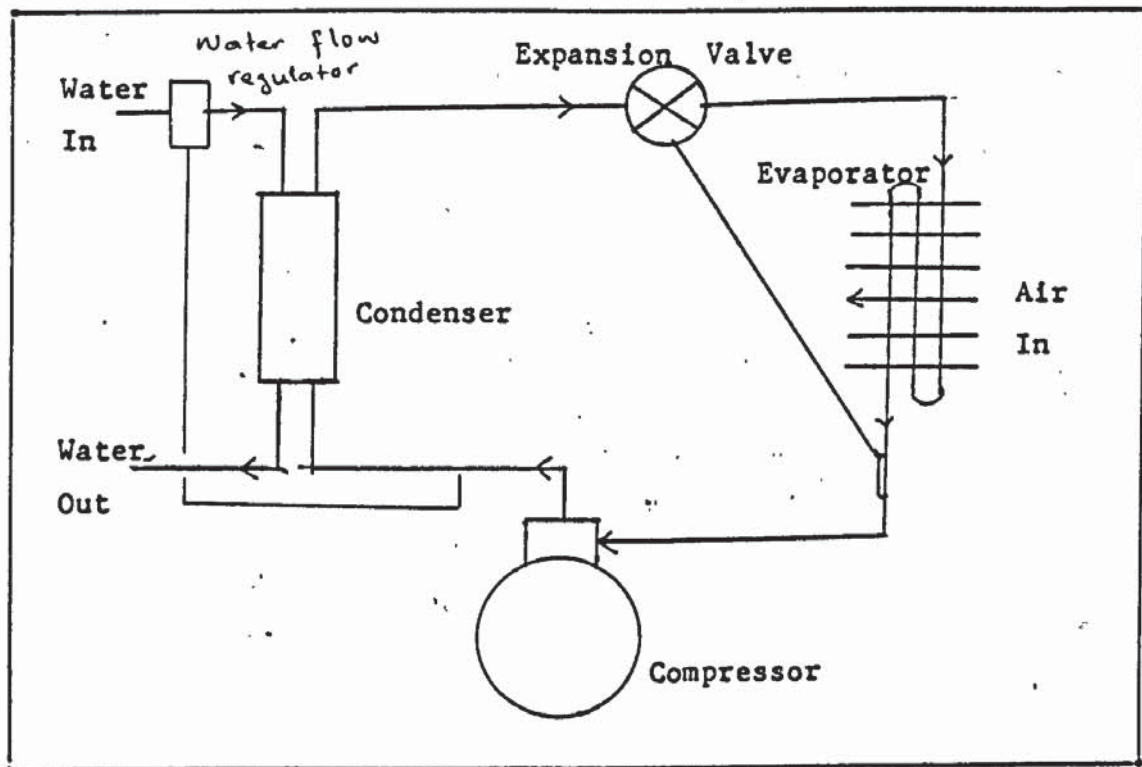


Fig (3.1) An air - water heat pump system showing the basic components.

3.1 Compressor

A compressor is a machine which is capable of increasing pressure and density of a working fluid. In a heat pump, the function of the compressor is to remove the refrigerant vapour from the evaporator, and raise the temperature and pressure to a state where condensation of the

vapour will produce useable heat. A reciprocating compressor was used in the present heat pump system.

3.1.1 The Danfoss SC10H

This reciprocating compressor is designed for small heat pump systems, mainly for heating of tap water for domestic use. It is of a hermetic type, i.e. the motor and compressor combination are hermetically sealed in one casing. The motor is a single-phase ac motor in which the input voltage range is from 198V to 255V at 50Hz. The motor size is 250W and the starting current is 10A. The stroke volume is 10.3 cm^3 and the total weight 12.1 kg without the electrical equipment. The refrigerant recommended for this compressor is R12.

Figure (3.2) shows the variation of input power to the compressor with the condensing and evaporating temperatures, as given by the manufacturer. Clearly there are two factors determining the input power to the compressor. First is the compression ratio, the ratio of the discharge pressure to the suction pressure. A higher compression ratio means that more work is required. The second factor is the density of the refrigerant vapour. When the density is increased, the mass of the refrigerant induced into the compressor is increased, and more work is required.

3.1.2 Reciprocating Compressors

Figure (3.3) shows a P-V diagram for a reciprocating vapour compressor.

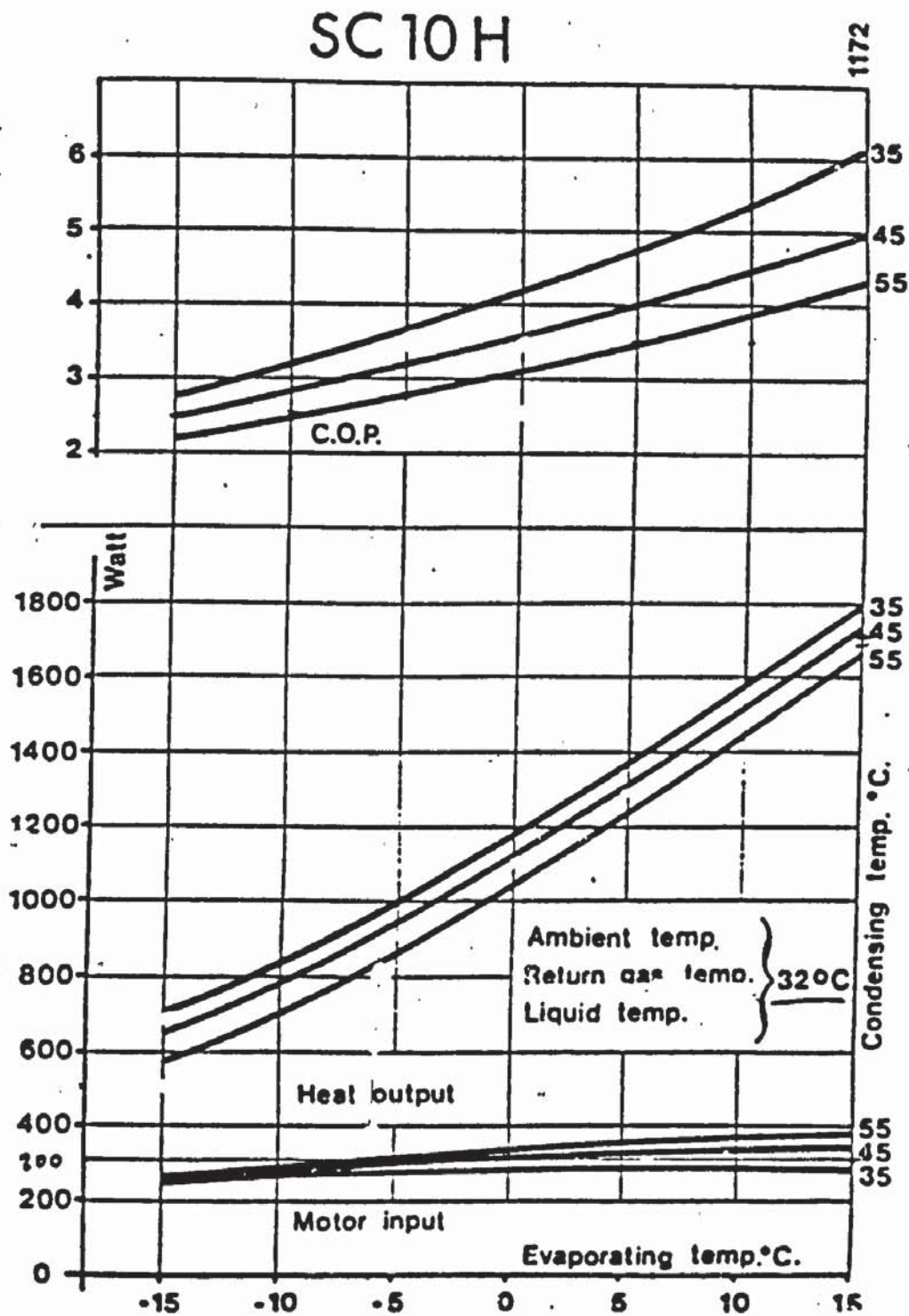


Fig (3.2) The compressor, Danfoss SC10H characteristics .

The clearance volume is the space between the valve plate and the top of the piston when the piston is at the top of its stroke . Practically this clearance space is very important in avoiding the piston striking and so damaging the valve. Normally the clearance volume varies from 4 to 10 % of the stroke volume (27).

The cycle of the reciprocating compressor consists of the following processes:

1. 3-4 : Piston moving down the cylinder and causing the expansion of the clearance vapour.
2. 4-1 : The inlet valve opens when clearance vapour pressure is equal to P_1 , and vapour is drawn in until the end of the suction stroke at 1. (V_1-V_4) is the volume of vapour drawn in.
3. 1-2 : Immediately after the piston starts on its return stroke , the vapour pressure inside the cylinder begin to rise and closes the inlet valve. Further movement of the piston will increase the pressure, density and temperature. At point 2, the pressure of the vapour has reached the delivery pressure, and further movement of the piston will open the outlet valve.
4. 2-3 : The vapour escapes into the discharge pipe until the end of the stroke is reached at 3.

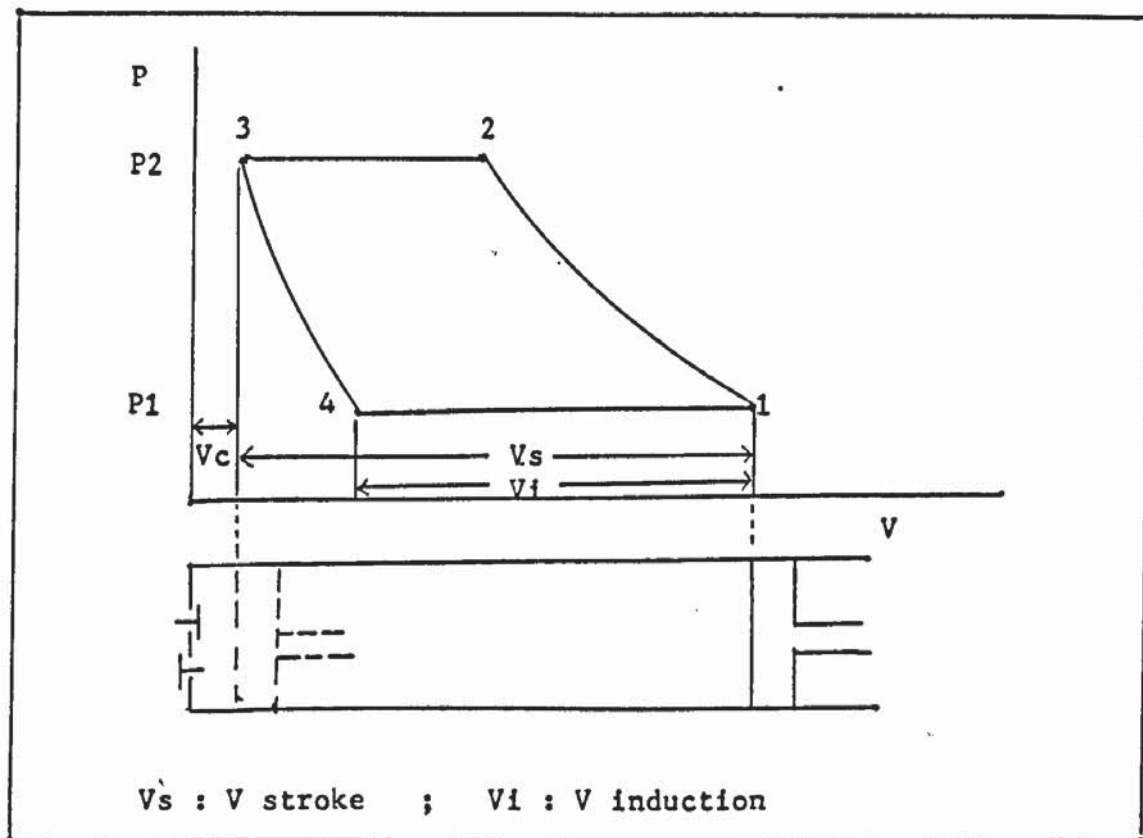


Fig (3.3) The P-V diagram of a reciprocating compressor

Process 1-2 is the compression of vapour from P_1 to P_2 according to the law of $PV^n = C$ (P :pressure , V : volume , C :constant) . The value of index n determines the type of compression . For $n=1$, the compression is isothermal , and for $n=\gamma$ ($\gamma = C_p/C_v$) it is an isentropic compression. The compression is known as polytropic when $n \neq 1$ and $n \neq \gamma$, and n is then called a polytropic index.

From figure (3.3) , the work W_r required to drive the reciprocating compressor is the area enclosed by the curve 1234 . In terms of pressure P , volume V and polytropic index n , the work done per cycle is,

$$W_r = \left(\frac{n}{n-1} \right) P_1 V_1 \left(1 - \frac{V_4}{V_1} \right) \left(\left(\frac{P_2}{P_1} \right)^{(n-1)/n} - 1 \right) \quad (3.1)$$

If V_c is the clearance volume , $V_c = V_3$, and using the relation $P_3 V_3^n = P_4 V_4^n$, equation (3.1) can now be expressed as ,

$$W_r = \left(\frac{n}{n-1} \right) P_1 V_1 \left(1 - \frac{V_c}{V_1} \left(\frac{P_2}{P_1} \right)^{1/n} \right) \left(\left(\frac{P_2}{P_1} \right)^{(n-1)/n} - 1 \right) \quad (3.2)$$

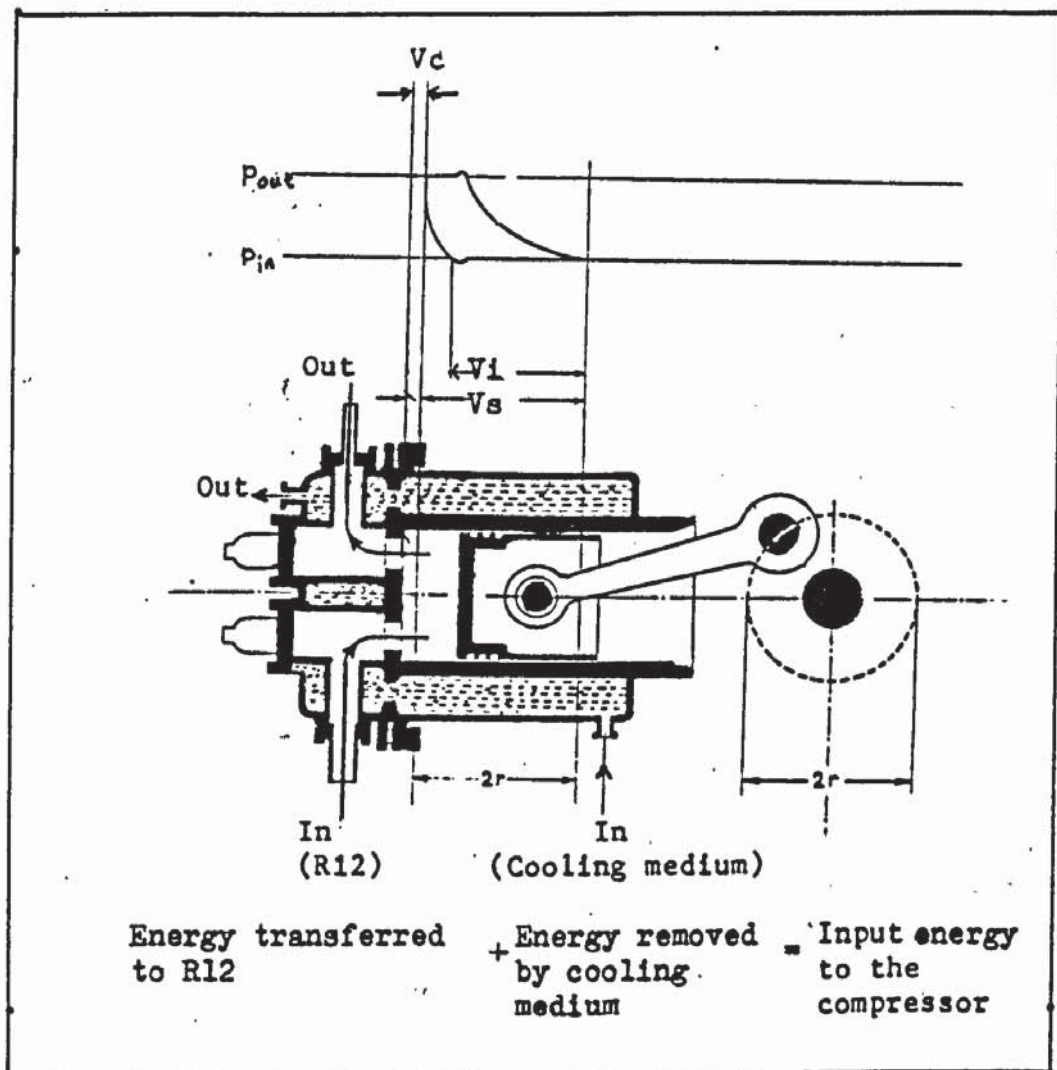


Fig (3.3 a) A schematic diagram of reciprocating compressor.

The work done W_r can also be expressed in terms of temperature by using the ideal gas law $pV = mR T$. m is the mass of freon discharged per cycle, R is the gas constant and T is temperature (appendix K).

$$W_r = \left(\frac{n}{n-1} \right) m R T_1 \left(\left(\frac{P_2}{P_1} \right)^{(n-1)/n} - 1 \right) \quad (3.3)$$

3.1.3 Compressor Efficiency

The work needed for the compression as expressed in equation (3.2) and (3.3) is called polytropic work. Isentropic work is for the ideal compression with $n = \gamma$. The ratio of the isentropic to the polytropic work is the isentropic efficiency, η_i . The actual work required to drive the compressor is greater than the polytropic work due to friction. Another efficiency known as mechanical efficiency η_m , is defined as the ratio of the polytropic work to the electrical input work for an electrically driven compressor. The overall isentropic efficiency, η_o , that is the ratio of the isentropic work to the electrical input work

$$\eta_o = \eta_i \eta_m \quad (3.4)$$

Another efficiency of the compressor arises as a result of the effect of clearance volume. This efficiency, known as volumetric efficiency η_v , is defined as the ratio of the volume of gas induced into the compressor to the stroke volume. Referring to figure (3.2),

$$\eta_v = \frac{(V_1 - V_4)}{(V_1 - V_3)} \quad (3.5)$$

Since the stroke volume $V_s = (V_1 - V_3)$ and the clearance volume is $V_c = V_3$, equation (3.5) can be expressed

$$\eta_v = 1 - \left(\frac{V_c}{V_s} \right) \left(\left(\frac{P_2}{P_1} \right)^{1/n} - 1 \right) \quad (3.6)$$

3.1.4 Compressor Cooling

In the interests of its working life, the manufacturer's recommendation

is that the compressor must not run in a system where the condensing temperature is higher than 60C and at the same time it must be cooled (28). The manufacturer suggests that the refrigerant itself (preferably in the state of saturated liquid) could be used as a cooling medium. In the system under investigation, the hot water (condenser outlet) is used as the cooling medium so that the final hot water temperature can be higher than the condensing temperature.

3.2 Condenser

The condenser is the component where the superheated refrigerant vapour is cooled, and then liquefied. In doing so heat is rejected and carried away by the cooling fluid, such as water. Normally the condenser is known by the cooling fluid, for example air cooled or water cooled. An air cooled condenser is usually a finned coil over which air is blown and the refrigerant is condensed inside the tube. The well known water cooled condensers are shell and tube, and concentric tube. In the system under investigation a simpler type of water cooled condenser, tube side by side is used.

3.2.1 Tube Side By Side Condenser

This condenser consists of two copper tubes joined together side by side by soldering material. One carries the water coolant and the other the refrigerant. This type of condenser is chosen because the temperature profile along the condenser tube can be more easily obtained. The condenser is 15 m in length with the tube carrying the refrigerant having an inside diameter of 0.004 m and the water tube with an inside diameter of 0.006 m.

Figure (3.4) shows the cross section of the condenser. The R12 and

water are flowing in opposite directions, and the condenser is more precisely known as a counter flow tube side by side condenser .

An accumulator , a copper tube of 2.5 cm in diameter and 25 cm in length is introduced into the condenser 12 m from the point where the refrigerant enters the condenser . The main purpose of putting the accumulator is to prevent liquid refrigerant flowing back into the compressor . Secondly , it is hoped to have a clear division between the subcooling and the condensing regions of the condenser.

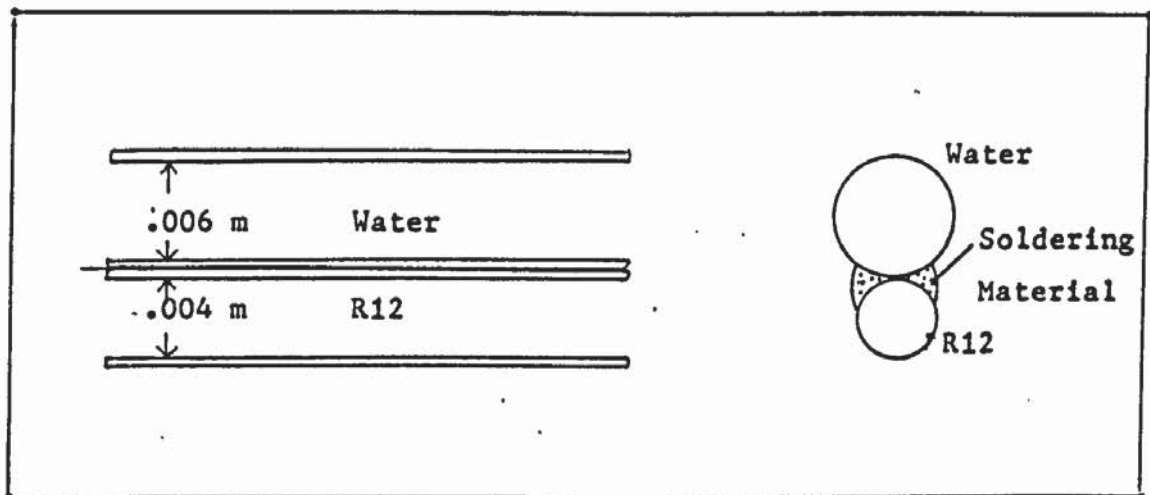
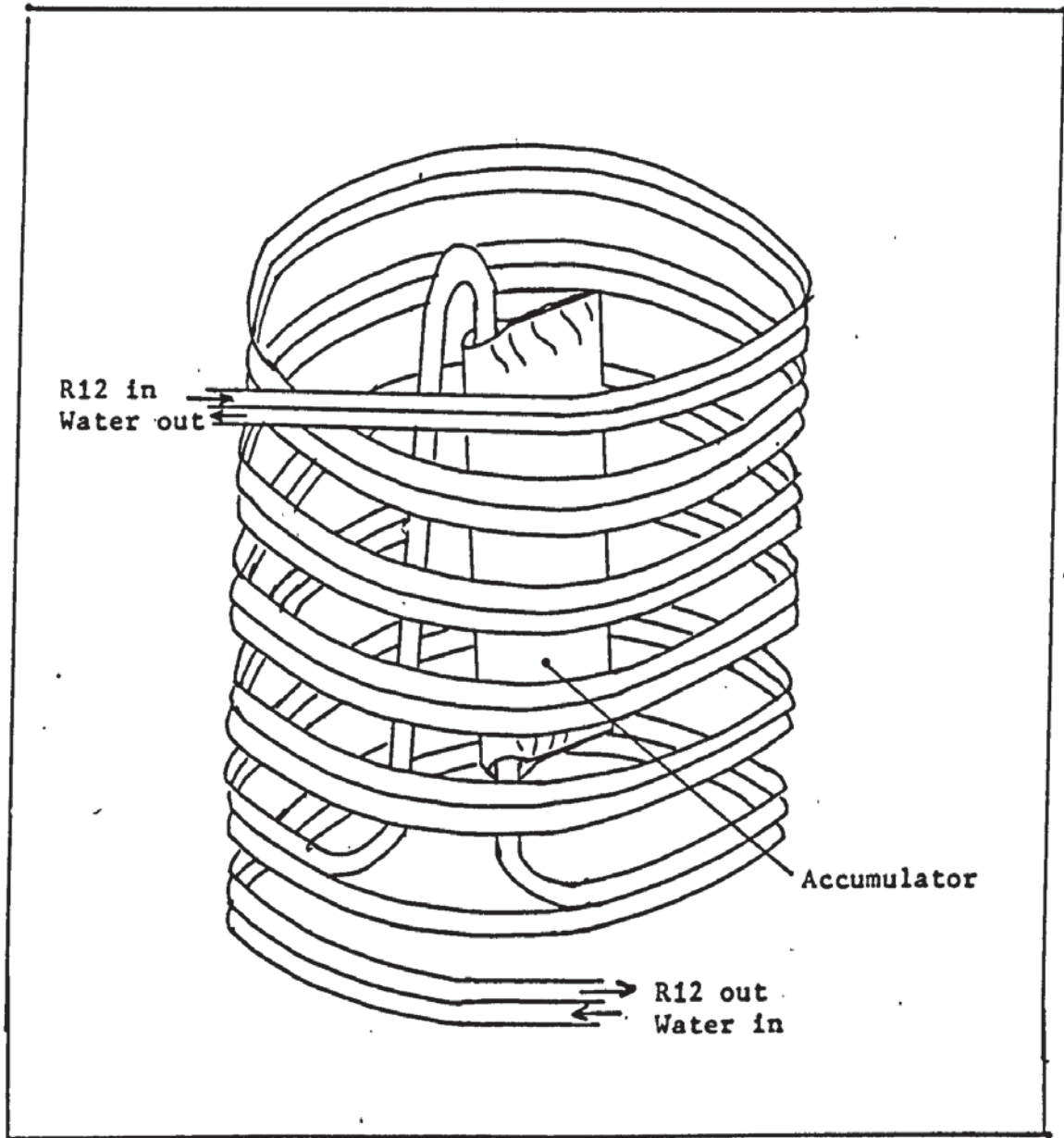


Fig (3.4) A cross section of the condenser .

3.2.2 Thermal Analysis Of The Condenser

For the purpose of thermal analysis , the condenser can be divide into three sections , desuperheating , condensing and liquid subcooling . In the desuperheating region , the superheated refrigerant vapour is cooled until it reaches its dew temperature ; the temperature below which condensation will take place. The overall heat transfer is from vapour to water. In the condensation region, the heat transfer is from a mixture of vapour and liquid refrigerant to water, and in the subcool region it is from liquid refrigerant to water.



Fig(3.4 a) The condenser.

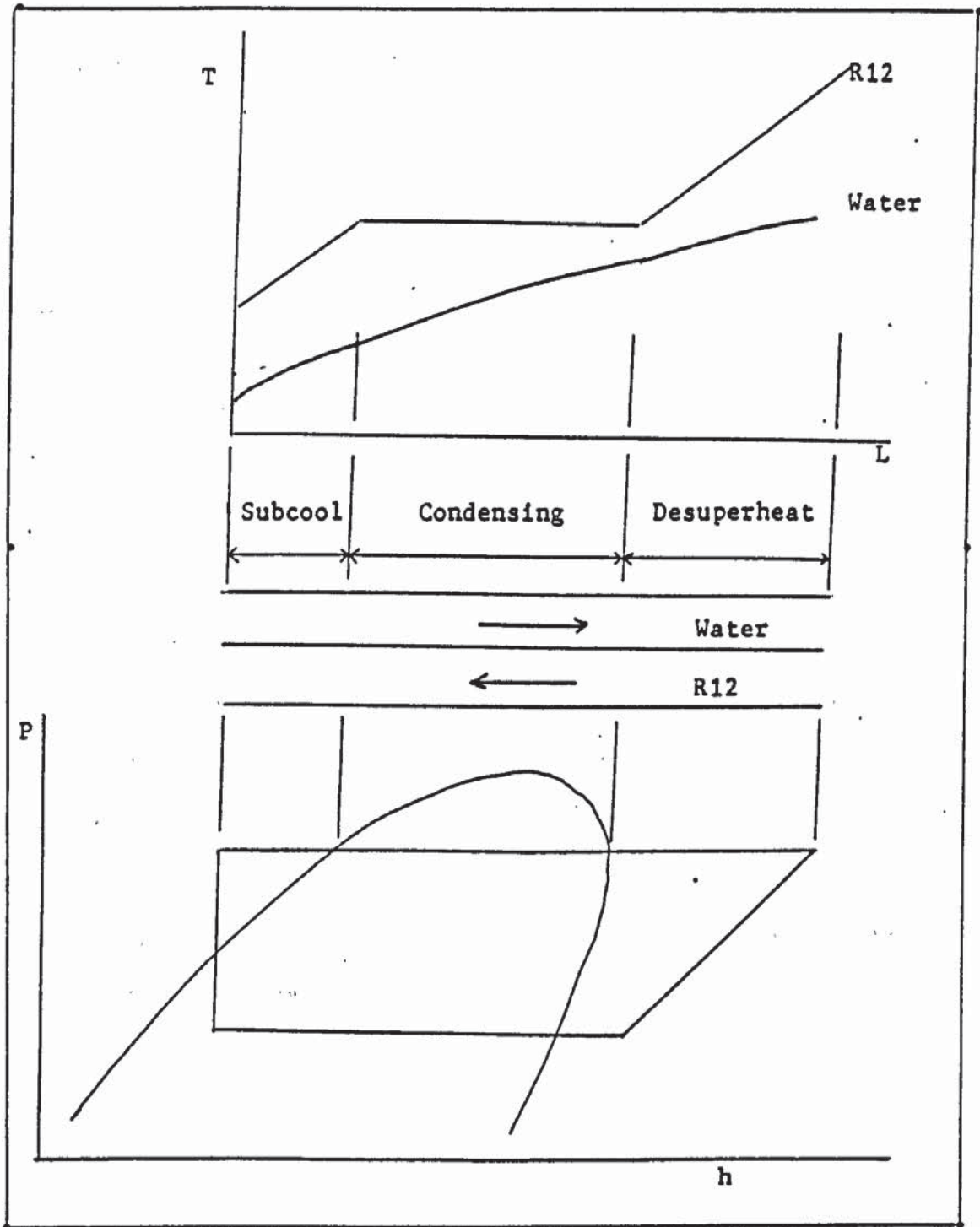


Fig (3-5) The variation of R12 and water temperature in the condenser .

In the thermal analysis of the condenser , there are six important parameters involved .

1. Prandtl Number : Pr
2. Reynolds Number : Ry
3. Nusselt Number : Nu
4. Heat transfer coefficient : Hc
5. Friction Factor and Pressure Drop : F , ΔP
6. Effectiveness : ε

1. Prandtl Number ; Pr (dimensionless)

The Prandtl number is a function of fluid properties and is defined as the ratio of the kinematic viscosity of the fluid to the thermal diffusivity of the fluid ,that is

$$Pr = \frac{\nu}{\alpha} = \frac{C_p \mu}{k} \quad (3.7)$$

2. Reynolds Number ; Ry (dimensionless)

The flow of fluid in tubes can be divided into two groups ; turbulent and laminar flows . In laminar flow fluid molecules move very smoothly parallel to each other along the tube, while in turbulent flow , the motion of fluid molecules is random . The type of fluid flow is characterized by a dimensionless parameter known as the Reynolds number and is defined as

$$Ry = \frac{V D}{\nu} = \frac{G D}{\mu} \quad (3.8)$$

3. Nusselt Number ; Nu (dimensionless)

The Nusselt number for flow inside tubes is defined as

$$Nu = \frac{Hc D}{k} \quad (3.9)$$

It has been shown (29) that Nu is a function of Reynolds and Prandtl numbers, $Nu = f(Ry, Pr)$. For turbulent flow of gas (30)

$$Nu = .023 \left(1 + \left(\frac{D}{L}\right)^{.8}\right) Re^{.8} Pr^{.3} \quad (3.10)$$

The term $(1 + (D/L)^{.8})$ is a correction due to the ratio of tube diameter to its length . For laminar flow (liquid) (31) ,

flow (liquid) (31) ,

$$Nu = 3.66 + \frac{.066 (D/L) Ry Pr}{1 + .04 ((D/L) Ry Pr)^{2/3}} \quad (3.11)$$

4. Heat Transfer Coefficient ; Hc

The heat transfer coefficient Hc is defined (29) as the constant of proportionality relating the heat transfer per unit time and unit area to the overall temperature difference . From figure (3.6) , if the heat is transferred from 1 to 2 and q is the heat energy at 2,

$$\dot{q} = Hc A (T1-T2) \quad (3.12)$$

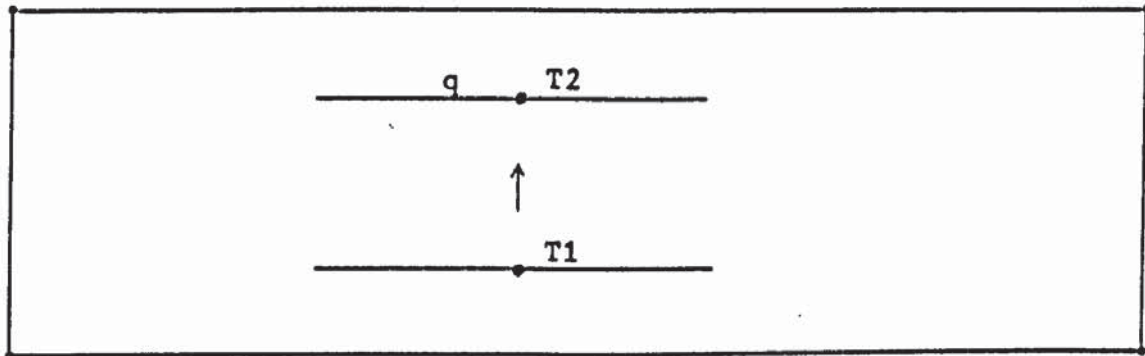


Fig (3.6) Heat is transferred from T1 to T2

From equation (3.9) , the heat transfer coefficient ,Hc can also be expressed in terms of Nusselt number, ^{thermal} conductivity and tube diameter,

$$Hc = \frac{Nu k}{D} \quad (3.13)$$

5. Friction Factor And Pressure Drop

The friction factor ,F arises due to the friction between the moving fluid with the inside surface of the tube . For turbulent flow of gas inside tube (30)

$$F = \frac{1}{((1.581 \log Ry - 3.28)^2 \left(\frac{\mu_B}{\mu_T}\right)^{.24})} \quad (3.14)$$

For fluid flow inside the tubes, the friction factor depends on Reynolds number and the ratio of fluid viscosity (bulk) with viscosity at wall temperature. The flow is taken as turbulent when $Ry > 7100$ and laminar when $Ry < 2100$. For Ry between 2100 and 7100, the flow is transitional between turbulent and laminar. The equations below are taken from (30).

1. $Ry < 2100$

$$F = \frac{16}{Ry} \quad (3.15)$$

2. $Ry > 7100, \mu_m > 1$ ($\mu_m = \frac{\mu_B}{\mu_T}$)

$$F = \frac{0.167 (7 - \mu_m)}{((1.581 \log Ry - 3.28)^2 \mu_m^{0.24})} \quad (3.16)$$

3. $Ry > 7100, \mu_m < 1$

F as in equation (3.14)

4. $2100 < Ry < 7100$

$$F = \frac{((7100 - Ry) F_1 + (Ry - 2100) F_2)}{5000} \quad (3.16a)$$

where F_1 : from equation (3.15)

F_2 : from equation (3.14) or (3.16) as $\mu_m < \text{or} > 1$

The pressure drop in the condenser results from core friction, flow acceleration and inlet and exit effects. The biggest contribution is from core friction, and inlet and exit effect can be neglected (30).

The pressure drop can be simplified to (32),

$$\Delta P = \frac{2 G^2 F L}{D} \quad (3.17)$$

6: Effectiveness ; ϵ

The effectiveness is the ratio of the actual heat transfer in the exchanger to the maximum which is thermodynamically possible for the prescribed inlet temperatures and flow rates (32). In other words, it is the ratio of the heat gain by water to the heat loss by the refrigerant.

$$\epsilon = \frac{\dot{M}_w C_{pw} (T_{w,o} - T_{w,i})}{\dot{M}_r C_{pr} (T_{r,i} - T_{r,o})} \quad (3.18)$$

The subscripts are w for water; r for refrigerant; i for inlet and o for outlet. The term $\dot{M} C_p$ is called the capacity rate, C. The capacity rate ratio is the ratio of minimum capacity rate to the maximum capacity rate. The effectiveness of a counter flow heat exchanger (condenser) can also be expressed as ,

$$\varepsilon = \frac{1 - \exp\left(-\left(\frac{Hc A}{C_{\min}}\right) + \left(\frac{Hc A}{C_{\max}}\right)\right)}{1 - \left(\frac{C_{\min}}{C_{\max}}\right) \exp\left(-\left(\frac{Hc A}{C_{\min}}\right) + \left(\frac{Hc A}{C_{\max}}\right)\right)} \quad (3.19)$$

3.3 Evaporator

The other heat exchanger incorporated in the heat pump system is called the evaporator; the component where refrigerant absorbs heat from the heat source and evaporates. The evaporator is designed, as with the other heat exchangers, to not only maximise heat transfer but also to suit the application. i.e with volume, weight and cost considered. For domestic application , a small, light, cheap and efficient heat exchanger is desired. This type of the heat exchanger is known as the compact heat exchanger .

3.3.1 An Air Source Compact Evaporator

The evaporator used in the present heat pump system was salvaged from an air conditioning unit manufactured by Versa Temp, model Vm220 . It is a wavy continuous fin type, with circular refrigerant tubes in staggered positions. Blundell (33) has made a comparison of several continuous fin evaporators and found that the wavy continuous fin has the lowest temperature difference between the air and refrigerant for a given operating condition.

The geometry of the evaporator is as follow.

Size	: .61 x .205 x .065 m
Depth	: 3 rows (.065 m)
Frontal(pace) area	: .125 m ²
Volume	: .00813 m ³
Freon tube outside diameter	: .01 m
Freon tube inside diameter	: .008 m
Freon side surface area	: .322 m ²
Freon tube length	: 7.32 m (2 parallel tubes)
Air side surface area	: 9.66 m ²
Fin area	: 8.12 m ²
Fin spacing	: .002 m
Fin metal thickness	: .0002 m
Freon tube spacing	: .025 m
Free flow area	: .055 m
Heat transfer area(air side)	: 9.66 m ²
Hydraulic radius	: 0.002 m

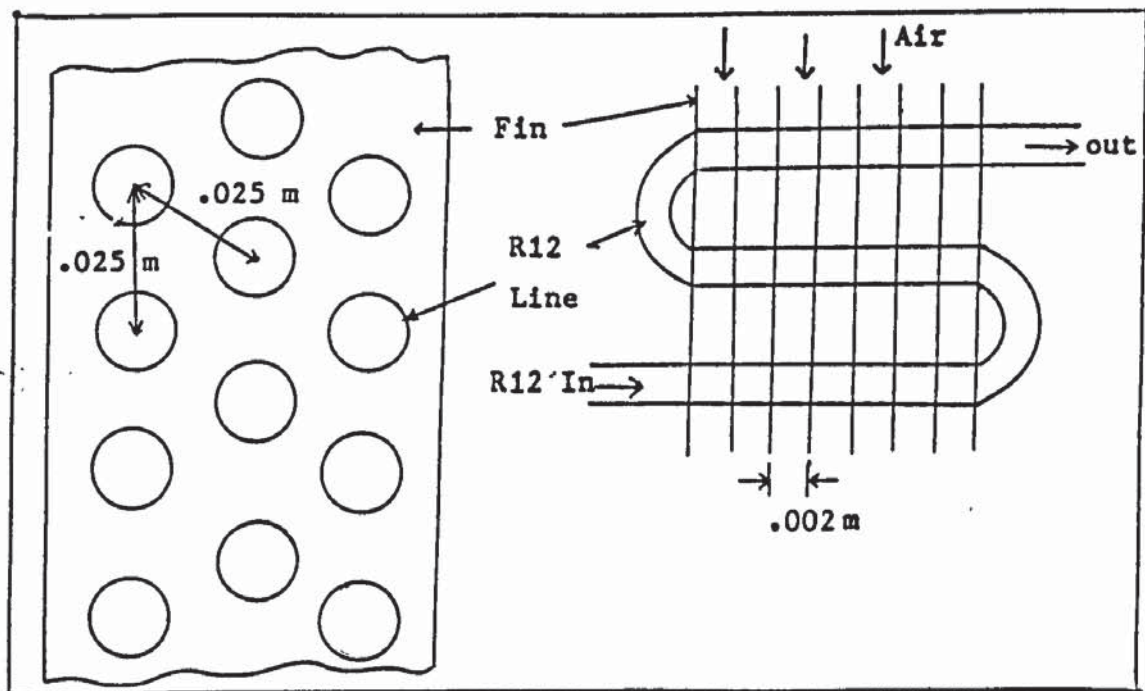


Fig (3.7) The cross section of the evaporator .

3.3.2 Thermal Analysis Of The Evaporator

The overall heat transfer coefficient for the evaporator can be expressed in terms of the outside air coefficient, inside (the tube) refrigerant film coefficient and fouling factors (34).

$$\frac{1}{H_c} = \frac{1}{E_o h_a} + R_c + \frac{A}{A_r h_r} + R_t \quad (3.20)$$

For the evaporator used, R_c is zero because the bond between the fin and tube is provided by galvanising . The inside fouling resistance R_t can also be neglected by assuming there is no corrosion inside the tube. The air heat transfer coefficient h_a is determined from (33) ,

$$h_a = F_s G_a C_{pa} \left(1 - \frac{0.72}{N}\right) \quad (3.21)$$

where N is the number of rows of freon tubes, which is 3 for the evaporator used. F_s is known as Stanton correlation and given by,

$$F_s = \frac{F_c'}{Pr^{2/3}} \quad (3.22)$$

F_c' in the above equation is called Colburn correlation ,

$$F_c' = (10.8 Ry^{.294})^{-1} \quad (3.23)$$

Both equations (3.22) and (3.23) were taken from (33).

E_o in equation (3.20) is called the overall air side surface effectiveness , which is given by ,

$$E_o = 1 - \left(\frac{A_f}{A}\right) (1 - \eta_f) \quad (3.24)$$

where η_f is the fin efficiency which is given by (33)

$$\eta_f = \frac{\tanh ml}{ml} \quad (3.25)$$

and
$$m = \sqrt{\frac{2 h_a}{k_f t}} \quad (3.26)$$

The refrigerant heat transfer coefficient h_r in equation (3.20) is

extremely difficult to calculate . This is because of the geometry of the evaporator makes it very difficult to estimate some of the required parameters, for example, R_y , Pr . Since hr is always ^{much} greater than ha (see (33)), for rough estimation of H_c , hr can be neglected.

One way of calculating hr will be described here. This method is by using the Dangler and Addom (43) equation , which is

$$hr = 3.5 \left(\frac{1}{X_t} \right)^{0.5} H_1 \quad (3.27)$$

where H_1 is a predicted heat transfer coefficient assuming the total flow is liquid, and is given by,

$$H_1 = 0.023 \left(\frac{k_L}{D} \right) (D G \left(\frac{1-X}{\mu_L} \right)^{0.8} \left(\frac{C_p \mu}{k} \right)_L \quad (3.28)$$

The X_t is the Lockhart and Martinelli parameter, where

$$\frac{1}{X_t} = \left(\frac{X}{(1-X)^{0.9}} \right) \left(\frac{f_L}{f_V} \right)^{0.5} \left(\frac{\mu_V}{\mu_L} \right)^{0.1} \quad (3.29)$$

The evaporator overall heat transfer coefficient, H_c , can now be calculated using equation (3.20) which is simplified to,

$$\frac{1}{H_c} = \frac{1}{E_o ha} + \frac{A}{Ar hr} \quad (3.30)$$

Using the Number Of Transfer Unit (NTU) method, the evaporator effectiveness is given by the equation below (32).

$$\xi_v = 1 - \exp \left(- \frac{H_c A}{C_a} + \frac{H_c A}{C_f} \right) \quad (3.31)$$

The effectiveness as defined on page 40 can also be expressed as

$$\eta_v = \frac{C_a (T_a(i) - T_a(o))}{C_{min} (T_a(i) - T_e)} \quad (3.31a)$$

The NTU method is a heat transfer technique for calculating the effectiveness of heat exchangers in terms of a dimensionless quantity, $NTU = \frac{H_c A}{C}$ (see (30)).

3.4 Expansion Valve

Two main functions of the expansion valve in the heat pump system are to reduce the liquid refrigerant pressure and temperature, and to regulate its flow to the compressor. The temperature of the refrigerant on entering the evaporator must be lower than the ambient temperature to enable heat to flow from the surroundings to the refrigerant. If too much refrigerant is passed by the expansion valve, it may not be completely evaporated in the evaporator, and as a result liquid refrigerant may be admitted into the compressor. If too little refrigerant is in the evaporator, heat absorbed is reduced, and so too the performance.

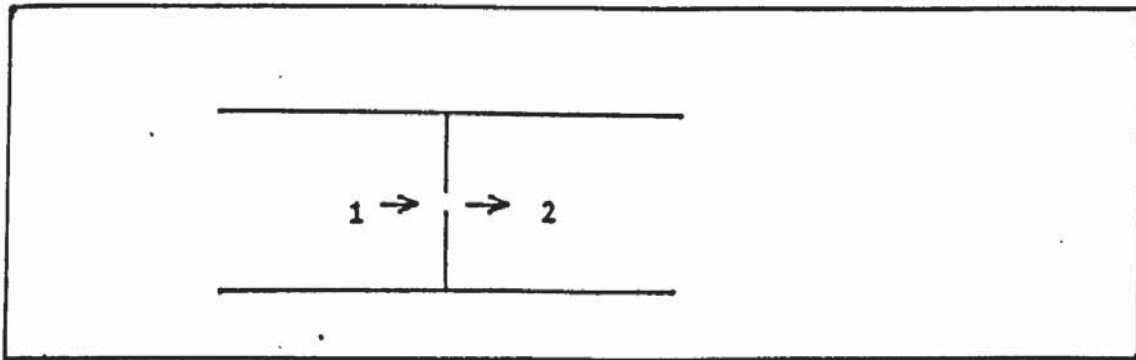


Fig (3.8) The throttling valve. Pressure and temperature at 1 is higher than at 2.

In figure (3.8) the steady flow equation from 1 to 2 (35) is given by,

$$Q-W = \dot{M} \left((h_2-h_1) + \frac{(C_2^2 - C_1^2)}{2} \right) \quad (3.32)$$

Since the area of the valve (or hole in figure (3.8)) is small and the device is thermally insulated, there is no energy loss by heat transfer so that $Q=0$. Further more no external work is done , therefore $W=0$.The change in kinetic energy is small (35), and so $C_2^2 - C_1^2 =0$. Equation (3.32) is now reduced to ,

$$h_2 = h_1 \quad (3.33)$$

That is the enthalpy before and after the expansion is the same. Practically when entering the expansion valve the refrigerant is in the liquid state, but after the expansion, it is in the two phase state. The process of expansion is an irreversible one. Though no heat is lost the expansion is not isentropic, in fact a small increase in entropy occurs.

3.4.1 Thermostatic Expansion Valve

In the heat pump system under study, a thermostatic expansion valve, manufactured by Danfoss (DF2) is used. A sketch of the valve is shown in figure (3.9). The feeler bulb is partially filled with liquid of the same type as the one used in the heat pump system; and is called the power fluid. The power fluid exerts pressure on top of the diaphragm. The pressure is opposed by the evaporating pressure from beneath the diaphragm. The pressure from the power fluid is always higher than the evaporating pressure because the feeler bulb is attached at the tube connecting the evaporator to the compressor. The difference in these two pressures determines the size of the opening of the valve, and so the refrigerant mass flow rate and the suction superheat. The valve setting can also be adjusted manually.

From figure (3.9) it can be seen that the inlet pressure (i.e. the condensing pressure) can also affect the freon mass flow rate. When pressure drop across the expansion valve (condensing pressure minus evaporating pressure) is large, the freon mass flow rate is higher.

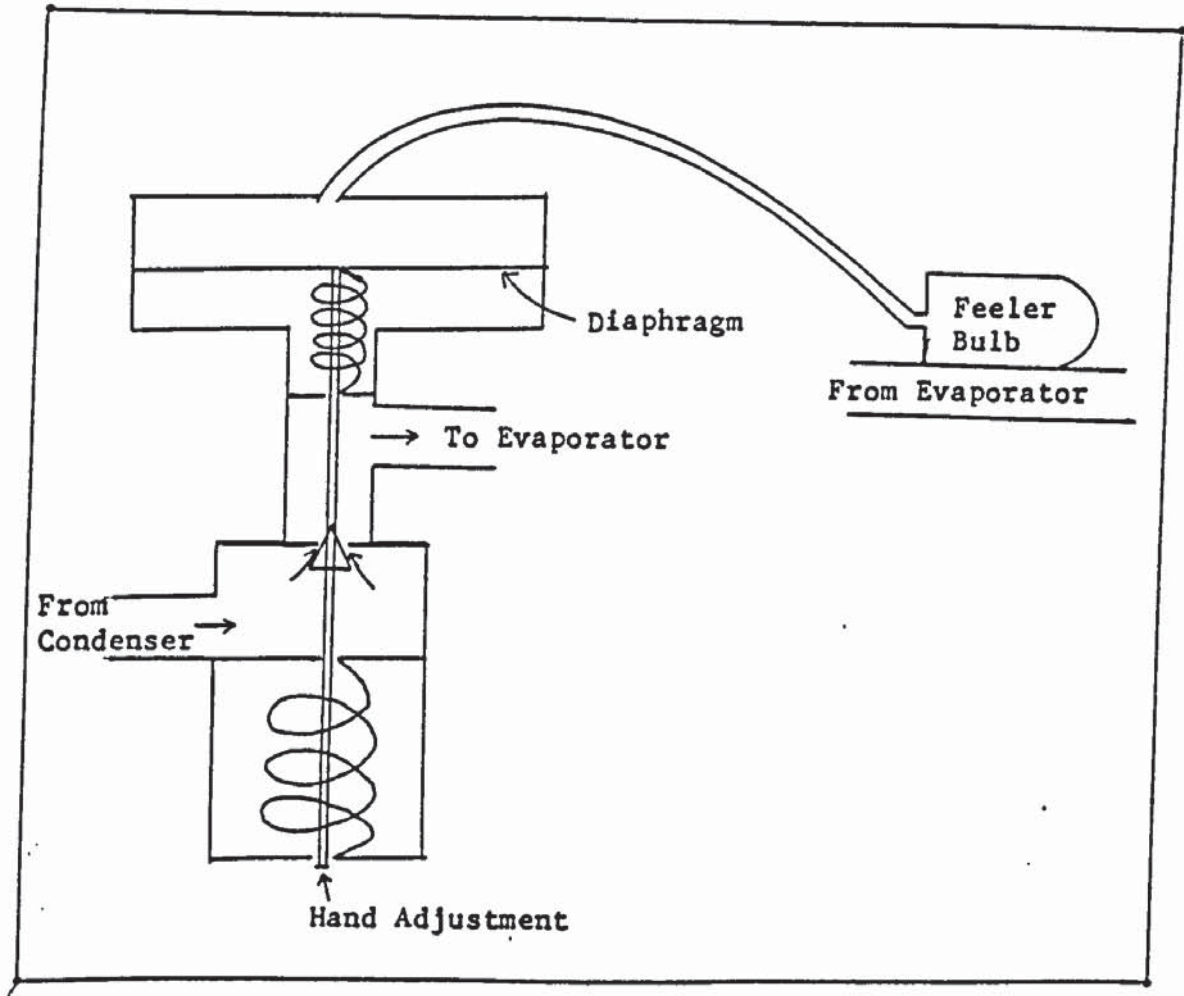


Fig (3.9) A schematic diagram of a thermostatic expansion valve.

3.5 Other Components

3.5.1 Fan

The main purpose of using the fan is to ensure efficient operation by increasing air circulation rates through the evaporator . Also it is used to ^{reduce} the frost formation on the evaporator . In this system a double centrifugal (backward curved blades) fan is used . The fan is taken from the Versa Temp air-water heat pump unit . The maximum air flow rate obtainable is $.16 \text{ m}^3 \text{ s}^{-1}$ with a power consumption of about 60W. In the experiments the air flow rate is changed by controlling the fan

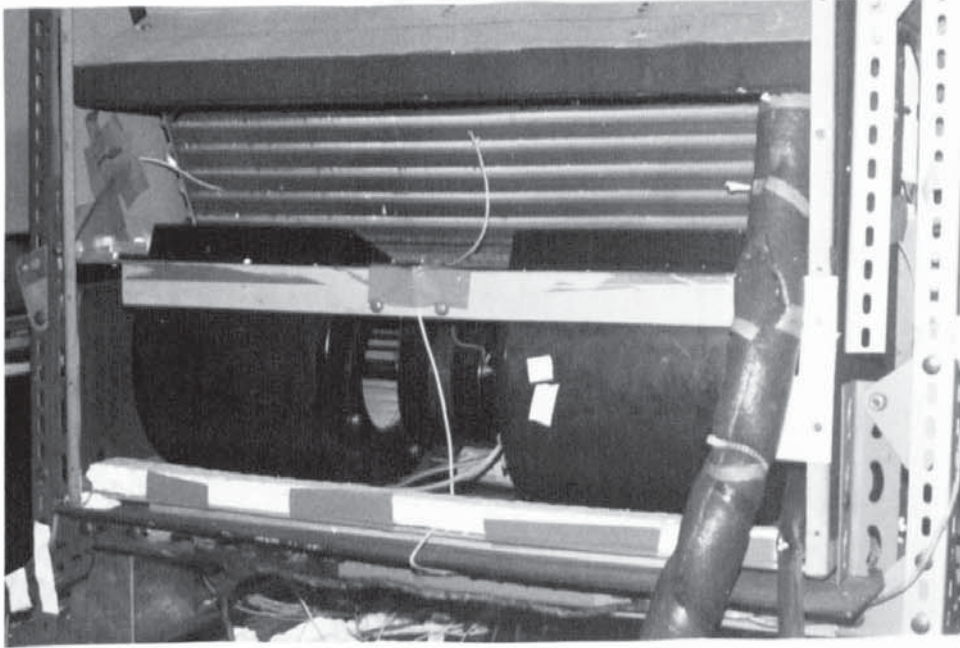


Photo (3.1) The position of the fan in the heat pump system .

input power using a variac . The minimum air flow rate across the evaporator is about $.04 \text{ m}^3 \text{ s}^{-1}$.

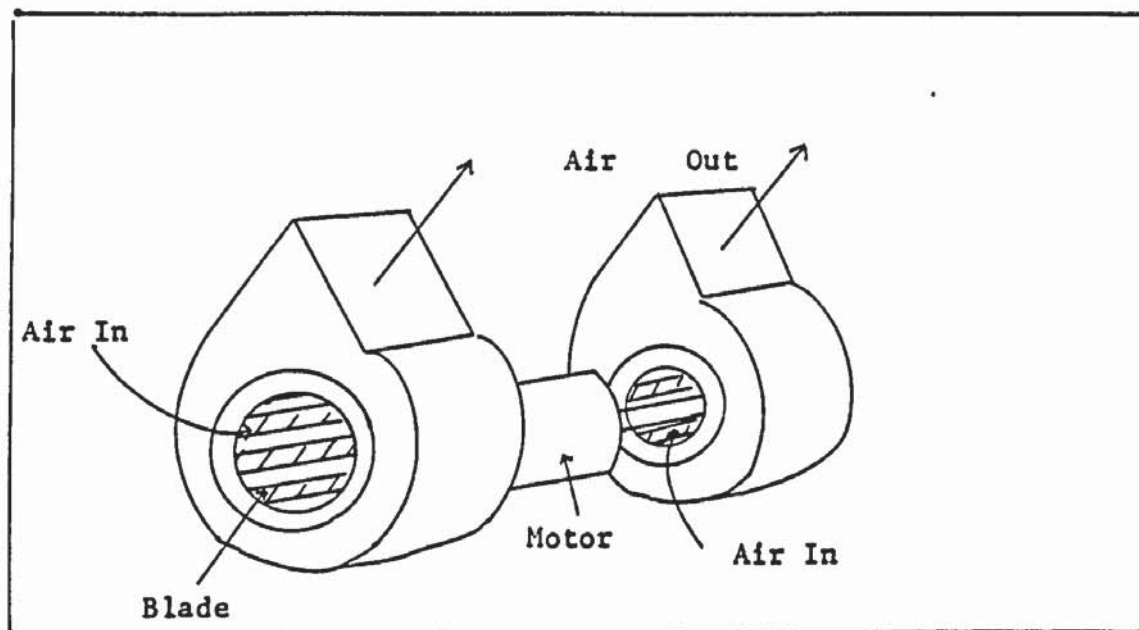


Fig (3.10) The fan.

3.5.2 Condenser Water Flow Regulator

The water flow regulator or valve is fitted in the water line just before the water enters the condenser. A capillary tube (inside diameter is 1 mm) connects the valve to the discharge line outside the condenser and about 20 cm from the compressor . The valve can be adjusted manually to control the water flow rate , and so the water outlet temperature . Changing the water flow rate , will change the condensing temperature and pressure . If anything happens in the heat pump system that changes the condensing pressure and temperature , the valve will automatically adjust the water flow to maintain the set condensing pressure.

The valve used here is Danfoss WAFX, which has a pressure range of 3.5 to 16 bar. A schematic diagram is shown in figure (3.11).

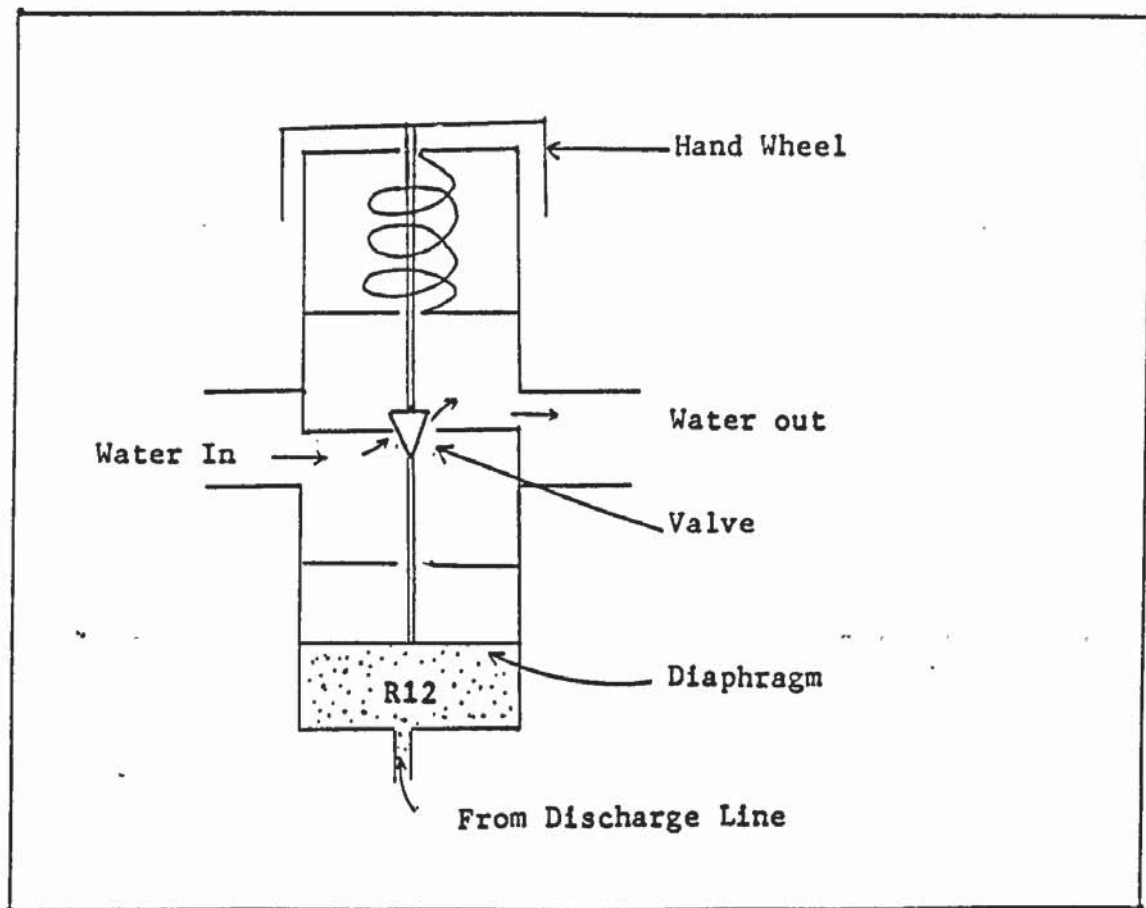


Fig (3.11) The condenser water flow regulator .

3.5.3 Filter Drier

Small particles of dirt and moisture which enter the system during construction can cause restriction to the liquid flow , particularly at the expansion valve where the opening is small . If operating at low evaporating temperature (below 0C) water moisture might freeze and block the expansion valve . The filter drier consists of a very fine filter to trap small particles of dirt , followed by a drying agent , usually silica gel . It is fitted before the expansion valve . The drier used is the Danfoss DC 032.

3.5.4 Sight Glass

This instrument with glass at one side, gives the facility of looking into the refrigerant line. It is fitted at the liquid section, that is between the drier and the expansion valve. It has a colour indicator to indicate the presence of water in the refrigerant.

The presence of vapour bubbles appearing in the sight glass indicates a fault in the system. Causes can be blockage in the drier or liquid line, or not enough refrigerant in the system, or a system leak.

3.5.5 The Air Heater

An air heater is needed in order to increase the air inlet temperature to the evaporator in the laboratory. It is made from a tin box of dimensions 0.75x0.5x0.15 m with four heating bars. Each bar can withstand current of 3 A. The maximum capability of this air heater is to heat the air temperature by 30 degree C.

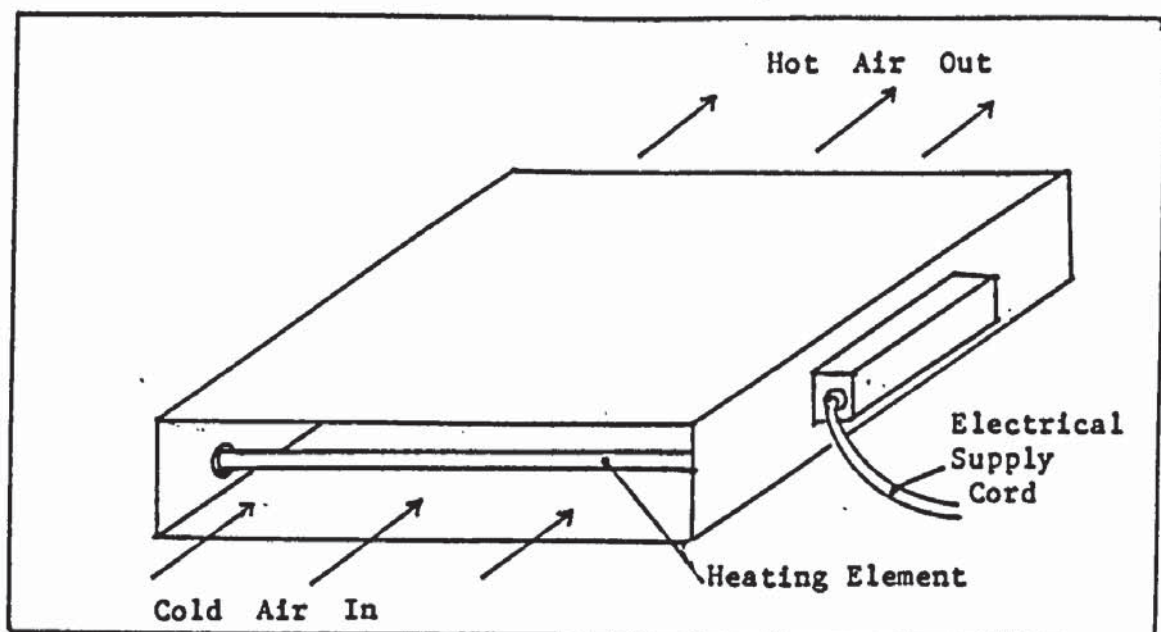


Fig (3.12) The air heater.

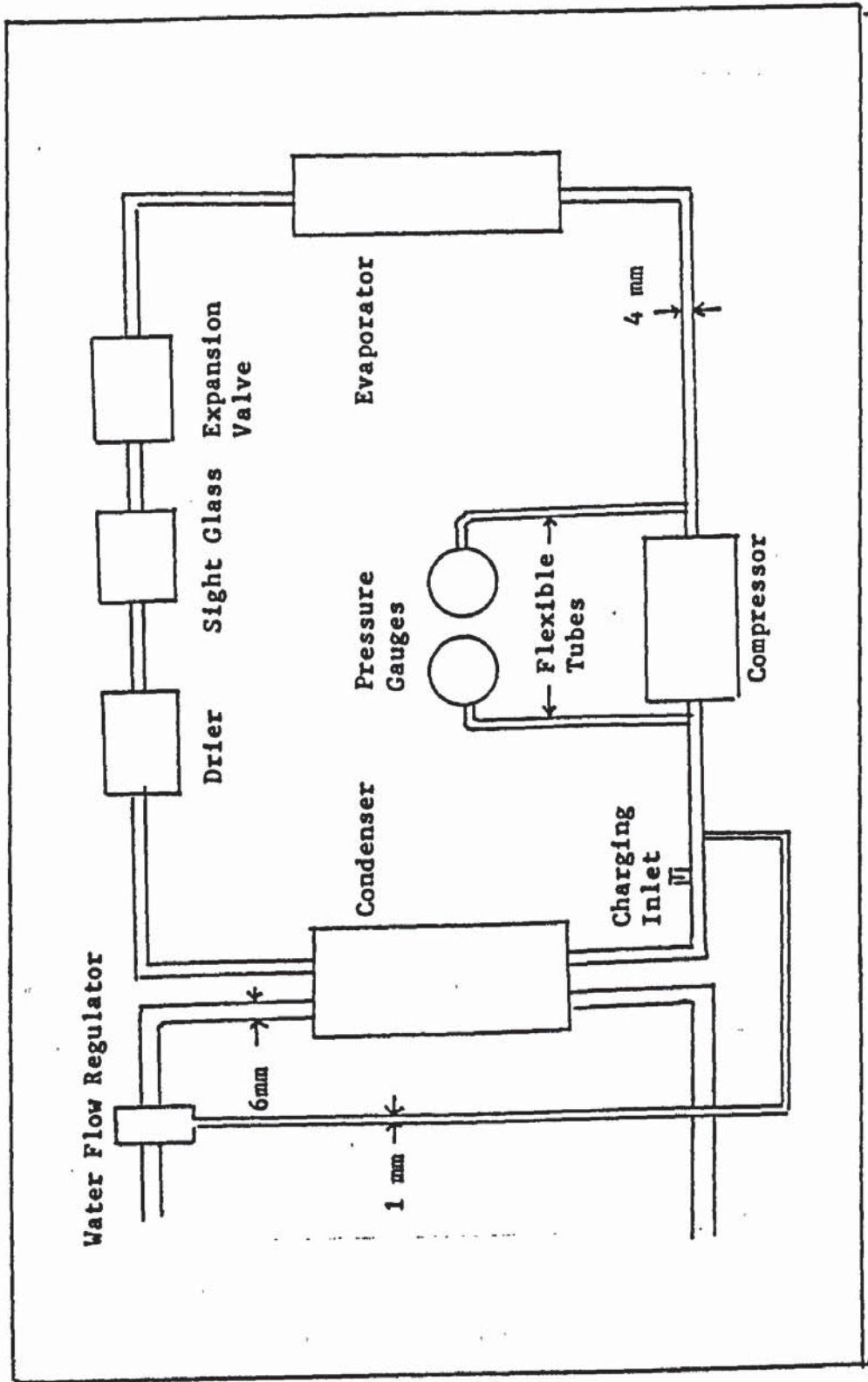


Fig (3.13) A block diagram of an air to water heat pump showing the internal diameters of pipes used.

3.6 The Construction

All components of the heat pump system are connected between each other by copper tube. The copper tube is chosen because of its strength, high resistance to corrosion and cost.

Pipes must be large enough to avoid excessive pressure drops and small enough to ensure adequate refrigerant flow velocity. Figure (3.13) shows the size of pipes used in the present system.

In the refrigerant circuit the compressor inlet and outlet terminals were soldered to the system, while the sight glass, drier and the expansion valve were flare fitted. In the water circuit the condenser water flow regulator was connected to the condenser through reinforced nylon tubing.

There are six compression fitted crosses in the refrigerant line and four compression fitted T-connectors in the condenser water line. They are used as access points for measurement of the refrigerant temperatures and pressures and the water temperatures.

The system was first evacuated to remove the air and water vapour before the refrigerant, R12 was admitted. The R12 was then let into the system through the charging inlet valve (figure (3.13)). The system was then switched on. Bubbles present in the sight glass indicated that there was insufficient R12 in the system. It should be noted that the amount of R12 circulated in the system varies according to the

operating condition. Therefore the sight glass should always be checked to ensure there is enough R12 in the system for the particular circumstances.

Bubbles in the sight glass could also indicate leaks . The area in which there was a leak was located using a halogen gas detector. This detector gave a high tune sound when R12 was detected. Soap solution was then used to pin point the leak.

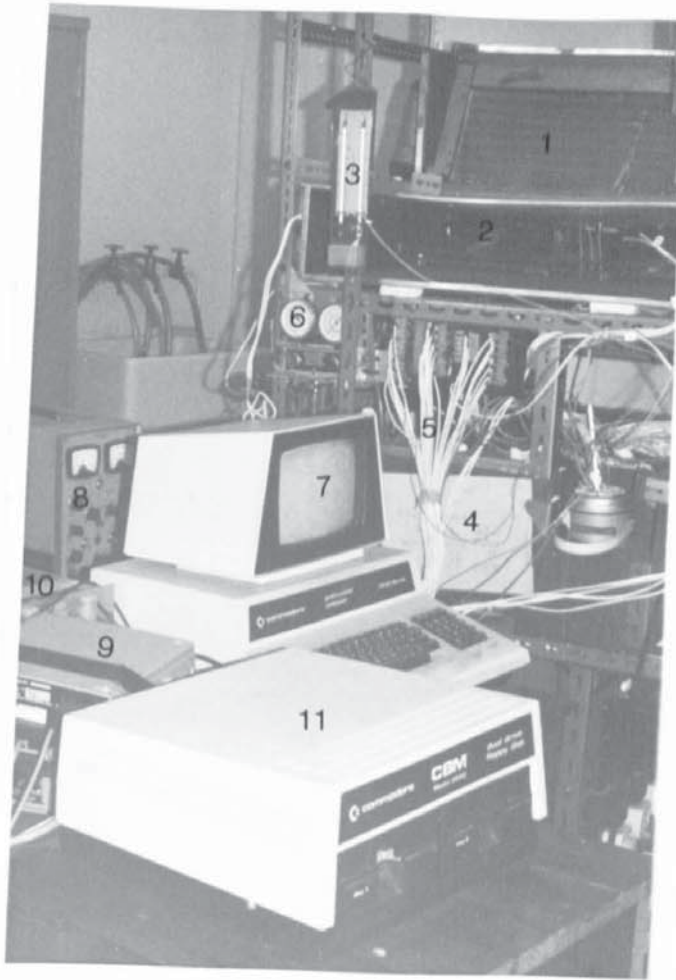


Photo (3.2) The heat pump and digital data acquisition system

1. Evaporator
2. Air heater
3. Wet and dry bulb thermometers.
4. Insulated box containing the compressor and condenser.
5. Cables connecting the transducers to the amplifiers.
6. Pressure gauge
7. Computer
8. Power supply
9. Analogue to digital converter
10. Amplifier
11. Disk drive

THE DIGITAL DATA ACQUISITION SYSTEM

In the experimental work, the digital data acquisition system is used to measure and record signals obtained from transducers, such as strain gauges for pressures measurement, and thermocouples. It is very helpful, because in this way, the calibrations and correction factors for the various parameters can be stored on file and used in online or offline computations. Major advantages include speed, continuous operation and acquisition of large quantities of data to improve the statistical interpretation of performance.

The essential functional operations within the digital data acquisition system include making the measurement, handling analogue signals, converting and handling digital data, and programming and control. Figure (4.1) shows the block diagram of the system elements whose functions are listed below.

1. Support System : Circuitry for the operation of transducers
e.g. excitation power supply.
2. Transducer : Translates physical parameters to electrical signals, ac or dc.
3. Signal Conditioning : Adjusts the transducer output signal (voltage) to a form acceptable by the analogue to digital converter. e.g. amplifier for amplifying low level voltage.
4. Analogue To Digital (ATD) Converter : Converts the analogue

voltage to its equivalent digital form. /

5. System Control : Microcomputer for system programming functions and digital data processing.

6. Digital Recorder: For programs and data storage. e.g. on magnetic disk.

7. Additional Accessories : Printer and graph plotter, for printing out and plotting of the results.

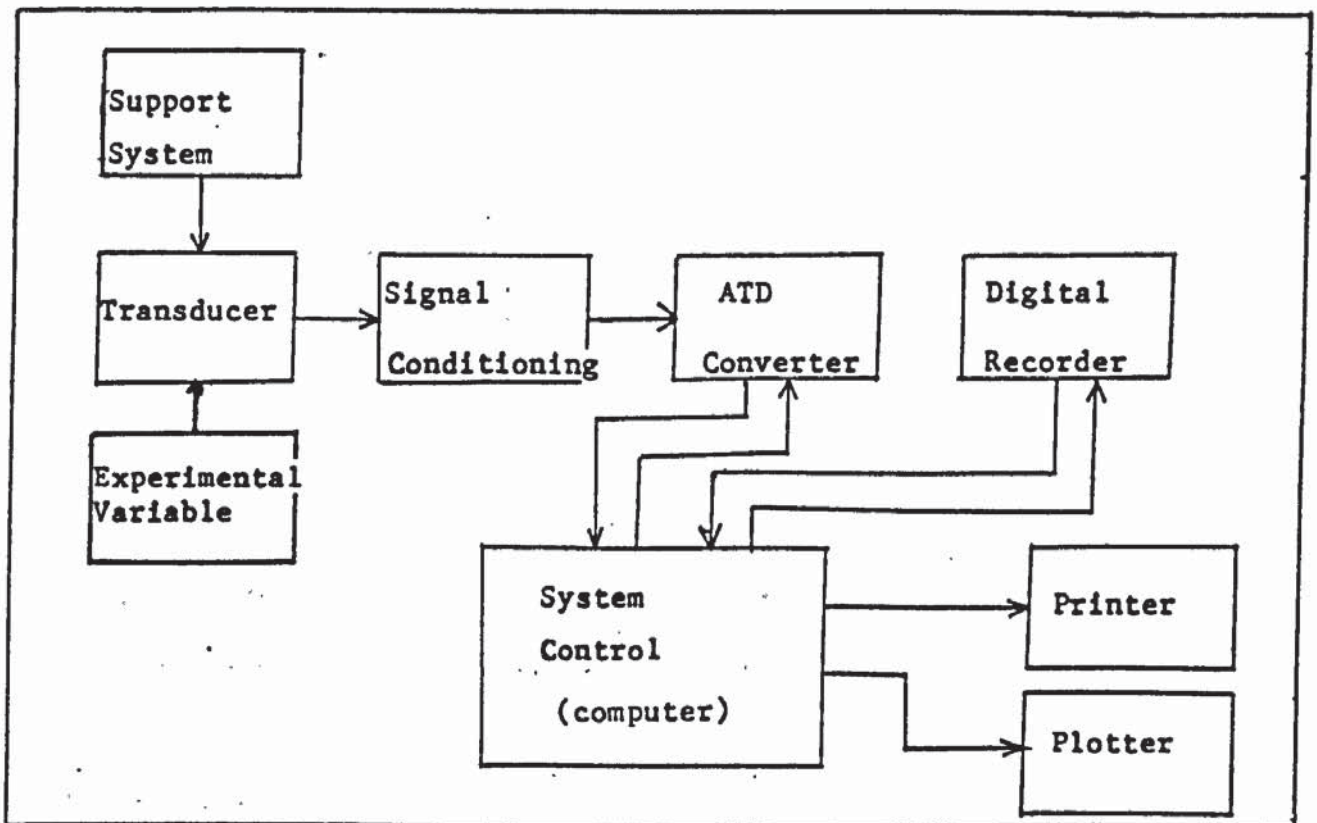


Fig (4.1) The digital data acquisition system.

4.1 The Microcomputer

The heart of this data acquisition system is a microcomputer manufactured by Commodore Business Machine (CBM) series 3032, and widely known as PET (Personal Electronic Transactor). Basically the microcomputer can be divided into 4 elements as listed below.

1. Central Processing Unit (CPU) : It is the most important part of the computer where all calculations and management of the whole system are done.
2. Read Only Memory (ROM) : It is used to store a special program that determines the characteristics of the computer. Interruption of the power supply will not alter the ROM. One of the facilities available is a computer clock.
3. Random Access Memory (RAM) : The RAM is a temporary memory and it is used for data and , or program storage.
4. An Expandable Input-Output Bus : It is a connection, path or circuit for input-output of data and peripheral equipment.

The peripheral equipment used in this data acquisition system is a floppy disk drive (IBM model 3040) for storage of programs and data files on magnetic disk. Also available are printer and graph plotter.

4.2 Analogue To Digital Converter (ATD)

The basis of the ATD converter is a comparator circuit, which is a high gain differential amplifier. The comparator compares an unknown input voltage with a reference voltage and indicates which of the two voltages is larger. For instance, if the input signal is higher than the reference, the output voltage is maximum, and the comparator is said to be 'on'. If the input voltage is lower than the reference, the comparator output is minimum, and the comparator is 'off'. The

comparator is said to act as a binary device . Figure (4.2) shows how the analogue input can be resolved in four equal steps depending on the 'on' or 'off' state of the comparator. The table alongside the diagram shows how the output can be expressed in the binary form.

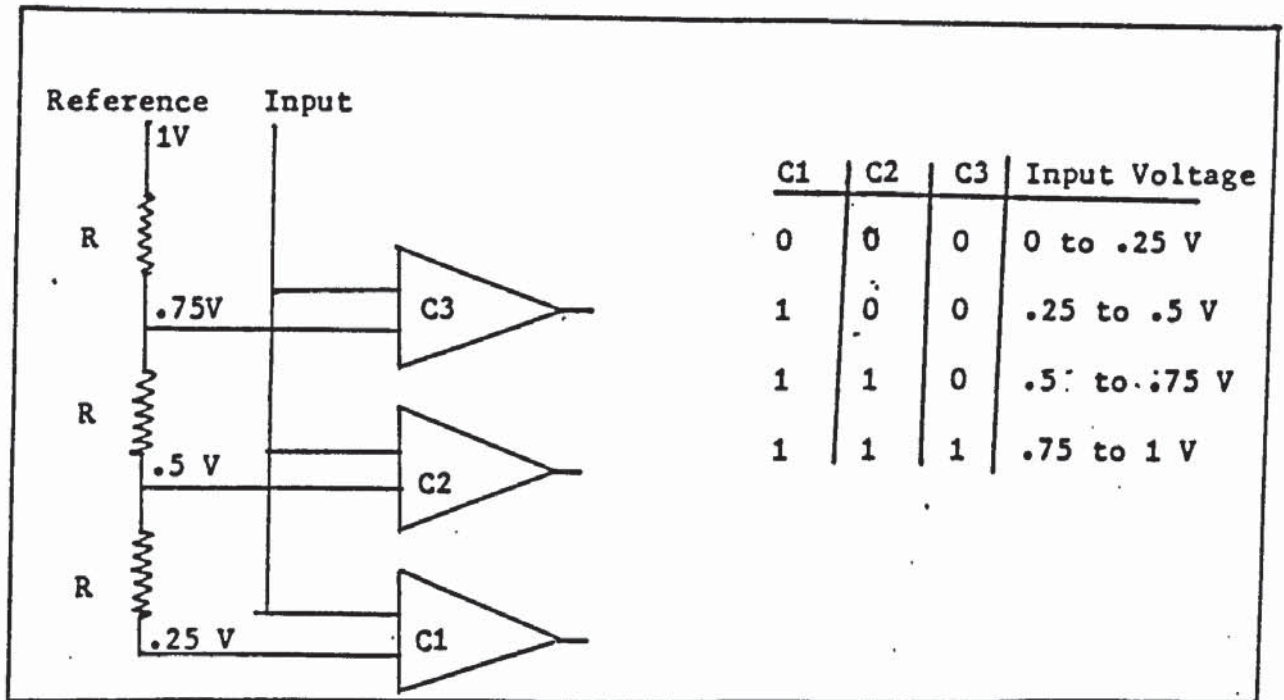


Fig (4.2) An analogue to digital converter.

Of course, for a higher accuracy a large number of comparators are needed. The latest converter uses a single integrated circuit as the comparator .The one used in this experimental work is manufactured by CIL Microsystem Ltd., model PCI 1000.The ATD is a 12 bit device with 16 channels and the analogue input range is 0 - 1 volt . The binary output range is 0 to 4095 bits. The accuracy is ± 1 bit or $\pm .25$ mV .

4.3 Instrumentation Operational Amplifier

Thermocouples do not produce output voltages high enough to permit them to be fed directly to the ATD; therefore the voltages must be amplified.

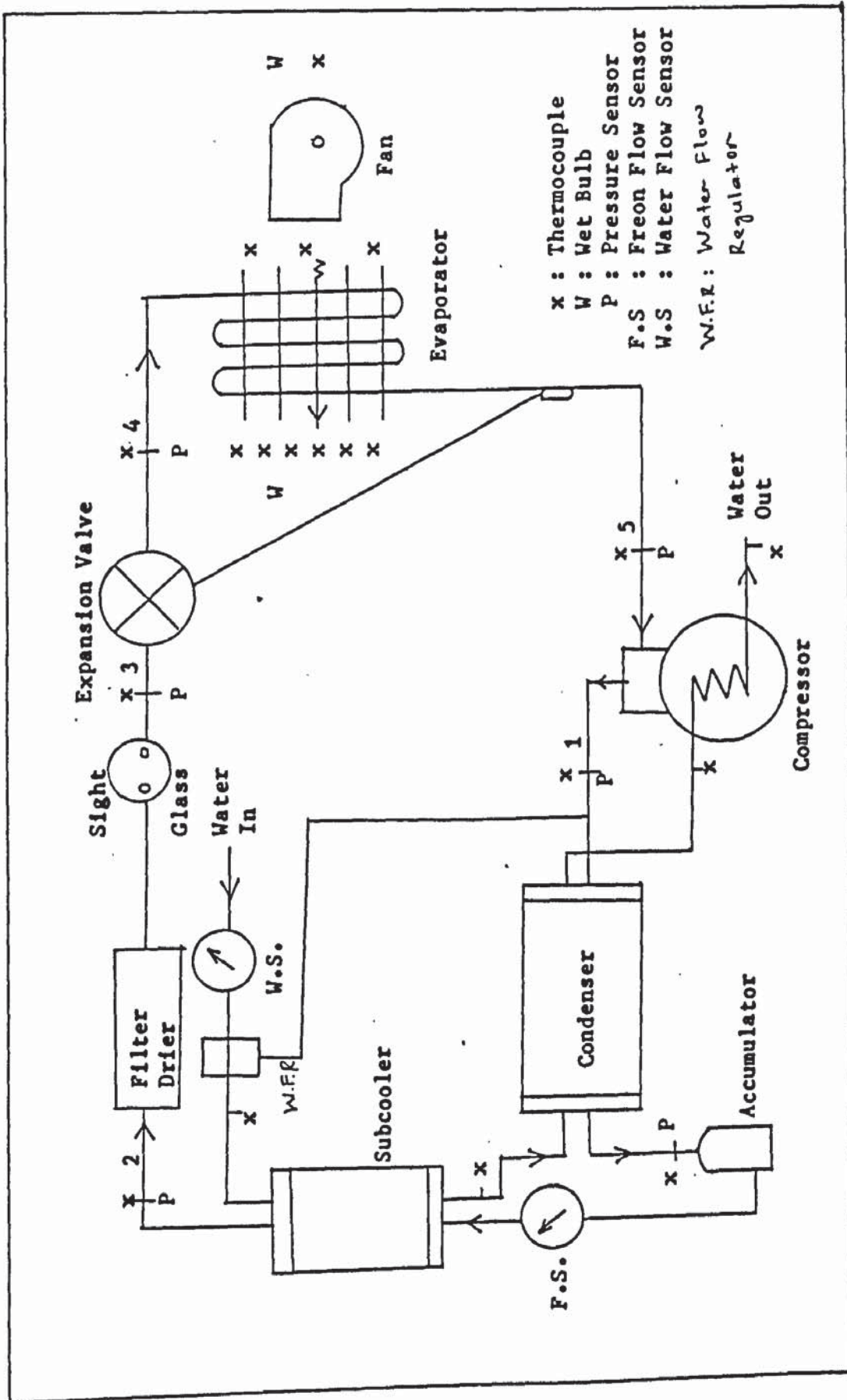


Fig (4.3) Arrangement of transducers in the air-water heat pump system.

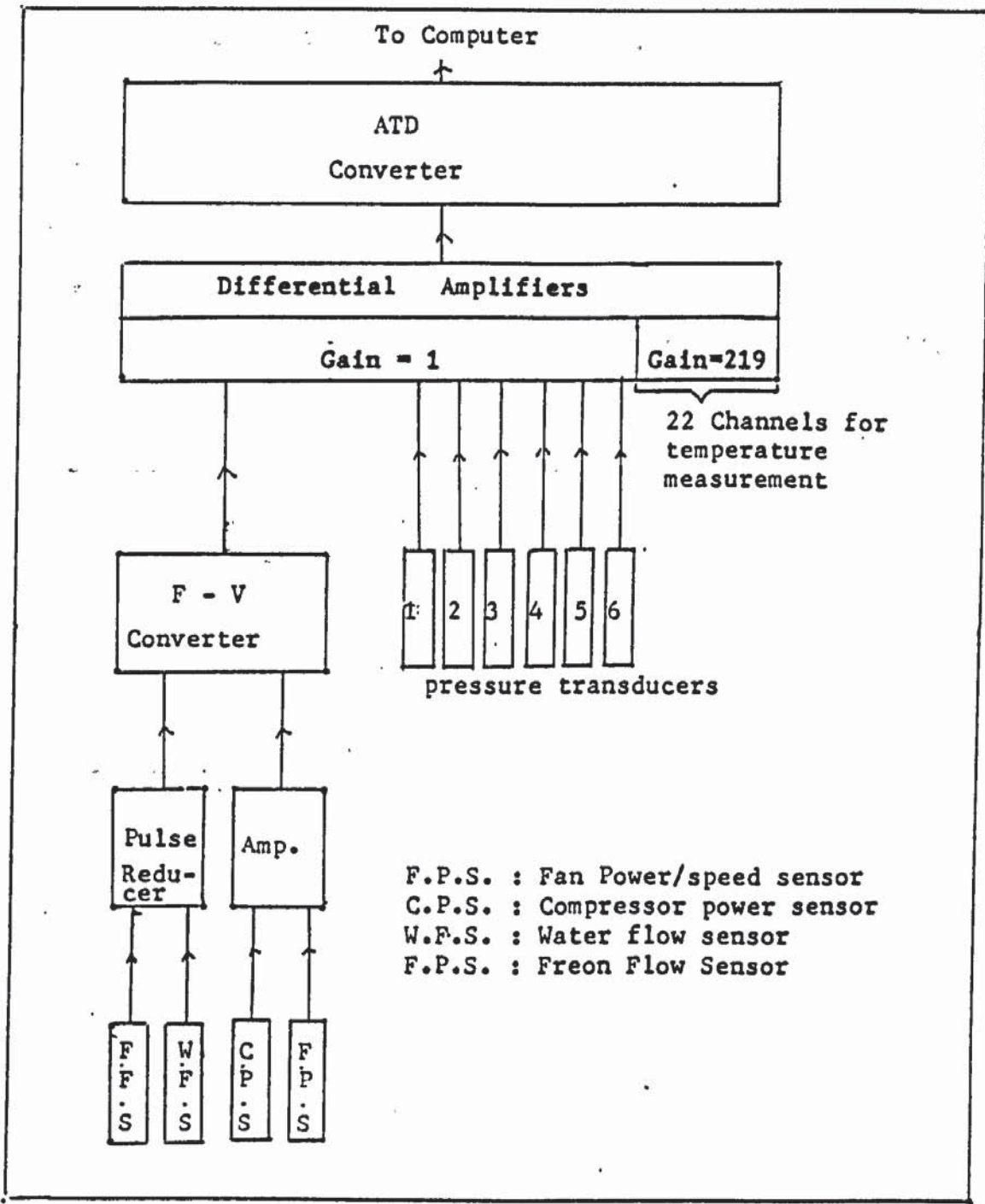


Fig (4.4) A block diagram of the transducers arrangement in the digital data acquisition system .

The output voltages of the transducers for measuring pressures are based on a negative output line, they therefore cannot be fed directly to the ATD converter which is ground based. To match the potentials a differential buffer amplifier is used. The same amplifiers are also used to feed flow rate and electrical power signals to the ATD converter. The type of amplifier used is an instrumentation operational amplifier. The integrated circuit (IC) used is 725 CN supplied by RS Component Limited.

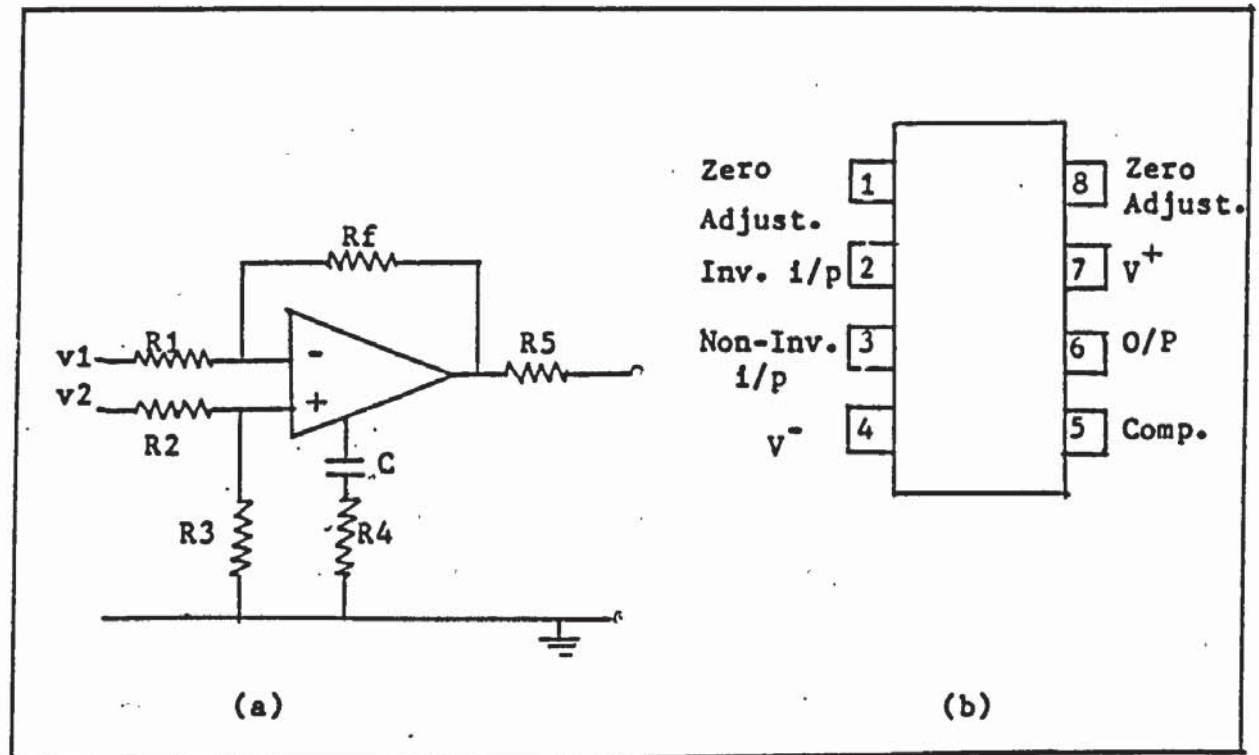


Fig (4.5) (a) Instrumental operational amplifier circuit.

(b) RS 725 CN integrated circuit.

Pin 1 and 8 (figure (4.5 b)) are for zero adjustment , pin 4 is for negative and pin 7 is for positive input power lines. Inverting input is to pin 2, while the non-inverting input is to pin 3, and output is from pin 6. Pin 5 is for compensation (stability) against noise and drift.

An operational amplifier IC is a solid state integrated circuit that uses external feedback to control its function . The feedback connection is made between the output and the inverting input pins , with resistors R1 and Rf as voltage dividers. The operational amplifier is said to have infinite input impedance and zero output impedance , and when there is no signal applied to either inputs , the output is zero (37) . Output polarity is in phase with the non-inverting input and out of phase with the inverting input . When both the inputs are connected the difference of the input voltages (v1 - v2) will be amplified , and this gives the name as the differential amplifier . The output voltage is,

$$V_o = \left(\frac{R_f}{R_1} \right) (v_1 - v_2) \quad (4.1)$$

for R1 = R2 and Rf = R3 . R5 at the output pin is to safeguard the IC in case of short circuit.

4.4 Frequency To Voltage Converter

It is necessary to convert the ac signal or pulses given out by some of the transducers into analogue dc signals, to match the ATD converter input requirement. For this purpose an IC RS 307-070 is used . The IC has 14 pins as shown in figure (4.6(a)) below.

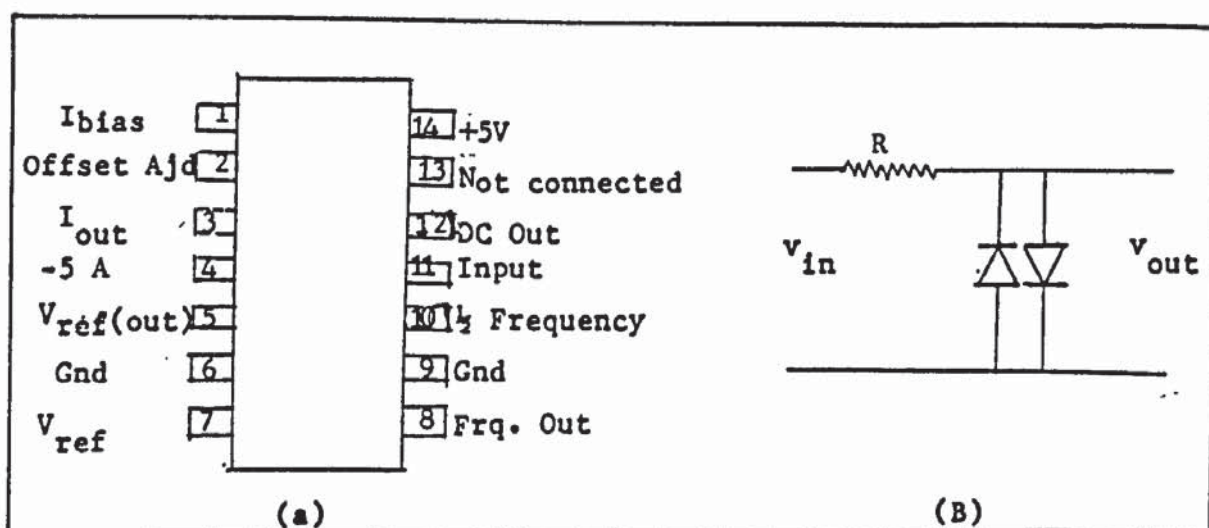


Fig (4.6) (a) RS 307-070, the frequency to voltage converter IC
(b) The voltage limiting circuit

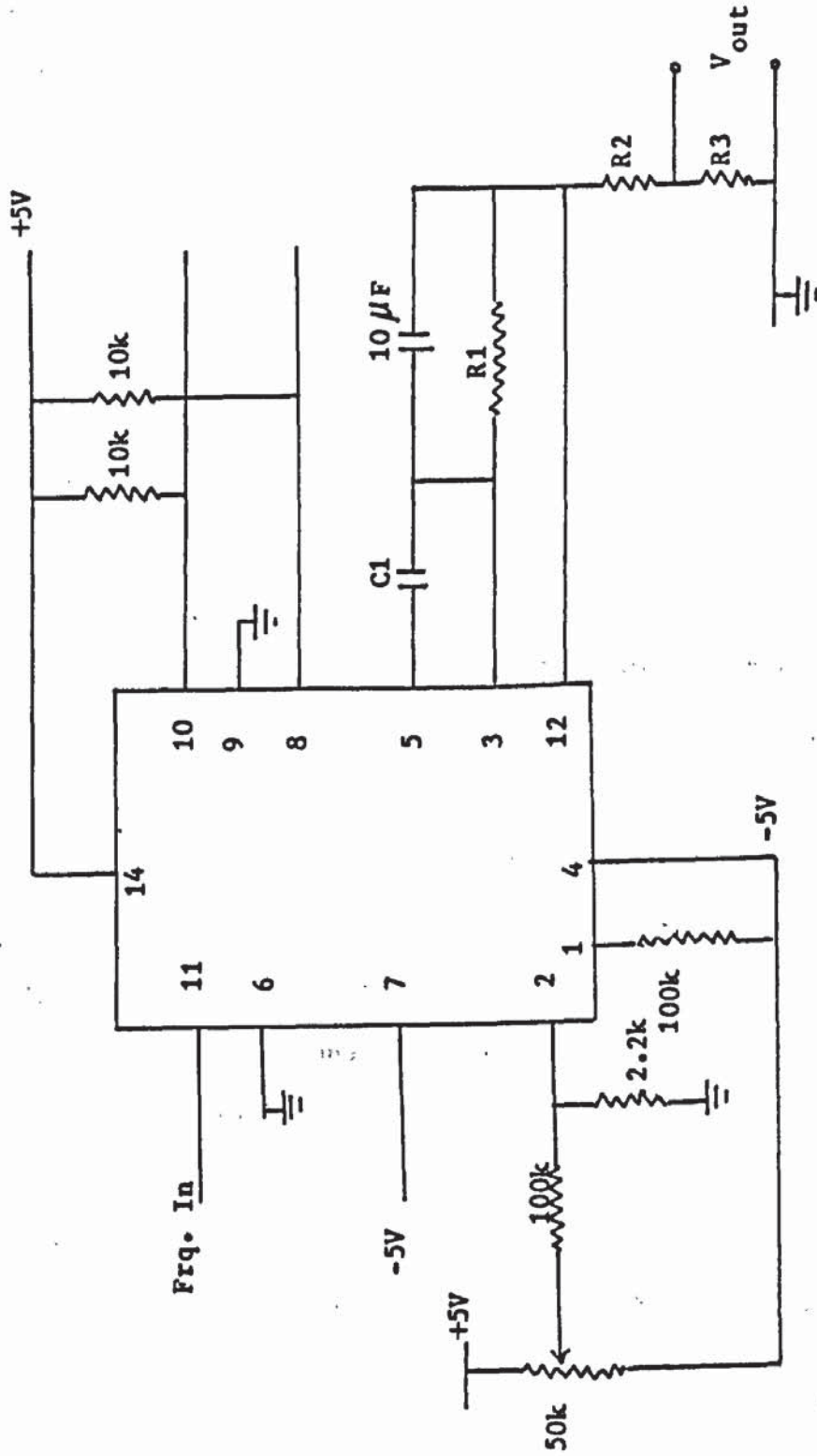


Fig. In

Fig (4.7) A circuit diagram of frequency to voltage converter. The values of R1,R2,R3 and C1 depend on the application.

Figure (4.6(b)) is the input voltage limiting circuit diagram. The purpose of the circuit, consisting of 2 silicon diodes and a resistor, is to limit the input voltage to less than 2.5 V and to make the signal cross zero, as required by the converter. The minimum input voltage permissible is 200mV. The parallel silicon diodes produce an output voltage not exceeding 1.2V (p-p). The manufacturer's recommended value for resistor R is given by,

$$R = (V_{i(p-p)} - 1) \cdot 10 \quad (4.2)$$

where R is in $k\Omega$ and $V_{i(p-p)}$ is input voltage peak-peak in volt.

The input signal is fed through pin 11 and the output is from pin 12. The values of R1 and C1 are chosen according to the magnitude of the input frequency (or application), so that the output voltage will be in the full range, which is 0-4 V. The range is then reduced to 0-1V to suit the ATD converter requirement by using the potential divider (R2 and R3 in figure (4.7)).

To smooth out ripples, a large capacitor, $10\mu F$ is put across resistor R1. A large capacitor in the output circuit means the response time is large, and will take a longer time to response to changes in the input frequency. The response time is made to be less than 5 seconds by adjusting the combination of C1 and R1 for each application.

The accuracy of this F-V converter as claimed by the manufacturer is .1 % of the full range output (FRO). Since the full range is 1V, the accuracy is $\pm 1mV$.

4.5 Temperature Measurement

4.5.1 Thermocouple

A thermocouple consists of a pair of dissimilar metal (e.g. copper and constantan) wires joined together at one end (sensing junction) and terminated at the other end (reference junction) at a known temperature , e.g. melting ice temperature (0 C) . When a temperature difference exists between the sensing junction and the reference junction , an emf is produced that causes current to flow in the circuit . The temperature difference associated with the emf is determined by measuring the voltage of the emf and converting it to a temperature using a , calibration table or equation.

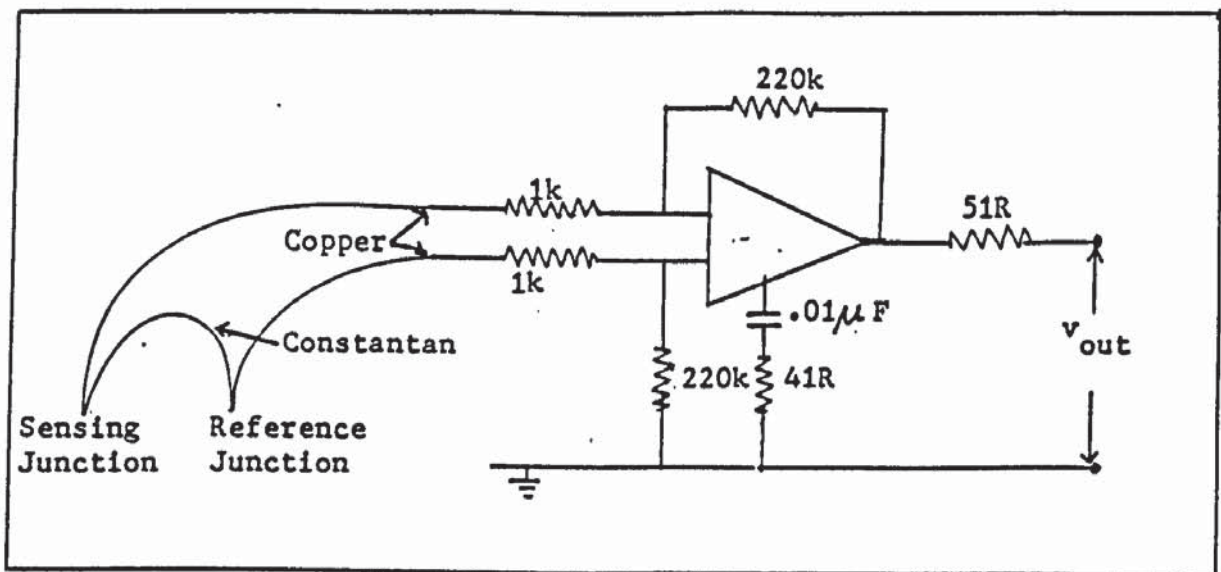


Fig (4.8) The output of the thermocouple is increased by the amplifier by 219 times.

When measuring the refrigerant temperature inside the refrigerant tube the thermocouple connection has to withstand a high pressure (3-12 bar).

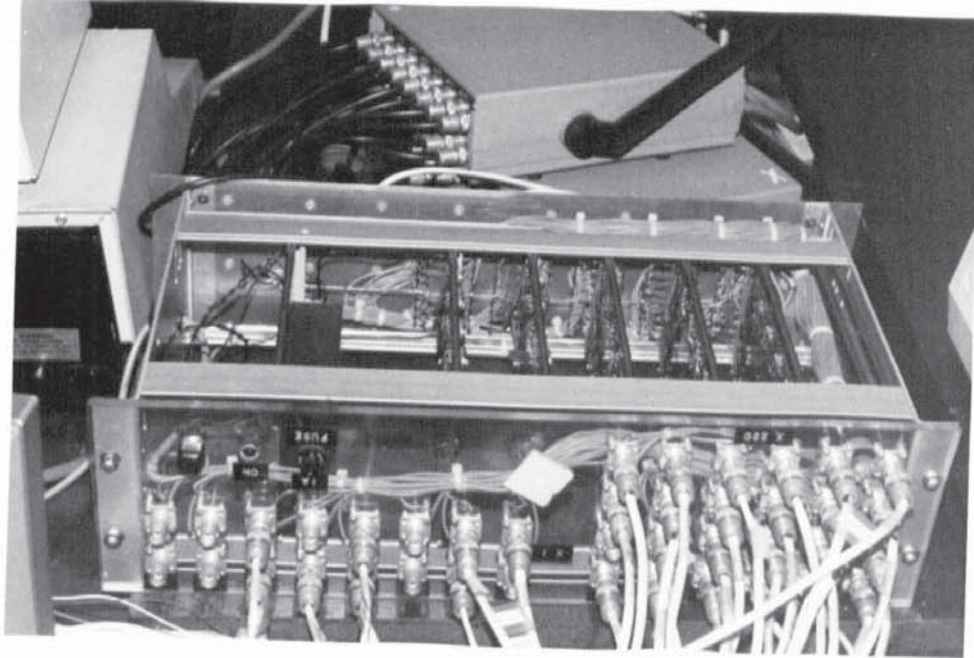


Photo (4.1) The amplifiers . At the top are the ATD converters.

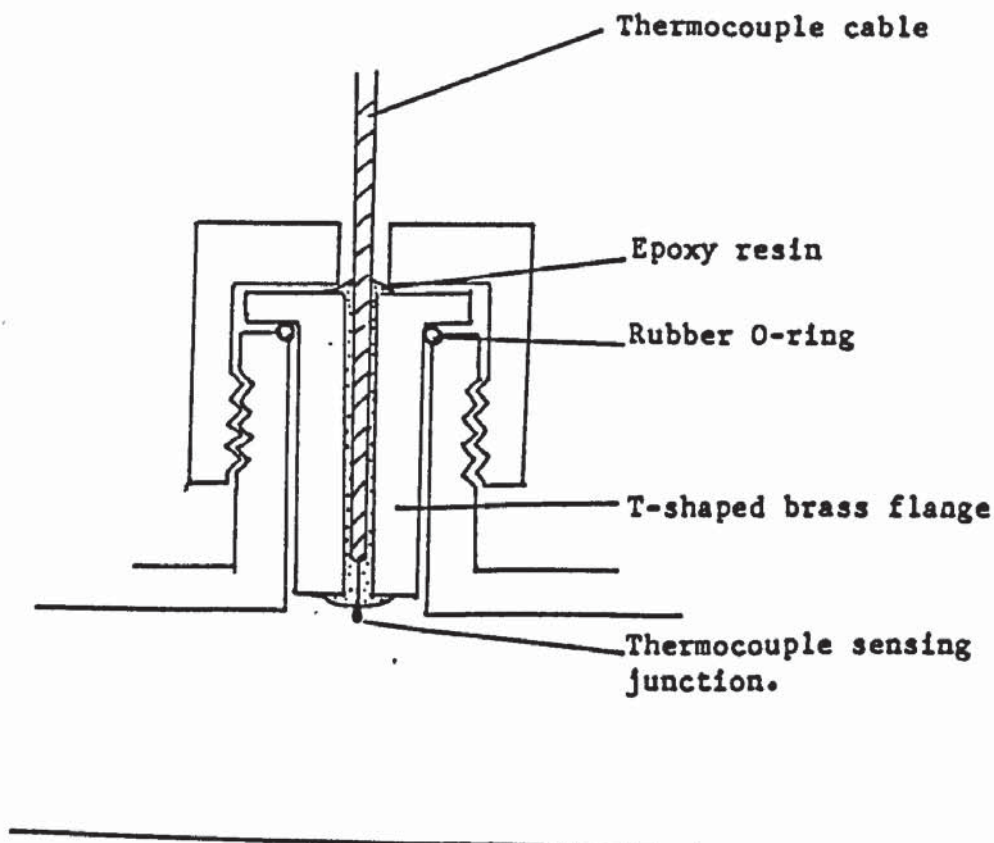


Fig (4.8) Connection of thermocouple to the R12 and water tubes.

The sensing junction is put through a hole in the middle of a T-shaped brass flange and covered with araldite epoxy resin. It is then connected to the refrigerant line using a compression cross-connector (the other outlet of the connector is for a pressure transducer).

4.5.2 The Calibration

The source of errors in the temperature measurement are the thermocouple itself, the amplifier, the ATD converter and the calibration equation. All the thermocouples were checked and those with output voltages within $5\mu\text{V}$ with the calibration table were chosen. The thermocouple outputs were amplified 219 times using the operational amplifier (figure(4.8)) with $R3=Rf=220k \pm 1\%$ and $R1=R2=1k \pm 1\%$. The accuracy of the amplification, confirmed by measurement, is 1%. The ATD converter gives an error $\pm .25\text{mV}$ as shown in section (4.2). A polynomial curve fitting program was developed and was used to obtain the equation shown below relating thermocouple output voltage to temperature.

$$T = 4.415 \times 10^{-3} + 25.830 \text{ Ev} - .606 \text{ Ev}^2 - .027 \text{ Ev}^3 + .012 \text{ Ev}^4 - 9.817 \times 10^{-4} \text{ Ev}^5 \quad (4.3)$$

where T is temperature in C and Ev is voltage in mV. The accuracy of equation (4.3) above is $\pm .05\%$ as shown in table (4.1) below.

voltage mV	temperature from table C	temperature from eq. C	$T_{\text{table}} - T_{\text{eq}}$ C	% of error
0	0	.0044	.0044	zero error
.789	20	19.9894	.0106	.05
1.611	40	39.9946	.0054	.02
2.467	60	59.9922	.0078	.02
3.357	80	80.0054	.0045	.01
4.277	100	99.9968	.0012	.001

Table (4.1) Comparison of equation (4.3) with values from the calibration table.

The experimental uncertainty in temperature measurement is calculated as follows. The previously mentioned experimental uncertainty of $\pm 5 \mu V$ was determined when the hot junction was at room temperature (about 20C or $800 \mu V$). The thermocouple thus has an inherent uncertainty of about $\frac{1}{2}\%$. If we assume the thermoelectric power to be $40 \mu V$ per C at temperature t the voltage after amplification is $219.40 t (1 \pm 1.5\%) V = 8.76 t (1 \pm 1.5\%) mV$. (Note: the amplification uncertainty is 1%). After the ATD converter, the voltage is $8.76 t (1 \pm 1.5\%) \pm .25 mV = 8.76 t (1 \pm (1.5 + \frac{25}{8.76t}) \%) mV$.

Temperature t (C)	% of error
2	3.0
5	2.0
10	1.8
20	1.7
50	1.6
100	1.5

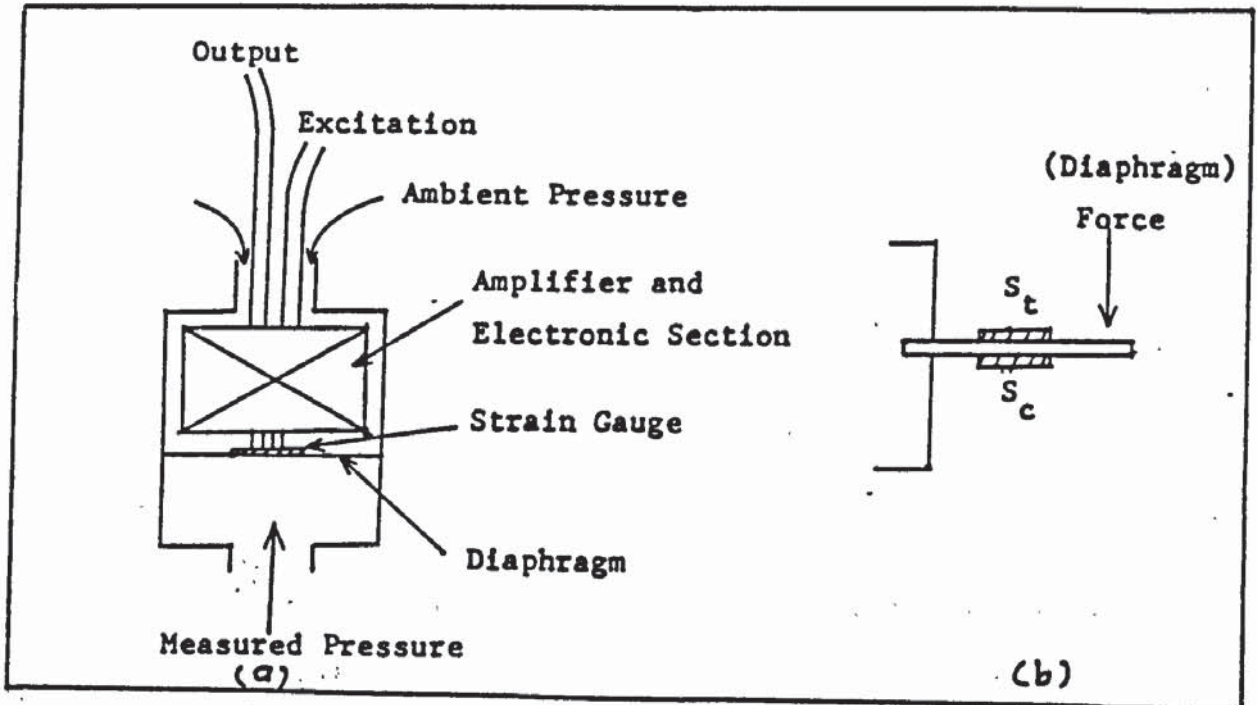
Table(4.2) The accuracy of temperature measurement

4.6 Pressure Measurement

4.6.1 The Strain Gauge

Pressure measurement is made by using a strain gauge. It consists essentially of a semiconductor mounted on a diaphragm, so that it undergoes small elongations or contractions due to tension or

compression stress, respectively in that surface. As a result, the strain gauge undergoes a corresponding change in resistance which is converted into a voltage signal by connecting the gauge as arms of a Wheatstone bridge, and applying excitation power to the bridge.



Fig(4.9) (a) A schematic diagram of a pressure transducer gauge.
 (b) Strain gauges for tensile and compression strains.

Figure (4.10) shows a typical Wheatstone bridge circuit with adjustment network used in the strain gauge transducer (38). The resistors R_1, R_2, R_3 and R_4 are the strain gauge components, where R_1 and R_3 sense the compression strain, S_c ; and R_2 and R_4 sense the tensile strain, S_t . The resistors R_a and R_b are for zero adjustment. The resistor R_c , determines the range of the transducer sensitivity.

4.6.2 The Calibration

All the transducers were supplied with their calibration certificates

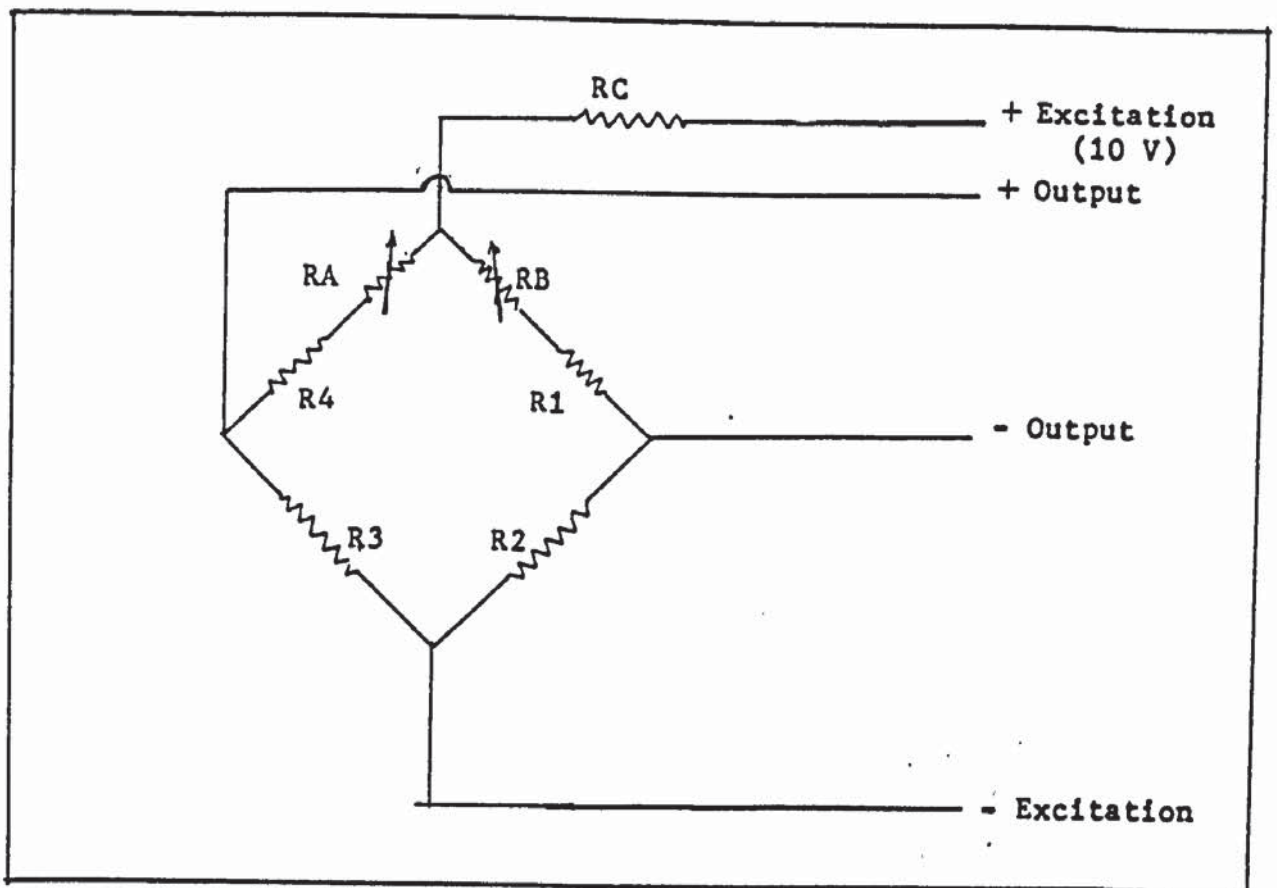
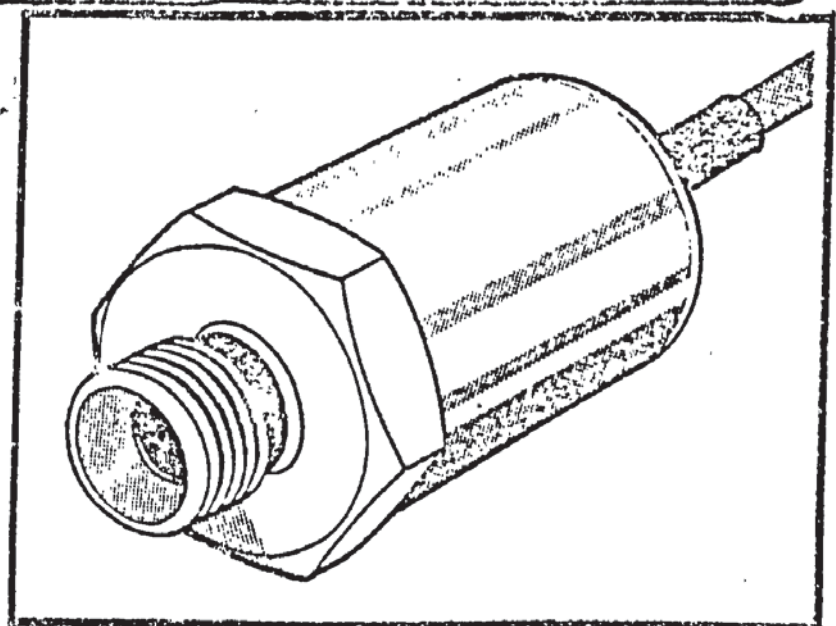


Fig (4.10) A circuit diagram of the strain gauge for measuring pressure

by the manufacturer, Maywood Instruments Limited. The error of each transducer as a percentage of the full range output (FRO) is shown in table (4.3).

The output signal of the transducer is matched with the converter input requirement by using a buffer amplifier. This is done by taking $R1=R2=R3=Rf=100k\pm 1\%$; $R4=41\Omega\pm 1\%$, and $R5=51\Omega\pm 1\%$; while $C=.01\mu F$ in figure(4.5). The maximum zero error of all the buffer amplifiers was found to be around $\pm .001$ mV.

Model Number	P102	
Serial Number	4707	
Range	0-2.00 PSIG	
Test Temperature	2.0	°C
Excitation	10	Volts DC
Non-Linearity	± 0.03	% FRO
Hysteresis & Non Repeatability	< 0.05	% FRO
Full Range Output	2.0133	mV
Input Resistance	14.03	Ohms
Output Resistance	4.77	Ohms
Compensated Temperature Range	-18	°C to +65 °C
Thermal Zero Shift	± 0.02	% FRO/°C
Thermal Sensitivity Shift	± 0.02	% FRO/°C
QUALITY CONTROL		
Signature	<i>M. Baker</i>	
Date	4.6.51	
ELECTRICAL CONNECTIONS		
Input +	RED (RED)	✓
Input -	BLUE (BLACK)	✓
Output +	GREEN (GREEN)	✓
Output -	YELLOW (WHITE)	✓
LEMO CONNECTOR		
	- IN	Orientation notch
	+ IN	
	+ OUT	
	- OUT	White line



Fig(4.10 a) The pressure transducer and the calibration certificate.

Transducers (Psig) ¹	FRO (mV)	Transducer Error ² (mV)	Total Error ³ (mV)	% Error of FRO
P1:0-500	203.96	± .31	± .57	± .28
P2:0-500	202.12	± .22	± .48	± .24
P3:0-200	200.76	± .22	± .48	± .24
P4:0-200	201.33	± .16	± .42	± .21
P5:0-200	200.23	± .22	± .48	± .23
P6:0-200	200.69	± .18	± .44	± .22

1 : As calibrated by the manufacturer in pounds per square inch .

2 : From the calibration certificate

3 : Total error = transducer error + ATD converter error + buffer amplifier error .

Table (4.3) Pressure transducer calibration

The six equations for automatic reading of the pressure are;

$$P1 = (Ev \times 2451.46 + 14.7) / 14.7 \quad (4.4 \text{ a})$$

$$P2 = (Ev \times 2473.78 + 14.7) / 14.7 \quad (4.4 \text{ b})$$

$$P3 = (Ev \times 996.56 + 14.7) / 14.7 \quad (4.4 \text{ c})$$

$$P4 = (Ev \times 998.85 + 14.7) / 14.7 \quad (4.4 \text{ d})$$

$$P5 = (Ev \times 993.39 + 14.7) / 14.7 \quad (4.4 \text{ e})$$

$$P6 = (Ev \times 996.23 + 14.7) / 14.7 \quad (4.4 \text{ f})$$

where Ev is the voltage output of the transducer in volt. The pressure is absolute and in bar (1 bar = 10⁵ Pa) .

4.7 The Compressor Input Power Measurement

4.7.1 The Opto Switch

The opto switch was purchased from RS Component Limited (stock no 307-913). It comprises a gallium arsenide infra red emitting diode with a silicon photodarlington transistor detector or 'switch' in a moulded package. An infra-red transmitting filter is fitted to eliminate ambient illumination problems.

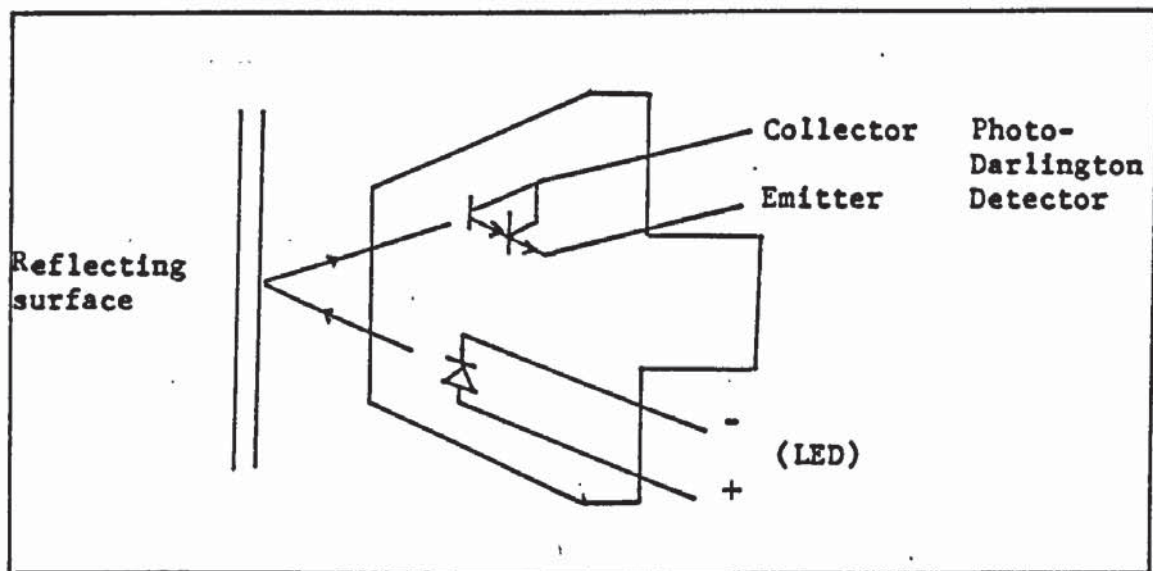


Fig (4.11) The RS opto-switch.

The infra-red light emitted by the LED will be reflected by a reflecting surface onto the photodarlington detector and switch the detector into a 'switch on' mode. When there is no light reflected onto the detector, the detector is in 'switch off' mode. Diode characteristics are such that the output current ratio in the on mode to the off mode is about 100. Values are typically of order $100\ \mu\text{A}$ and $1\ \mu\text{A}$ (reference (36)). Thus in the off mode the voltage at pin 2

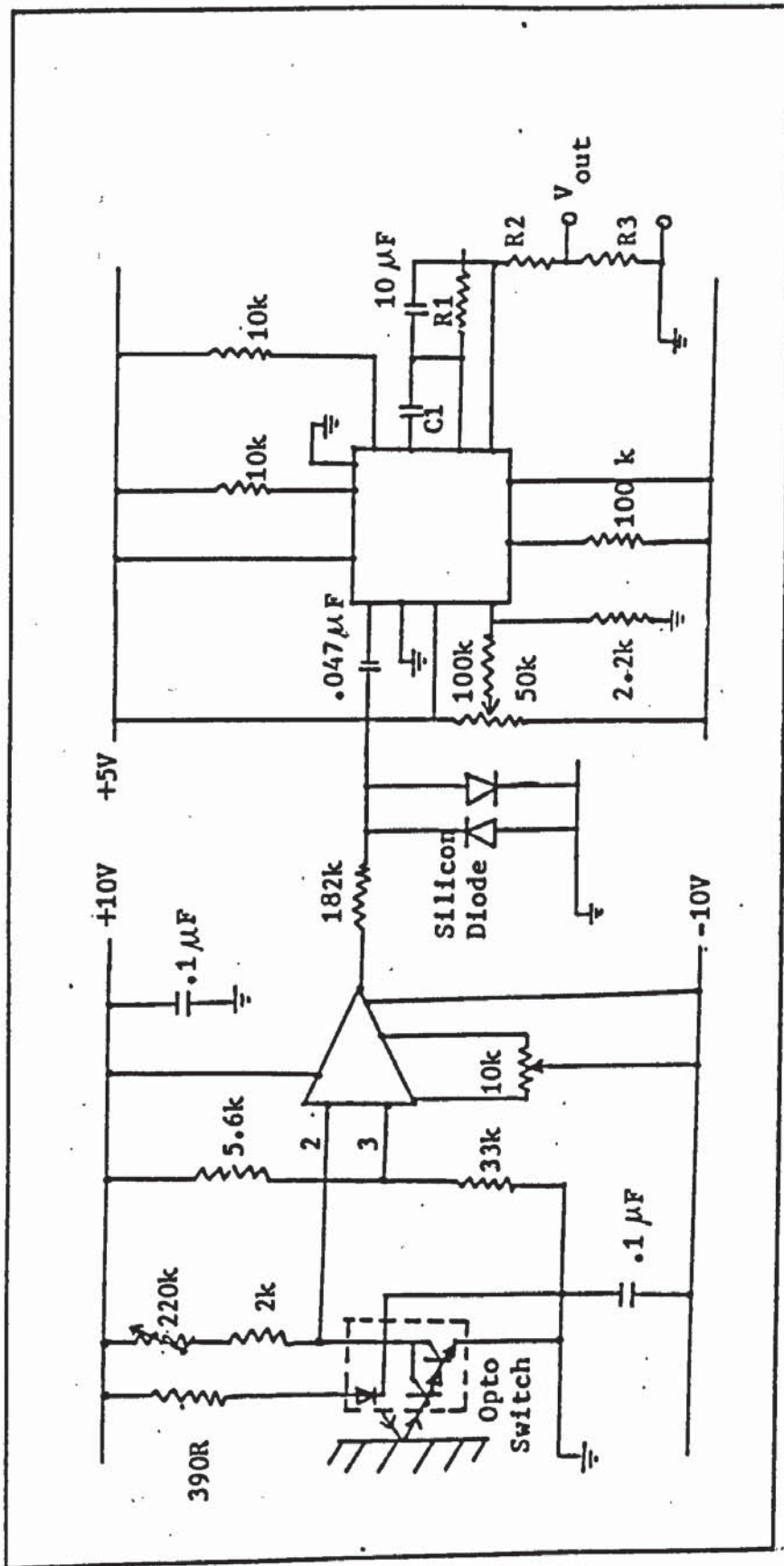


Fig (4.12) Circuit diagram for measuring compressor input power and air speed.

1. Compressor power : $R1 = 1\text{ M}$; $R2 = 1\text{ k}$; $R3 = 330\text{ R}$; $C1 = .047\text{ F}$
2. Air Speed : $R1 = 570\text{ k}$; $R2 = 1\text{ k}$; $R3 = 330\text{ R}$; $C1 = .04705\text{ F}$

is little different from the supply voltage of +10V, whereas in the on mode suitable adjustment of the variable 220k resistor produces a low voltage at pin 2. The resistors that determine the voltage at pin 3 are chosen to give a value between the two pin 2 voltages. The operational amplifier output will be -10V for the off mode ,but +10V for the on mode. The circuit thus acts to produce a square wave output. The frequency to voltage conversion circuit as described earlier, then follows to give a dc output proportional to the rate of switching mode.

To measure the compressor input power , the opto switch is made to count the lines on the light-reflecting disc inside the watt-hour meter (figure (4.13)). On the disc there are 200 dark lines of equal thickness and equally separated . When the light strikes the disc , the detector is switched 'on' and when the light strikes the dark lines , the detector is switched 'off' .

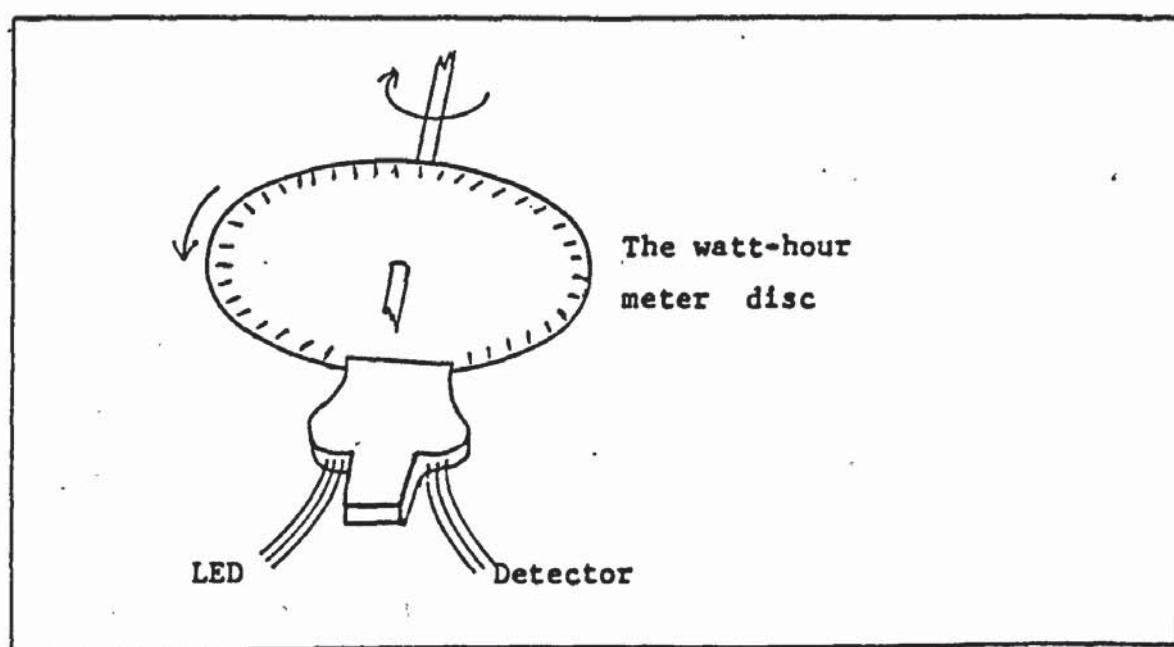


Fig (4.13) The opto-switch is made to count the lines on the watt hour meter disc.

4.7.2 The Calibration

It was calibrated by using known loads ; light bulbs of 100 , 150 , 200 , 250 , 300 , 350 and 400 W . The voltages across the light bulbs and current were measured . The accuracy of the output signals is $1\text{mV} + .25\text{mV} + .001\text{mV} = 1.251 \text{ mV}$ (the FV converter + ATD converter + the amplifier) . The accuracy of the volt meter is $.1\text{V}$ in 240 V ;and the accuracy of the ammeter is $\pm .003 \text{ A}$. The power, calculated from $P=(I \pm \Delta I)(V \pm \Delta V)$ gives an average error of $.3\%$. Table (4.4) below shows the data for the calibration.

Transducer Output ($\pm 1.251\text{mV}$) V	Voltage Across light bulb ($\pm .04\%$) V	Current A	Power $P = I \times V$ W
.9733	239.6	1.650 $\pm .2\%$	395.34 $\pm .2\%$
.8473	239.5	1.425	341.29
.7331	239	1.225	292.78
.6137	239.8	1.025 $\pm .3\%$	245.8 $\pm .3\%$
.4840	239.8	.800	191.84
.3770	240.8	.620	149.3
.2481	240.1	.400 $\pm .8\%$	96.04 $\pm .8\%$

Table (4.4) Calibration of the compressor input power .

An equation relating the power P_e to the transducer output voltage E_v was fitted from the data in table (4.4).

$$P_e = 406.25 \times E_v - 3.12 \quad (4.5)$$

Where P_e is in W and E_v in V.

The disagreement between the power calculated from equation (4.5) above and the power from experiment is typically 1%. That means for power in the range of 100W to 400W, the error is between 1 to 4W. The error due to the uncertainty of the transducer output signal is 1.251 mV, which is equivalent to $\frac{1}{2}$ W.

In the actual experiment, the error is higher than the one which has been discussed above. A small error is due to the unsteadiness of the disc rotation due to the fluctuation of the main power supply. Another source of error is due to the low frequency of the disc rotation, which is in the region of $\frac{1}{20}$ cycle/second. Thus any irregularity in the line spacing produces further experimental uncertainty. A comparison of direct measurement from the watt hour meter and from equation (4.5) gives an error of about 3-4%. Therefore it can be concluded that an error in the region of 4% is expected in the instantaneous compressor power measurement.

4.8 Water Flow Rate Measurement

4.8.1 Water Flow Sensor

The transducers used to measure the water and refrigerant flow rates are of the rotor type. They consist of three main parts. The body to which the water pipes are attached; the electronic compartment and the rotor assembly unit which consists of a ring carrying sapphire cups.

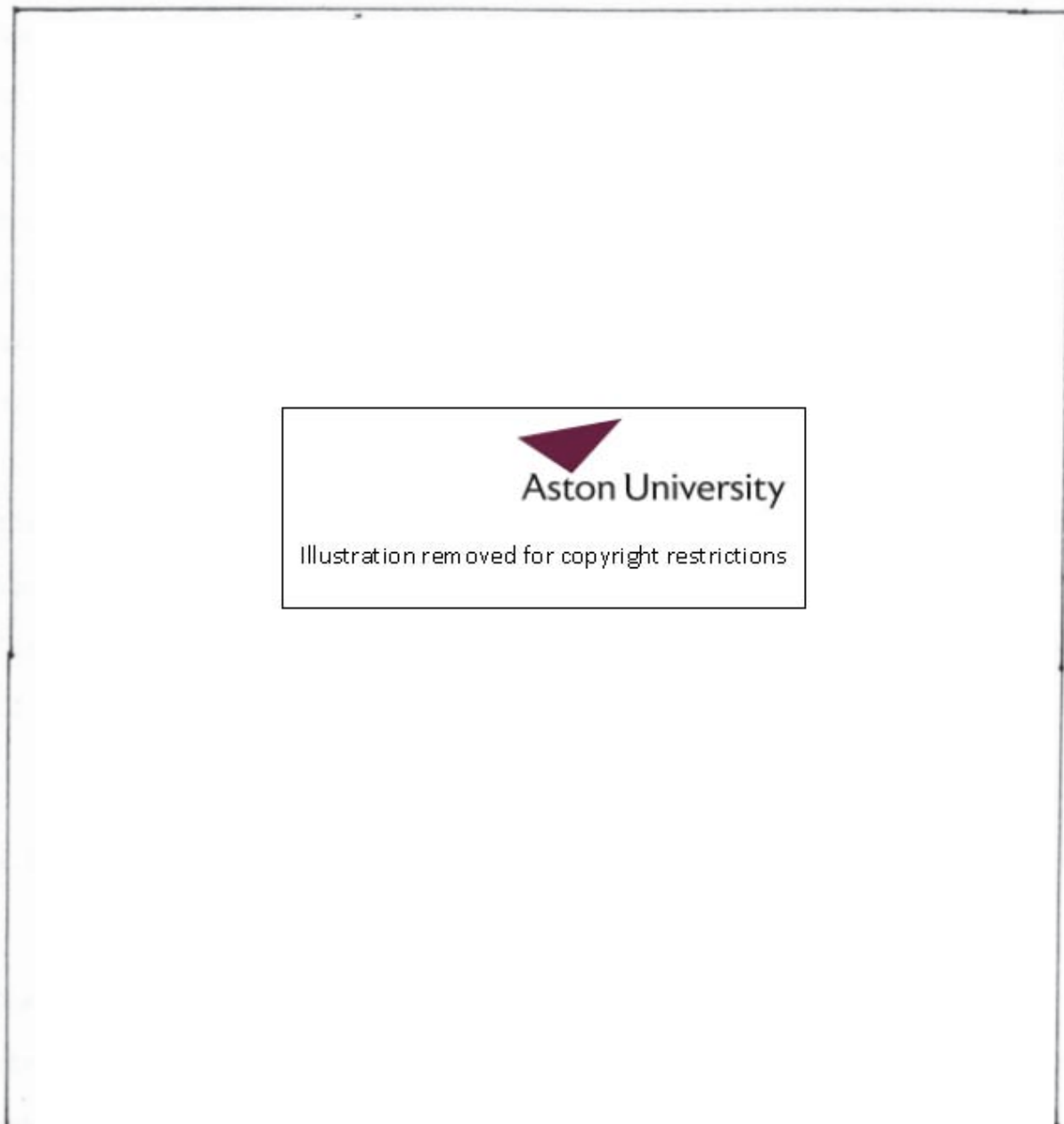


Fig (4.14) (a) The water flow sensor

(b) A schematic diagram of the flow sensor showing the rotor and the sensing coil.

bearings, which in their turn carry the rotor mounted on a shaft. The tips of the rotor contain ferrite rods. Inside the electronic compartment, there is an electromagnetic coil. In operation when the magnet in the rotor tips cuts the field of the electromagnetic coil, a current is induced, which is taken as output signal. The frequency of the output signal is proportional to the angular velocity of the rotor, which in turn is proportional to the liquid volume flow rate. X

The output signal of the water flow sensor is pulsed. The frequency is converted to a dc voltage using a F-V converter as described earlier (chapter(4.4)). Figure (4.15) shows the circuit diagram with the value of the required components.

4.8.2 The Calibration

The calibration was done by measuring the amount of water flow for a given period, using measuring cylinder and stop clock. The error of the measuring cylinder is .5ml and of the stop clock is .5s, by taking the error as $\frac{1}{2}$ of the smallest scale division. The water mass flow rate is determined by taking water density as 1 kg per litre. The error of the transducer signal is $1\text{mV} + .25\text{mV} + .001\text{mV} = 1.251\text{mV}$ (the error of F-V converter + ATD converter + amplifier).

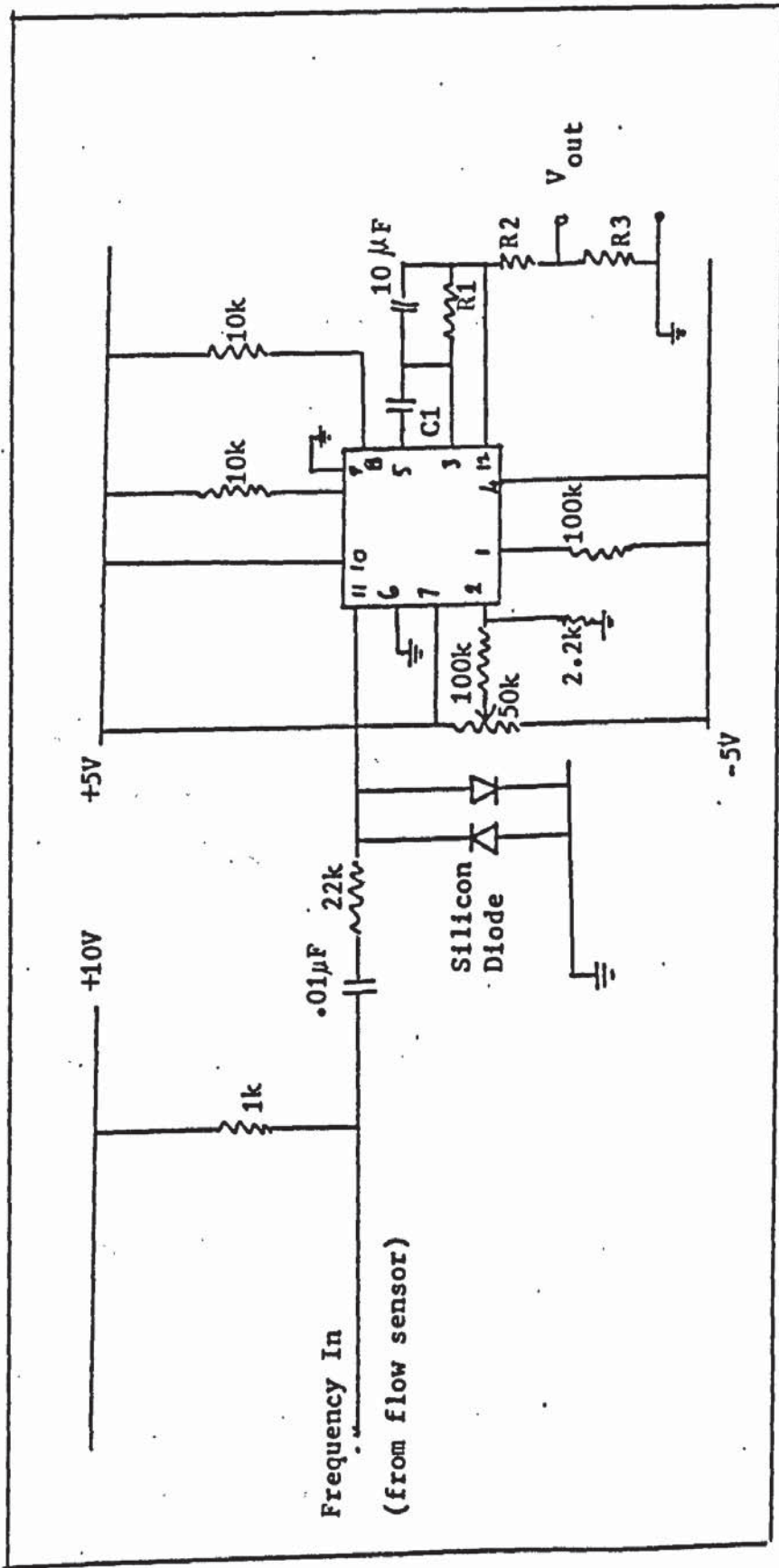


Fig (4.15) Frequency to voltage converter for liquid flow sensor.

1. Water : R1 = 1 M ; R2 = 440R ; R3 = 190R

2. Freon : R1 = 470 R ; R2 = 440R ; R3 = 288R

Ev (exp) V	\dot{M}_w (exp) $\times 10^{-3}$ kg s ⁻¹	\dot{M}_w (eq) $\times 10^{-3}$ kg s ⁻¹
.21105	7.12 ± .09	7.05
.23234	7.67 ± .15	7.76
.25713	8.67 ± .16	8.59
.30681	10.30 ± .17	10.25
.36018	11.92 ± .18	12.03
.48869	16.18 ± .22	16.31
.61132	20.60 ± .52	20.41
.69101	23.01 ± .58	23.07

Table(4.5) The calibration of the water flow sensor.

An equation relating the water mass flow rate \dot{M}_w (kgs⁻¹) and the transducer signal Ev (V) was developed using the experimental data from table (4.5) above.

$$\dot{M}_w = (.009 + 33.37 Ev) 10^{-3} \quad (4.6)$$

As shown in table (4.5) above, the values of the \dot{M}_w (eq) is within the error range of the \dot{M}_w (exp); therefore equation (4.6) can be accepted.

4.9 The Refrigerant (R12) Flow Measurement

4.9.1 The Flow Sensor

The type and operational principle is the same as the water flow

sensor, except the casing is made from stainless steel instead of hard plastic, and the electronic compartment (not including the signal pick up coil) is about 14 cm from the rotor assembly. The sensor is connected to the refrigerant liquid line of the heat pump by flexible tubes to reduce the vibration caused by the compressor. The F-V converter circuit diagram for the R12 flow sensor is in figure (4.15).

4.9.2 The Calibration

The calibration is based on the manufacturer's certificate since it cannot be done simply in the laboratory. The calibration certificate shows that the sensor was calibrated using water at constant temperature. The R12 density, ρ_r is obtained from equation (4.7) below, which was developed using data from (48).

$$\rho_r = 1.400 - 3.823 \times 10^{-3} t + 1.500 t^2 - 2.635 \times 10^{-7} t^3 \quad (4.7)$$

where ρ_r is the density in kg/litre and t is temperature in C.

Using data from the manufacturer's calibration certificate, a relationship between the frequency Fq and mass flow rate \dot{M}_r was developed (table (4.6a)).

$$\dot{M}_r = (1.845 + 4.475 Fq) \rho_r \cdot 10^{-4} \quad (4.8)$$

where \dot{M}_r is in kg/s and Fq is in Hertz.

Several readings of the analogue dc outputs of the transducer Ev and the equivalent frequency Fq were measured experimentally in the laboratory. Then using equation (4.8) above the mass flow rates at the measured frequency were calculated (table (4.6b)). An equation relating the mass flow rate and the analogue output of the transducer was found as below.

$$\dot{M}_r = (-2.458 \times 10^{-4} + .0147 \text{ Ev}) \rho_r \quad (4.9)$$

where Ev is in V and \dot{M}_r is in kg s^{-1}

Water F-rate kg/min	R12 F-rate $\times \rho_r$ kg/s	Pulse rate Hz
6.26	0.104	233.39
5.51	0.092	206.07
4.25	0.071	156.05
3.26	0.054	122.96
1.39	0.023	53.61
0.38	0.006	14.32
0.1	0.002	3.76

Table (4.6a) Data from the manufacturer's calibration certificate.

Transducer Voltage Ev V	Frequency Fq Hz	Mass F-rate \dot{M}_r $\times \rho_r$ kg/s
0.3236	10.5	0.00451
0.3372	11.1	0.00478
0.3460	11.2	0.00483
0.3840	12.3	0.00532
0.4152	13.5	0.00586
0.4356	14	0.00608
0.4487	14.4	0.00626
0.5722	18.9	0.00827
0.6610	21.6	0.00948
0.7700	25	0.0110

Table (4.6b) The calibration of R12 flow sensor

The accuracy of the analogue signal is $1\text{mV} + .25\text{mV} + .001\text{mV} = 1.251\text{mV}$. The accuracy of R12 mass flow rate is about 5% at 10 Hz.

It is essential to place the R12 flow sensor in the liquid line to avoid the vapour which could be a problem.

4.10 The Air Speed Measurement

4.10.1 The Transducer

The same type of transducer used for measuring the compressor input power is used here. The sensor was made to count the frequency of the shaft rotation. This was done by putting a strip of paper as non - reflecting material on the shaft. The light will be reflected to the detector when it falls on the shaft but not when it falls on the paper. The output square wave is converted to dc voltage using a F-V converter as described earlier and the circuit diagram is shown in figure (4.12).

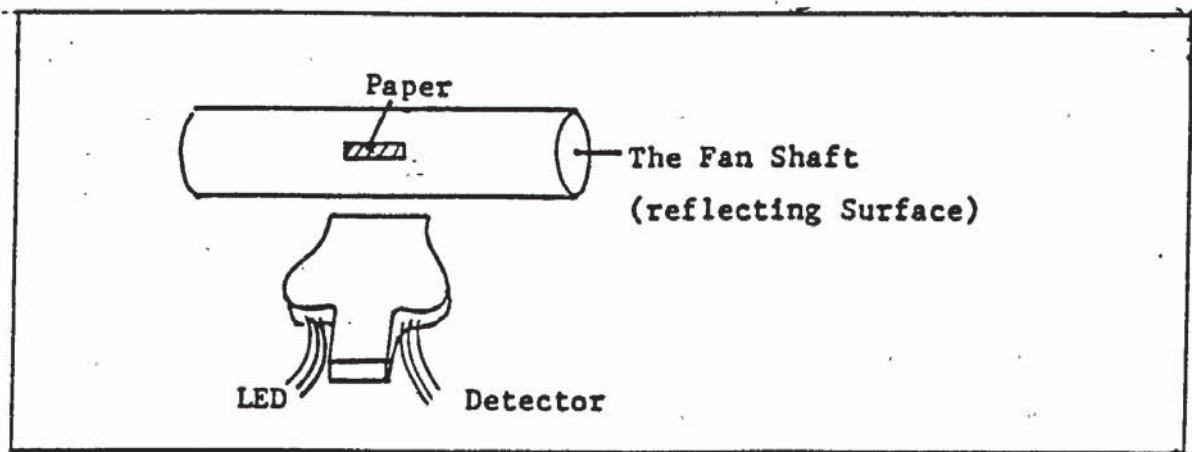


Fig (4.16) The opto switch is made to count the number of revolution of the fan shaft.

4.10.2 The Calibration

There is a variation of air speed over the evaporator surface due to the type of fan used, and it is extremely difficult to measure it precisely. The method adopted here is to divide the evaporator surface into 24 sections and measure the air speed at every section using a vane anemometer. The bilateral symmetry of the evaporator gave rise to 12 different air speeds for any one fan frequency.

	Detector Output Voltage (V)						
	.387	.448	.516	.585	.656	.721	.783
	Air speed (ms ⁻¹)						
A1	.406	.734	.952	1.172	1.385	1.590	1.801
A2	.293	.622	.802	1.051	1.325	1.450	1.693
A3	.258	.492	.709	.871	1.051	1.172	1.297
A4	.476	.802	1.033	1.325	1.647	1.905	2.201
A5	.423	.677	.924	1.219	1.451	1.590	1.793
A6	.288	.517	.692	.847	1.016	1.170	1.297
A7	.179	.363	.535	.709	.910	1.016	1.219
A8	.280	.469	.622	.824	.983	1.108	1.270
A9	.188	.406	.535	.726	.871	.983	1.219
A10	(0)	(.105)	.218	.381	.476	.598	.709
A11	(.16)	.252	.376	.510	.635	.726	.847
A12	(.08)	.169	.293	.429	.586	.663	.781
Aver.	.253	.467	.638	.820	1.033	1.185	1.343
Fitted Eq.	.313	.463	.642	.829	1.021	1.191	1.343

Table(4.7) The evaporator air speeds at several fan frequency, values in parentheses are estimated by extrapolation.

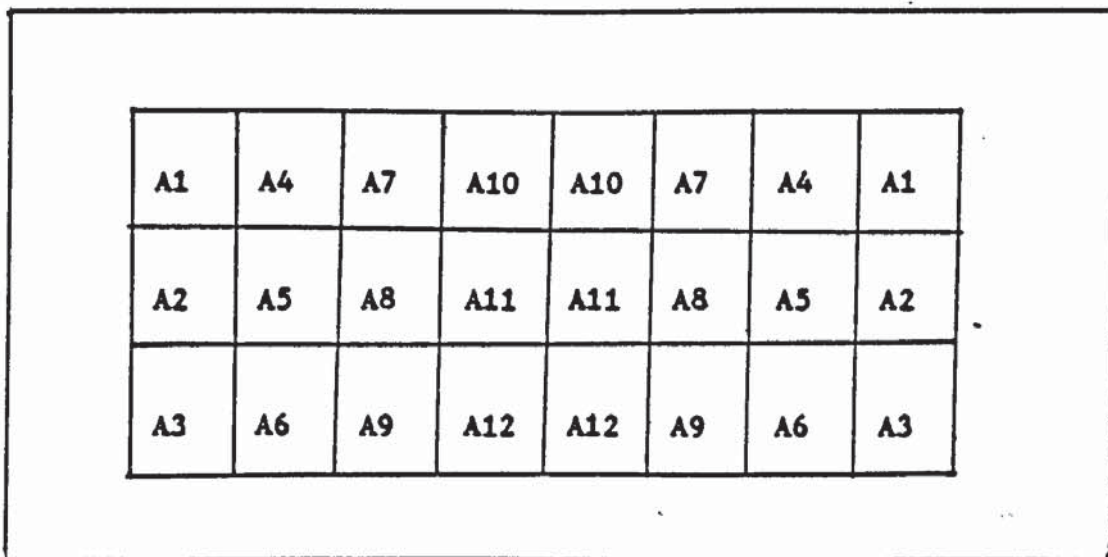


Fig (4.17) The evaporator face area is divided into 24 sections.

Table(4.7) shows the air speed at all the 12 sections of the evaporator (figure (4.17)) for several fan frequencies. For a given fan frequency the air speed is taken as the average of the speeds at all the sections. The transducer output voltage is related to the air speed by equation (4.10) below, which is fitted from the experimental data.

$$As = 2.64 Ev - 0.71 \quad (4.10)$$

where As is the air speed in ms^{-1} and Ev is the transducer output voltage in V. The evaporator air flow rate (in m^3s^{-1}) is the product of the evaporator face area (which is $.125 m^2$) with the air speed, As .

The error of the air flow rate is extremely difficult to estimate. The total error of the F-V converter, ATD converter and the amplifier is less than 1% (about 1.251 mV). The error of fitting the equation of air speed to the transducer's output voltage is very small, (see table (4.7)), and can be neglected. The biggest uncertainty is the vane anemometer, which is very difficult to estimate. One way of determining the overall error of the air flow rate measurement is by comparing it with the manufacturer's specification. The manufacturer gives the air flow rate as $.16 m^3s^{-1}$. From the experiment the maximum air flow rate is $.168 m^3s^{-1}$ (which is $1.343 \times .125$). This gives an error of around 5%.

4.11 The Fan Input Power Measurement

4.11.1 The Sensor

The same sensor is used as in the air speed measurement (section 4.10).

4.11.2 The Calibration

The fan input power and also the air speed were made variable by controlling the voltage of the input power using a variac . The experimental data shown in the table (4.8) below .

Ev(sensor) V	Current mA	Voltage(variac) V	Power P=I V W
.3532	169	150	25.35
.4475	190	170.5	32.4
.5281	212	193	40.92
.602	231	214.7	49.60
.6878	248	234	58.03
.7515	265	257.6	68.26
.8345	277	278.2	77.06

Table(4.8) The fan input power calibration .

An equation was developed by fitting the above data (Ev and P).

$$F_p = 109.64 E_v - 252.79 E_v^2 + 505.47 E_v^3 - 272.15 E_v^4 \quad (4.11)$$

where F_p is fan input power in Watt and E_v the transducer voltage in volt. The error here is the same with the measurement of compressor input power, in the range of 2to 3% .

4.12 The Air Relative Humidity Measurement

4.12.1 The Sensor

A psychrometer, which consists of two thermometers, one having a bulb covered with a wick that has been wetted with water, known as the wet bulb, and the other as the dry bulb, is used to determine the air relative humidity. The wet and dry temperatures were measured using thermocouples. At the wet bulb, the wick covered both the bulb and the sensing junction of the thermocouple.

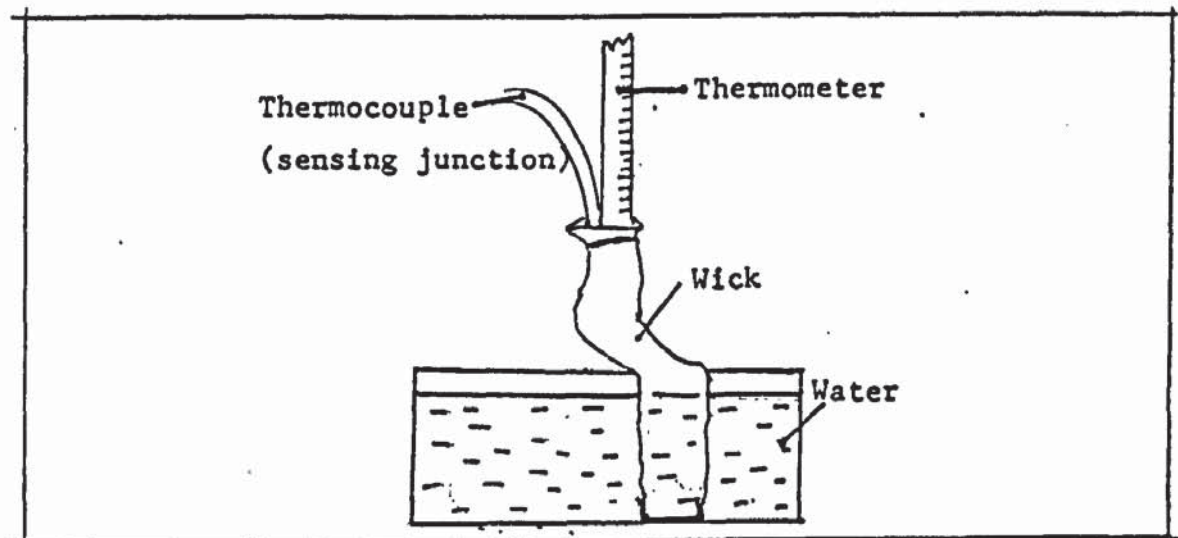


Fig (4.18) Measuring the wet bulb temperature .

4.12.2 The Calculation Of Air Relative Humidity

The calculation is based on the thermodynamic wet bulb temperature, (definition in (19)), which is a unique property of a given moist air sample independent of the measurement technique utilized. The wet bulb temperature is the equilibrium temperature of the bulb-as water evaporates from the wick of the psychrometer . The difference between

the thermodynamic wet bulb temperature and the wet bulb temperature is small (19) , and in this case it is assumed to be zero. The calculation of relative humidity from wet and dry bulb temperatures is done by the following procedure.

1. The saturated water vapour pressure P_s at a given temperature is calculated from

$$\ln(P_s) = - \frac{5800.2206}{T} + 1.3914993 - 0.04860293 T + 0.41764768 \times 10^{-4} T^2 - 0.14452093 \times 10^{-3} T^3 + 6.5459673 \ln(T) \quad (4.12)$$

where P_s : saturation pressure in Pa

T : absolute temperature in K.

Let the saturation vapour pressure at dry bulb temperature be P_s and P_{s^*} at the wet bulb temperature.

2. The humidity ratio at wet bulb temperature, W_{s^*} , which is the ratio of the mass of water vapour to mass of dry air in saturated air at the wet bulb temperature.

$$W_{s^*} = 0.62198 \frac{P_{s^*}}{P_a - P_{s^*}} \quad (4.13)$$

where P_a is the atmospheric pressure (in Pa). The constant 0.62198 is the ratio of the molecular weight of water to the molecular weight of dry air.

3. The humidity ratio W , which is defined as the mass of water vapour to the mass of dry air is determined from equation (4.14).

$$W = \frac{(LH + (C_{pv} - C_{pw})W_{s^*} - C_{pa}(t - t^*))}{LH + C_{pv} t - C_{pw} t^*} \quad (4.14)$$

where LH : Latent heat of evaporation of water at 0C taken as 2501 kJkg^{-1}

C_{pv} : The mean specific heat of water vapour over the range of

interest, taken as 1.84 kJ/kg C .

Cpw : Specific heat of water, taken as 4.195 kJ/kg C

Cpa : The mean specific heat of air over the range of interest ,
taken as 1 kJ/kg C .

t,t*: the wet and dry bulbs temperature in C

Putting in figures for the constants, equation (4.14) now become,

$$W = \frac{(2501 - 2.355 \times t^*) \times W_s - (t - t^*)}{2501 + 1.84 \times t - 4.195 \times t^*} \quad (4.15)$$

(for derivation of equation see (49)).

4. From equation (4.13) above, the humidity ratio at dry bulb temperature W_s is calculated using P_s .

5. The degree of saturation μ , which is the ratio of the air humidity W to the humidity ratio of saturated air at the same temperature,

$$\mu = \frac{W}{W_s} \quad (4.16)$$

6. Finally the relative humidity is calculated from

$$RH = \frac{\mu}{1 - (1 - \mu) \left(\frac{P_s}{P_a}\right)} \quad (4.17)$$

4.13 The Computer Program

Figure (4.19) shows the flow chart of the computer program for the data acquisition system. The inputs to the program are the number of samples required, n , and the time interval between the sets of readings, t . After reading transducer output signals, the computer then saves the data on the magnetic disc for a complete analysis at some later time. The voltages are then converted to the appropriate units and some calculations are done. The result is then displayed on the computer screen. The full computer program is shown in the appendix .

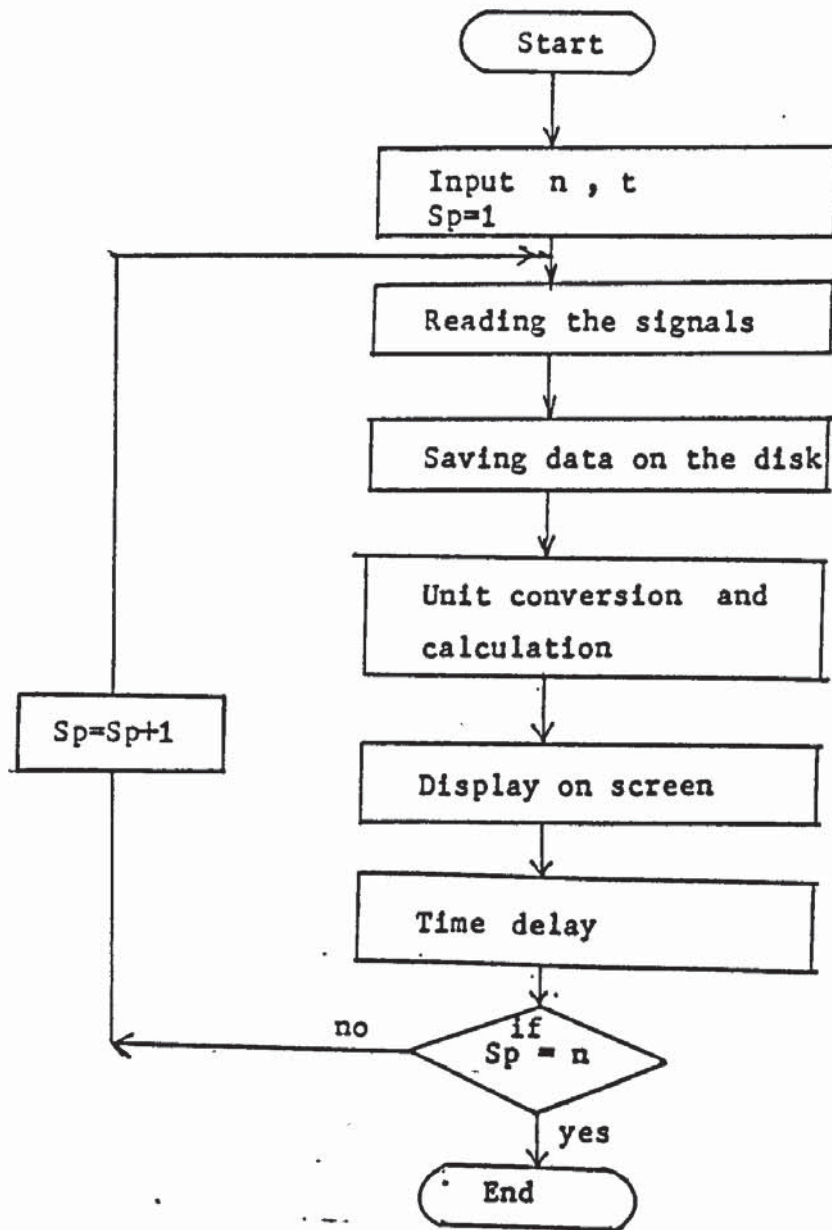


Fig (4.19) The flow chart for the data acquisition program.

READING NO: 1 :FILE :10 :DISC 3

R12 TEMP	73.84	40.50	23.44
	4.30	13.7	9.40
WATER TEM	12.00	44.50	45.00
WET B:OUT	8.00	IN	10.10
R HUM:OUT	85	IN	70
AIR T:OUT	9.95	IN	15.50
R12 COND.	40.50	35.50	36.20
PRES PSI	135.8	126.5	120.2
	119.5	52.5	50.4
IFR KG/S:CON	.0085	: R12 :	.00756
AIR M3/S	.100		
ELC J/S:COM	305	: FAN :	50.4
HEATJ/S:OUT	1200	IN	900
COP	3.42	TIME(M)	10.20

Fig (4.20) Display on the computer screen during a typical experiment.

CHAPTER 5

EXPERIMENTAL RESULTS

The objects of the experimental programme of work were to study the thermodynamic characteristics of the components of the heat pump system , and the behaviour of the system as a whole , under various operating conditions , and also to obtain the empirical relationships required by the computer model.

The first experiment was to find the optimum suction superheat of the system . The suction superheat was varied by adjusting the setting of the expansion valve. The second experiments were to investigate the effects of air inlet temperatures and flow rates on the evaporator and heat pump system. The following experiments were for the determination of the compressor efficiencies and energy balance. Experiments were also conducted to investigate the condenser characteristics ; temperature profiles along the condenser length, the effect of subcooling and the variation of hot and cold water temperatures. The final experiments were on the transient response of the heat pump to the changing in the air inlet temperatures.

Since some of the relationships required by the computer model cannot be derived theoretically data from these experiments were used. The data were fitted for the required relationships using computer programs which were developed in the present work. The information required from the experimental work for the computer model and the fitting of the required equations will be discussed in chapter 6 .

5.1 The Expansion Valve: Variation Of Suction Superheat

The expansion valve is factory adjusted to give a superheat of 6 C in the suction line at an evaporating temperature of 0 C. This adjustment was varied in order to investigate the effect of changes in the degree of the superheat. Figure (5.1) shows that increasing the superheat will reduce the evaporating temperature T_e . The input power to the compressor is decreasing (figure(5.3)) because of the decreasing in T_e . Since the freon mass flow rate is decreasing with increasing superheat (figure (5.2)), the heat output (at condenser) is also decreasing (figure (5.3)).

The suction superheat is increased by reducing the opening of the expansion valve (chapter 3). This will reduce the freon flow rate. With less freon present the area of evaporator used for evaporation is reduced, and that for superheating of freon vapour is increased. Thus the evaporator becomes less effective and the amount of suction superheat increases. This will bring down the evaporating temperature, T_e , and so the COP, as shown by the experimental results (figure(5.4)), therefore it can be concluded that excessive suction superheat will reduce the evaporator capacity and the heat pump COP. The experimental results show that for this heat pump, the most effective suction superheat is less than 10 degree C for an air inlet temperature of about 23 C.

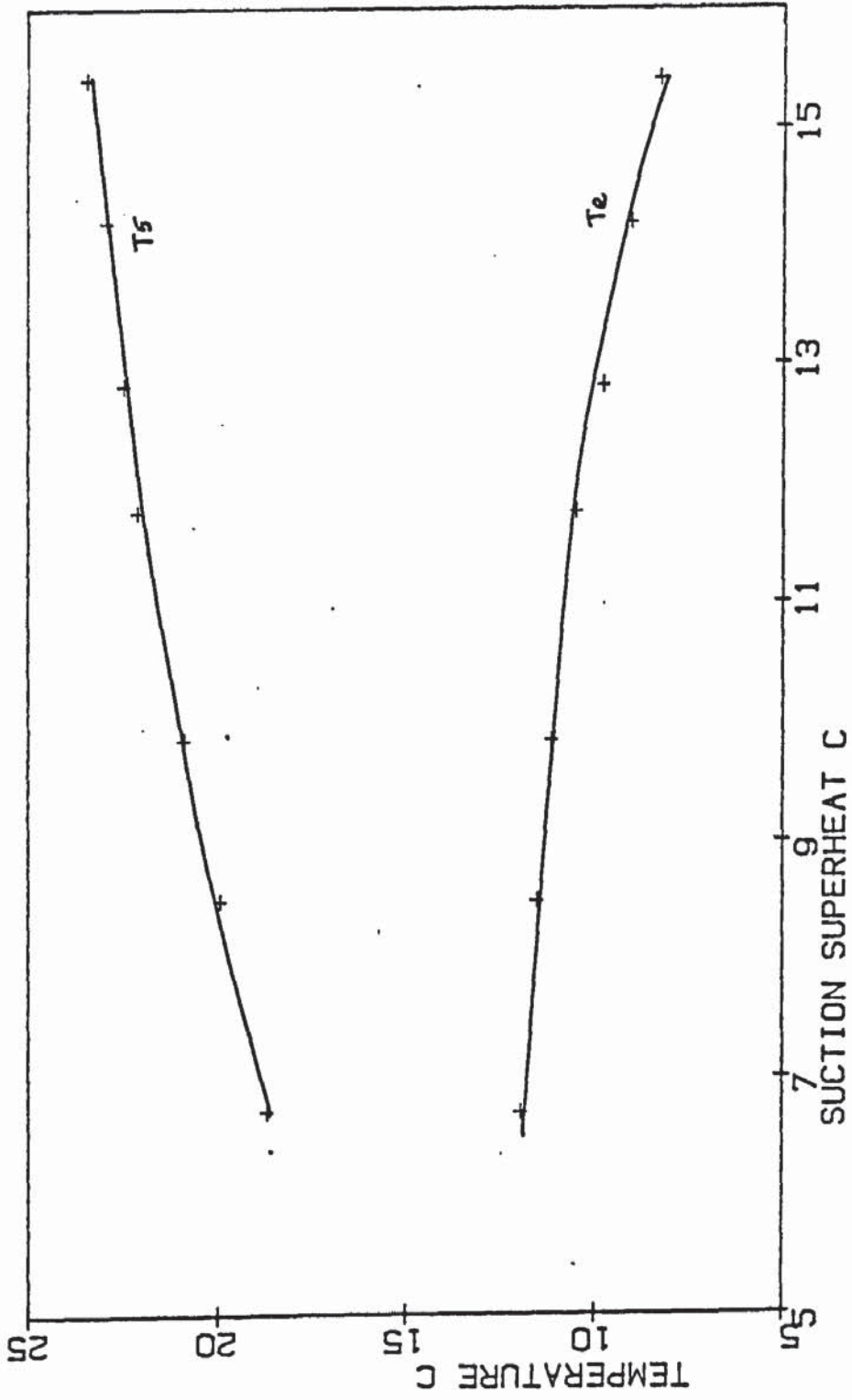
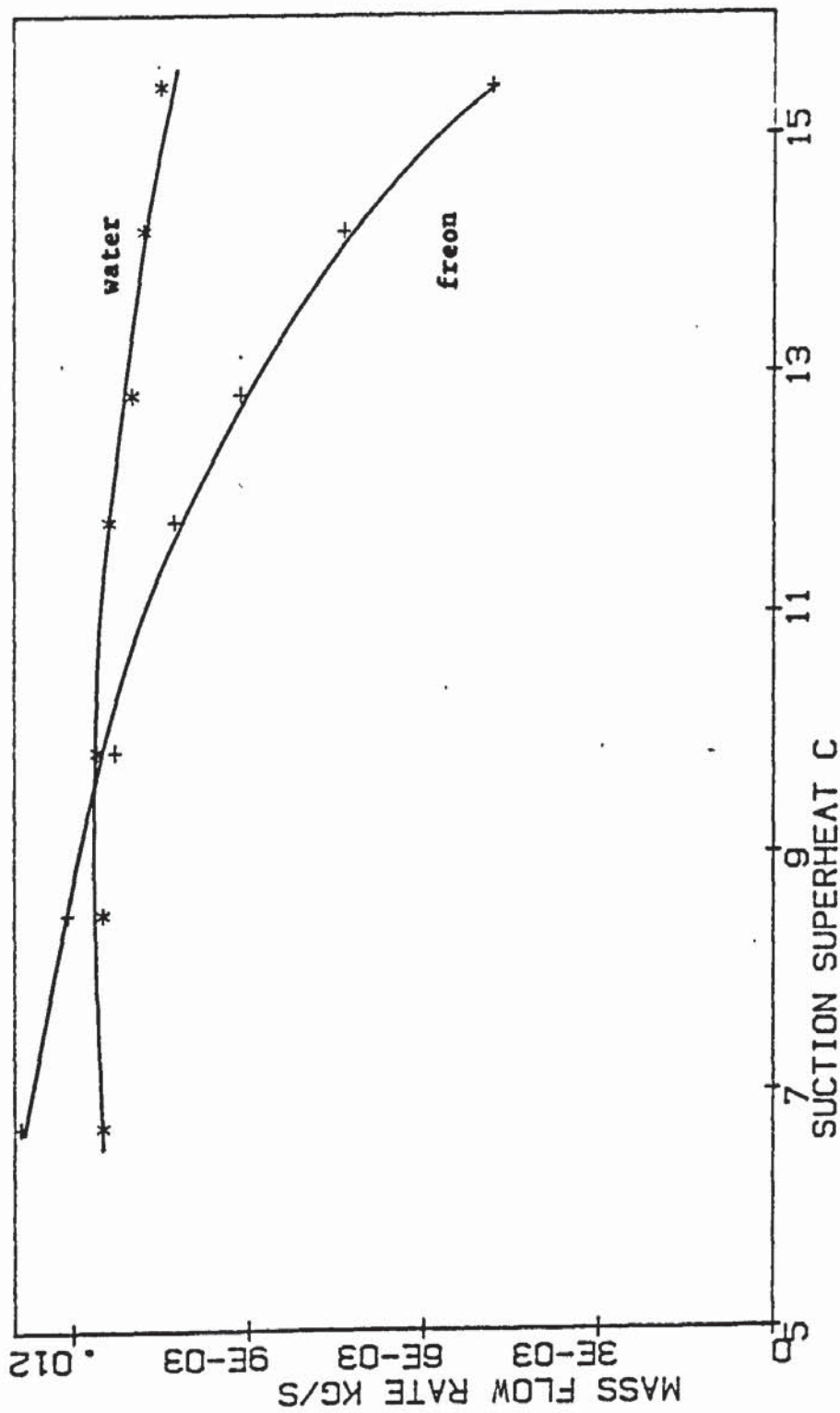


Fig (5.1) The variation of T5 and Te with suction superheat. The operating condition are; $A_1=23C$, $A_s=0.1m\ s^{-1}$, $T_w(1)=12\ C$, $T_w(o)=45C$.



Fig(5.2) The variation of freon and water mass flow rates with suction superheat. Operating under the same condition as in fig(5.1).

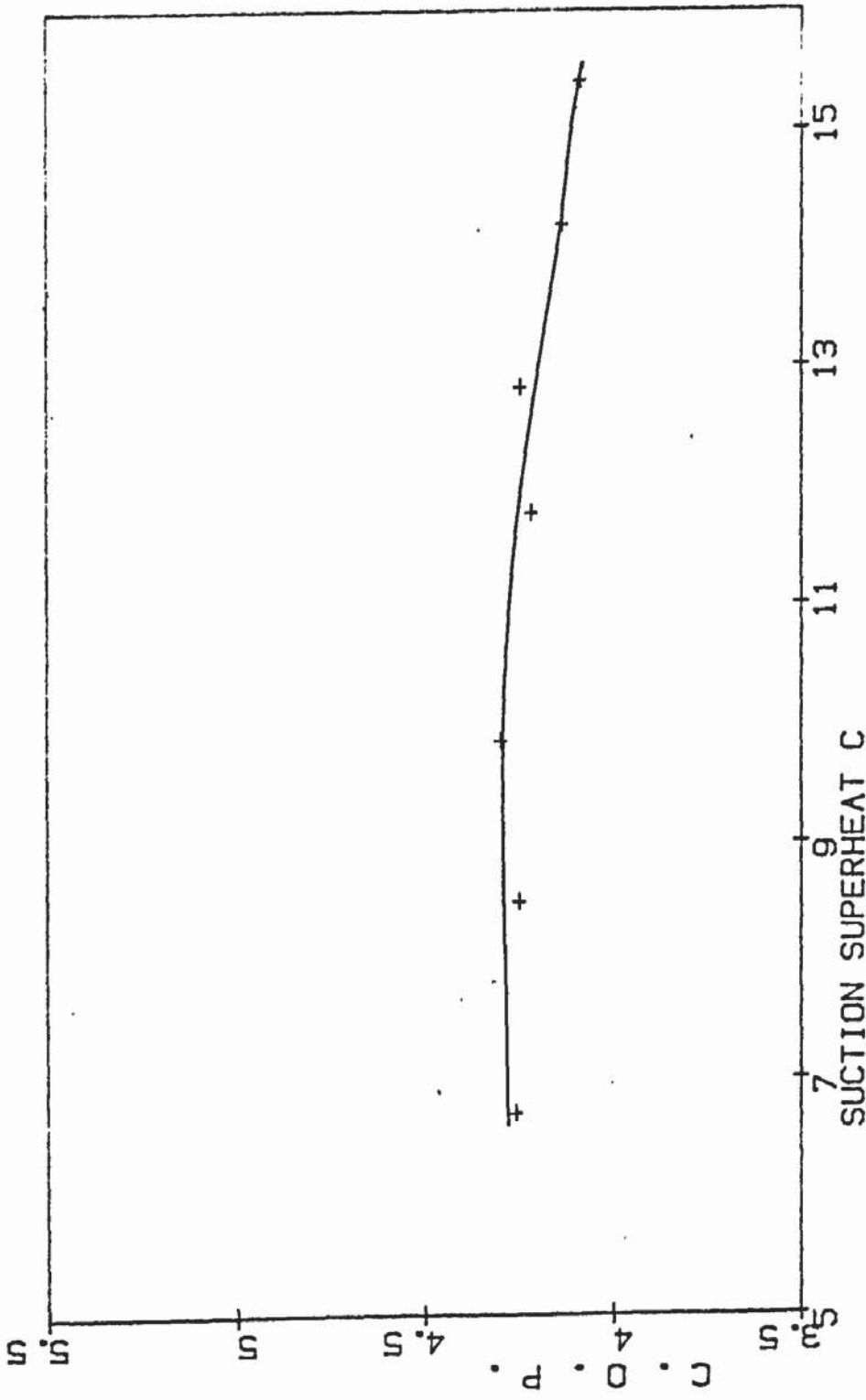


Fig (5.3) The plot of COP against suction superheat. Operating under the same condition as in fig(5.1).

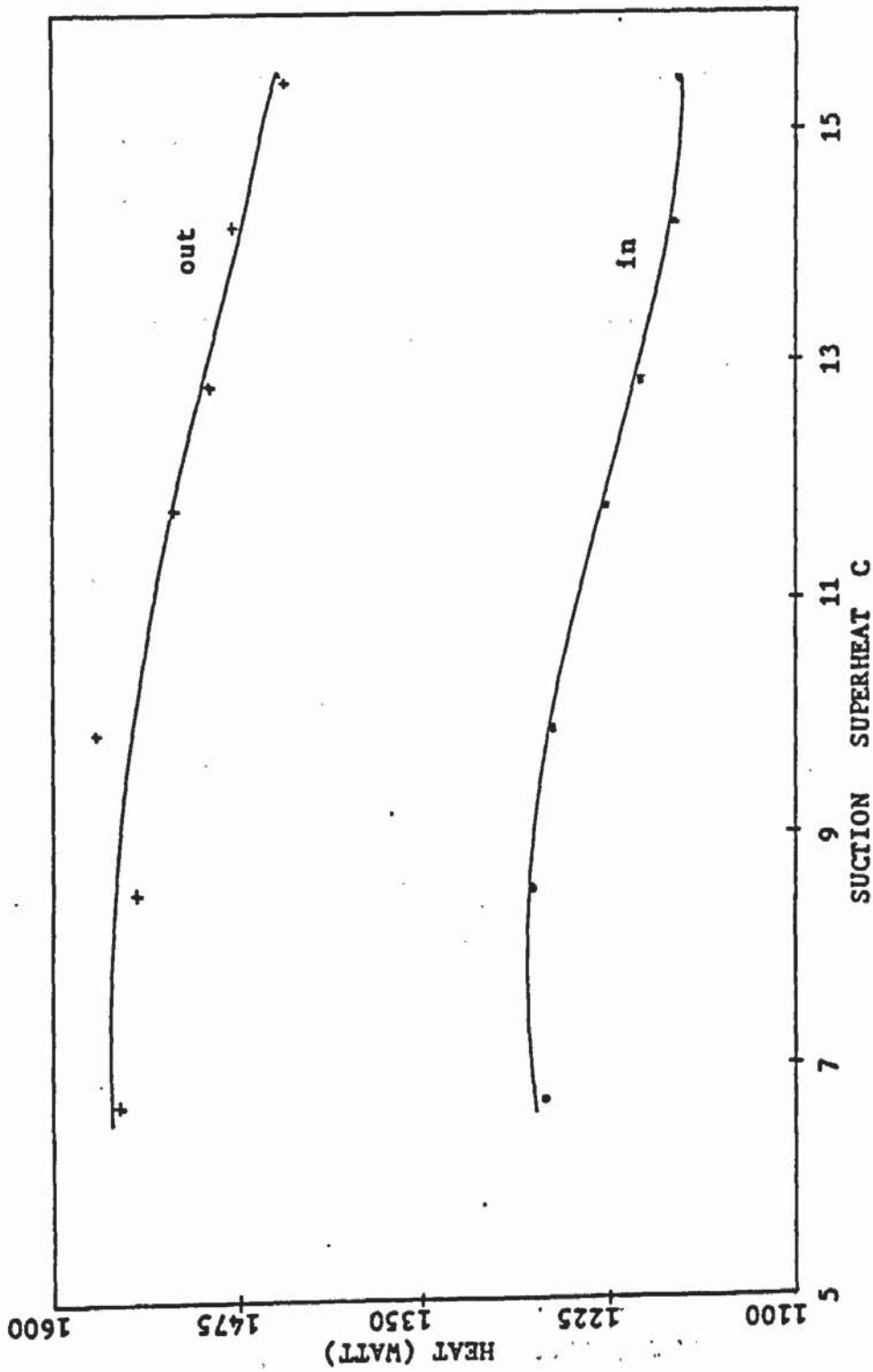


Fig (5.4) The variation of heat input and output with the suction superheat. Operating under the same condition as in fig(5.1).

5.2 The Evaporator

There are two main factors affecting the evaporator performance, air inlet temperature and air speed. The air inlet temperatures were varied in the experiment by using an air heater, while the air speeds were changed by controlling the input power to the fan via a variac (chapter (3)).

5.2.1 The Effect Of Air Inlet Temperature

Figure (5.5) shows the relationship between air inlet and evaporating temperatures. The air inlet temperature $T_a(i)$, evaporating temperature T_e and evaporating pressure were all measured in the experiment. The evaporating temperature T_e' was calculated from P_4 , the evaporating pressure. The values of T_e and T_e' as shown in table (5.1) are agreed to a good accuracy.

$T_a(i)$ (C)	T_e (C)	P_4 (bar)	T_e' (C)
23.57	10.62	4.303	10.53
19.65	7.96	3.993	8.08
16.12	5.25	3.649	5.19
14.63	3.2	3.373	2.72
10.78	0.8	3.149	0.61
7.76	-0.3	3.027	-0.6
7.04	-1.8	2.891	-1.98

Table (5.1) The evaporating temperature as measured by the thermocouple and pressure transducer.

The experimental results show that increasing the air inlet temperature will increase the evaporating pressure and temperature, because more heat is now available to the freon. As a result, the pressure of the

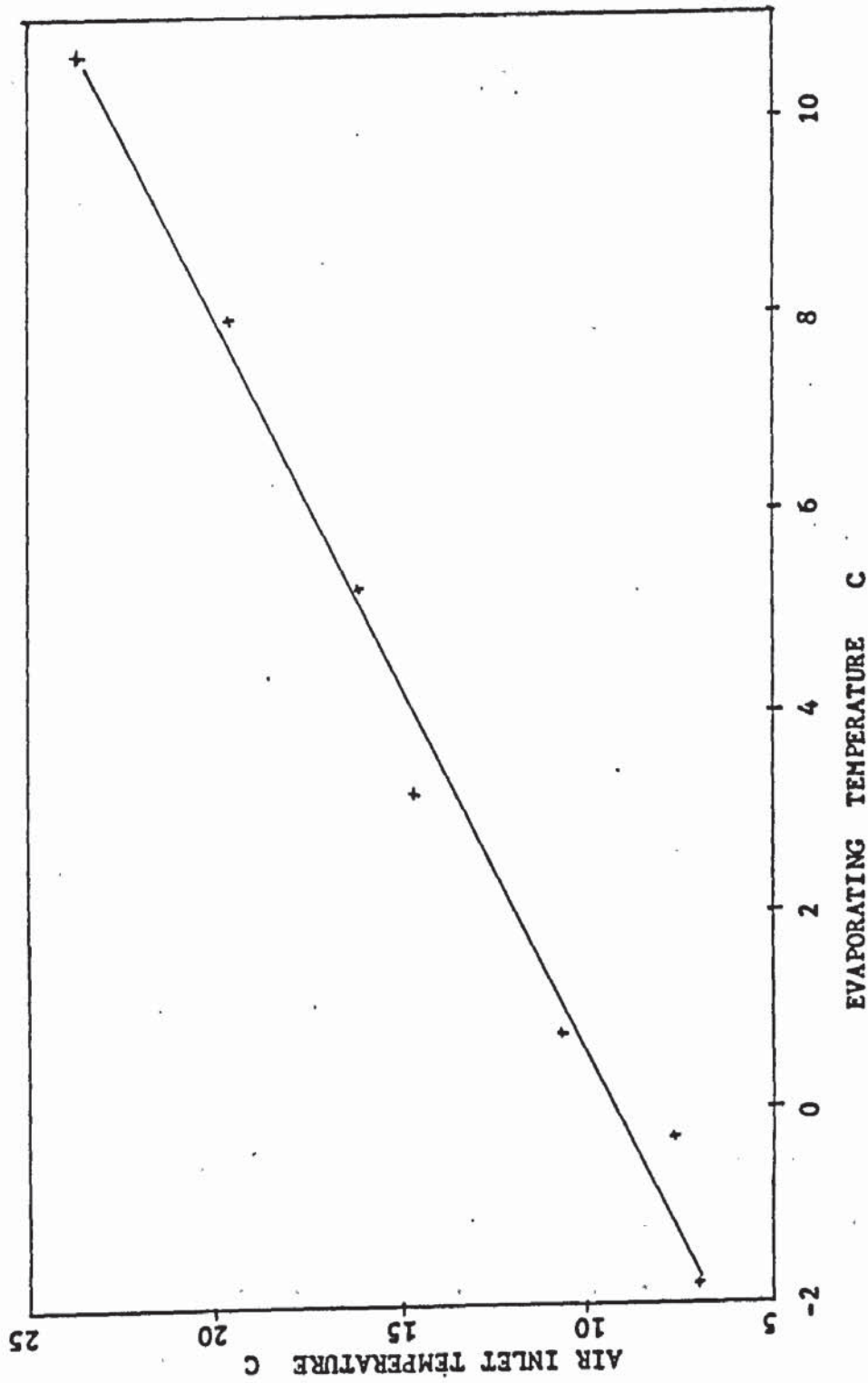


Fig (5.5) The evaporating temperature is increasing with the air inlet temperature.
 Operating condition; $T_w(1)=12.4\text{ C}$, $T_w(0)=45\text{ C}$, $A_s=0.1\text{ m s}^{-1}$.

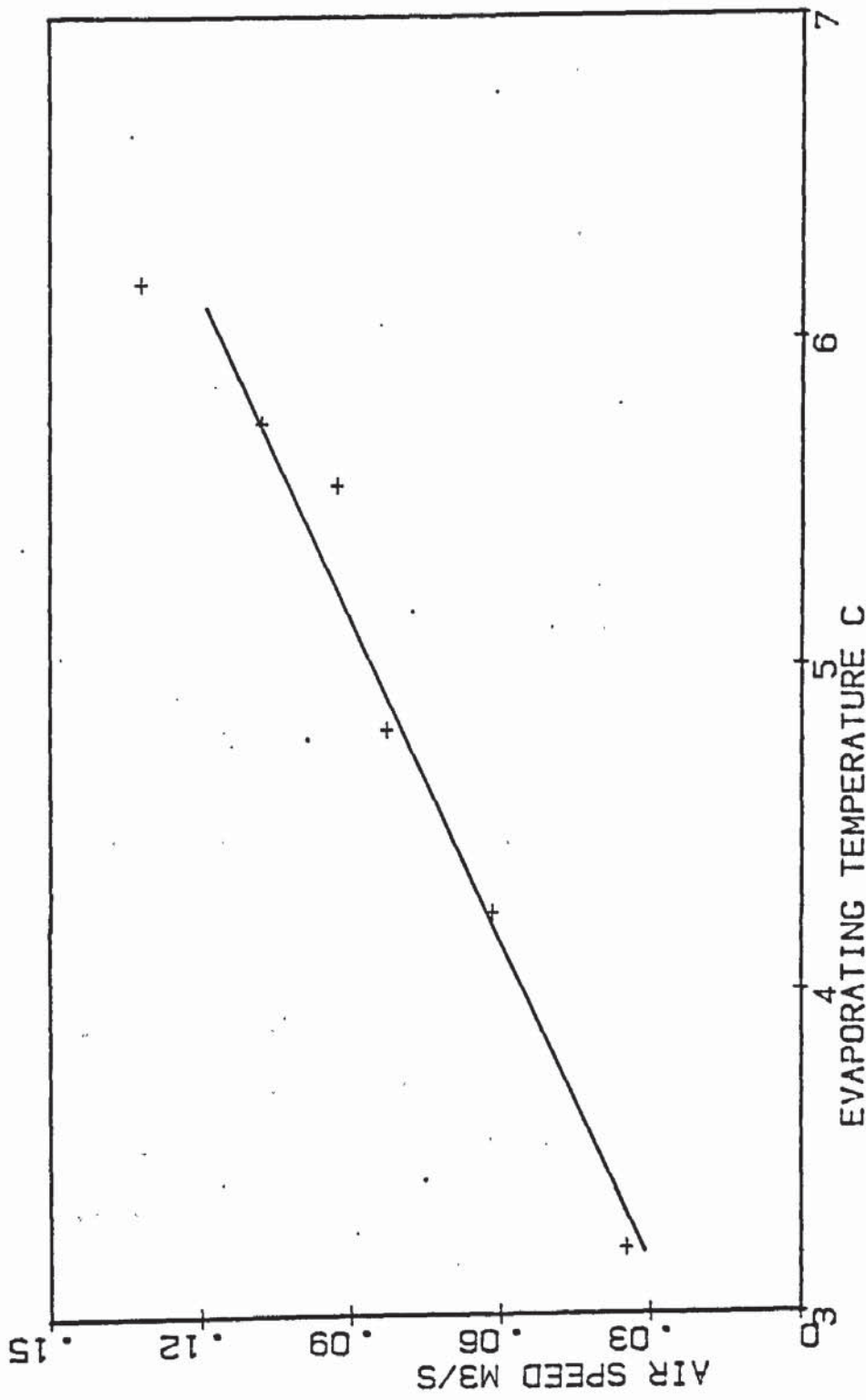
power fluid of the expansion valve is also increased and forces the valve to open wider, therefore allowing more freon to flow. When the input energy (from air) is higher, so is the output energy (to water). Since the work done increases only slightly, the COP is higher at higher air temperature, as shown in table (5.1a) below. The operating conditions of readings in table (5.1a) are the hot water temperature is 45C (Tc=40C), the inlet cold water temperature is 12C and air speed is $0.1 \text{ m}^3 \text{ s}^{-1}$ (relative humidity is about 60 %).

Ta(i) (C)	Qout (W)	Wcomp (W)	COP
23.57	1670	322	4.49
19.65	1535	316	4.19
16.12	1403	310	3.90
14.63	1286	305	3.62
10.78	1130	300	3.23
7.76	930	294	2.70
7.04	895	285	2.67

Table (5.1a) The COP is higher at higher air temperature Ai

5.2.2 The Effect Of Air Speed

The main function of the fan in the heat pump system is to increase the air circulation through the evaporator in order to provide heat input and to ^{reduce} the formation of frost on the evaporator outside surface. Increasing the air circulation means more heat is transferred to the freon, increasing the evaporating temperature and so the COP. Since the fan requires input power for operation, there is an optimum air speed for a given heat pump system.



Fig(5.6) Increasing air speed will increase the evaporating temperature.

$T_w(1) = 11.8C$, $T_w(0) = 45C$, $A_1 = 15 C$

In table (5.2) the input power required for several air flow rates are given for the fan as described in chapter (3). The result shows that the maximum COP is achieved when the air speed is $0.11 \text{ m}^3\text{s}^{-1}$. To produce this speed, the fan required 52 W of input power. This represents about 4% (or $\frac{1}{25}$) of the heat output. For the air speed higher than $0.11 \text{ m}^3\text{s}^{-1}$, the heat output is increased, but not the COP.

Air Speed (m^3s^{-1})	Fan Power (W)	Comp. Power (W)	Heat Out (W)	COP
0.04	29.8	301	1168	3.53
0.06	36.0	303	1258	3.71
0.08	44.3	304	1297	3.72
0.11	52.0	305	1334	3.73
0.13	63.3	306	1367	3.70
0.16	70.1	306	1390	3.69

Table (5.2) The effect of air speed on the system COP

5.2.3 The Effect Of Relative Humidity

Apart from the air temperature and speed, the air humidity also affects the heat pump performance. In this experiment, the air humidity is not a controlled parameter, but the humidity at the inlet and outlet of the evaporator was measured. In general it was found that for an air speed of $0.1 \text{ m}^3\text{s}^{-1}$, and air temperature about 14C , the relative humidity difference between the inlet and outlet of the evaporator is about 20%.

The experimental results also show that the relative humidity difference across the evaporator increases while the air speed decreases (table (5.3)). At the lowest air speed (about $.04\text{m}^3\text{s}^{-1}$), the outlet

Relative Humidity (IN) %	Relative Humidity (OUT) %	Air Speed (m s^{-1})	Heat Out E_o (W)	Moist Air Energy E_m (W)	Dry Air Energy E_d (W)	Comp Energy E_c (W)	T_e (C)	(i) $\frac{(E_m - E_d)}{E_m} \times 100$ %	(ii) $\frac{(E_m - E_d)}{(E_m + E_c)} \times 100$ %
70.2	92.9	0.131	1360	1160	955	306	6.21	17.7	14.0
72.7	92.5	0.108	1334	1100	823	305	5.61	25.2	19.7
71.2	95.1	0.083	1297	1000	708	305	4.81	29.3	22.4
73.2	97.7	0.066	1280	980	598	304	4.53	39.0	29.8
73.4	99.0	0.045	1214	926	480	297	3.62	38.1	36.5

Table(5.3) Shows the effect of relative humidity and air speed on the heat pump performance.

Column (i) indicates the percentage contribution of condensed water to the heat input .

Column (ii) indicates the percentage contribution of condensed water to the heat output.

relative humidity was about 100%. It was observed the water vapour had condensed on the evaporator surface. Over a period of 45 minutes, 156 ml of condensed water was collected, which is equivalent to a heat of condensation of 130 W. Since it was not possible to collect all the condensed water and some of it evaporated back into the air before it could be measured, this energy is a lower estimate of the exact amount of energy transferred to freon from the process of condensation.

From table (5.3) it can be seen that the heat pump energy balance agrees within an error of 5% when the air relative humidity is used in the calculation. Neglecting the humidity gives an error of about 14% at air speed of $0.13 \text{ m}^3 \text{ s}^{-1}$. and 36% at speed of $0.04 \text{ m}^3 \text{ s}^{-1}$ in the heat output and COP.

5.2.4 The Heat Transfer Coefficient

The heat transfer coefficient of the evaporator for the air side, H_c is calculated using the method described in chapter 3. Rewriting equation (3.20), neglecting terms of minor effect,

$$\frac{1}{H_c} = \frac{1}{E_o h_a} + \frac{A}{A_r h_r} \quad (5.1)$$

where E_o is the evaporator overall efficiency. The value of E_o and h_a are evaluated using equation (3.24) and (3.21) respectively. There are several methods of determining h_r , the heat transfer coefficient of the freon. The methods as described by Blundell (33) and Dengler and Addom (43) (also applied by Tassou (39) in his heat pump model) are chosen here. The results from these two methods are then compared with the heat transfer coefficient measured in the experiments (figure (5.7)).

The experimental heat transfer coefficient $H_c(\text{exp})$ was calculated from,

$$H_c(\text{exp}) = \frac{\text{Energy Input}}{\text{Heat Transfer Area} \times \Delta T} \quad (5.2)$$

Where $\Delta T = (T_a(i) - T_a(o)) / \log((T_a(i) - T_e) / (T_a(o) - T_e))$ and the energy input was calculated from $\dot{M}_a C_p (T_a(i) - T_a(o))$. In the experiment the air was recycled to produce the lower temperatures, and by the time the steady state was reached, almost all the water vapour had been removed. Therefore the experimental calculation, as with both theoretical models, ignored the effect of the air relative humidity. As can be seen from figure (5.7), the experimental curve is closer to the Dengler and Addom curve than that of Blundell. This is because Blundell used only the liquid properties of the refrigerant in his calculation, while Dengler and Addom used both the liquid and vapour properties. The non-uniform flow of air through the evaporator gave rise to a range of values of $T_a(o)$. The average value of $T_a(o)$ was estimated to be uncertain to 0.5 degree C. This gives rise to an uncertainty in the $H_c(\text{exp})$ of about 15 % .

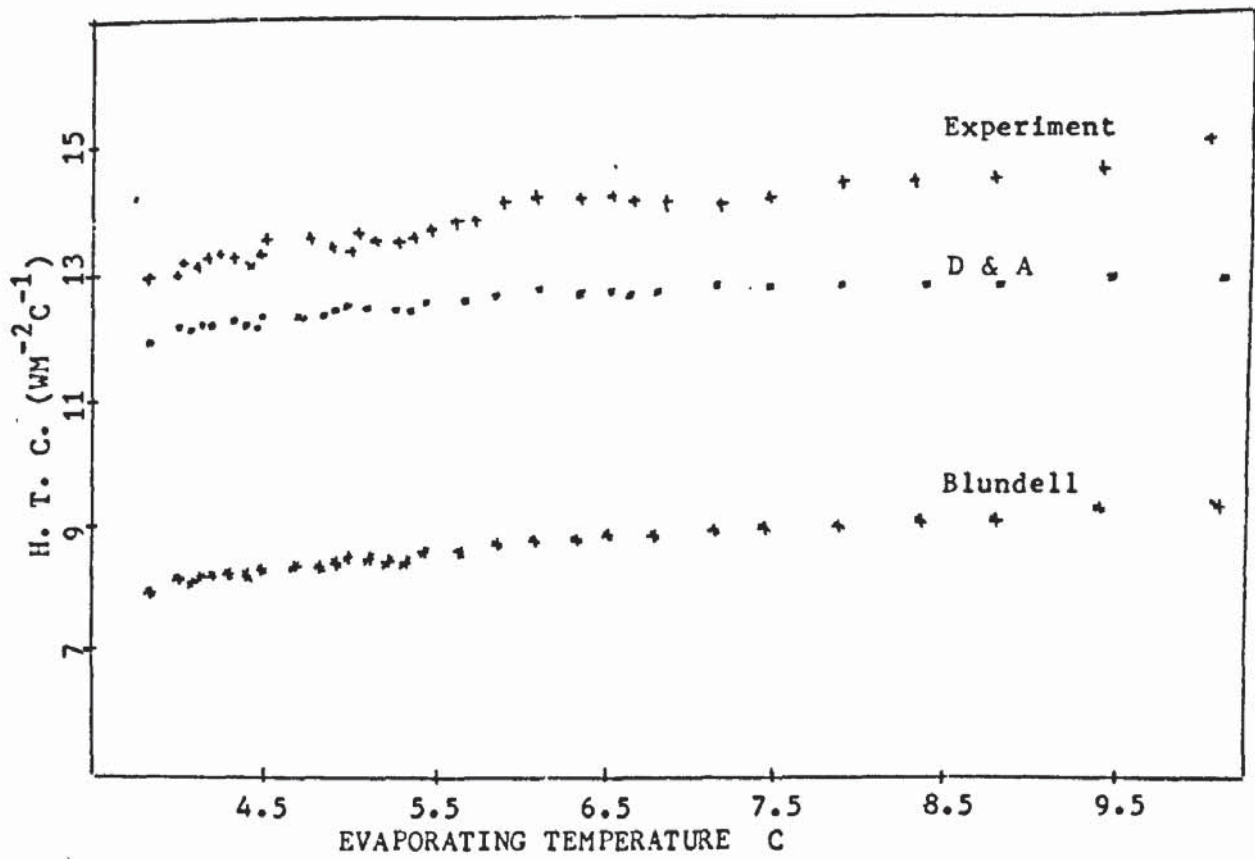
5.3 The Compressor

5.3.1 Variation Of Polytropic Index With Compression Ratio

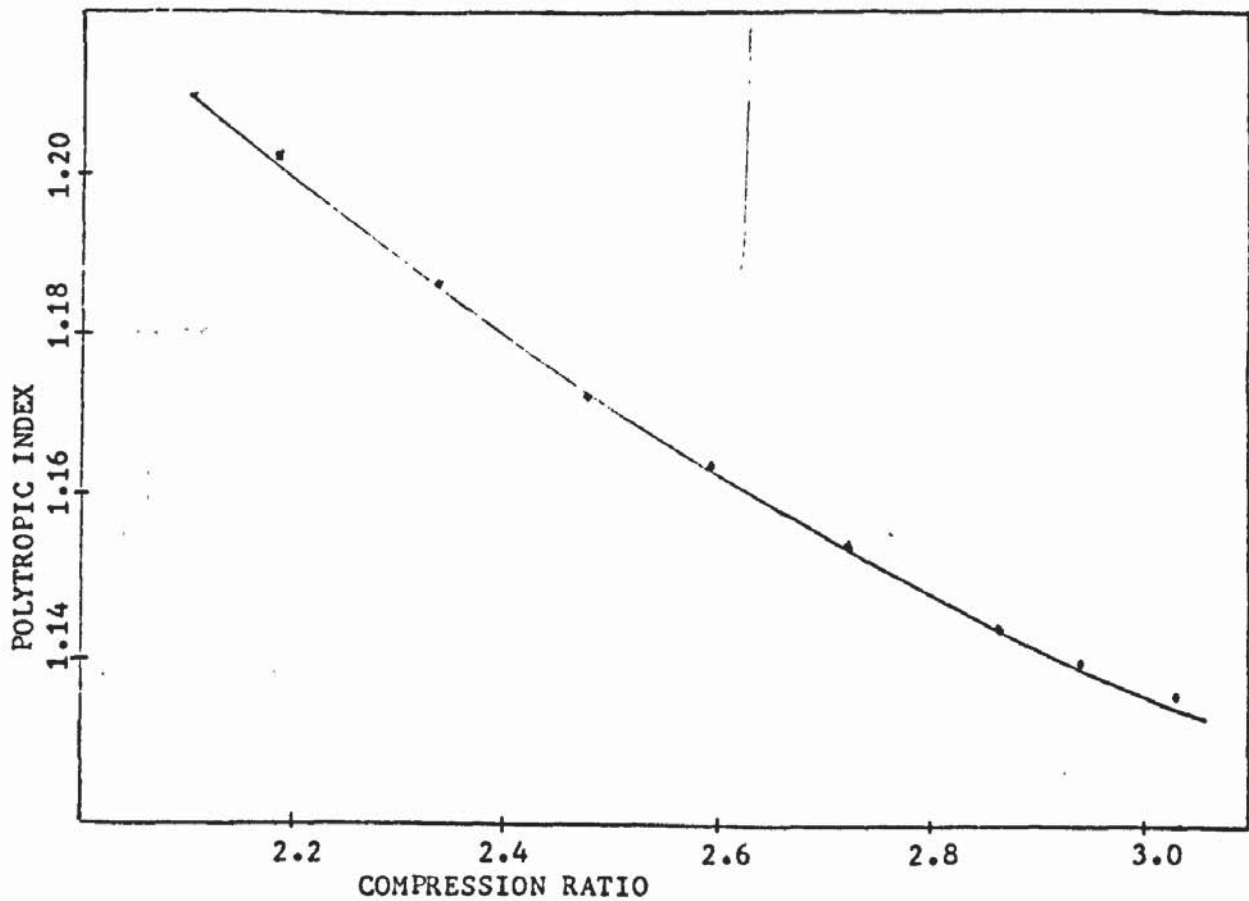
Figure (5.8) shows a plot of polytropic index n against compression ratio C_r (discharge pressure/suction pressure) for a reciprocating compressor which is cooled by water discharged from the condenser (figure(5.9)). The graph shows that n decreases, or approaches γ (isentropic index), with increasing C_r . The heat extracted from the compressor by the cooling water is also decreasing, at higher C_r . This is because at higher C_r , the coefficient of performance is lower.

5.3.2 Variation Of Hot Water With Compression Ratio

The main aim of cooling the compressor with hot water from the condenser is to increase the final water outlet temperature by about 1 degree C.



Fig(5.7) Evaporator heat transfer coefficient at several evaporating temperatures .



Fig(5.8) Polytropic index versus compression ratio. $T_w(1)=12\text{C}$, $A_s=.1 \text{ m}^3 \text{ s}^{-1}$

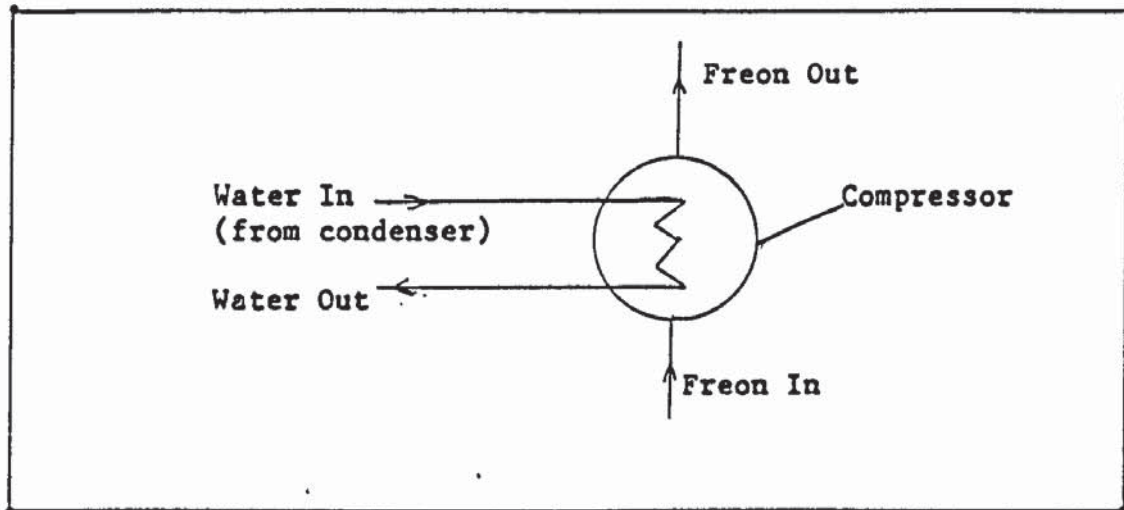


Figure (5.9) The compressor is cooled by water from the condenser.

The experimental results (figure (5.10)) show that the maximum temperature increase is achieved when Cr is between 2.4 and 2.6 . When Cr is higher than 2.6, the water temperature is high ,therefore reducing the amount of heat that can be absorbed from the compressor. As a result the increase in water temperature is small. When Cr is lower than 2.4, the water temperature is low but the flow rate is high. Even though more heat can be absorbed from the compressor , because of the large amount of water involved, the water temperature increases only slightly.

The compressor Cr can be changed manually by adjusting the water flow regulator valve. Reducing the opening of the valve, that is reducing the water flow rate will increase the Cr . This is because at lower flow rate, the water temperature is increased.As a result the energy that can be transferred from freon to water is reduced. The 'untransferred' heat will increase the temperature and pressure of the freon. Since the evaporating pressure is unchanged, Cr is increased.

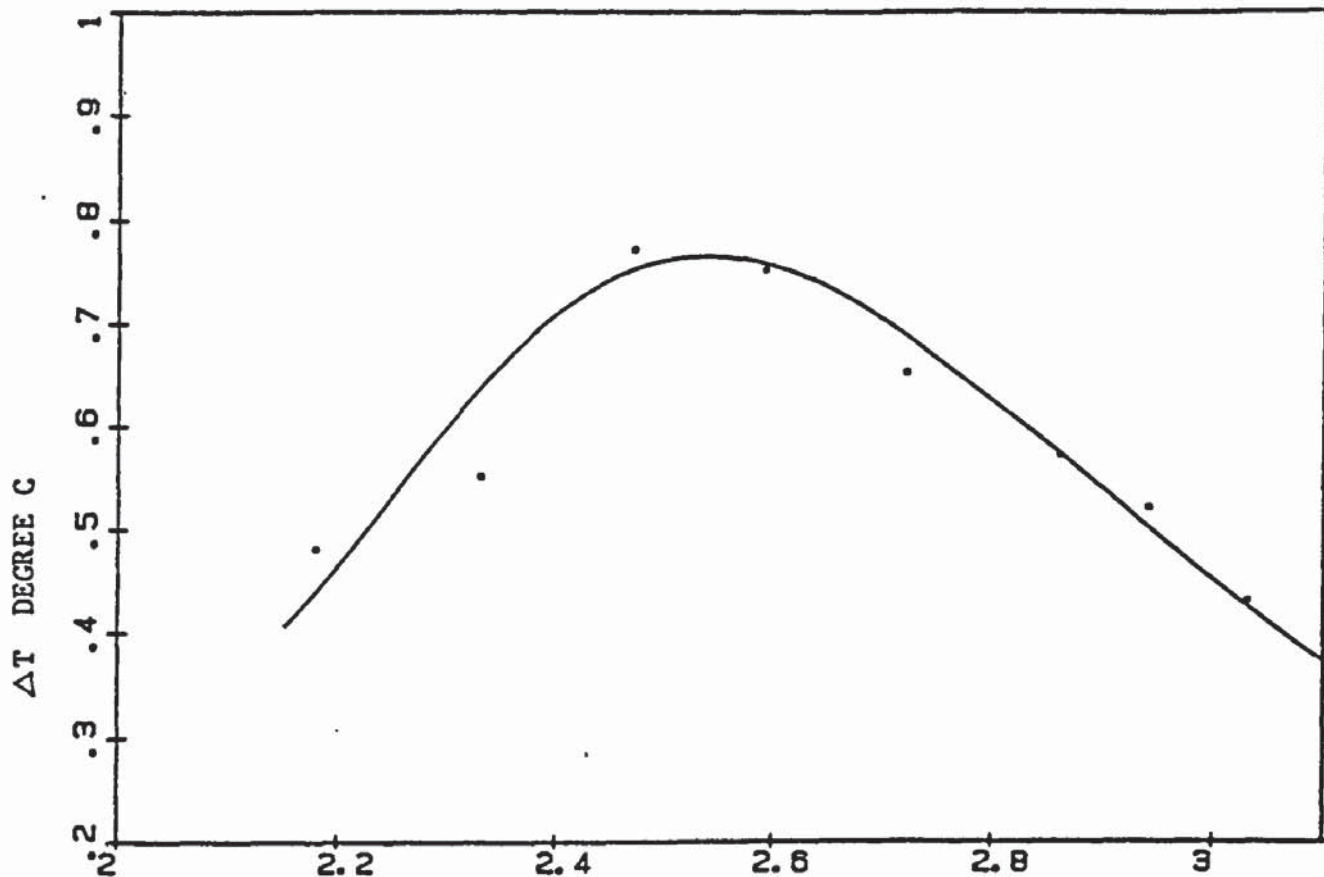


FIG. (5-10) The increase in water temperature after cooling the compressor. Operated under the same condition as fig (5.8).

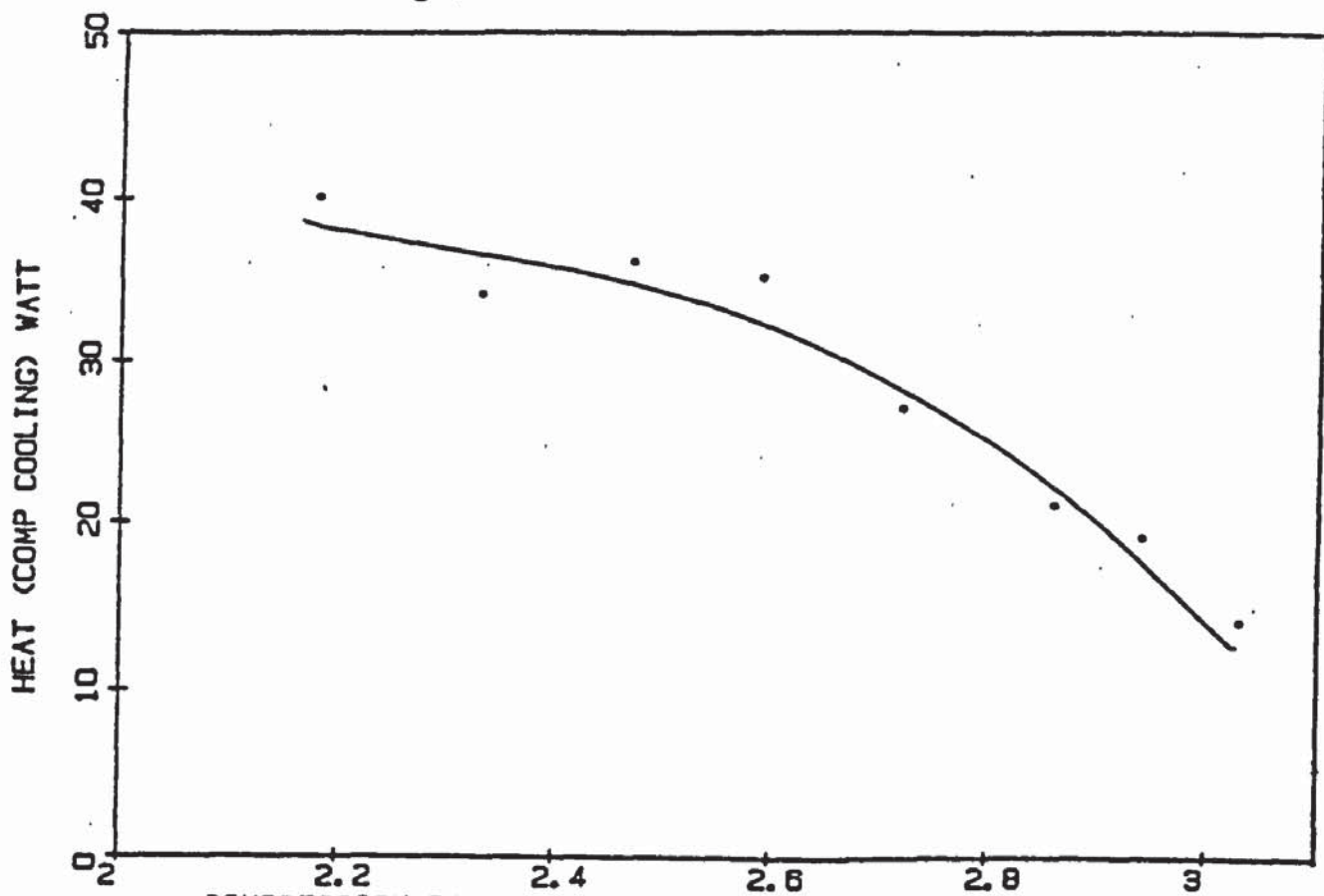


FIG. (5-11) Heat extracted by the cooling water from the compressor. Operated under the same condition as in fig (5.8)

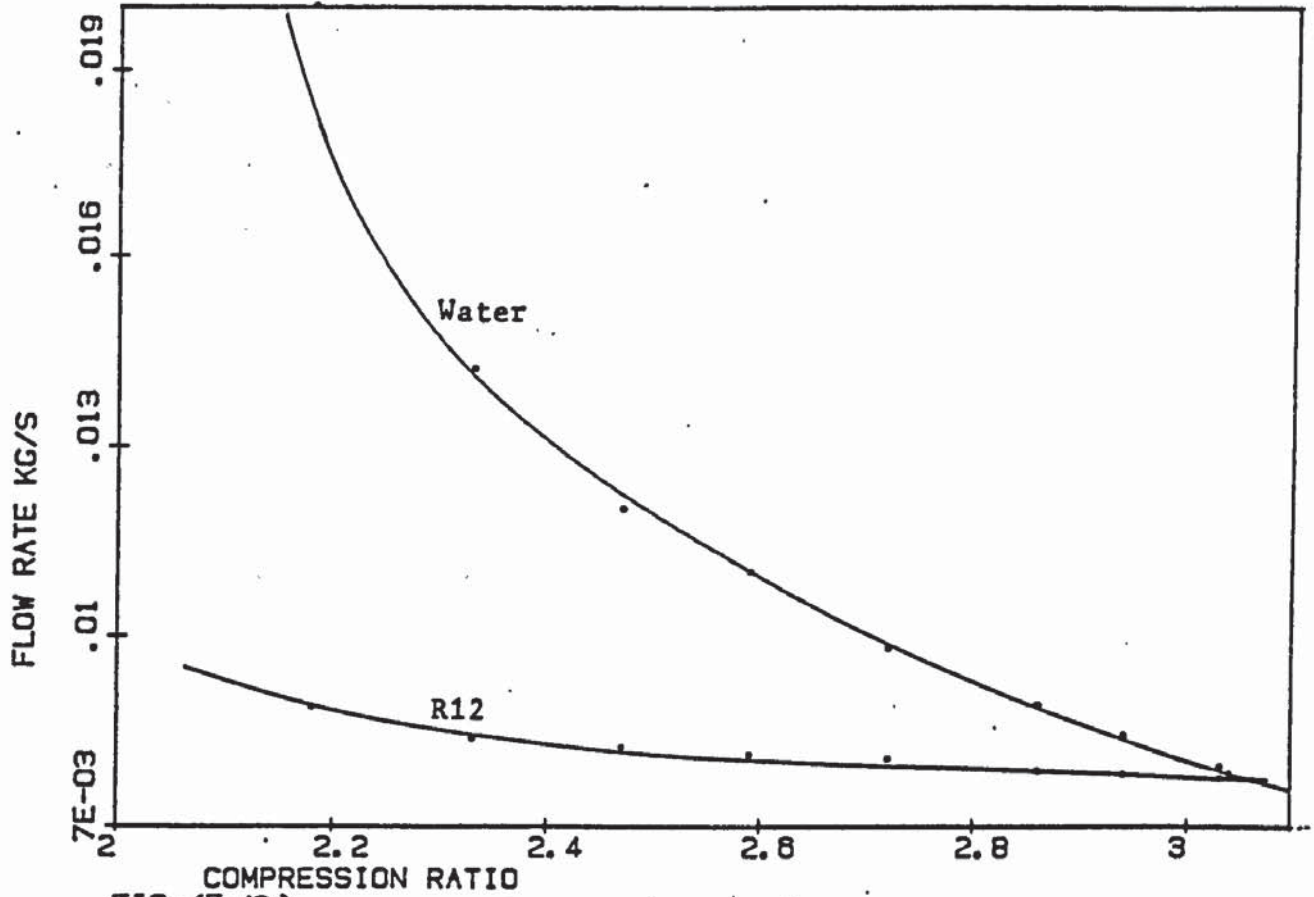


FIG. (5-12) Water and freon mass flow rates change with the compression ratio. Operating condition as in figure (5.8).

Figure (5.12) shows the plot of water and freon mass flow rates against Cr for Cr between 2.18 and 3. As explained above the water flow rate is decreasing with increasing Cr. The plot also shows that the freon mass flow rate is decreasing with increasing Cr. This can be explained from equation (3.6), which shows that η_v is decreasing with increasing Cr (assume n is constant). This reduction in η_v is due to the smaller induce volume V_i as Cr increases so reducing the amount of freon that can be admitted into the compressor. Also at higher Cr the amount of back-leakage from the high pressure side toward the low pressure side is higher (40). This will reduce the freon mass flow rate.

5.3.3 Variation In Condensing And Evaporating Temperatures

Table (5.4) below shows three sets of experimental results where T_e was kept constant at 5C and T_c was set at three different values. The refrigerant cycles of the three results are shown in figure (5.13).

T_c (C)	T_1 (C)	T_3 (C)	Heat Out (W)	Water Flow Rate (kgs ⁻¹)	Freon Flow Rate (kgs ⁻¹)	COP
44.02	77.37	26.43	1294	0.0079	0.0075	3.70
40.41	73.68	24.71	1302	0.0089	0.0087	3.73
36.11	69.07	21.38	1356	0.0109	0.0098	3.86

Table (5.4) Three set of results at $T_e=5$ C.

Another set of results is obtained by keeping T_c constant ($T_c=40C$) and letting T_e takes three values, as shown in table (5.5). The refrigerant cycles are shown in figure (5.14).

Te (C)	T1 (C)	T3 (C)	Heat Out (W)	Water Flow Rate (kgs ⁻¹)	Freon Flow Rate (kgs ⁻¹)	COP
10.65	72.03	26.56	1532	0.0118	0.0111	4.38
5.45	73.54	24.54	1303	0.0093	0.0077	3.72
3.73	75.54	22.29	1250	0.0089	0.0061	3.57

Table (5.5) Three set of result with Tc=40C.

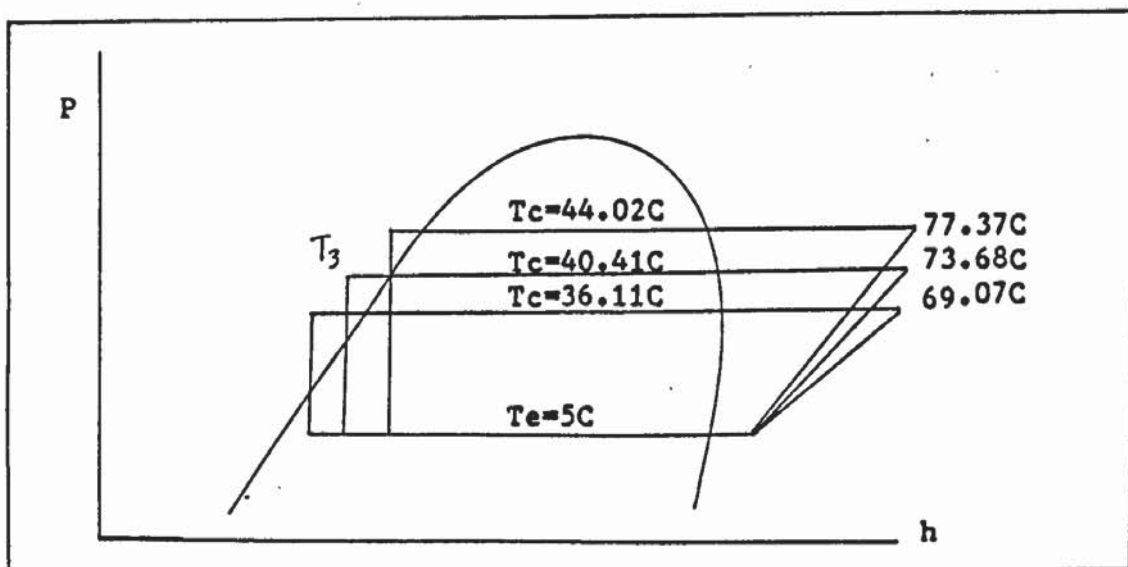


Fig (5.13) The freon cycles with different Tc but constant Te.

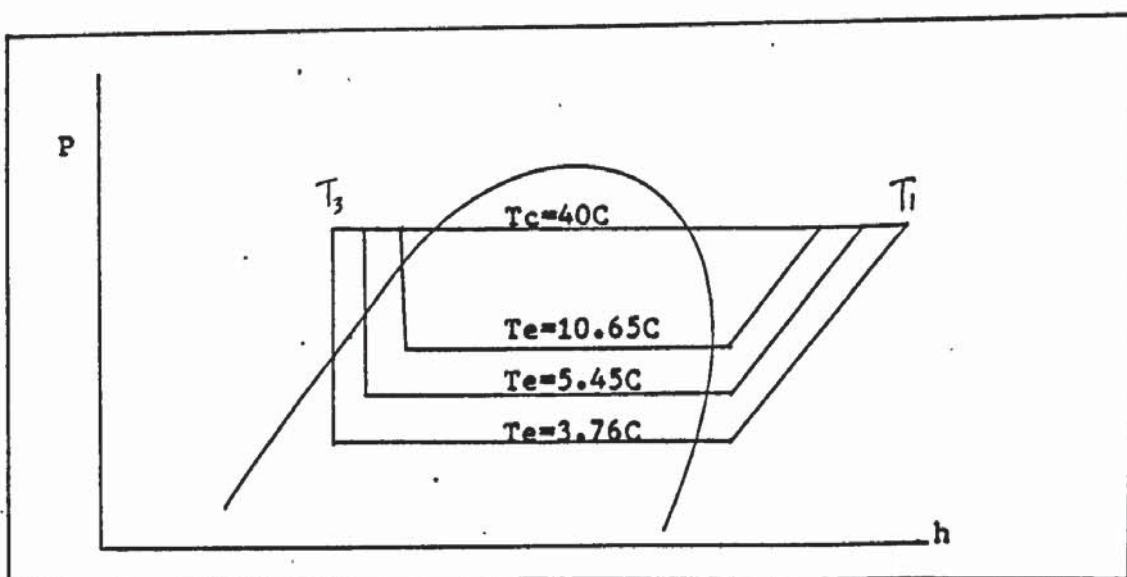


Fig (5.14) The cycles with different Te but constant Tc.

In the first set of experiments (table (5.4)). The Cr is changed by changing the water flow rate, while in the second set (table (5.5)) by changing the air temperature. Both results show that increasing Cr will increase the freon discharge temperature T1 and also the freon liquid temperature T3. In the first case the quality of freon entering the evaporator is increasing with Cr, while in the second set it remains almost unchanged. The most interesting feature here is the water flow rate in the second set of the experimental results. It shows that the water flow rate changes with Cr even though the condensing pressure P1 is unchanged. This is best explained by considering the energy balance in the cycle. At low Te and hence low freon flow rate the COP and output energy are also low. In consequence, to produce approximately the same rise in water temperature, the water flow rate must be lower.

5.3.4 Compressor Energy Balance

Further consideration is given to the compressor energy balance. The increase in enthalpy of any process is given by

$$dh = dQ + VdP$$

If this is integrated over a compression cycle,

$$\Delta h = \Delta Q + \oint VdP$$

The last term $\oint VdP$ is the area enclosed by the cycle on an indicator diagram and is therefore numerically equal to $\oint PdV$ which is known to be the work done by the gas. Algebraically the two terms will differ in sign

$$\Delta h = \Delta Q - \oint PdV$$

Thus if Q_r is the rate of heat gain by freon we have

$$\dot{M}_r (h_1 - h_5) = \dot{Q}_r + F_c W_r \quad (5.3)$$

where W_r the work done on the gas per cycle, is given by equation (3.2), and F_c is the compressor frequency. Since F_c is not known an approximation to the last term is obtained by a perfect gas approach.

$$\dot{M}_r (h_1 - h_5) = \dot{Q}_r + \frac{n}{n-1} \dot{M}_r R (T_1 - T_5) \quad (5.4)$$

The energy flow equation (3.32) would also achieve the same result. Equation (5.4) simply states that in the polytropic process, the total energy transferred to the freon is the sum of the work done by the compressor and the quantity of heat transferred to the freon from the cylinder wall.

In the equation (5.4) above, the value of the gas constant R cannot be taken as the value of the assumed perfect freon gas. This is because at high pressures, the freon gas is not a perfect gas (appendix D). In the experiment, the pressure and temperature at suction P_5 and T_5 and at discharge P_1 and T_1 were measured. The specific volumes at suction and discharge are determined from the values of pressure and temperature ($V=f(P,T)$). The gas constant R is calculated from $R = \frac{PV}{T}$. In table (5.6) R_5 is the gas constant at suction and R_1 at discharge points. The average of R_1 and R_5 is in the right column, and the overall average of R is $61.93 \text{ Jkg}^{-1}\text{C}^{-1}$, this is about 10% lower than the reported value for a perfect gas which is $68.77 \text{ Jkg}^{-1}\text{C}^{-1}$.

Figure (5.15) shows the freon cycle with the symbols used. Line 5i is the isentropic line, where the entropy at 5 is equal to the entropy at i .

Cr	R5 $J(kgC)^{-1}$	R1 $J(kgC)^{-1}$	R ave. $J(kgC)^{-1}$
3.03	63.12	59.85	61.49
2.94	63.13	60.08	61.61
2.85	63.17	60.29	61.73
2.72	63.16	60.52	61.84
2.58	63.19	60.88	62.04
2.47	63.23	61.10	62.17
2.18	63.36	61.88	62.62
Average value of R is $61.93 J(kgC)^{-1}$			

Table (5.6) The value of freon gas constant before and after the compression. If freon is considered as a perfect gas R is $68.77 J(kgC)^{-1}$.

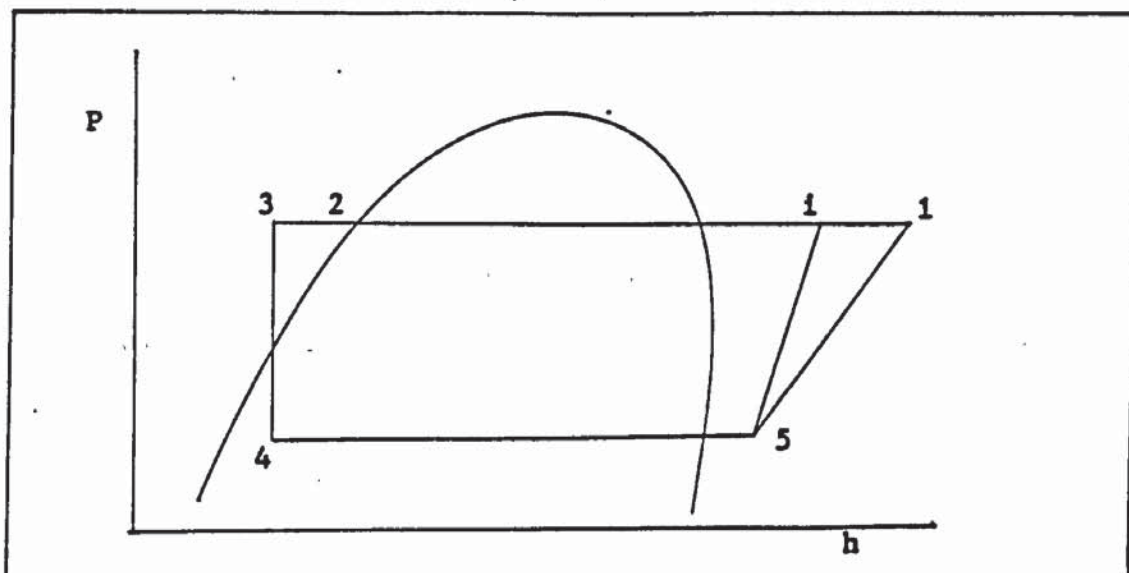


Fig (5.15) The freon cycle with the symbols used.

A set of an experimental results is shown in table (5.7), where $\dot{W}_x = \frac{n}{n-1} R \dot{M}_r \Delta T$, $\Delta \hat{H} = \dot{M}_r (h_1 - h_5)$, $\dot{Q}_r = \Delta \hat{H} - \dot{W}_x$, P_e is the electrical power supplied to the compressor and \dot{Q}_c is the heat removed from the compressor by the cooling water. It can be seen that $\Delta \hat{H} + \dot{Q}_c$, the sum of the total energy transferred to the freon gas and the energy removed by the cooling water, and P_e are equal within the limit of experimental error, which confirms the energy balance in the compressor. Only about half of the electrical energy is used for compression and the difference is to overcome the friction and all other resistances. A part of the heat resulting from the friction between the piston and the cylinder wall is removed by the cooling water \dot{Q}_c and the rest is transferred to the freon gas \dot{Q}_r . This \dot{Q}_r has a considerable effect on the freon discharge temperature. From figure (5.15), if $\dot{Q}_r = 0$ (adiabatic compression), the discharge temperature is T_1 . In the polytropic process, $\dot{Q}_r \neq 0$, the discharge temperature is increased from T_1 to T_1 .

In table (5.8) the percentage of \dot{W}_x , \dot{Q}_r and \dot{Q}_c to the input power P_e are shown. The result shows that about 55% of P_e is transferred to the freon from the work done by the compressor, 35% from the frictional heat, and so a total of 90% is transferred to the freon gas. The rest is removed from the compressor by the cooling water.

Tc (C)	Te (C)	Cr	\dot{M}_x (W)	\dot{Q}_r (W)	\dot{Q}_c (W)	$\Delta \dot{H}$ (W)	Pe (W)
44.02	5.60	3.03	178	105	14	283	317
42.4	5.52	2.94	174	104	19	278	311
40.6	5.06	2.85	171	105	21	274	298
38.79	5.18	2.73	164	106	27	270	294
36.21	4.81	2.59	158	107	34	265	287
34.15	4.52	2.47	155	107	38	262	283
27.88	3.16	2.18	141	114	41	255	264

Table(5.7) The compressor energy balance. Where,

$$\dot{M}_x = (n/(n-1)) R \dot{M}_r (T1-T5)$$

$$\dot{Q}_r = \Delta \dot{H} - \dot{M}_x$$

$$\Delta \dot{H} = \dot{M}_r (h1 - h5)$$

Pe = Electrical input to the compressor

$$Q_c = \dot{M}_w C_{pw} \Delta T$$

Table (5.9) shows the compressor efficiencies, volumetric η_v and isentropic η_i for Cr between 2.18 and 3.03. η_v is calculated from equation (3.6), while η_i is from $(T_i - T_5)/(T_1 - T_5)$. At higher Cr the isentropic efficiency is higher. This is due to the changes in n with Cr. Also at higher Cr the proportion of the stroke volume that admits freon gas into the compressor is reduced and so the η_v is lower.

Cr	$\frac{W_x}{P_e} \cdot 100$	$\frac{Q_r}{P_e} \cdot 100$	$\frac{Q_c}{P_e} \cdot 100$
3.03	56.2 %	39.4 %	4.4 %
2.94	55.9	38.0	6.1
2.85	57.4	35.6	7.0
2.73	55.8	35.0	9.2
2.59	55.1	33.1	11.8
2.47	54.8	31.8	13.4
2.18	53.4	31.1	15.5

Table (5.8) About 55% of the electrical input power is transferred to the freon gas by compression and about 35% by heating. The cooling liquid removes about 10% of the input power.

Cr	η_i	η_v
3.03	0.63	0.925
2.94	0.62	0.929
2.85	0.61	0.932
2.72	0.60	0.937
2.58	0.59	0.942
2.18	0.56	0.957

Table (5.9) The compressor efficiencies η_i and η_v with $\frac{V_i}{V_s} = 0.95$

5.4 The Condenser

5.4.1 Variation of Hot Water Temperature

The condenser is designed to always give the water outlet temperature $T_w(o)$ greater than the freon condensing temperature T_c , by utilizing the discharge superheat. Figure (5.16) shows that at $T_c=27.8$ C, the outlet water temperature is 1.9 C above T_c , and at $T_c=43.9$ C, it is 7.7 C. Also it can be seen that the water outlet temperature varies almost linearly with T_c .

The water flow rate is higher at lower Cr , about $.02 \text{ kgs}^{-1}$ at $Cr=2.18$; and lower, $.0075 \text{ kgs}^{-1}$ at higher Cr ($Cr=3.03$). As shown by the graph (figure(5.16)), the water flow rate is not linear with T_c .

The water outlet temperature is made higher than the condensing temperature T_c , by making the freon and water tube diameters very small compared to their length. This produces high and turbulent flow rates which yield maximum heat transfer, and brings the water temperature near to the T_c in the condensing region. Extra heat picked up in the desuperheating region will increase the water temperature higher than T_c . The disadvantage is that the pressure drop across the condenser (in the refrigerant circuit) will be increased.

5.4.2 Pressure Drop Across The Condenser

Figure (5.17) shows the pressure drop across the condenser against the freon flow rate. It shows that operating at higher

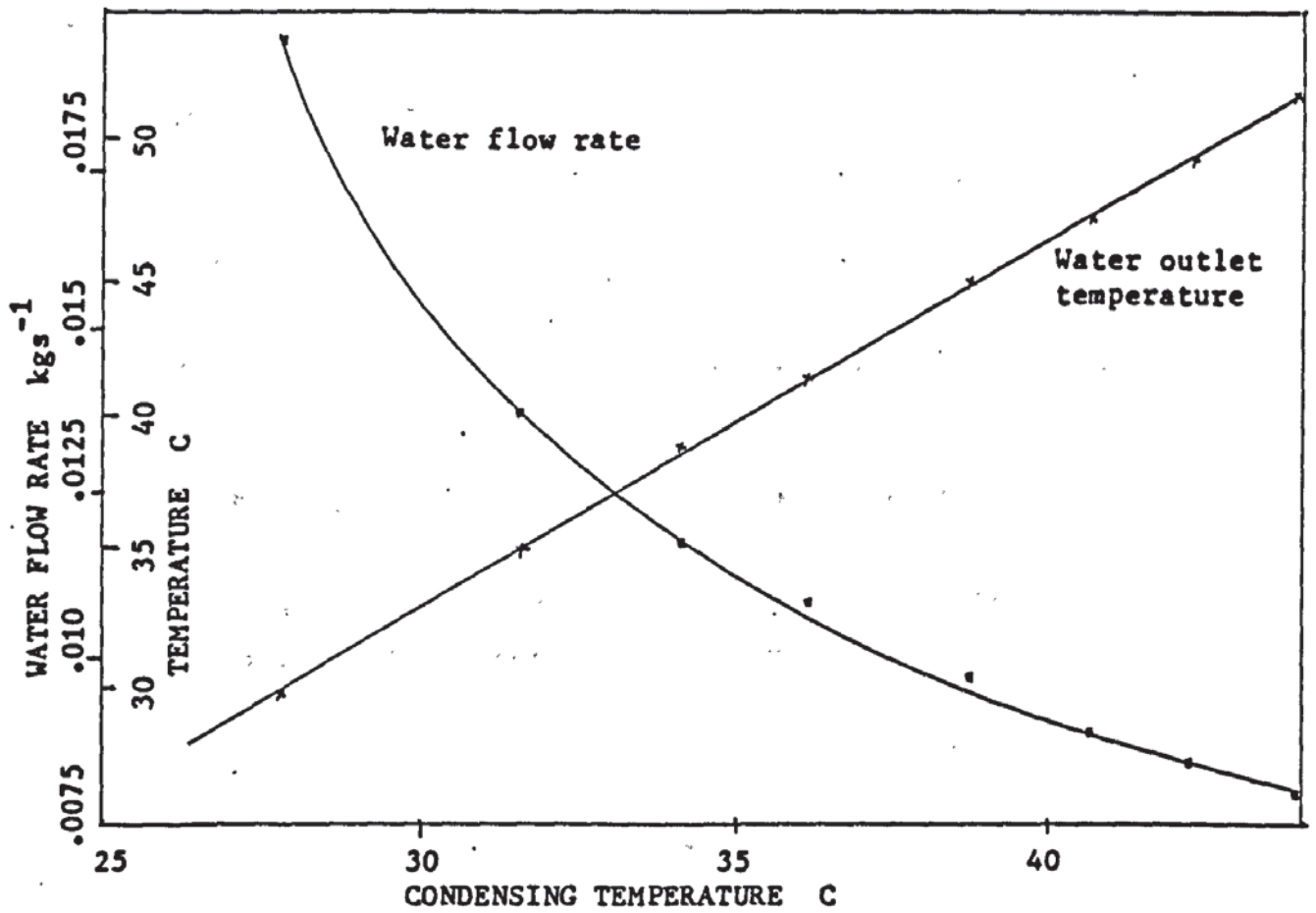


Fig (5.16) The variation of water flow rates and outlet temperatures with T_c . $T_w(i)=12.2$, $A_s=0.1\text{m}^3\text{s}^{-1}$, $T_a(i)=14\text{C}$

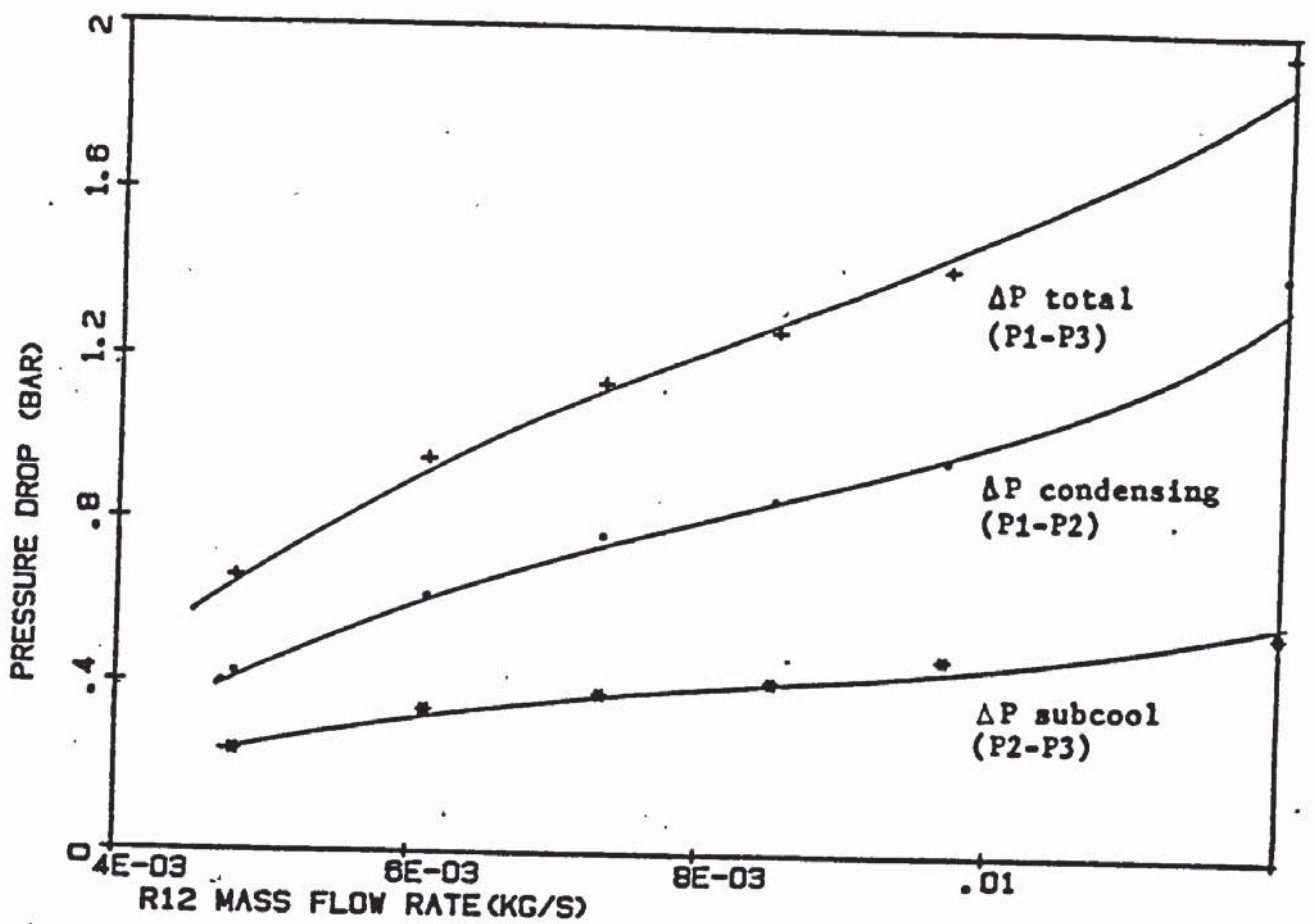


Fig (5.17) The condenser pressure drop. The pressure drop in the condensing region is about 2/3 of the total pressure drop. The pressure drop at the condensing region is based on the pressure measurement at the accumulator.

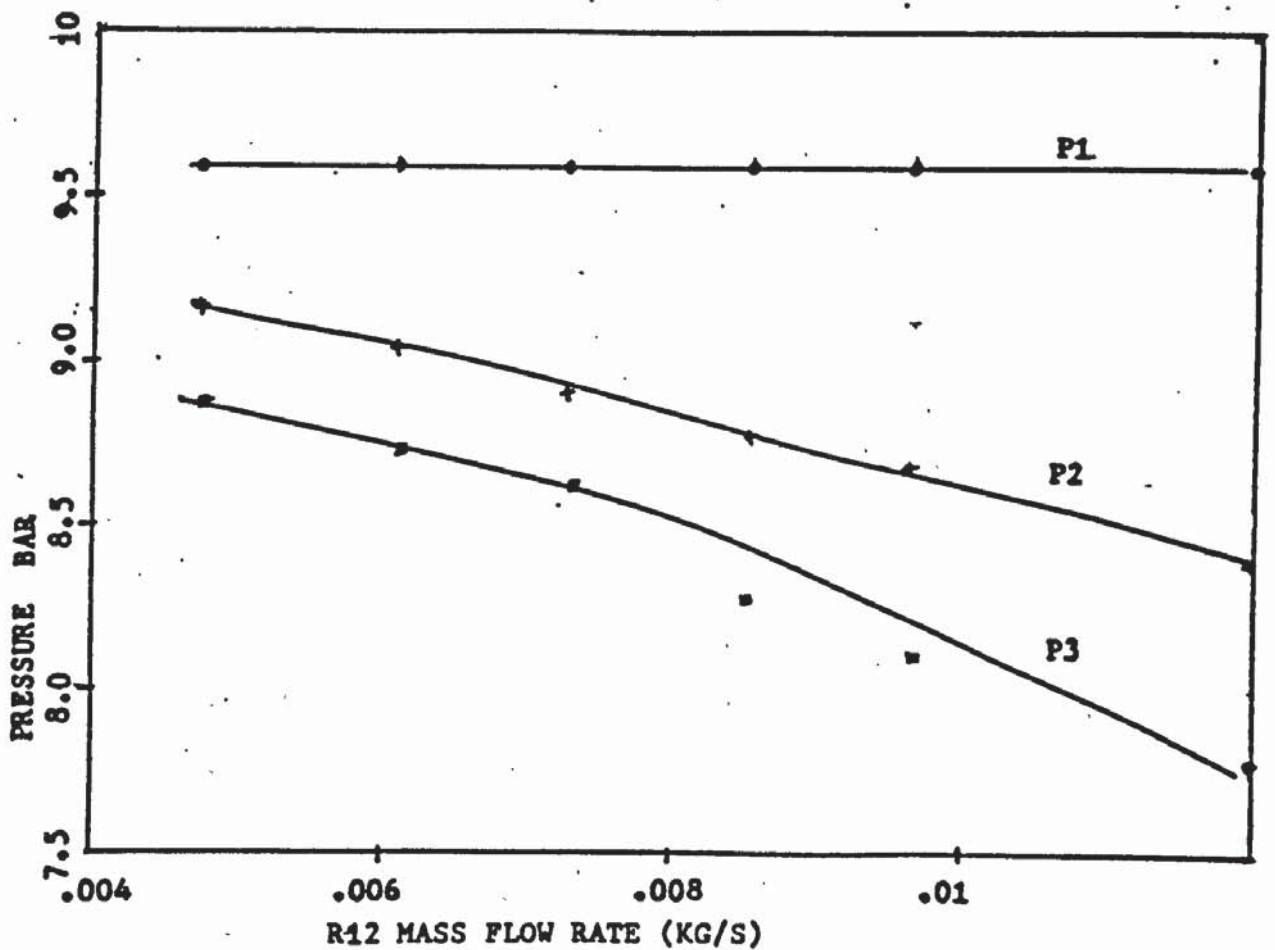


Fig (5.17a) Condenser pressures plotted against freon flow rate.

freon flow rate will cause a higher pressure drop across the condenser (at constant T_c). As an example of the effect on freon temperature when operating at $T_e = 5\text{ C}$ and $T_c = 45\text{ C}$, about 3 or 4 deg C are lost due to the pressure drop. That is $T_c = 45\text{ C}$ on entering the condenser and $T_c = 42\text{ C}$ on leaving.

Figure (5.18) is a sketch illustrating the effect of pressure drop across the condenser in reducing the condenser capacity. The dashed lines are the temperature profiles of freon and water without pressure drop, and the continuous lines are with pressure drop.

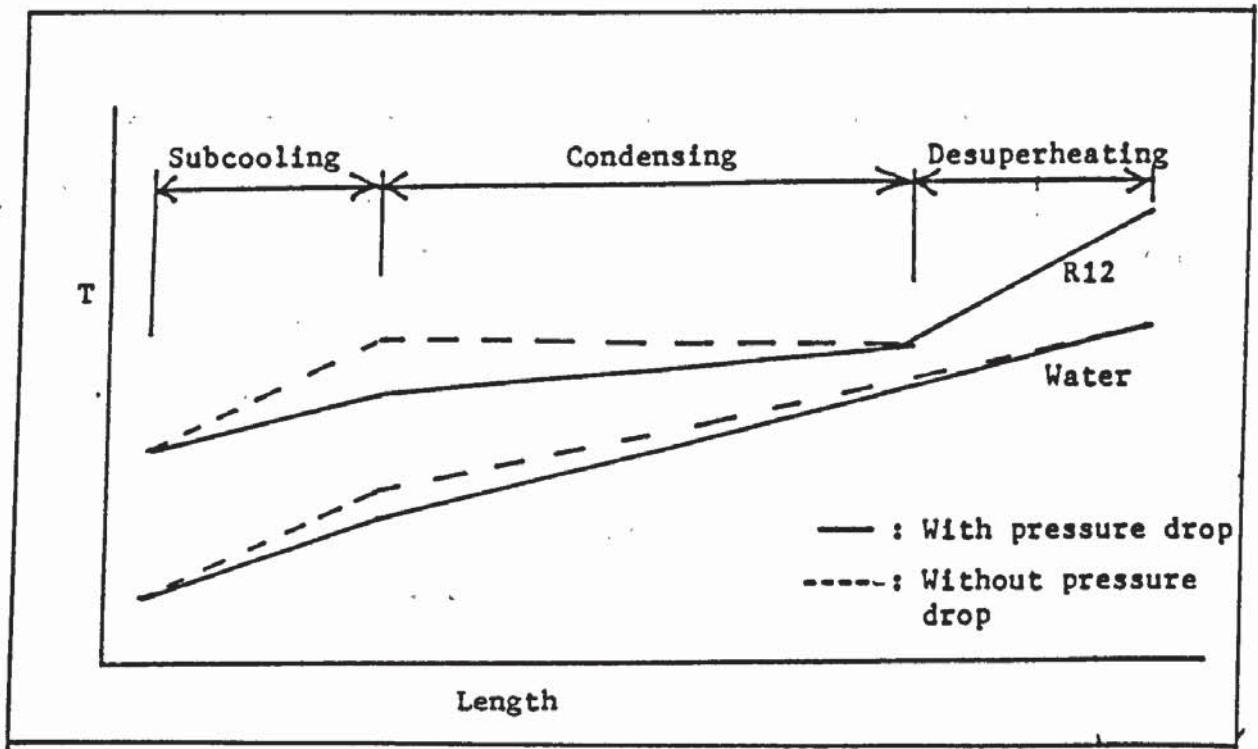


Fig (5.18) The condenser temperature profiles with and without pressure drop.

Without the pressure drop, the water is heated more quickly than in the case with pressure drop, because the effect of the pressure drop is to reduce the temperature gradient. Therefore to arrive at the same

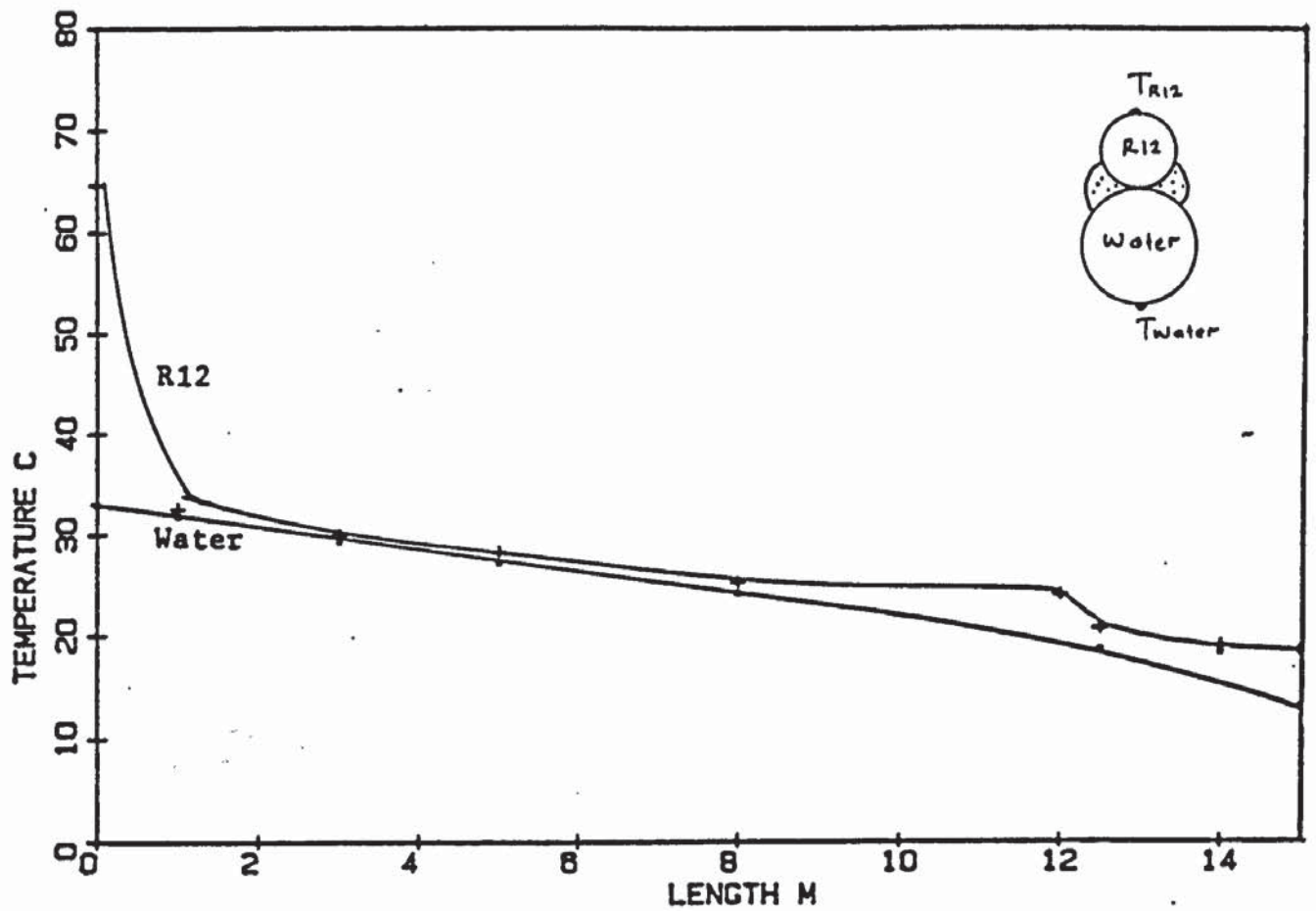
outlet temperature, the water flow rate in the case with pressure drop must be less than the flow rate without pressure drop. As a result the heat output with pressure drop is less than the case without pressure drop.

The equation $dH=dQ + VdP$ may be applied to the condenser. It shows that in the absence of a pressure drop the heat rejected has its maximum value of H_1-H_3 . In the real experimental situation as described a pressure drop exists and so the heat rejected is reduced.

5.4.3 The Freon and Water Temperature Profiles

The temperature profile of the condenser is obtained by measuring the temperatures of freon and water along the condenser tubes on the outside wall, except at the outlet and inlet where the thermocouples were inserted into the tubes. The measurements were made for three different condensing temperatures $T_c = 30, 40$ and 45°C . One feature of all three figures (figures (5.19,20,21)) is that T_3 for freon is always 20°C (water inlet temperature is 12°C). Thus in the liquid region the temperature drop over the last 3 meter of the condenser , the subcooling region, is 2 , 5 and 7 degC per meter for $T_c=30,40$ and 45°C respectively.

Subcooling has a considerable effect on the system performance. This can be seen from the two sets of the experimental results in table (5.10). The COP of a system without subcooling can be increased by about 15%, from 2.6 to 3 by subcooling the liquid freon , for certain operating conditions. The system with the subcooler also shows a higher air temperature drop across the evaporator than the one without. This



Fig(5.19) Condenser temperature profile at $T_c = 30\text{ C}$. $T_w(i) = 12\text{ C}$,
 $A_s = 0.1\text{ m}^3/\text{s}$. $T_a(i) = 15\text{ C}$

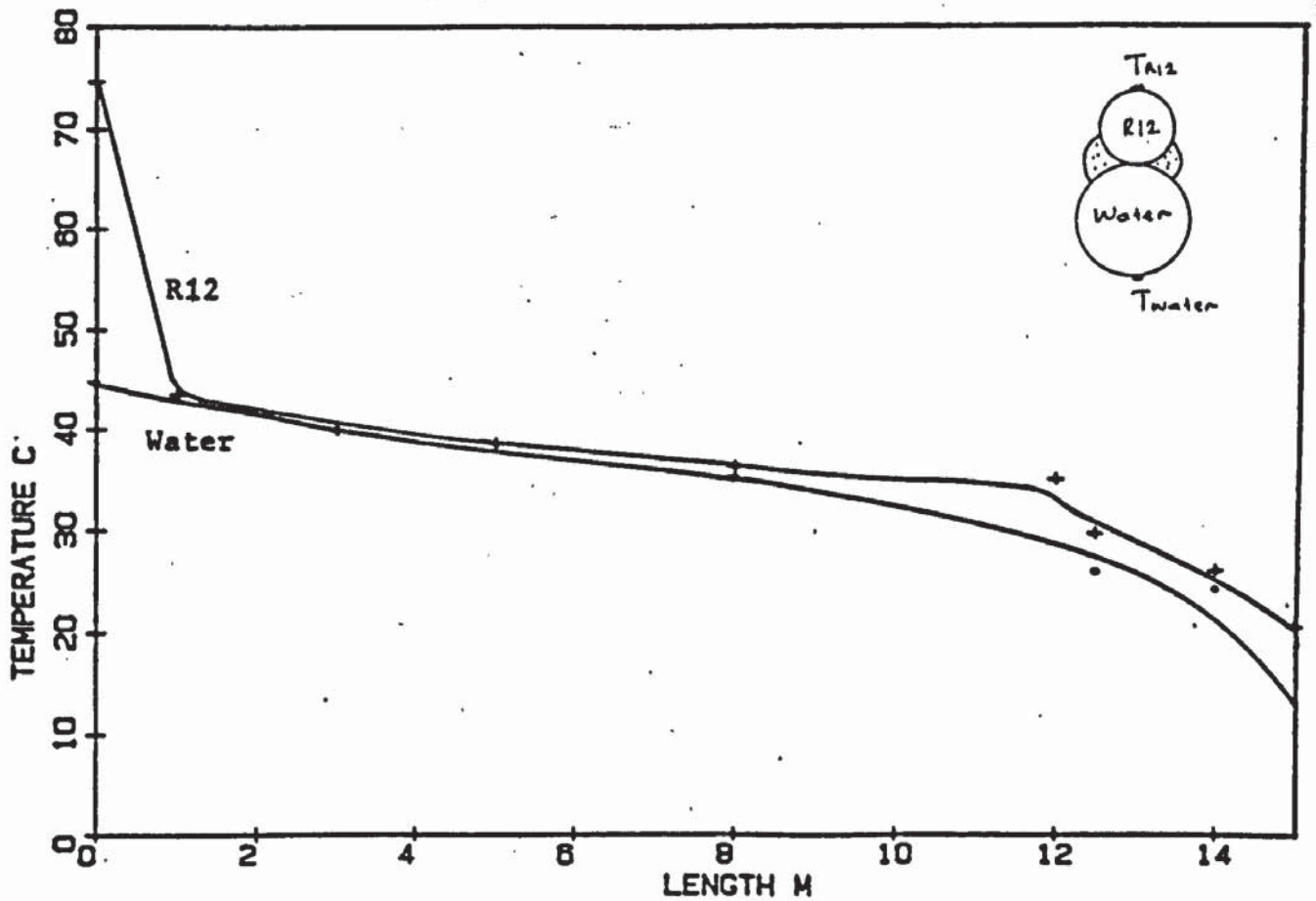


Fig (5.20) Condenser temperature profile at $T_c = 40\text{ C}$. Other operating condition as in fig(5.19).

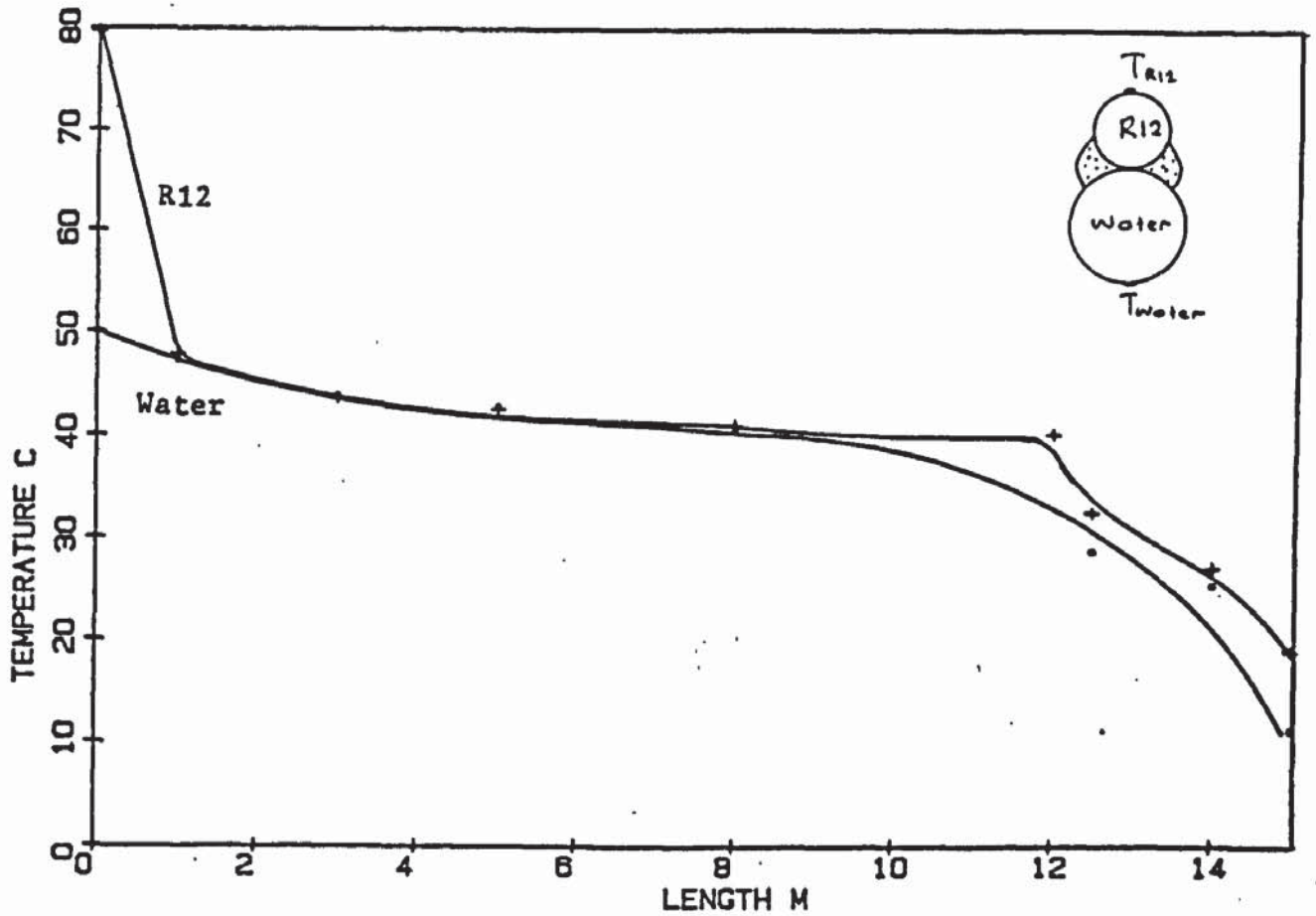


Fig (5.21) Condenser temperature profile at $T_c = 45$ C ; Other operating condition as in fig (5.19)

In figures (5.19) to (5.21) temperatures, other than at the end points, were measured on the outer wall of the condenser as indicated.

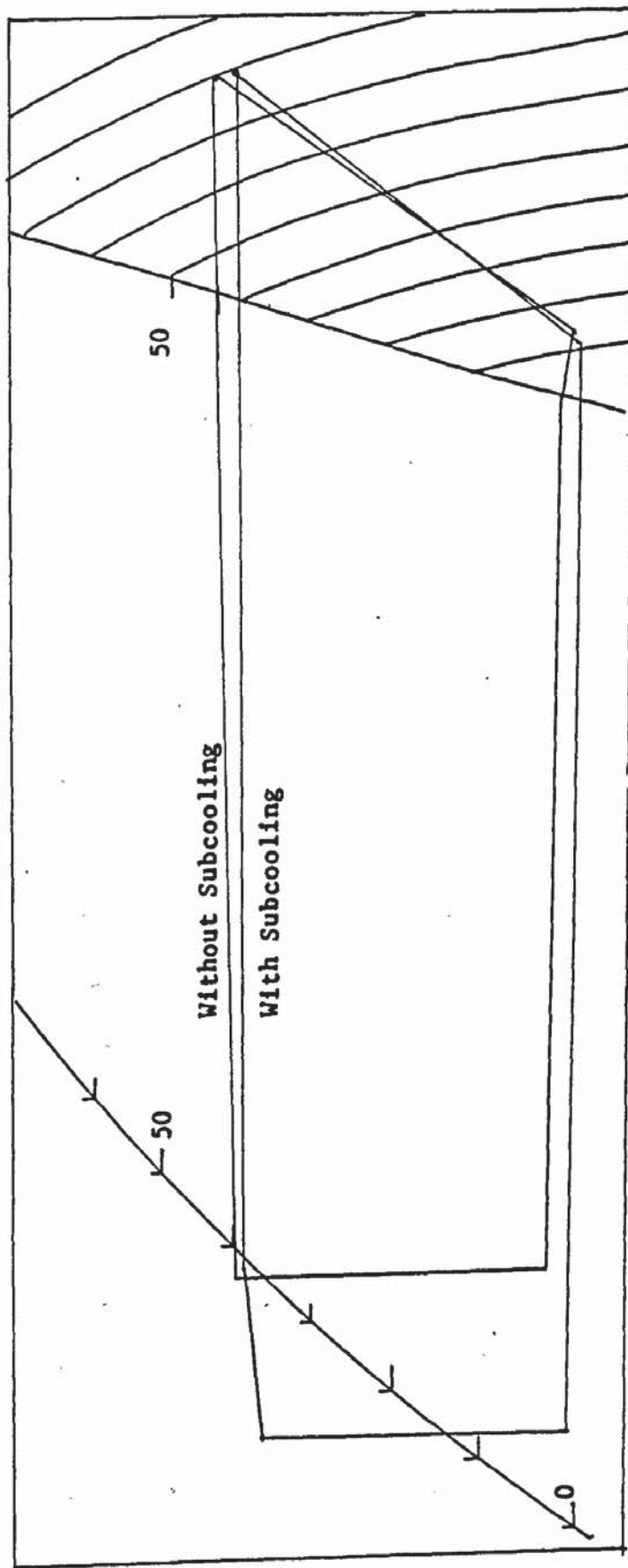


Fig (5.22) The freon cycles, with and without subcooling.

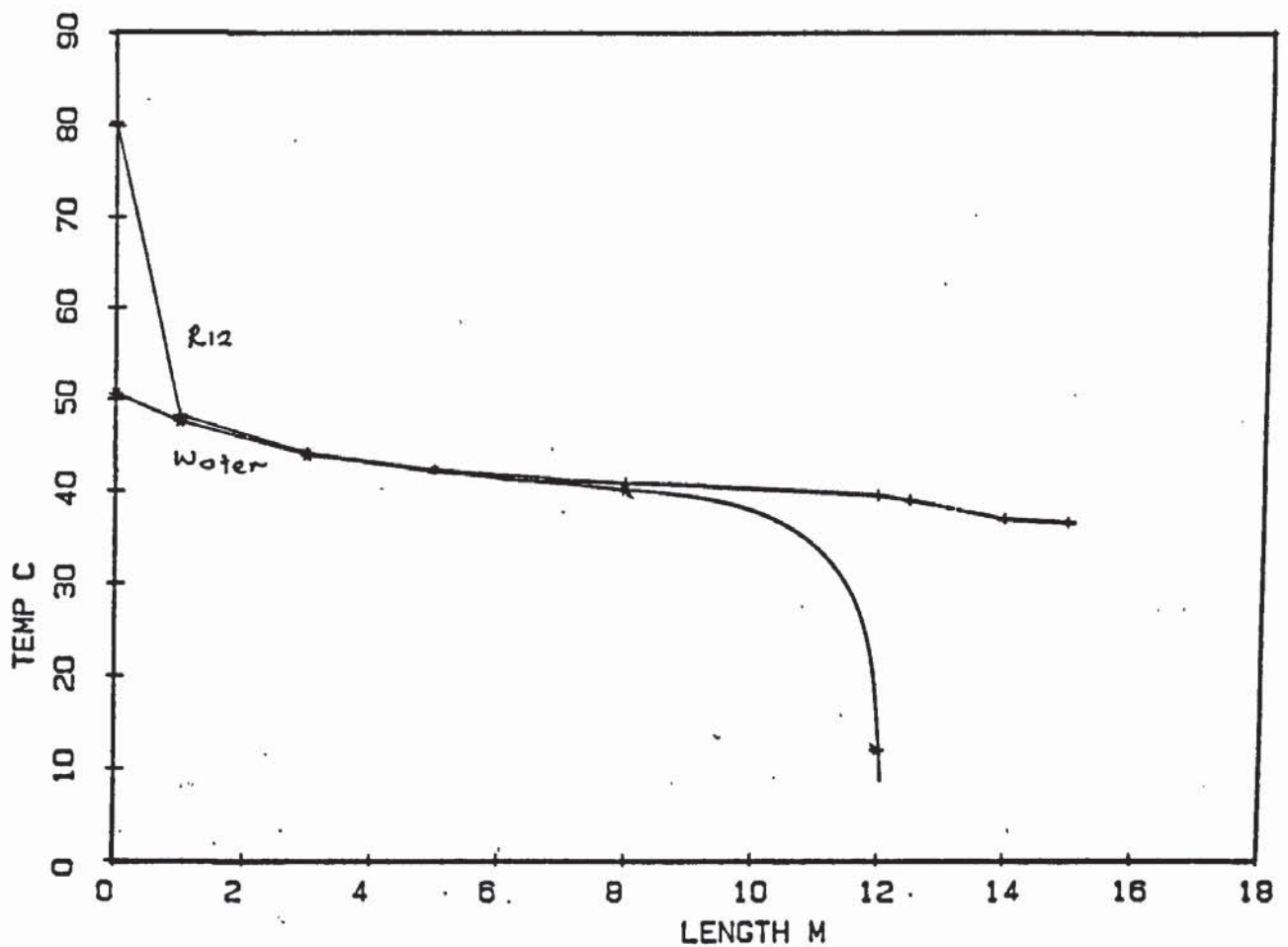


Fig (5.23) Condenser temperature profile without the subcooling section . Operating at $T_w(i) = 12.3 \text{ C}$, $A_s = 0.1 \text{ m}^3/\text{s}$, $T_a(i) = 15\text{C}$

means the evaporator absorbed more heat from the air in the case with the subcooler than the one without. It can be concluded here that subcooling the liquid freon can increase the heat output, heat input and the system performance. The freon cycle for both cases is shown in

figure (5.22). Figure (5.23) shows the condenser temperature profile for the system without the subcooler. In this case the freon liquid temperature is about 4 deg C below T_c .

	P1 (bar)	T1 (C)	T3 (C)	Mw kgs ⁻¹	Te (C)	Wcomp (W)	Heat Out (W)	COP
Cond. + Subcooler	9.5	79.9	19.06	0.0063	4.71	305	1056	3.0
Cond.	9.5	80.1	38.20	0.0057	4.37	309	921	2.6

Table(5.10) Comparison of the condenser with and without subcooler.

5.4.4 The Operation Of The Water Flow Regulator

The experimental results show that, apart from T_c , the water flow rate is also a function of inlet conditions. Changes in the inlet condition, for example in air temperature and air speed, will change T_e but not T_c . The water flow regulator sets in such a way as to maintain a constant condensing pressure and therefore a constant condensing temperature T_c . In table (5.11) it can be seen that at constant P_1 or T_c , the condenser water flow rate increases with a rise in T_e as obtained from the experimental results. The dependance of water flow rate on T_e (which is also means freon flow rate) is as a result of the 'action' by the water flow regulator. The water flow regulator is operated by three pressures : a manually set pressure, using hand wheel, P_h ; freon pressure, P_1 ; and water pressure, P_w which is constant (λ pressure), see figure (5.24). Since P_1 is set by P_h , therefore at equilibrium $P_1 = P_h$; and in this experiment $P_1 = P_h = 9.4$ bar and $T_e = 4.6$ C initially. When T_e increases the freon flow rate also increases. As a result the condensing temperature T_c will increase and so P_1 ; and

Discharge Pressure bar	Discharge Temp C	Water Flow Rate kg/s	Water Outlet Temp C	Te (Evap) C	T5 (suction) C
9.421	74.13	.00938	44.46	4.58	14.54
9.379	74.08	.00949	44.59	5.28	15.34
9.428	73.95	.00982	44.49	5.95	16.14
9.379	73.95	.01006	44.46	6.68	16.74
9.510	73.60	.01025	44.27	7.35	17.28
9.428	73.32	.01050	44.16	7.96	17.68
9.428	73.06	.01056	44.11	8.16	18.11
9.414	72.80	.01069	43.97	8.68	18.37
9.510	72.58	.01080	43.89	9.00	18.62
9.379	72.35	.01094	43.95	9.09	18.79
9.510	71.94	.01102	43.73	9.38	19.10
9.469	71.65	.01121	43.76	9.75	19.28
9.428	71.12	.01131	43.62	10.02	19.56
9.510	70.84	.01147	43.49	10.30	19.62
9.510	70.12	.01164	43.30	10.56	19.70
9.510	69.60	.01173	43.16	10.65	19.98

Table (5.11) The water flow rate is increasing with increasing T_e eventhough the discharge pressure P_1 is almost unchanged.

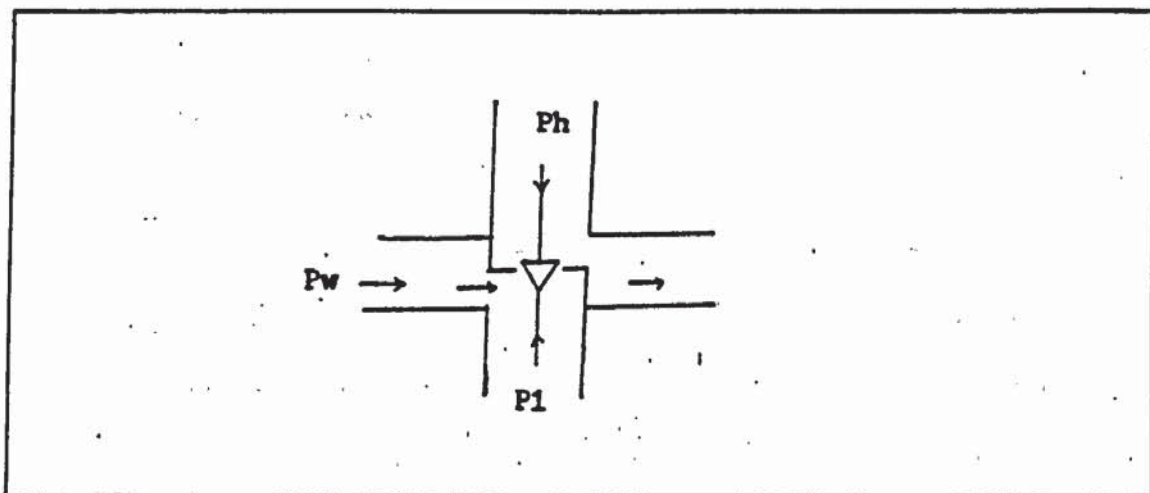


Figure (5.24) The pressure involved in the water flow regulator.

since P_1 is opposed by P_h , increases in P_1 will cause the valve of the regulator to open wider, and so increase the water flow rate. The 'extra' heat of freon due to the increase in freon flow rate can now be transferred to the water. This will bring back P_1 to the initial pressure, $P_1 = P_h$, but at a different water flow rate.

5.4.5 Effect of Water Inlet Temperature

Another parameter which can effect the water flow rate and so the system COP is the water inlet temperature, $T_w(i)$. Experimental results for three values of $T_w(i)$ are shown in table (5.12). The results show that increasing $T_w(i)$ will increase water flow rate. The COP is decreasing because of two factors. The heat output is decreasing due to a reduction in the amount of subcooling, while the electrical input is increasing due to a small rise in C_r with increasing $T_w(i)$.

The fact that the COP is dropping with increasing $T_w(i)$, (also agreed by Danfoss (8)), is causing considerable problems in the application of this type of condenser for heating and storage of hot water. ^{in a continuous cycling operation} Normally the cold water is taken from the bottom of the tank, and after passing through the condenser, the hot water is returned back to the tank through an inlet at the top. In order to maintain a high COP the temperature at the bottom of the tank $T_w(i)$ should be kept as low as possible. The problem here is in order to maintain $T_w(i)$ at a lowest temperature as possible how is the hot water to be injected back into the tank without mixing it with the cold water. The second problem is of what type of material should the tank be made so that no heat can be conducted to the bottom of the tank through the

Water In (C)	Water Out (C)	P1 (bar)	P3 (bar)	P4 (bar)	T1 (C)	T3 (C)	T4 (C)	Water F-Rate (kgs ⁻¹)	Heat Out (W)	Work Done (W)	COP
12.01	45.90	9.586	8.48	3.544	73.85	18.08	3.55	0.00897	1283	300	3.6
21.09	45.48	9.931	8.897	3.607	74.20	23.49	5.06	0.01213	1270	308	3.5
31.81	44.30	10.41	9.517	3.703	75.80	32.14	6.21	0.0202	1056	317	2.9

Table (5.12). Increasing water inlet temperature will reduce the COP.

the tank wall faster than conduction through the water. The most suitable draw off point for this system is at the top of the tank. During draw off the hot water temperature will fall due to the necessary stratification in the tank.

5.5 Transient Response: Decreasing And Increasing Air Inlet Temperatures

The response of the heat pump to the changing of air inlet temperature is studied for two conditions, decreasing and increasing air inlet temperatures. In the first case the air was heated to a temperature of about 24C, and then the heater was switched off. The readings were taken at intervals of 30 seconds from the moment the heater was switched off and up to about half an hour, when the air temperature is about the ambient temperature.

Figure (5.25) shows that the biggest air temperature drop occurred in the first 10 minutes. The freon mass flow rate is decreasing, as is the water mass flow rate and so the heat output (figure (5.26)). This is because T_e is decreasing with the air temperature and T_c is almost unchanged. The COP is also decreasing with T_e as shown in figure (5.27).

The second experiment is increasing the air temperature as shown in figure (5.28). The freon and water mass flow rates are increasing with air temperature (figure(5.29)), and also the COP. The freon mass flow rate drops sharply in the first 3 minutes and then rises again. The drop is due to sudden increase in T_e and P_4 while the opening of

the expansion valve remains unchanged. After 3 minutes the new P4 is balanced by the pressure from the expansion valve fluid.

In both cases, the biggest interruption occurs in the first 10 minutes and becomes steady after about 20 minutes.

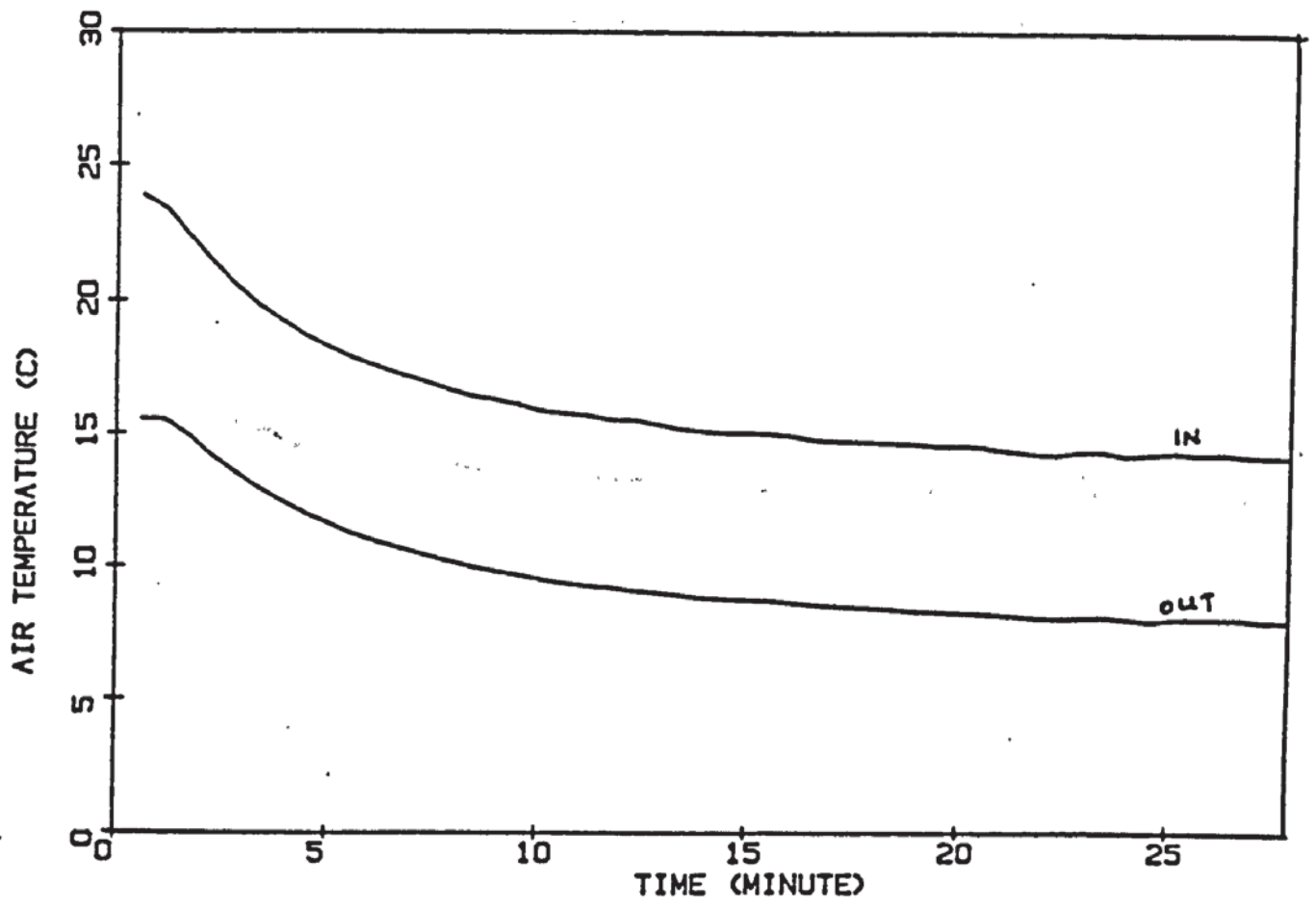


Fig (5.25) The air inlet temperature is allowed to drop from 25 C to 15 C in 30 minutes . $T_w(i) = 12.5$ C , $A_s = 0.1$ m³/s , $T_w(o) = 45$ C

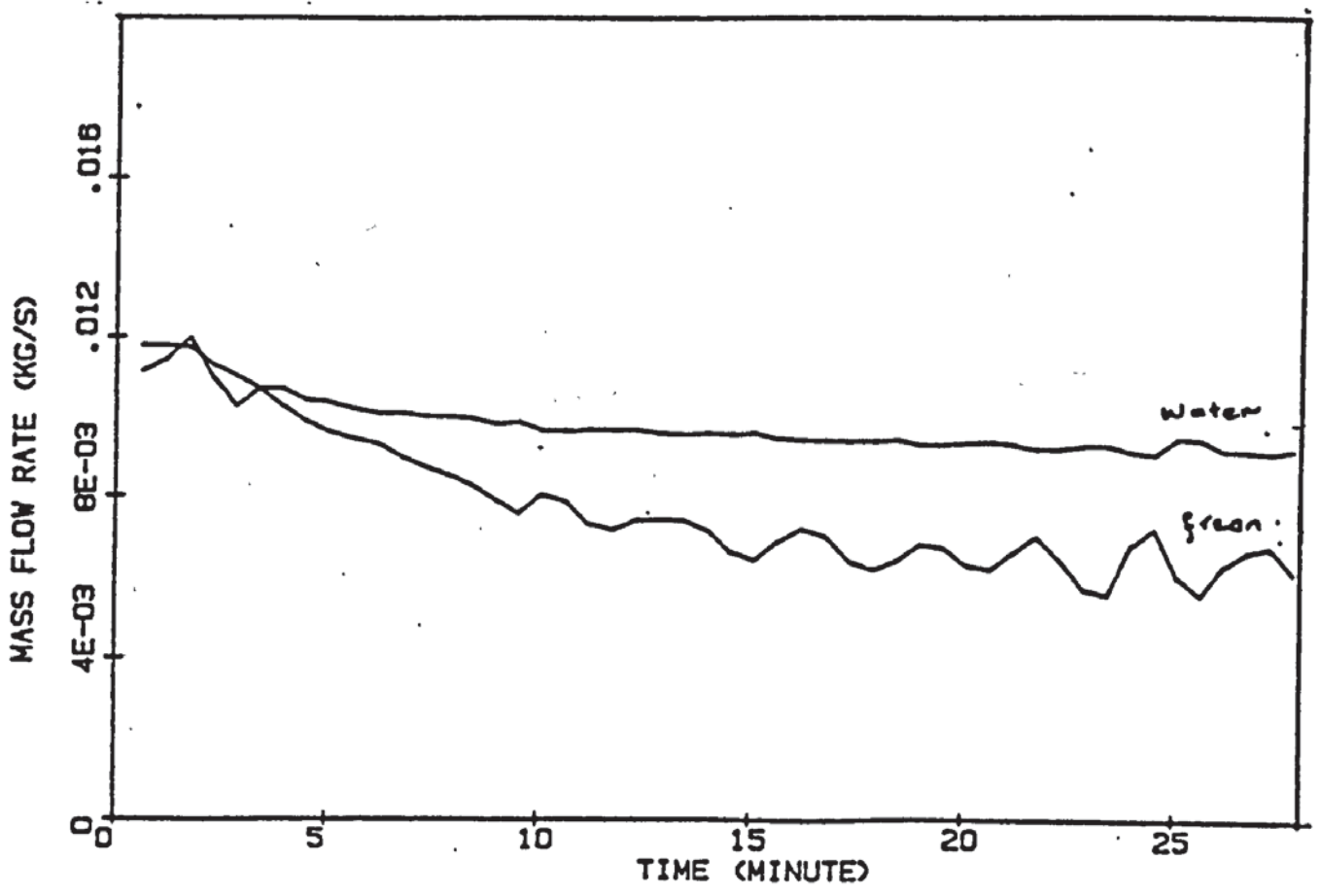


Fig (5.26) The water and freon mass flow rates also decreasing with air inlet temperature . Other condition as in fig(5.25).

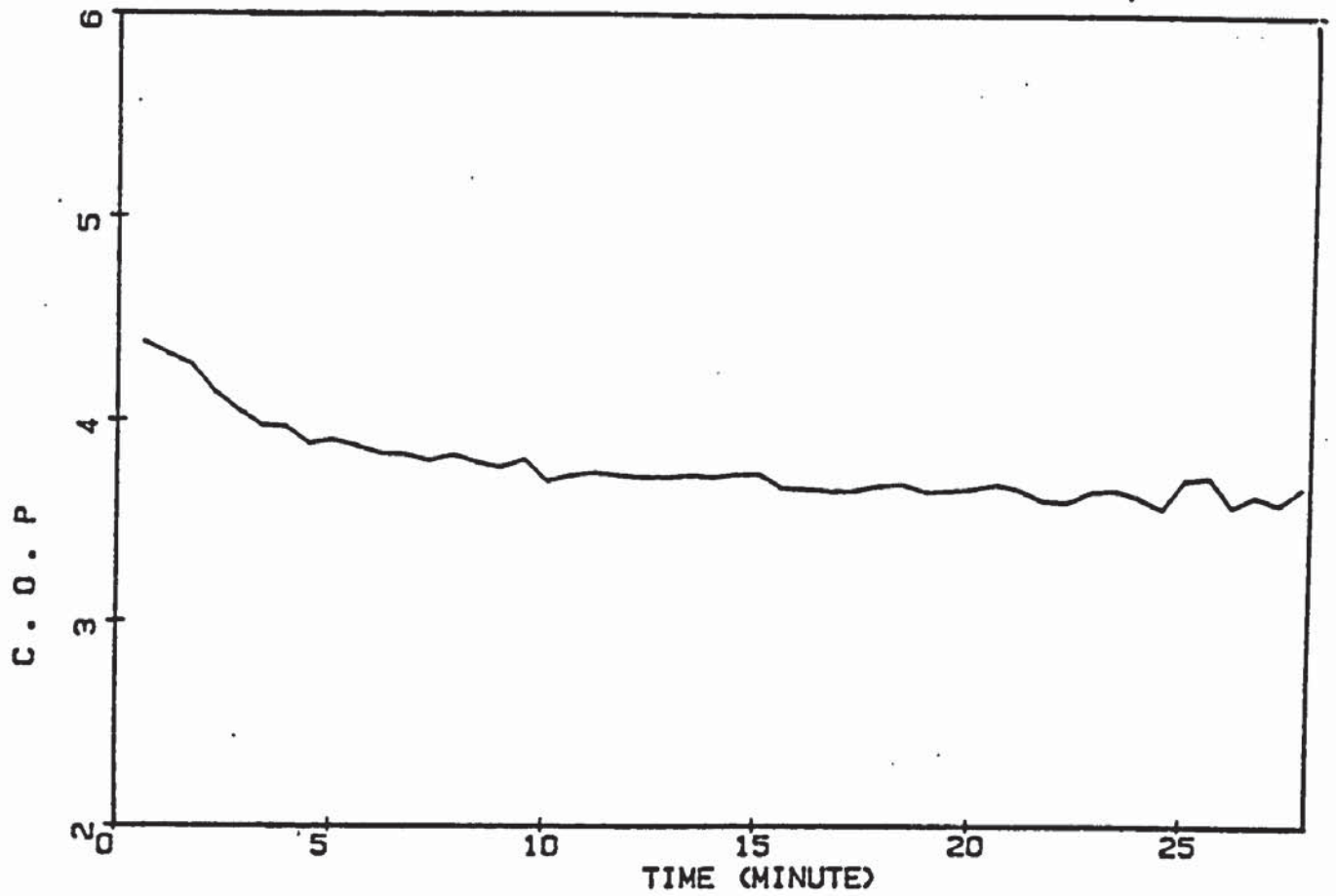


Fig (5.27) The COP also decreasing with air temperature . Operating as in fig (5.25)

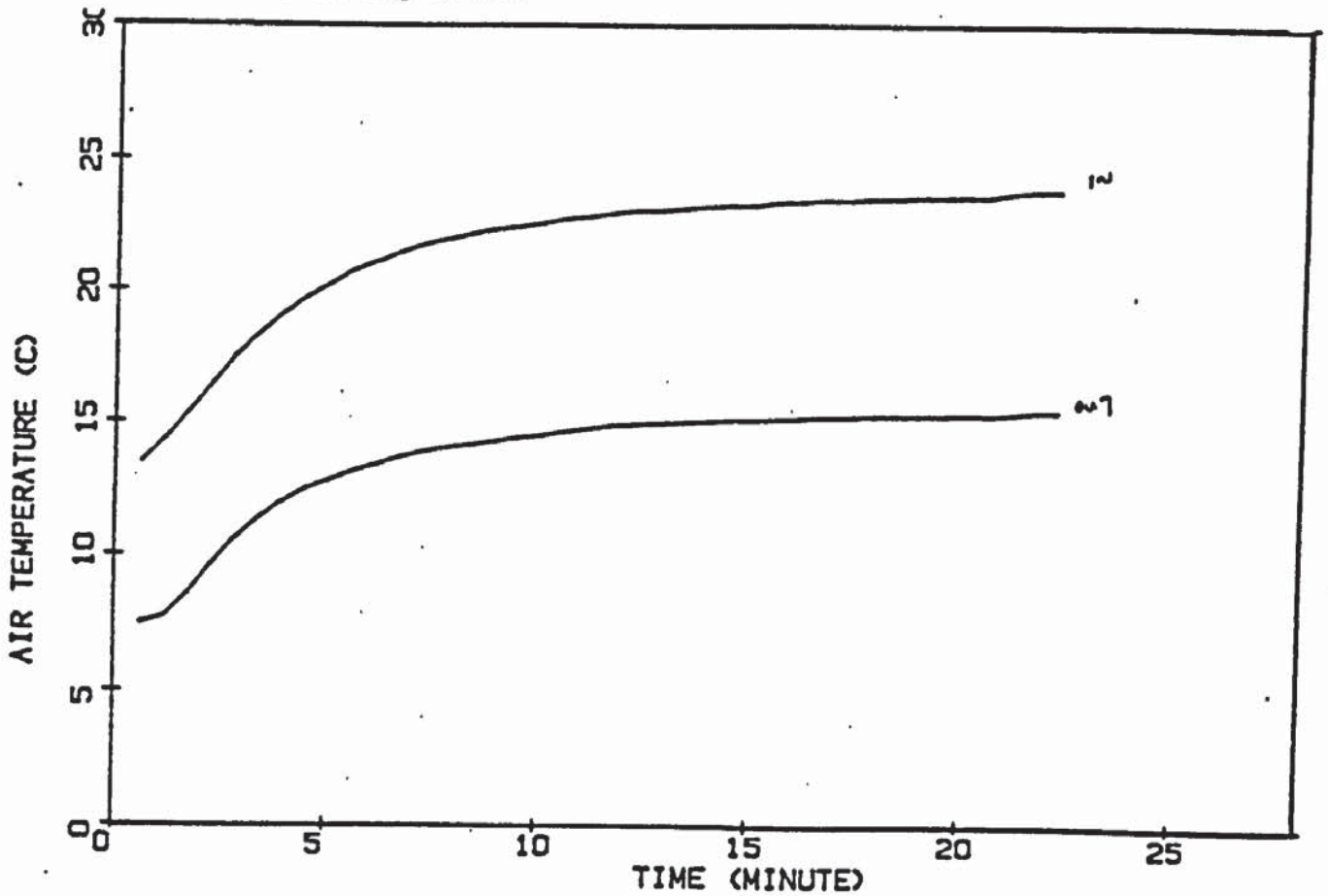


Fig (5.28) Air temperature is increased from about 14 C to 25 C in about 25 minutes . Operating as in fig (5.25)

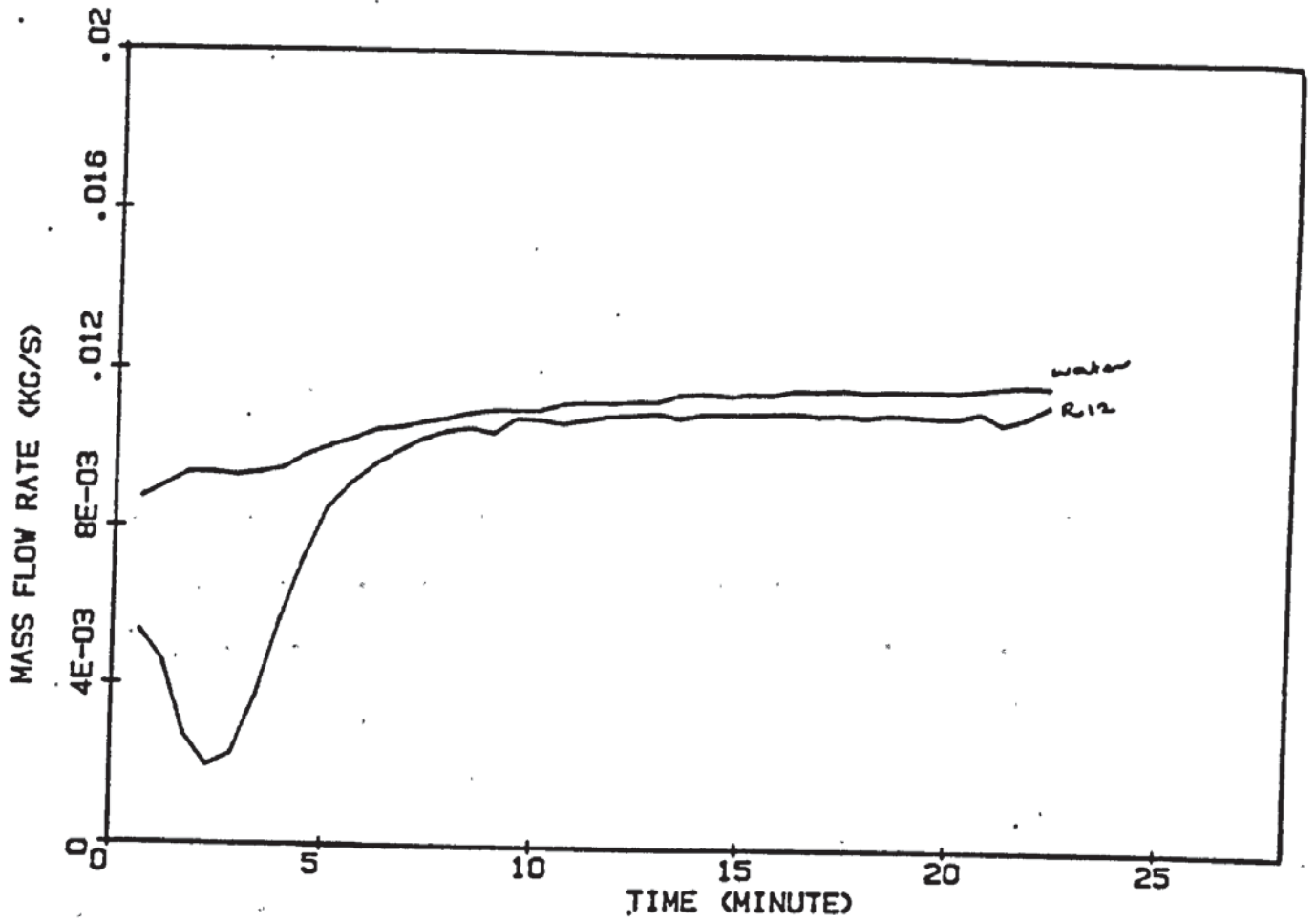


Fig (5.29) The water and freon mass flow rates adjust themselves with the increasing temperature . Operating as in fig (5.25)

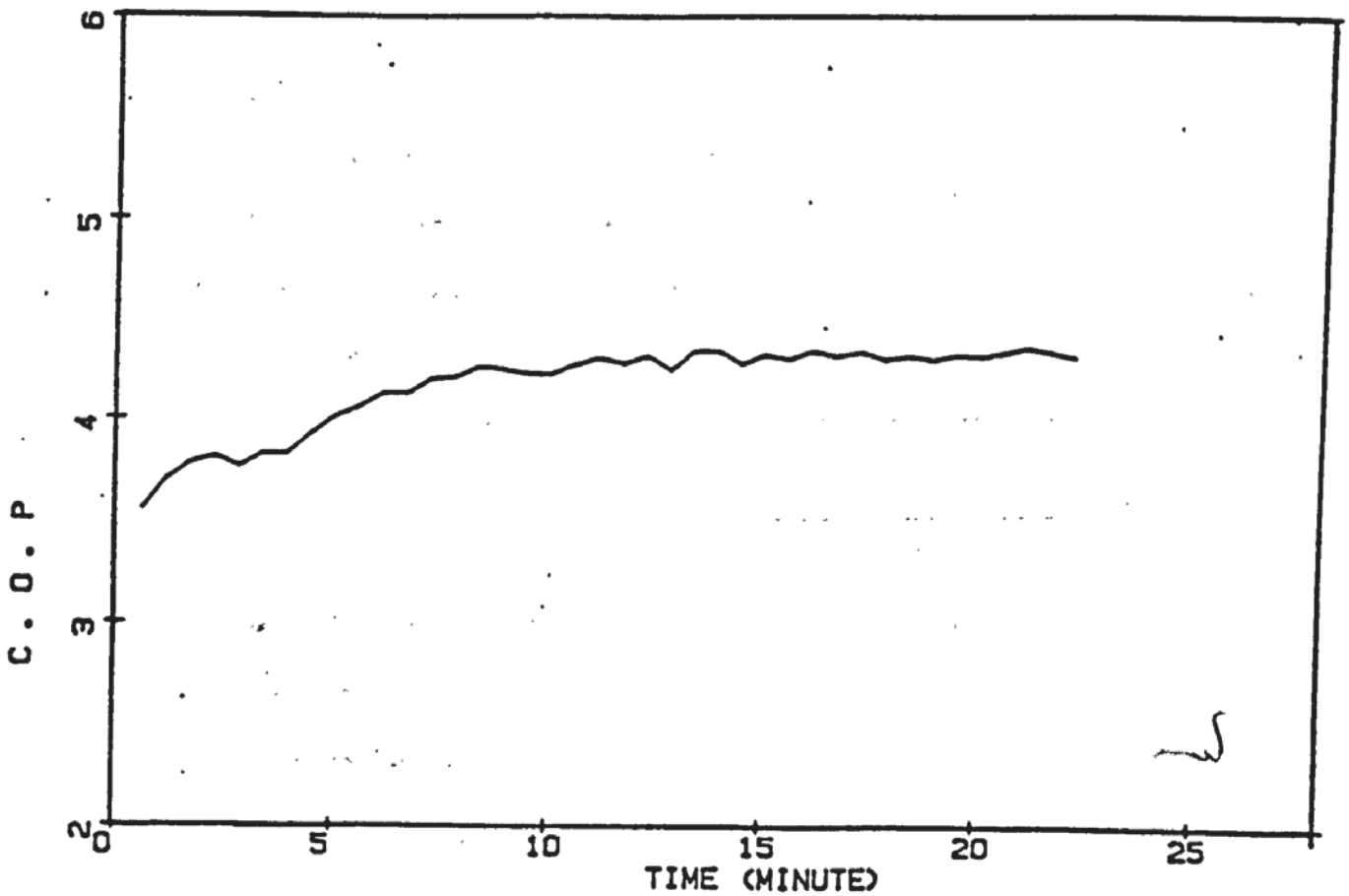


Fig (5.30) The COP also increased with the air temperature . Operating under the same condition as in fig (5.25)

THE COMPUTER MODEL

6.1 Introduction

A mathematical model of a steady state heat pump system based on theoretical analysis and experimental work has been developed. This model can predict the thermodynamic characteristics at any point on the heat pump cycle for a given operating condition. With this model the effect of various disturbances, such as variation in air inlet temperature, air speed, required outlet water temperature and others can be investigated.

The model is different from other models, for example Tassou (39), Ahrens (40) and James (41), because the heating load is not made an input parameter. This will make the theoretical analysis more complicated, and a few empirical equations, determined from the experimental work, have to be used. One is for an initial guess of the evaporating temperature, T_e and subsequently calculating the condensing temperature, T_c . The others are for determination of compressor polytropic index, compressor frequency and the pressure drop in the condenser.

Inputs to the model include the desired hot water, the cold water and air inlet temperatures, the air speed and the expected amount of freon suction superheat. The effect of relative humidity is included in the calculation through the empirical equation for determination

of compressor frequency. In calculating the compressor frequency from the experimental data, the freon mass flow rate is taken as $Q_{out}/\Delta h$; where Q_{out} is heat rejected and Δh is the freon enthalpy difference at the condenser. Effect of relative humidity on the system is included in both values, Q_{out} and Δh . Outputs from the model include the refrigerant and water mass flow rates, the refrigerant thermodynamic state at appropriate points in the cycle, the compressor and the system energy balances, the heat load and the system COP.

6.2 Component Model

The heat pump model is divided into three main sections: the compressor, the condenser and the evaporator models. The pressure drops across the evaporator and condenser are considered but not in the pipes for connecting the components. Heat transfer between the heat pump components and piping with the ambient, except the evaporator is neglected since the system is well insulated. Oil circulation in the system is not considered.

6.2.1 Compressor Model

For a high speed reciprocating compressor the discharge temperature is higher than that indicated by an isentropic process. The discharge temperature is a function of suction temperature, compression ratio and polytropic index. The polytropic index is calculated from T_5, P_5, T_1 and P_1 using equation below,

$$n = \frac{\log\left(\frac{P_1}{P_5}\right)}{\log\left(\frac{V_5}{V_1}\right)} \quad (6.1)$$

This calculation of n is different from the method used by James et al (39) , because in this work the polytropic index , n , is not considered to be constant . An equation relating n to P_5, T_5 and P_1 is developed using experimental data.

$$n = 1.273 - 0.0166 P_1 + 0.020 P_5 - 0.00437 T_5 \quad (6.2)$$

where P_1 and P_5 are pressure in bar and T_5 is temperature in C. Experimental and fitted values of n are listed in table (6.1). When the values of T_5, P_5, P_1 and n are known, the temperature T_1 can be calculated using the freon equation of state (equation (6.3)) having determined V_5 ($V_5=f(T_5, P_5)$) and then V_1 from equation (6.1).

$$P_1 = \frac{R T_1}{V_1 + b} + C \quad (6.3)$$

From equation (3.6), the compressor η_v can also be written as,

$$\eta_v = 1 + C - C \left(\frac{V_5}{V_1} \right) \quad (6.4)$$

where $C = \frac{V_c}{V_s}$ is the ratio of the clearance volume to the stroke volume of the compressor. The refrigerant mass flow rate is given by,

$$\dot{M}_r = F_c V_s \eta_v \rho_5 \quad (6.5)$$

where F_c is the compressor frequency. The freon mass flow rate can also be determined from the condenser energy balance by assuming the condenser efficiency is η_c

$$\dot{M}_r = \frac{\dot{M}_w C_{pw} (T_w(o) - T_w(i))}{(h_1 - h_3) \eta_c} \quad (6.6)$$

Rearranging equations (6.5) and (6.6), the F_c becomes,

$$F_c' = \frac{\dot{M}_w C_{pw} (T_w(o) - T_w(i))}{(h_1 - h_3) V_s \eta_v \rho_5} = F_c \eta_c \quad (6.7)$$

All the terms, except F_c and η_c in equation (6.7) are either measured directly in the experiment or calculated from the measured data. By replacing F_c with F_c' in equation (6.5), the effect of η_c is included in the calculation of \dot{M}_r .

Therefore equation (6.7) can be used to determine the compressor frequency. Since the compressor frequency depends on the inlet and outlet conditions of the compressor, F_c can be related to V_1 and V_5 . An equation, developed by fitting of the experimental data, is given below,

$$F_c' = 31.25 + 1289.88 V_1 - 372.13 V_5 \quad (6.8)$$

After F_c' , the compressor frequency is determined, the freon mass flow rate is then calculated from equation (6.5) above. Experimental and fitted values of compressor frequency and freon mass flow rate are given in table (6.2).

The electrical power consumed by the compressor is calculated from the equation below, which is also fitted from the manufacturer's data.

$$P_e = 162.12 + 2.71 T_e + 3.10 T_c \quad (6.9)$$

Validation of this equation is given in table (6.3).

The power transferred to the freon is

$$W_1 = (h_1 - h_5) \dot{M}_r \quad (6.10)$$

For an isentropic compression the power transferred is,

$$W_1 = (h_1 - h_5) \dot{M}_r \quad (6.11)$$

It can be shown that the work done by the reciprocating compressor is given by,

$$W_r = \left(\frac{n}{n-1} \right) P_5 V_s \left(\left(\frac{P_1}{P_5} \right)^{(n-1)/n} - 1 \right) \eta_v \quad (6.12)$$

The heat which accompanies the polytropic compression is (refer to equation (5.3)) ,

$$Q_r = W_1 - F_c W_r \quad (6.13)$$

The compressor overall efficiency, which is the ratio of heat

T1 (C)	T5 (C)	P1 (bar)	P5 (bar)	n (exp)	n (eq)
61.65	13.35	6.91	3.19	1.206	1.198
64.13	13.71	7.17	3.21	1.205	1.194
65.88	14.17	7.67	3.29	1.191	1.187
68.32	15.00	7.92	3.18	1.173	1.179
69.27	13.59	8.38	3.32	1.181	1.182
69.83	19.87	9.46	4.16	1.170	1.159
70.12	19.70	9.38	4.09	1.171	1.159
70.84	21.03	9.20	4.16	1.166	1.153
71.27	14.91	8.59	3.34	1.176	1.175
72.14	22.14	9.46	4.09	1.163	1.148
72.23	11.85	9.36	3.41	1.174	1.180
72.74	11.43	9.28	3.47	1.189	1.184
73.10	15.50	9.30	3.47	1.164	1.166
73.14	22.47	9.46	4.01	1.159	1.145
73.43	14.71	9.26	3.38	1.164	1.168
73.48	13.98	9.13	3.37	1.173	1.173
73.84	9.73	9.50	3.27	1.177	1.185
73.85	13.92	9.19	3.28	1.165	1.171
73.91	12.67	9.37	3.39	1.175	1.176
74.03	22.98	9.50	3.91	1.151	1.140
74.16	12.70	9.17	3.24	1.171	1.175
74.40	11.81	9.34	3.21	1.168	1.177
74.55	11.03	9.07	3.07	1.171	1.180
74.56	12.79	9.05	3.10	1.167	1.174
75.00	23.43	9.42	3.84	1.152	1.137
75.86	14.23	9.67	3.41	1.167	1.166
77.10	7.07	9.67	2.88	1.165	1.187
77.75	15.76	10.06	3.42	1.154	1.155
78.33	5.73	9.78	2.75	1.163	1.189
79.59	15.93	10.46	3.43	1.150	1.150
80.08	11.43	10.07	3.14	1.166	1.168
83.93	7.23	10.01	2.93	1.191	1.183
84.21	7.29	10.05	2.95	1.193	1.183
84.21	6.44	10.01	2.89	1.193	1.186
84.51	4.43	9.80	2.71	1.194	1.194
85.23	6.91	9.88	2.84	1.195	1.184
85.56	4.93	9.97	2.74	1.194	1.190

Table (6.1) Validation of equation (6.2) ,the polytropic index as a function of P1,P5 and T5.

Frq (Exp) (Hz)	Frq(Eq) (Hz)	Mr (Exp) (kg/s)	Mr (Eq) (kg/s)	V ₁ (m ³ /kg)	V ₅ (m ³ /kg)
33.2	35.4	0.0049	0.0052	0.0216	0.0636
34.3	35.6	0.0050	0.0051	0.0219	0.0644
34.4	36.4	0.0054	0.0057	0.0213	0.0600
34.9	37.2	0.0056	0.0059	0.0216	0.0588
35.3	36.5	0.0056	0.0058	0.0213	0.0595
35.7	36.3	0.0055	0.0056	0.0214	0.0605
39.0	41.0	0.0074	0.0078	0.0222	0.0507
39.1	39.3	0.0067	0.0068	0.0222	0.0553
39.1	40.3	0.0073	0.0075	0.0219	0.0517
39.2	39.3	0.0067	0.0068	0.0222	0.0553
39.7	39.3	0.0065	0.0065	0.0229	0.0578
39.9	40.1	0.0073	0.0073	0.0220	0.0524
40.0	40.0	0.0070	0.0070	0.0225	0.0546
40.0	39.6	0.0067	0.0066	0.0230	0.0572
40.2	40.6	0.0075	0.0076	0.0222	0.0516
40.4	39.3	0.0072	0.0070	0.0217	0.0537
40.6	40.3	0.0073	0.0073	0.0223	0.0531
40.8	39.4	0.0074	0.0072	0.0214	0.0523
41.0	41.8	0.0083	0.0084	0.0220	0.0480
41.1	42.8	0.0091	0.0095	0.0216	0.0440
41.3	40.0	0.0072	0.0070	0.0226	0.0549
41.6	41.8	0.0086	0.0086	0.0217	0.0470
41.6	42.3	0.0089	0.0090	0.0217	0.0456
41.7	42.6	0.0091	0.0093	0.0216	0.0445
41.7	42.8	0.0094	0.0097	0.0214	0.0432
42.2	42.7	0.0095	0.0096	0.0214	0.0434
42.2	40.8	0.0076	0.0074	0.0227	0.0531
42.2	40.8	0.0077	0.0074	0.0227	0.0531
42.5	42.9	0.0076	0.0077	0.0246	0.0538
43.8	43.8	0.0075	0.0075	0.0261	0.0568
44.9	42.3	0.0081	0.0076	0.0241	0.0538
46.6	45.5	0.0084	0.0082	0.0268	0.0544
50.6	48.5	0.0089	0.0085	0.0296	0.0561

Table(6.2) Validation Of equation (6.8)

Tc (C)	Te (C)	Pe (Exp) (W)	Pe' (Eq) (W)
27.64	3.2	254	265
29.06	3.67	260	269
31.65	4.16	269	272
32.86	3.17	270	277
35.08	4.74	285	293
36.03	4.84	288	286
38.24	1.67	282	291
38.48	5.34	293	295
38.72	3.26	288	291
39.03	4.74	292	299
39.14	5.26	294	295
39.23	5.44	295	304
39.40	2.88	294	302
39.49	4.35	293	297
39.61	10.68	310	301
39.76	8.10	304	303
39.93	9.81	309	306
39.93	10.39	311	314
39.93	11.46	314	314
40.11	3.65	293	303
40.11	8.86	307	306
40.11	11.29	314	319
40.83	5.58	300	306
40.83	0.63	287	294
41.26	-1.35	283	294
41.34	-1.36	283	298
41.88	1.61	293	308
42.19	1.44	301	307
42.19	0.54	302	309
42.39	1.47	298	306
42.44	5.52	305	310
42.47	2.91	299	306
44.01	5.60	310	316

Table(6.3) Validation of equation (6.9).

transferred to the freon to the electrical input power is given by,

$$\eta_o = \frac{W1}{P_e} \quad (6.15)$$

The isentropic efficiency is calculated from,

$$\eta_i = \frac{(T1 - T5)}{(T1 - T5)} \quad (6.16)$$

6.2.2 Evaporator Model

The analysis here is following a method suggested by Blundell (33). The heat transfer coefficient is calculated for the air side by neglecting the effect of suction superheat. Other effects such as fouling factor and resistance to the heat transfer by the tube and the fin are also neglected because of the reasons given in chapter(3.3).

The heat transfer coefficient for the evaporator H_c is calculated as described in chapter 3. Since the thermal capacity of freon during the evaporation process is very much greater than air ($C_r \gg C_a$), the equation for the evaporator effectiveness (equation (3.31)) can be simplified to ,

$$\xi_v = 1 - \exp\left(-\frac{H_c A}{C_a}\right) \quad (6.17)$$

The effectiveness of the evaporator (see also chapter 3) can also be expressed by the equation below,

$$\xi_v = \frac{C_a (T_a(i) - T_a(o))}{C_{min} (T_a(i) - T_e)} \quad (6.18)$$

where $T_a(i)$ and $T_a(o)$ are air inlet and outlet temperatures respectively.

The heat rejected by the air is equal to the heat absorbed

by the freon.

$$C_a (T_a(i) - T_a(o)) = (h_5 - h_4) \dot{M}_r \quad (6.19)$$

From equation (6.18) and (6.19), the air inlet temperature $T_a(i)$ is

$$T_a(i) = T_e + \frac{(h_5 - h_4) \dot{M}_r}{\dot{M}_a C_{pa} \zeta_v} \quad (6.20)$$

The evaporating temperature T_e is calculated from equation (6.21) (for its first estimate) which was developed from experimental data.

$$T_e = -3.595 + 0.786 T_a(i) + 13.10 A_s - 0.485 S_h \quad (6.21)$$

where S_h is the suction superheat and A_s is the air speed. Values of T_e derived from this equation are compared with those from the experiment in table (6.5). It is believed that it is not possible to obtain a better fit because the variation of freon flow rate is an unknown factor which will also affect the evaporating temperature. Nevertheless, as a first guess for T_e in the computer model, equation (6.21) is a better estimate than some simpler assumption.

It is assumed that the pressure drop in the evaporator is about 0.13 bar (2 psi). Therefore the suction pressure $P_5 = (P_4 - 0.13)$ bar. The suction temperature is $T_5 = T_e + S_h$.

Since some of the equations are empirical, it is therefore necessary to validate the model before it can be accepted. For this validation, all the input required (points 1 to 5 of the freon cycle on P-h diagram) are taken from the present experimental work. The model calculates air inlet temperature from equation (6.20) (say $T_a(i)'$). The results show that $T_a(i)'$ and $T_a(i)$ (from the experiment) agreed within an error $\pm 2^\circ\text{C}$, which is acceptable (see table (6.4)).

Tc (C)	Te (C)	As m ³ /s	Ta(i) (Exp) (C)	Ta(i)' (Model) (C)
27.64	3.20	0.096	14.63	16.61
29.06	3.67	0.092	14.62	16.83
31.65	4.16	0.093	15.34	16.98
32.86	3.17	0.095	14.70	14.55
35.08	4.74	0.092	14.84	16.37
36.03	4.84	0.093	15.37	16.29
38.24	1.67	0.100	11.44	11.67
38.48	5.34	0.096	15.03	15.92
38.72	3.26	0.103	14.00	13.67
38.76	3.96	0.080	13.89	16.33
39.03	4.74	0.111	14.25	15.09
39.14	5.26	0.098	15.77	17.15
39.23	5.44	0.149	14.47	14.29
39.40	2.88	0.095	13.54	13.66
39.49	4.35	0.123	13.28	14.36
39.61	10.68	0.111	24.00	24.01
39.76	8.10	0.121	23.50	20.55
39.93	9.81	0.121	23.00	22.15
39.93	10.39	0.121	23.00	22.88
39.93	11.46	0.123	23.00	23.81
40.11	3.65	0.092	14.07	14.73
40.11	8.86	0.121	23.00	21.04
40.83	5.58	0.094	15.13	15.95
40.83	0.63	0.113	7.78	7.52
41.26	-1.35	0.107	7.05	6.17
41.34	-1.36	0.082	6.28	6.81
41.88	1.61	0.122	8.67	8.64
42.05	-0.89	0.080	7.05	7.54
42.19	0.54	0.114	7.83	7.52
42.39	1.47	0.122	8.56	8.31
42.44	5.52	0.094	15.58	15.68
42.47	2.91	0.093	10.45	11.19
44.01	5.60	0.092	15.58	15.60

Table(6.4) Validation of evaporator model.

Air Temperature (C)	Air Speed (m ³ /s)	Suction S-Heat (C)	Te(Exp) (C)	Te(Eq) (C)
6.28	0.082	5.79	-1.36	-0.39
7.05	0.080	5.85	-0.89	0.17
7.05	0.107	7.08	-1.35	-0.08
7.78	0.113	6.44	0.63	0.88
7.83	0.114	5.90	0.54	1.19
7.97	0.118	6.71	0.20	0.96
8.32	0.084	5.79	1.44	1.24
8.56	0.122	5.82	1.47	1.97
8.67	0.122	5.85	1.61	1.98
10.45	0.093	8.52	2.91	1.71
11.44	0.100	9.36	1.67	2.17
13.12	0.040	10.40	2.39	2.20
13.28	0.123	7.50	4.35	4.82
13.89	0.080	10.16	3.76	3.45
14.00	0.103	9.40	3.26	4.20
14.25	0.111	9.97	4.74	4.23
14.47	0.149	10.06	5.44	4.86
14.62	0.092	10.04	3.67	4.24
14.63	0.096	10.15	3.20	4.24
14.70	0.095	11.23	3.17	3.76
14.84	0.092	8.85	4.74	4.99
15.00	0.096	8.64	5.34	5.27
15.03	0.096	8.60	5.34	5.31
15.13	0.094	8.65	5.58	5.34
15.40	0.093	10.07	4.84	4.85
15.58	0.094	10.24	5.52	4.92
15.58	0.092	10.33	5.60	4.85
23.00	0.121	13.88	8.86	9.36
23.00	0.121	12.66	9.81	9.94
23.00	0.121	11.75	10.39	10.34
23.00	0.121	9.74	11.29	11.35
23.00	0.123	8.41	11.46	12.02
23.50	0.121	15.33	8.10	9.03

Table(6.5) Te(Eq) is from equation (6.32). Te is adjusted in the model.

6.2.3 The Condenser Model

For the purpose of predicting freon liquid temperature T3 and adjusting the condensing temperature Tc in the heat pump model, a very simple condenser model is developed. In this model the condenser is divided into three sections; desuperheating, condensing, and liquid cooling. It can be shown diagrammatically as in figure (6.1)

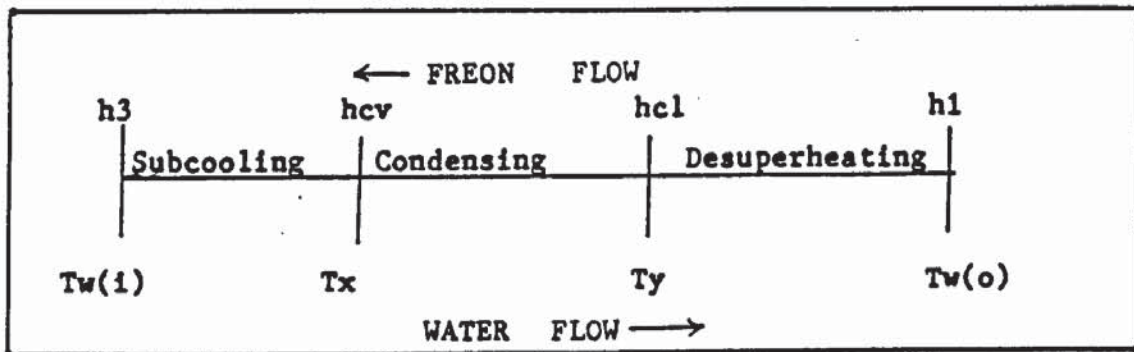


Fig (6.1) The condenser can be divided into three regions; desuperheating , condensing and liquid cooling.

It is assumed that the water temperature Ty at the start of the desuperheating region is equal to Tc. For this type of condenser, where the Tw(o) is higher than Tc, this assumption is reasonable and is confirmed by experimental results (chapter 5). The water temperature Tx, at the end of the condensing region is calculated from,

$$\frac{T_y - T_x}{T_w(o) - T_x} = \frac{h_{cv} - h_{cl}}{h_1 - h_{cl}} \quad (6.22)$$

In practice Tx is always higher than water inlet temperature Tw(1). If from the calculation of Tx by equation (6.22) above, the resulting Tx is less than Tw(1), then the condensing temperature, first estimated using equation (6.24), must be increased.

The enthalpy of the liquid freon h3 is calculated from the relation below.

$$\frac{h1 - h3}{h1 - h3} = \frac{T_x - T_w(i)}{T_w(o) - T_w(i)} \quad (6.23)$$

The freon liquid temperature T3 is determined from h3 (see appendix G). It should be noted that the final value of T3 is checked and if necessary adjusted by the evaporator model.

For a given hot water temperature Tw(o) and evaporating temperature Te, there is a unique condensing temperature Tc. This Tc depends on the type of the heat pump system. Therefore it is reasonable to estimate Tc from Te and Tw(o), as given by the empirical equation (6.24).

$$T_c = 5.23 + 0.159 T_e + 0.735 T_w(o) \quad (6.24)$$

A comparison of Tc calculated from this equation with the experimental results is given in table (6.6).

The refrigerant pressure drop in the condenser is a function of the square of the refrigerant velocity (44). Therefore it is reasonable to develop an empirical equation to predict the pressure drop as a function of freon mass flow rate. The equation is,

$$P_3 = (P_1 - 3238.72 \dot{M}_r^{1.08}) \frac{1}{14.7} \quad (6.25)$$

Validation of this equation is given in table (6.7).

6.3 The Heat Pump Model

This model incorporates all the component models which have been described above. The main purpose of the model is to predict the heat

Hot water (C)	T _e (C)	T _c (Exp) (C)	T _c (Eq) (C)
29.72	3.20	27.65	27.57
31.95	3.67	29.06	29.28
35.17	4.16	31.72	31.73
36.68	3.17	32.86	32.68
39.74	4.74	35.08	35.18
41.28	4.84	35.97	36.32
43.30	10.68	39.58	38.74
44.32	11.46	39.93	39.61
44.40	11.29	40.11	39.64
44.62	5.34	38.48	38.86
44.70	10.39	39.93	39.72
44.73	3.26	38.66	38.61
44.74	1.67	38.24	38.36
44.80	3.76	38.72	38.74
44.84	9.81	39.93	39.73
44.86	2.39	38.12	38.56
44.94	8.86	40.11	39.65
44.95	4.35	39.61	38.94
45.02	8.10	39.76	39.59
45.02	5.44	39.23	39.17
45.09	4.74	39.02	39.11
45.29	4.25	39.61	39.18
46.54	-1.35	41.26	39.20
46.81	0.63	40.83	39.72
47.91	5.58	40.77	41.31
49.21	5.52	42.47	42.26
49.80	-1.36	41.34	41.60
50.26	0.54	42.19	42.24
50.81	0.20	41.63	42.59
50.91	1.44	42.22	42.86
50.99	1.47	42.47	42.92
51.21	-0.89	42.19	42.71
51.62	5.60	44.01	44.04

Table(6.6) T_c(eq) is calculated from equation (6.36) . T_c is adjusted in the model.

Te (C)	Tc (C)	Suction S-Heat (Deg C)	P3(Exp) (bar)	P3(Eq) (bar)
-1.36	41.34	5.79	9.38	9.20
-1.35	41.26	7.08	9.10	9.25
-0.89	42.19	5.82	9.52	9.40
0.20	41.63	6.71	9.33	9.29
0.54	42.19	5.90	9.45	9.32
0.63	40.83	6.44	8.74	8.90
1.44	42.22	5.79	9.24	9.35
1.47	42.47	5.82	9.38	9.38
1.61	41.91	5.85	9.34	9.24
1.67	38.24	9.36	8.39	8.22
2.39	38.12	10.40	8.28	8.12
2.91	42.47	8.52	9.39	9.37
3.17	32.86	11.23	6.72	6.89
3.20	27.65	10.15	5.69	5.64
3.26	38.66	9.40	8.32	8.21
3.67	29.06	10.04	5.81	6.08
3.76	38.72	10.16	8.14	8.25
4.16	31.72	10.01	6.44	6.51
4.35	39.61	7.50	8.34	8.42
4.74	35.08	8.85	6.99	7.34
4.74	39.02	9.97	8.14	8.27
4.84	35.97	10.07	7.35	7.46
5.34	38.48	8.60	7.84	8.10
5.44	39.23	10.06	8.07	8.29
5.52	42.47	10.24	8.85	9.82
5.58	40.77	8.65	8.43	8.66
5.60	44.01	10.33	9.31	9.42
8.10	39.76	15.33	8.16	8.28
8.86	40.11	13.88	7.97	8.32
9.81	39.93	12.66	7.80	8.23
10.39	39.93	11.75	7.68	8.18
11.29	40.11	9.74	7.49	8.17
11.46	39.93	8.41	7.35	8.14

Table(6.7) Validation of equation (6.25).

pump behaviour for a given operating condition. The inputs required by the model are,

1. Air inlet temperature, $T_a(i)$ in C
2. Air speed , A_s in $m^3 s^{-1}$
3. Suction superheat , Sh in deg C
4. Hot water outlet temperature, $T_w(o)$ in C
5. Cold water inlet temperature, $T_w(i)$ in C

The model first estimates T_e from equation (6.21). This allows T_5 , P_4 and P_5 to be found. Equation (6.24) is used to estimate T_c , and P_1 calculated. It then determines the polytropic index n from equation (6.2). Specific volumes V_5 and V_1 are then obtained from equations (6.3) and (6.1) respectively. T_1 is then calculated from the equation of state (6.3). The compressor frequency F_c and freon mass flow rate \dot{M}_r are calculated from equation (6.7) and (6.5) respectively.

The analysis then proceeds to the evaporator model, where T_3 is taken as $T_3 = T_w(i) + 5$, for an initial guess. The air inlet temperature $T_a(i)'$ is then calculated from equation (6.20). Within the program a subroutine is available for the determination of specific enthalpy h at any given temperature and pressure. This $T_a(i)'$ is made to agree with the input $T_a(i)$ within $\pm 0.9C$ (based on experimental uncertainty) by adjusting T_e .

The condensing temperature T_c is adjusted by varying T_x (equation (6.22)), until T_x is at least 2 deg C above $T_w(i)$.

At this stage T_c , T_e and \dot{M}_r are assumed to be the final values. The liquid temperature T_3 is then adjusted until $T_a(i)'$ agrees to within ± 0.3 deg C with $T_a(i)$.

The pressure at point 3 is calculated from equation (6.25). The freon cycle at this stage is completed. The water flow rate is calculated by taking the effectiveness of the condenser to be 100% (no heat loss). The compressor power and evaporator and condenser heat transfers are determined as a system COP evaluated.

Figure (6.32) shows that the flow chart of the heat pump model. While tables (6.8) to (6.16) show the comparison of the experimental results with the computer outputs at 9 operating conditions. Generally both results show a very close agreement with other. The heat output, water and freon mass flow rates agree within 5% . The agreement of the four points on the freon cycle is also very close. At point 3 the agreement is not as close as at other points. This is due to the assumption made in the condenser and evaporator model.

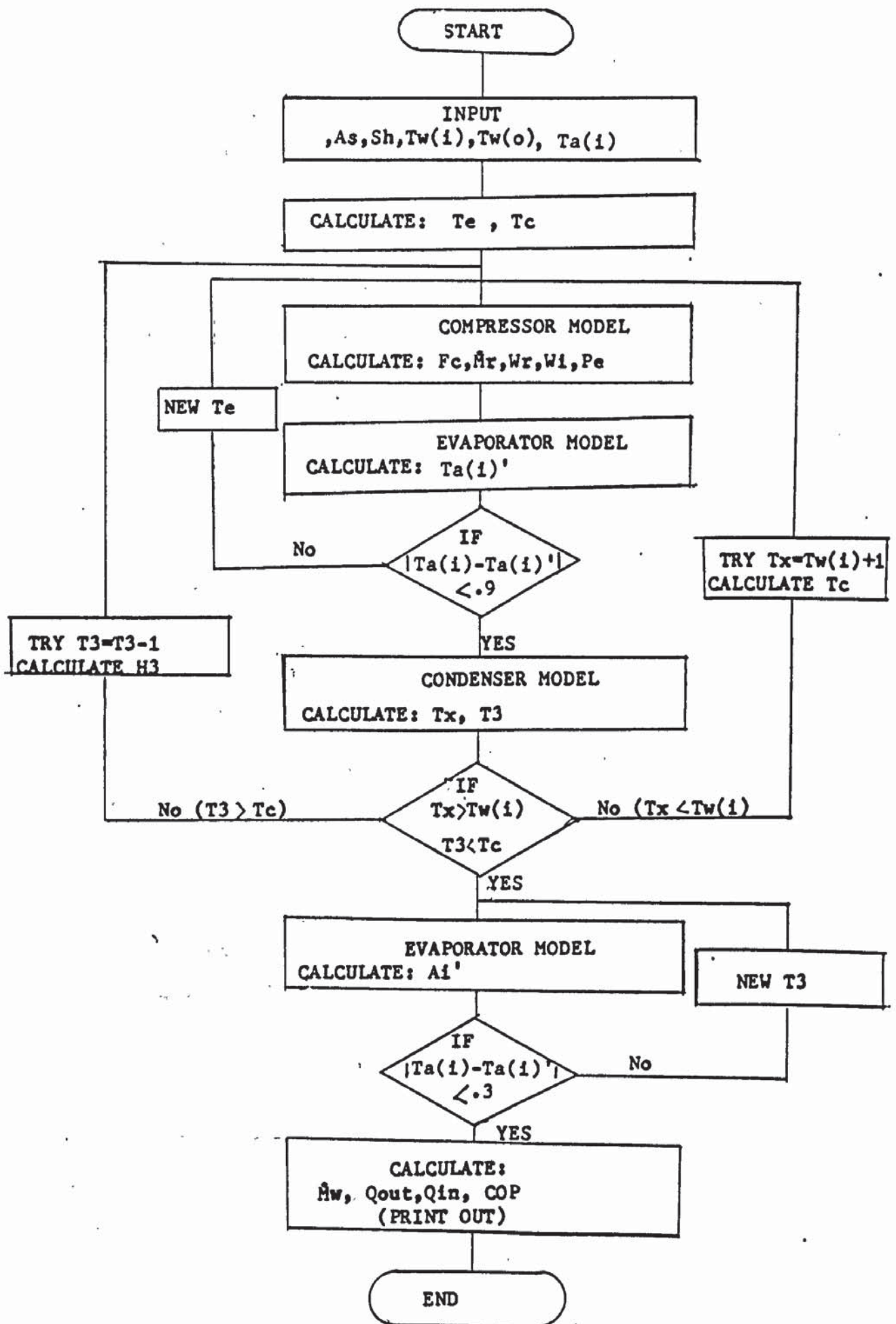
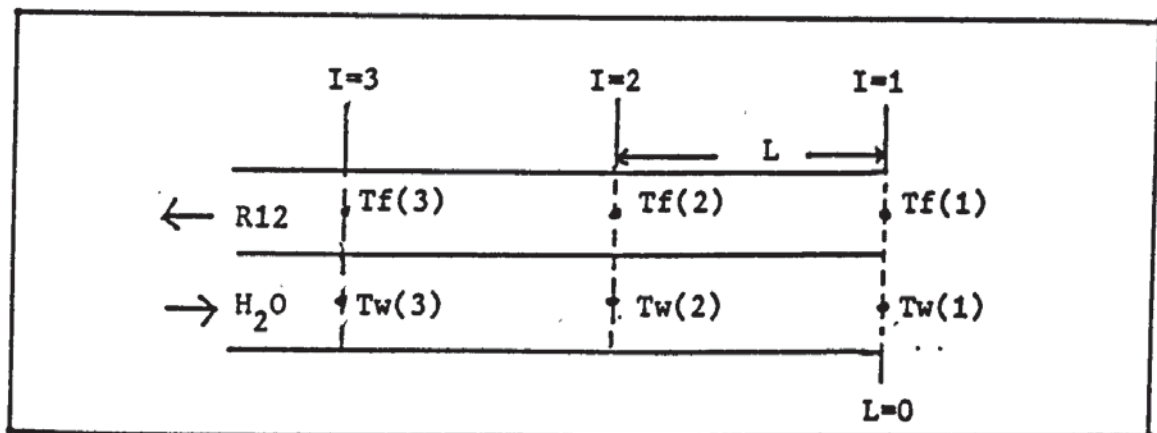


Fig (6.2) Flow chart of the heat pump model.

6.4 The Detailed Model Of The Condenser

This model is capable of predicting the freon and water temperature profiles along the condenser tube. The model is based on the model developed by Carrington (30). Basically the condenser is divided into three sections containing superheated vapour , condensing and liquid refrigerant . The three regions are treated as separate heat exchangers connected in series, and the sum of their heat transfer areas is equal to the fixed total heat transfer area of the condenser.



Fig(6. 3) The condenser is divided into 15 sections each of length 1m .

The analysis is started from the beginning of the superheated section over a certain length . The length increment can be chosen to be any value, but to speed up the computation , the length increment is taken as equal to 1 m.

Inputs to the model are the freon vapour temperature $T_f(1)=T_1$, pressure $P_f(1)=P_1$, the hot water temperature $T_w(0)=T_w(1)$, water inlet temperature $T_w(i) = T_w(16)$, freon and water mass flow rates, \dot{M}_r and \dot{M}_w .

The thermodynamic properties of freon and water (viscosity, density and specific heat), and then Prandtl, Reynolds and Nusselt numbers are calculated using temperatures and pressures at the beginning of every section. Using these values the heat transfer coefficients are calculated (chapter 3). The freon side H_r is the rate of heat being transferred from freon to the tube, and the water side H_w is from the tube to the water. The heat transfer from the freon tube to the water tube is assumed to be $500 \text{ Wm}^{-2}\text{C}^{-1}$ as suggested by Carrington (30). The linear heat transfer coefficient (in a side by side tube condenser) is calculated from,

$$UL = \left(\frac{1}{500} + \frac{1}{3.142 D_r H_r} + \frac{1}{3.142 D_w H_w} \right)^{-1} \quad (6.25)$$

The heat exchanger effectiveness is then

$$\epsilon_c = \frac{1 - \exp\left(-\frac{\Delta L UL}{C_f} + \frac{\Delta L UL}{C_w}\right)}{1 - \frac{C_r}{C_w} \exp\left(-\frac{\Delta L UL}{C_f} + \frac{\Delta L UL}{C_w}\right)} \quad (6.26)$$

The next water and freon temperatures, for the next segment are $T_w(I+1)$ and $T_f(I+1)$ respectively, are calculated from,

$$T_w(I+1) = \frac{(T_w(I) - \epsilon_c \frac{C_f}{C_w} T_f(I))}{(1 - \epsilon_c \frac{C_f}{C_w})} \quad (6.27)$$

and

$$T_f(I+1) = T_f(I) - \epsilon_c (T_f(I) - T_w(I+1)) \quad (6.28)$$

In the desuperheating region the pressure drop is assumed to be very small and negligible. The analysis exists from the desuperheating region when freon temperature equals the condensing temperature, T_c .

In the two phase or condensing region, the freon temperature is the

condensing temperature, $T_f(I) = T_c$; and since there is a pressure drop the condensing temperature is decreasing. The pressure drop in the two phase region is determined using the method due to Lockhart and Martinelli as described by Carrington (30). It is given by,

$$P_d = A_4(A_5(A_1+A_2+A_3)) + A_6 A_7 \quad (6.29)$$

where $A_1 = X^{1.8}$

$$A_2 = 5.7 \left(\frac{\nu_1}{\nu_v}\right)^{.0523} (1-X)^{.47} X^{1.3} \left(\frac{\rho_v}{\rho_l}\right)^{.26} \quad (6.29a)$$

$$A_3 = 8.11 \left(\frac{\nu_1}{\nu_v}\right)^{.105} (1-X)^{.94} X^{.86} \left(\frac{\rho_v}{\rho_l}\right)^{.522} \quad (6.29b)$$

$$A_4 = \frac{Gr^{1.95}}{(\rho_v Df)^2} \quad (6.29c)$$

$$A_5 = .09 \left(\frac{\nu_v}{Gr \cdot Df}\right)^{.2} \quad (6.29d)$$

$$A_6 = 2X + (1-2X)\left(\frac{\rho_v}{\rho_l}\right)^{.333} + (1-2X)\left(\frac{\rho_v}{\rho_l}\right)^{.667} - 2(1-X)\left(\frac{\rho_v}{\rho_l}\right) \quad (6.29e)$$

$$A_7 = Df \left(\frac{X}{\delta L}\right) \quad (6.29f)$$

X is the quality (X=1 for vapour and X=0 for liquid)

The condenser effectiveness for the two phase region is given by,

$$\xi_c = 1 - \exp\left(-\frac{\Delta L U_L}{C_w}\right) \quad (6.30)$$

The next water temperature is calculated from equation (3.18).

It is also assumed that 98% of freon is in the vapour state when entering the two phase region ($X(I) = .98$). The next value of X is calculated by first calculating the enthalpy at the end of the length.

$$H(I+1) = H(I) - \frac{C_w(T_w(I) - T_w(I+1))}{\dot{M}_r} \quad (6.31)$$

By knowing the pressure, the latent heat HL and the enthalpy of saturation liquid $H_s(\text{liq})$ can be determined. The next value of the quality

$$X(I+1) = \frac{H(I+1) - H_s(\text{liq})}{HL} \quad (6.32)$$

The analysis in the two phase region is completed when the quality X , becomes negative or close to zero (less than 10%).

In the subcooling section, the method of analysis is the same as the desuperheating region, except the freon is now liquid. The same equations are used in calculating the freon and water heat transfer coefficients.

This is^a somewhat crude model of the condenser, being based on only 15 segments of condenser, and so unable to determine with any great accuracy the boundaries from vapour to two phase to liquid. Nevertheless it does show the general features observed in the condenser (see figure (6.4) and (6.5)). Because of its inaccuracy and the length of the program it was not used in the heat pump model.

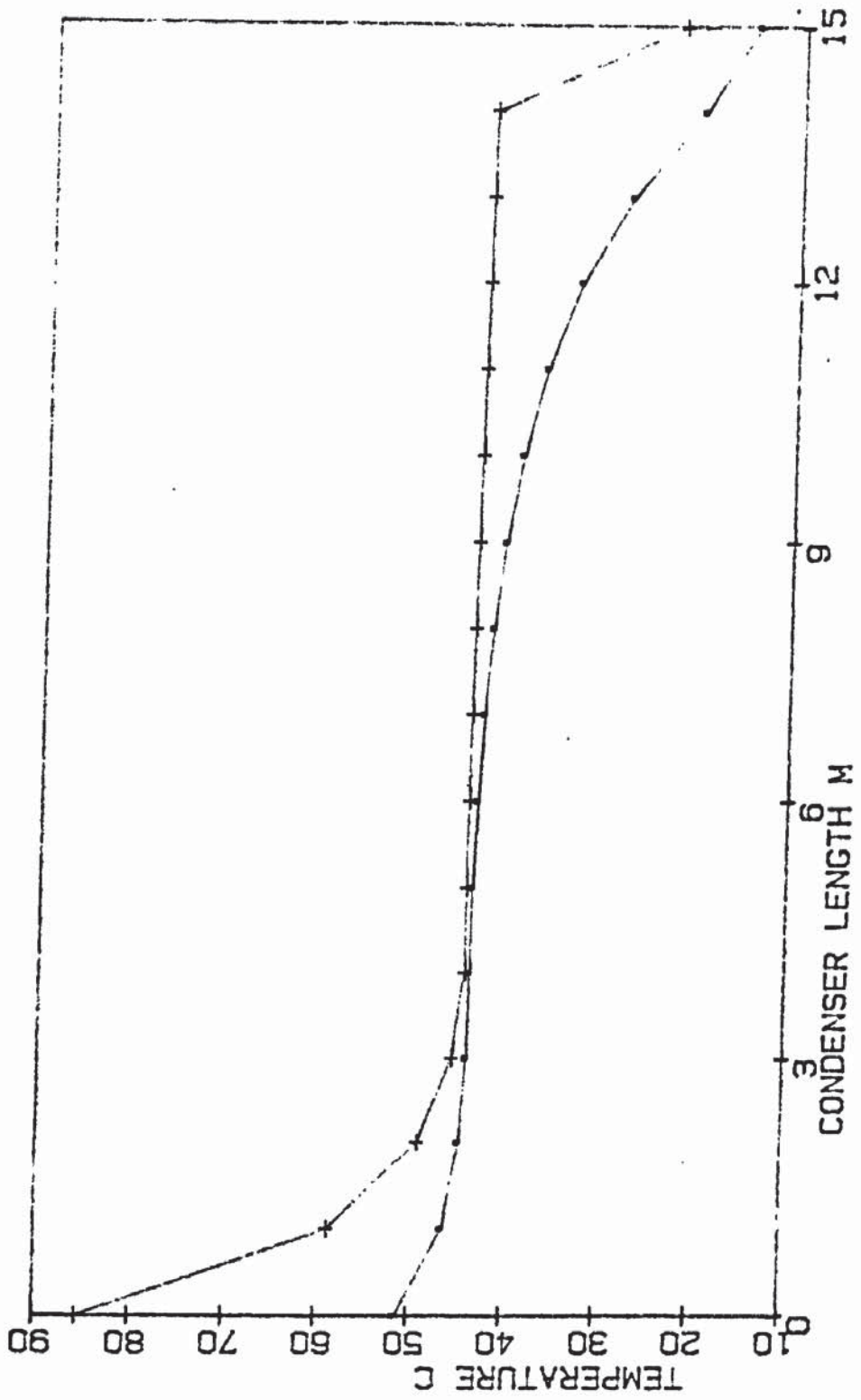


Fig (6.4) Temperature profile of freon and water inthe condenser at Tw(o)= 51C.

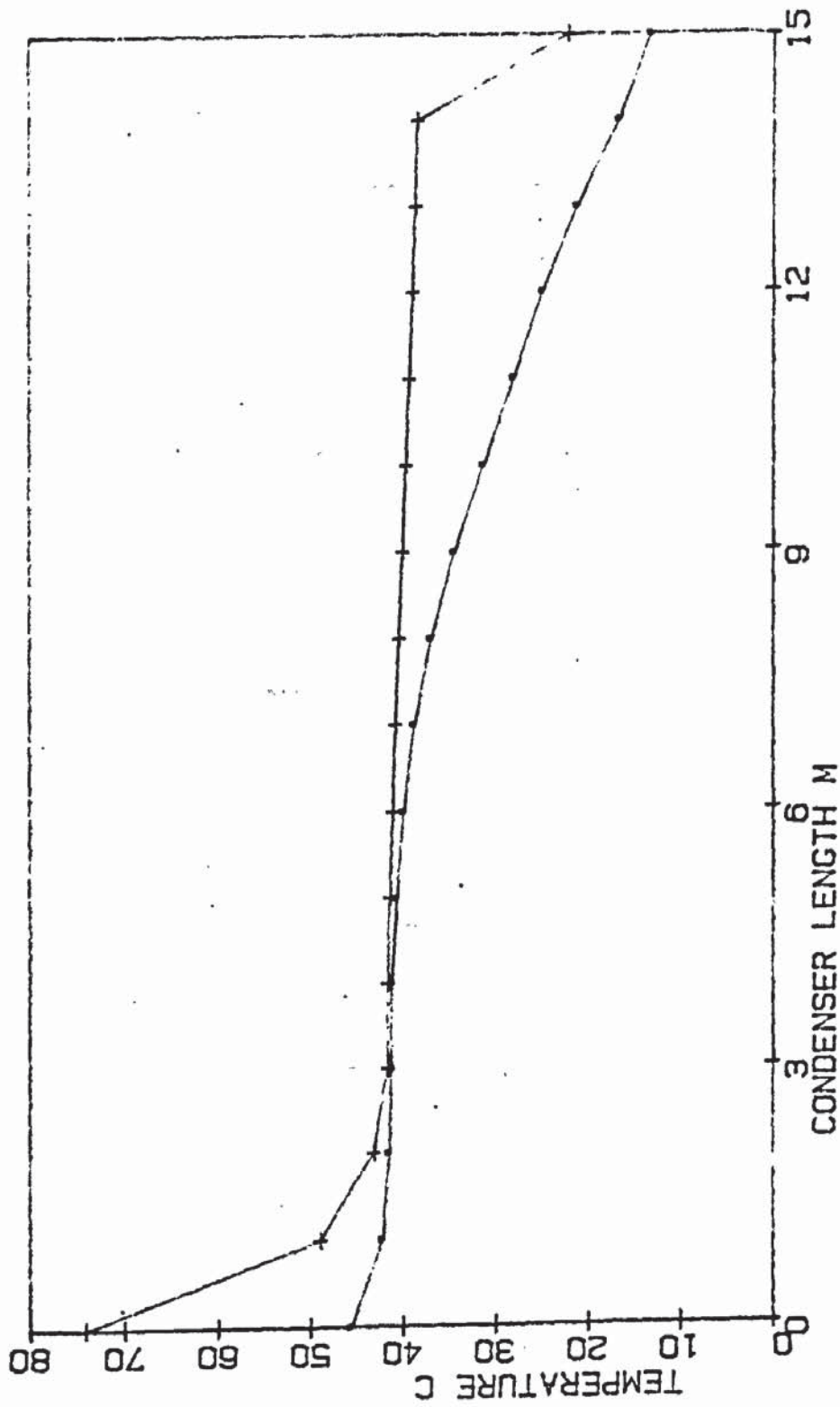


Fig (6. 5) Temperature profile of freon and water in the condenser at $T_w(o) = 45$ C.

HEAT PUMP MODEL:	RESULT	EXPERIMENT
<u>INPUT</u>		
Air Inlet Temperature	C: 24.00	24.00
Air Speed	$m^3 s^{-1}$: 0.111	0.111
Suction Super Heat	C: 9.02	9.02
Hot Water (out) Temperature	C: 43.30	43.30
Cold Water (in) Temperature	C: 12.38	12.38
<u>OUTPUT</u>		
Evaporating Temperature	C: 10.26	10.26
Condensing Temperature	C: 39.30	
Compressor Frequency	Hz: 42.70	
Freon Mass Flow Rate	kgs^{-1} : 0.00949	0.00914
Water Mass Flow Rate	kgs^{-1} : 0.0120	0.01164
Compressor Work	W: 253	
Compressor Isentropic Work	W: 152	
Compressor Electric Input	W: 308	301
Heat Out (Condenser)	W: 1579	1533
Heat Input (Evaporator)	W: 1349	
COP Carnot	: 10.79	
COP Cycle	: 6.24	
COP Practical	: 4.38	
* Evaporator:		
Air H.T.C	$W(m^2C)^{-1}$: 41.78	
Freon H.T.C	$W(m^2C)^{-1}$: 884.41	
Evaporator H.T.C	$W(m^2C)^{-1}$: 18.31	
Evaporator Effectiveness	: 0.74	
* Compressor:		
Volumetric Efficiency	: 0.95	
Isentropic Efficiency	: 0.60	
Polytropic Index	: 1.161	
* The Cycle (T in C ; P in bar) :		
Point : 1	: P = 9.347 T = 68.23	P = 9.381 T = 70.12
Point : 3	: P = 7.918 T = 21.24	P = 7.238 T = 23.32
Point : 4	: P = 4.224 T = 10.26	P = 4.259 T = 10.68
Point : 5	: P = 4.088 T = 19.28	P = 4.088 T = 19.70

Table(6. 8) Validation of the heat pump model.

HEAT PUMP MODEL:	RESULT	EXPERIMENT
<u>INPUT</u>		
Air Inlet Temperature	C: 23.50	23.50
Air Speed	$m^3 s^{-1}$: 0.121	0.121
Suction Super Heat	C: 15.30	15.30
Hot Water (out) Temperature	C: 45.02	45.02
Cold Water (in) Temperature	C: 12.07	12.07
<u>OUTPUT</u>		
Evaporating Temperature	C: 9.65	8.36
Condensing Temperature	C: 40.24	
Compressor Frequency	Hz: 41.69	
Freon Mass Flow Rate	$kg s^{-1}$: 0.00787	0.00829
Water Mass Flow Rate	$kg s^{-1}$: 0.01086	0.0106
Compressor Work	W: 225	
Compressor Isentropic Work	W: 149	
Compressor Electric Input	W: 310	303
Heat Out (Condenser)	W: 1521	1462
Heat Input (Evaporator)	W: 1319	
COP Carnot	: 10.24	
COP Cycle	: 6.29	
COP Practical	: 4.17	
* Evaporator:		
Air H.T.C	$W(m^2 C)^{-1}$: 44.49	
Freon H.T.C	$W(m^2 C)^{-1}$: 692.08	
Evaporator H.T.C	$W(m^2 C)^{-1}$: 16.29	
Evaporator Effectiveness	: 0.66	
* Compressor:		
Volumetric Efficiency	: 0.94	
Isentropic Efficiency	: 0.66	
Polytropic Index	: 1.133	
* The Cycle (T in C ; P in bar) :		
Point : 1 :	P = 9.565 T = 72.47	P = 9.422 T = 75.00
Point : 3 :	P = 8.238 T = 15.94	P = 8.05 T = 17.68
Point : 4 :	P = 4.143 T = 9.65	P = 3.973 T = 8.36
Point : 5 :	P = 4.007 T = 24.95	P = 3.837 T = 23.40

Table(6.9) Validation of the heat pump model.

HEAT PUMP MODEL:	RESULT	EXPERIMENT
<u>INPUT</u>		
Air Inlet Temperature	C: 7.05	7.05
Air Speed	$m^3 s^{-1}$: 0.08	0.08
Suction Super Heat	C: 5.82	5.82
Hot Water (out) Temperature	C: 51.21	51.21
Cold Water (in) Temperature	C: 11.37	11.37
<u>OUTPUT</u>		
Evaporating Temperature	C: -1.43	-1.64
Condensing Temperature	C: 43.75	
Compressor Frequency	Hz: 34.49	
Freon Mass Flow Rate	kgs^{-1} : 0.00509	0.00485
Water Mass Flow Rate	kgs^{-1} : 0.00523	0.00499
Compressor Work	W: 234	
Compressor Isentropic Work	W: 123	
Compressor Electric Input	W: 290	301
Heat Out (Condenser)	W: 883	858
Heat Input (Evaporator)	W: 665	
COP Carnot	: 7.01	
COP Cycle	: 3.78	
COP Practical	: 2.65	
* Evaporator:		
Air H.T.C	$W(m^2C)^{-1}$: 35.61	
Freon H.T.C	$W(m^2C)^{-1}$: 822.13	
Evaporator H.T.C	$W(m^2C)^{-1}$: 16.39	
Evaporator Effectiveness	: 0.79	
* Compressor:		
Volumetric Efficiency	: 0.90	
Isentropic Efficiency	: 0.53	
Polytropic Index	: 1.188	
* The Cycle (T in C ; P in bar) :		
Point : 1 :	P = 10.422 T = 86.12	P = 9.966 T = 85.56
Point : 3 :	P = 9.68 T = 24.60	P = 9.608 T = 24.27
Point : 4 :	P = 2.912 T = -1.43	P = 2.884 T = -1.64
Point : 5 :	P = 2.776 T = 4.39	P = 2.741 T = 4.93

Table(6.10) Validation of the heat pump model.

HEAT PUMP MODEL:	RESULT	EXPERIMENT
<u>INPUT</u>		
Air Inlet Temperature	C: 14.07	14.07
Air Speed	$m^3 s^{-1}$: 0.092	0.092
Suction Super Heat	C: 6.08	6.08
Hot Water (out) Temperature	C: 45.31	45.31
Cold Water (in) Temperature	C: 11.96	11.96
<u>OUTPUT</u>		
Evaporating Temperature	C: 3.43	3.43
Condensing Temperature	C: 40.16	
Compressor Frequency	Hz: 39.35	
Freon Mass Flow Rate	$kg s^{-1}$: 0.00702	0.00718
Water Mass Flow Rate	$kg s^{-1}$: 0.00841	0.0088
Compressor Work	W: 257	
Compressor Isentropic Work	W: 139	
Compressor Electric Input	W: 292	303
Heat Out (Condenser)	W: 1191	1251
Heat Input (Evaporator)	W: 953	
COP Carnot	: 8.53	
COP Cycle	: 4.63	
COP Practical	: 3.51	
* Evaporator:		
Air H.T.C	$W(m^2 C)^{-1}$: 38.14	
Freon H.T.C	$W(m^2 C)^{-1}$: 909.2	
Evaporator H.T.C	$W(m^2 C)^{-1}$: 17.83	
Evaporator Effectiveness	: 0.78	
* Compressor:		
Volumetric Efficiency	: 0.93	
Isentropic Efficiency	: 0.54	
Polytropic Index	: 1.186	
* The Cycle (T in C ; P in bar) :		
Point : 1 :	P = 9.551 T = 75.42	P = 9.503 T = 73.84
Point : 3 :	P = 8.503 T = 22.80	P = 8.49 T = 18.86
Point : 4 :	P = 3.415 T = 3.43	P = 3.401 T = 3.41
Point : 5 :	P = 3.279 T = 9.51	P = 3.272 T = 9.73

Table(6.11) Validation of the heat pump model.

HEAT PUMP MODEL:	RESULT	EXPERIMENT
<u>INPUT</u>		
Air Inlet Temperature	C: 15.77	15.77
Air Speed	$m^3 s^{-1}$: 0.098	0.098
Suction Super Heat	C: 6.17	6.17
Hot Water (out) Temperature	C: 44.44	44.44
Cold Water (in) Temperature	C: 12.31	12.31
<u>OUTPUT</u>		
Evaporating Temperature	C: 4.83	5.25
Condensing Temperature	C: 39.71	
Compressor Frequency	Hz: 40.28	
Freon Mass Flow Rate	kgs^{-1} : 0.00755	0.0074
Water Mass Flow Rate	kgs^{-1} : 0.00934	0.00936
Compressor Work	W: 261	
Compressor Isentropic Work	W: 143	
Compressor Electric Input	W: 295	301
Heat Out (Condenser)	W: 1276	1286
Heat Input (Evaporator)	W: 1035	
COP Carnot	: 8.96	
COP Cycle	: 4.90	
COP Practical	: 3.72	
* Evaporator:		
Air H.T.C	$W(m^2C)^{-1}$: 39.6	
Freon H.T.C	$W(m^2C)^{-1}$: 909.83	
Evaporator H.T.C	$W(m^2C)^{-1}$: 18.15	
Evaporator Effectiveness	: 0.77	
* Compressor:		
Volumetric Efficiency	: 0.93	
Isentropic Efficiency	: 0.55	
Polytropic Index	: 1.183	
* The Cycle (T in C ; P in bar) :		
Point : 1 :	P = 9.442 T = 73.24	P = 9.279 T = 72.74
Point : 3 :	P = 8.313 T = 21.93	P = 8.17 T = 18.88
Point : 4 :	P = 3.565 T = 4.80	P = 3.605 T = 5.26
Point : 5 :	P = 3.429 T = 10.97	P = 3.469 T = 11.43

Table(6.12) Validation of the heat pump model.

HEAT PUMP MODEL:	RESULT	EXPERIMENT
<u>INPUT</u>		
Air Inlet Temperature	C: 8.32	8.32
Air Speed	$m^3 s^{-1}$: 0.084	0.084
Suction Super Heat	C: 5.79	5.79
Hot Water (out) Temperature	C: 50.91	50.91
Cold Water (in) Temperature	C: 10.85	10.85
<u>OUTPUT</u>		
Evaporating Temperature	C: -0.36	0.30
Condensing Temperature	C: 43.63	
Compressor Frequency	Hz: 35.21	
Freon Mass Flow Rate	kgs^{-1} : 0.00542	0.00537
Water Mass Flow Rate	kgs^{-1} : 0.00547	0.00536
Compressor Work	W: 240	
Compressor Isentropic Work	W: 128	
Compressor Electric Input	W: 293	307
Heat Out (Condenser)	W: 928	923
Heat Input (Evaporator)	W: 705	
COP Carnot	: 7.2	
COP Cycle	: 3.83	
COP Practical	: 2.73	
* Evaporator:		
Air H.T.C	$W(m^2C)^{-1}$: 36.67	
Freon H.T.C	$W(m^2C)^{-1}$: 857.1	
Evaporator H.T.C	$W(m^2C)^{-1}$: 16.98	
Evaporator Effectiveness	: 0.79	
* Compressor:		
Volumetric Efficiency	: 0.90	
Isentropic Efficiency	: 0.53	
Polytropic Index	: 1.186	
* The Cycle (T in C ; P in bar) :		
Point : 1	: P = 10.388 T = 84.47	P = 10.007 T = 83.93
Point : 3	: P = 9.599 T = 25.55	P = 9.116 T = 28.53
Point : 4	: P = 3.02 T = -0.36	P = 3.075 T = 0.30
Point : 5	: P = 2.884 T = 5.43	P = 2.925 T = 7.23

Table(6.13) Validation of the heat pump model.

HEAT PUMP MODEL:	RESULT	EXPERIMENT
<u>INPUT</u>		
Air Inlet Temperature	C: 6.28	6.28
Air Speed	$m^3 s^{-1}$: 0.082	0.082
Suction Super Heat	C: 5.79	5.79
Hot Water (out) Temperature	C: 49.80	49.80
Cold Water (in) Temperature	C: 12.76	12.76
<u>OUTPUT</u>		
Evaporating Temperature	C: -1.69	-1.99
Condensing Temperature	C: 42.94	
Compressor Frequency	Hz: 34.83	
Freon Mass Flow Rate	kgs^{-1} : 0.00511	0.00495
Water Mass Flow Rate	kgs^{-1} : 0.00560	0.00542
Compressor Work	W: 234	
Compressor Isentropic Work	W: 122	
Compressor Electric Input	W: 287	307
Heat Out (Condenser)	W: 879	871
Heat Input (Evaporator)	W: 660	
COP Carnot	: 7.08	
COP Cycle	: 3.75	
COP Practical	: 2.66	
* Evaporator:		
Air H.T.C	$W(m^2C)^{-1}$: 36.36	
Freon H.T.C	$W(m^2C)^{-1}$: 844.8	
Evaporator H.T.C	$W(m^2C)^{-1}$: 16.76	
Evaporator Effectiveness	: 0.79	
* Compressor:		
Volumetric Efficiency	: 0.90	
Isentropic Efficiency	: 0.52	
Polytropic Index	: 1.191	
* The Cycle (T in C ; P in bar) :		
Point : 1 :	P = 10.218 T = 85.58	P = 9.796 T = 84.51
Point : 3 :	P = 9.476 T = 27.01	P = 9.272 T = 24.92
Point : 4 :	P = 2.891 T = -1.69	P = 2.85 T = -1.99
Point : 5 :	P = 2.755 T = 4.10	P = 2.701 T = 4.43

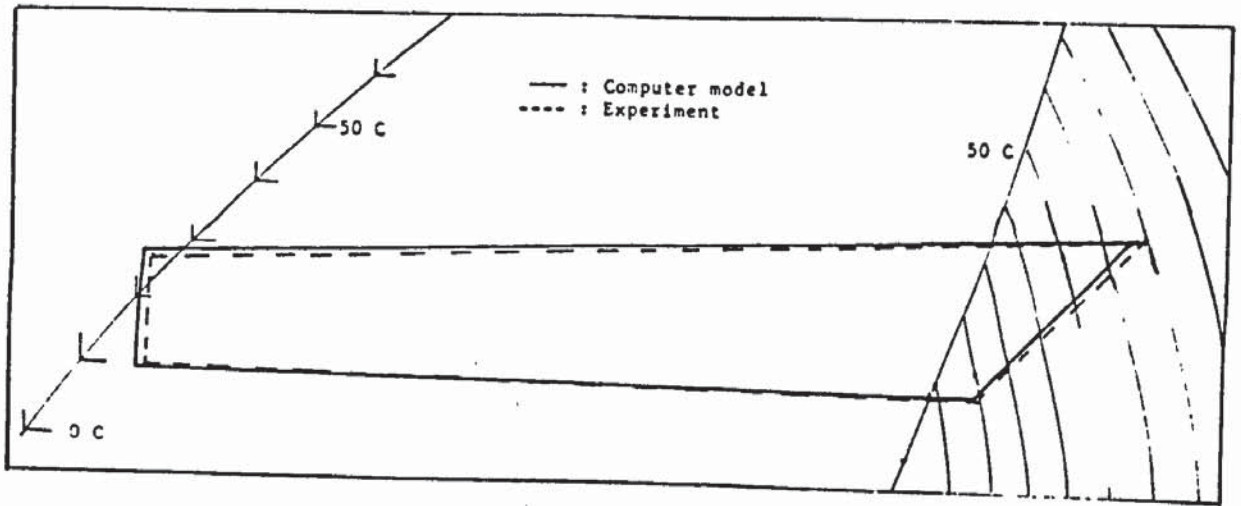
Table(6.14) Validation of the heat pump model.

HEAT PUMP MODEL:	RESULT	EXPERIMENT
<u>INPUT</u>		
Air Inlet Temperature	C: 8.56	8.56
Air Speed	$m^3 s^{-1}$: 0.122	0.122
Suction Super Heat	C: 5.82	5.82
Hot Water (out) Temperature	C: 50.99	50.99
Cold Water (in) Temperature	C: 11.92	11.92
<u>OUTPUT</u>		
Evaporating Temperature	C: 1.31	0.63
Condensing Temperature	C: 44.2	
Compressor Frequency	Hz: 35.8	
Freon Mass Flow Rate	kgs^{-1} : 0.00585	0.00556
Water Mass Flow Rate	kgs^{-1} : 0.00598	0.00572
Compressor Work	W: 246	
Compressor Isentropic Work	W: 136	
Compressor Electric Input	W: 299	306
Heat Out (Condenser)	W: 991	963
Heat Input (Evaporator)	W: 762	
COP Carnot	: 7.4	
COP Cycle	: 4.02	
COP Practical	: 2.80	
* Evaporator:		
Air H.T.C	$W(m^2C)^{-1}$: 47.68	
Freon H.T.C	$W(m^2C)^{-1}$: 890.4	
Evaporator H.T.C	$W(m^2C)^{-1}$: 19.44	
Evaporator Effectiveness	: 0.70	
* Compressor:		
Volumetric Efficiency	: 0.91	
Isentropic Efficiency	: 0.55	
Polytropic Index	: 1.18	
* The Cycle (T in C ; P in bar) :		
Point : 1	: P = 10.531 T = 82.88	P = 10.048 T = 84.21
Point : 3	: P = 9.673 T = 26.18	P = 9.272 T = 27.30
Point : 4	: P = 3.188 T = 1.31	P = 3.109 T = 0.63
Point : 5	: P = 3.052 T = 7.13	P = 2.946 T = 7.29

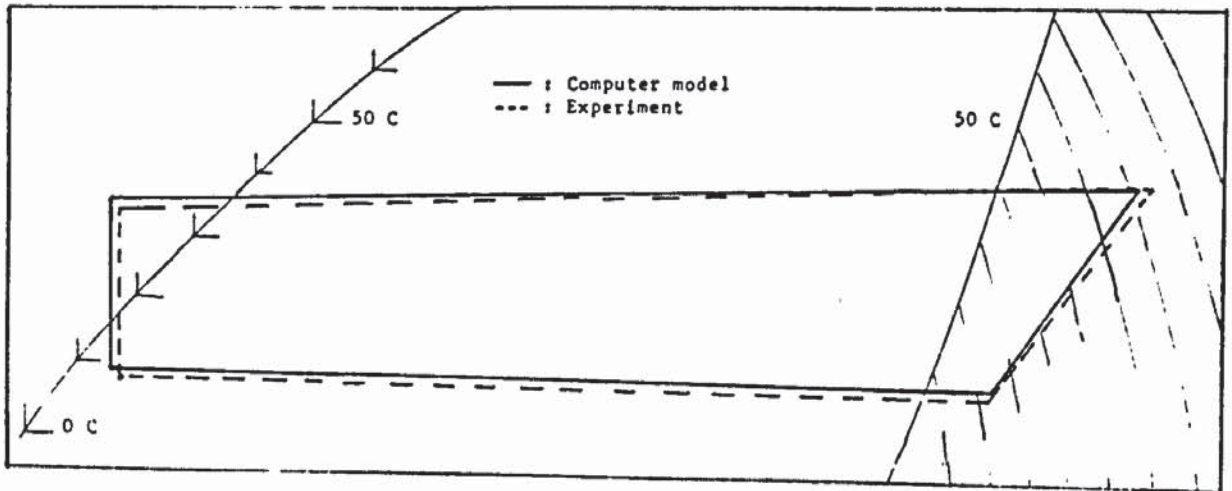
Table(6.15) Validation of the heat pump model.

HEAT PUMP MODEL:	RESULT	EXPERIMENT
<u>INPUT</u>		
Air Inlet Temperature	C: 23.00	23.00
Air Speed	$m^3 s^{-1}$: 0.121	0.121
Suction Super Heat	C: 12.66	12.66
Hot Water (out) Temperature	C: 44.84	44.84
Cold Water (in) Temperature	C: 11.95	11.95
<u>OUTPUT</u>		
Evaporating Temperature	C: 9.94	9.87
Condensing Temperature	C: 40.25	
Compressor Frequency	Hz: 41.28	
Freon Mass Flow Rate	$kg s^{-1}$: 0.00902	0.00889
Water Mass Flow Rate	$kg s^{-1}$: 0.01094	0.011
Compressor Work	W: 237	
Compressor Isentropic Work	W: 151	
Compressor Electric Input	W: 310	306
Heat Out (Condenser)	W: 1530	1520
Heat Input (Evaporator)	W: 1316	
COP Carnot	: 10.34	
COP Cycle	: 6.44	
COP Practical	: 4.18	
* Evaporator:		
Air H.T.C	$W(m^2 C)^{-1}$: 44.57	
Freon H.T.C	$W(m^2 C)^{-1}$: 808.39	
Evaporator H.T.C	$W(m^2 C)^{-1}$: 17.86	
Evaporator Effectiveness	: 0.69	
* Compressor:		
Volumetric Efficiency	: 0.94	
Isentropic Efficiency	: 0.64	
Polytropic Index	: 1.14	
* The Cycle (T in C ; P in bar) :		
Point : 1 :	P = 9.569 T = 71.23	P = 9.463 T = 73.14
Point : 3 :	P = 8.197 T = 18.91	P = 7.694 T = 22.08
Point : 4 :	P = 4.184 T = 9.94	P = 4.16 T = 9.87
Point : 5 :	P = 4.068 T = 22.6	P = 4.007 T = 22.47

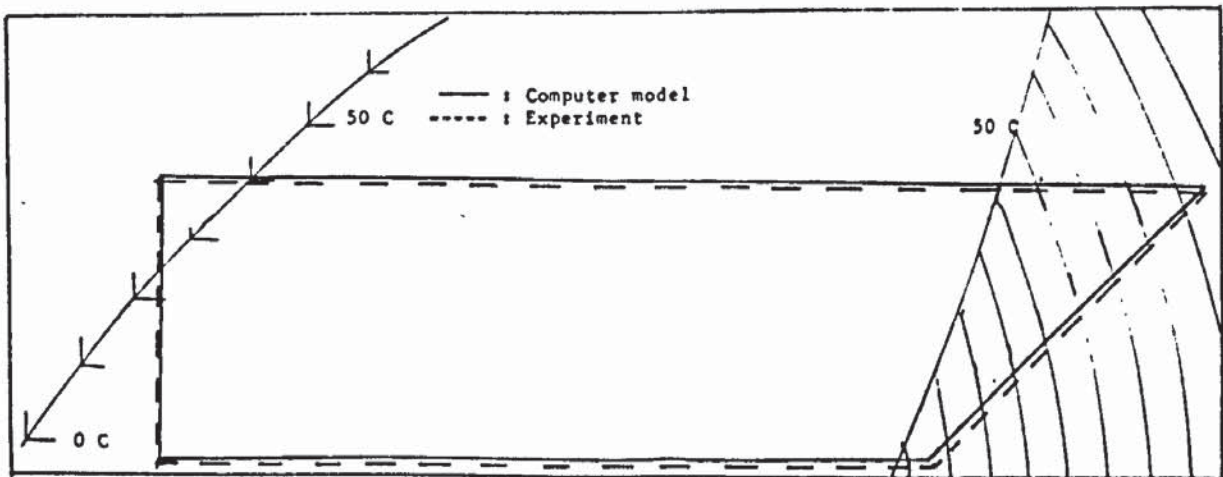
Table(6.16) Validation of the heat pump model.



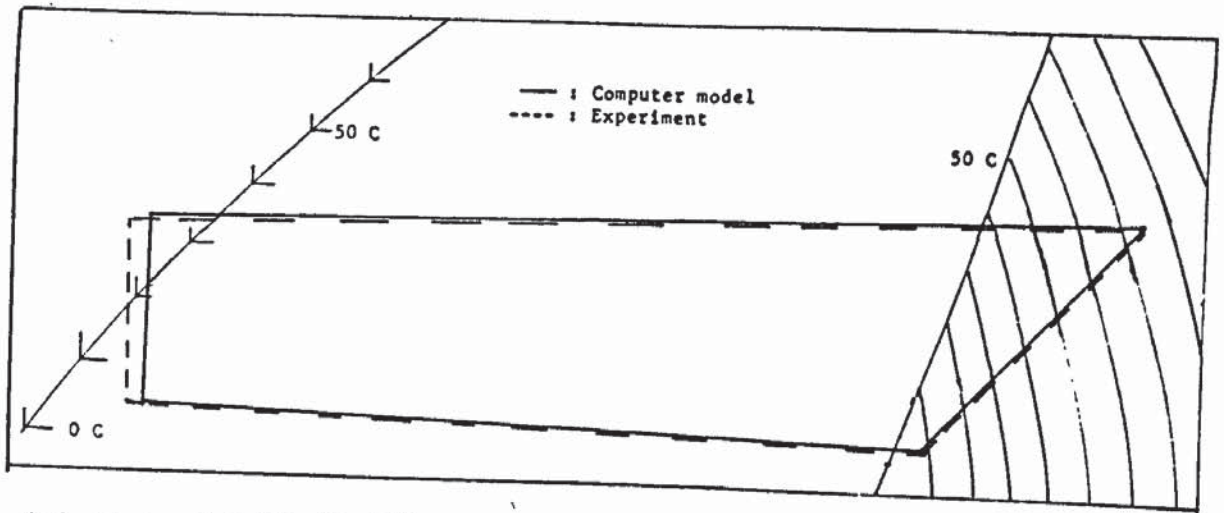
(a) Plot of table(6.8)



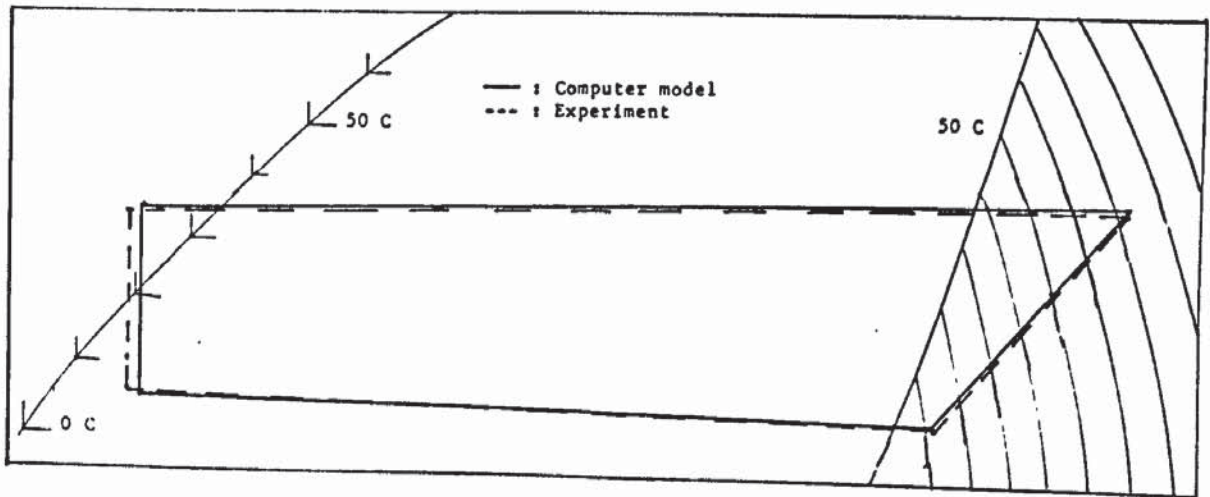
(b) Plot of table(6.9)



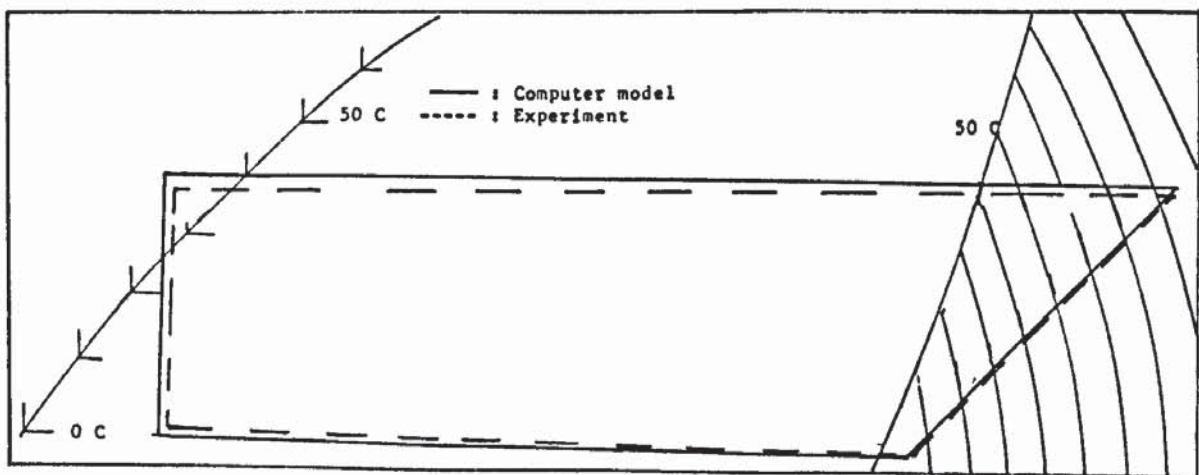
(c) Plot of table(6.10)



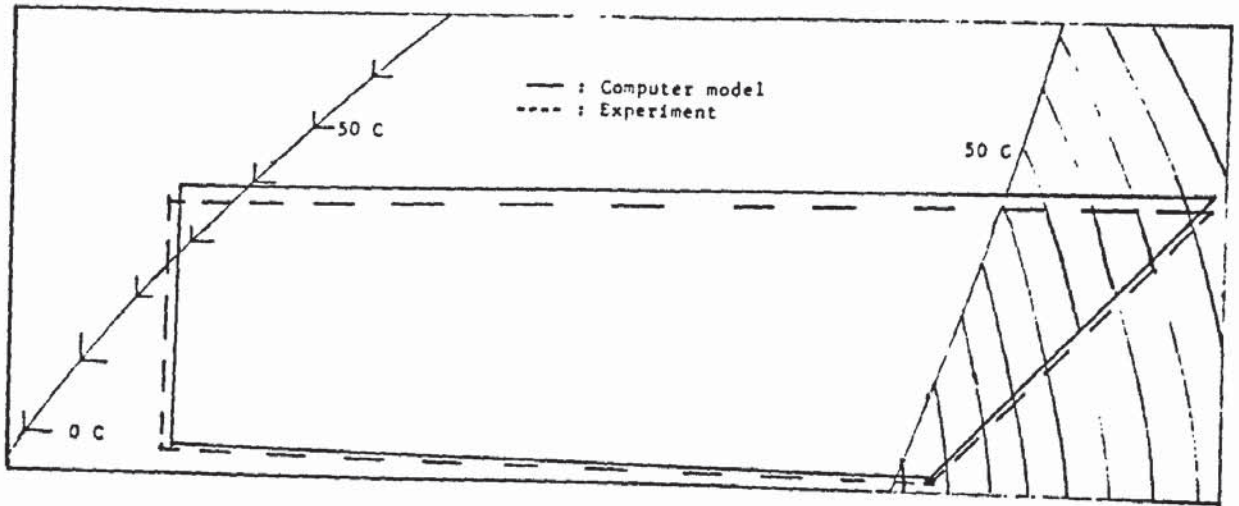
(d) Plot of table(6.11)



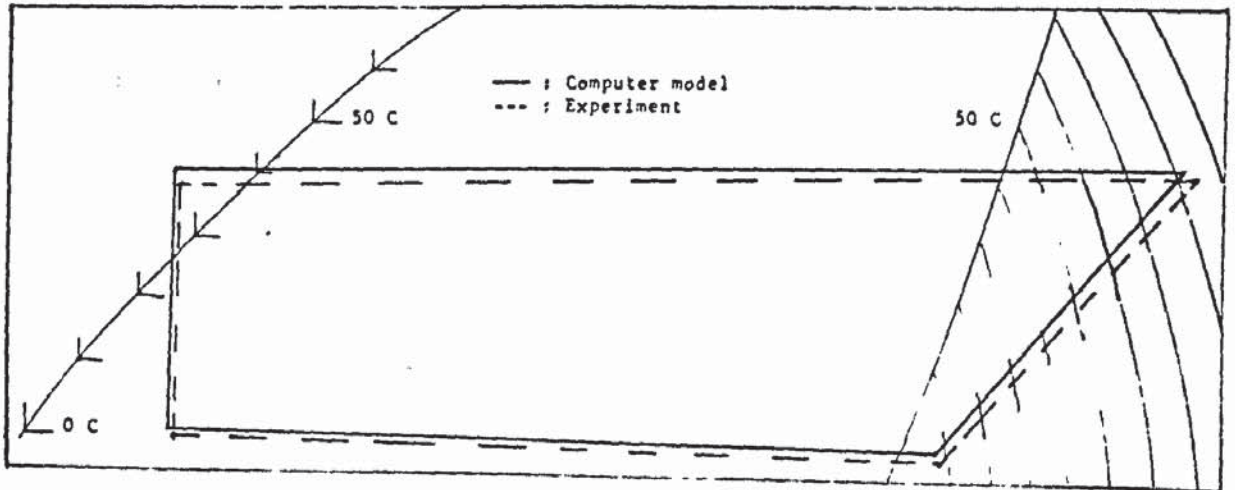
(e) Plot of table(6.12)



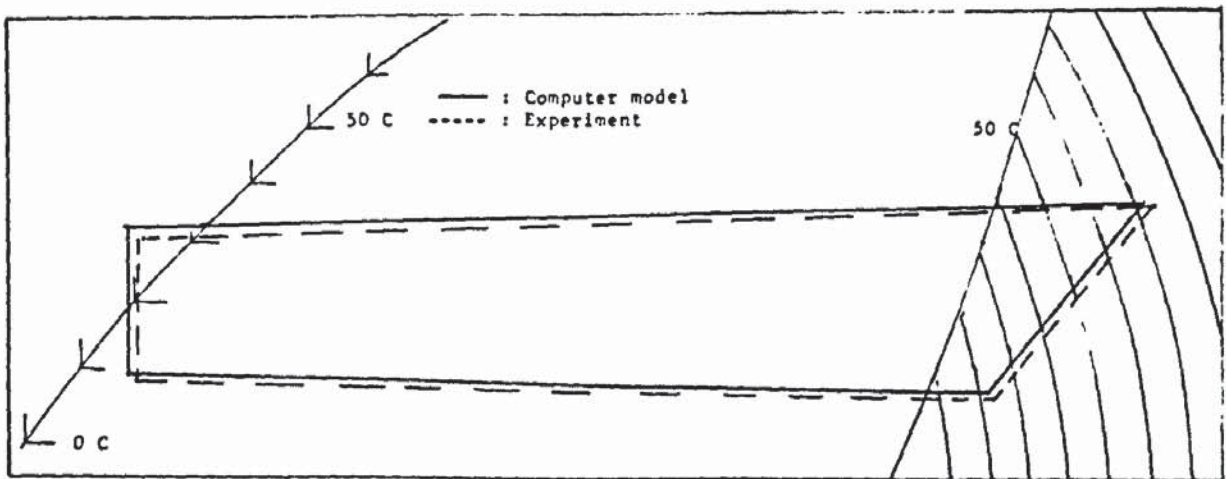
(f) Plot of table(6.13)



(g) Plot of table(6.14)



(h) Plot of table(6.15)



(i) Plot of table(6.16)

Fig(6.6) (a) to (i) Validation of the heat pump model.

THERMODYNAMIC CHARACTERISTICS OF AN AIR TO
WATER HEAT PUMP DETERMINED FROM THE MODEL

7.1 Air Inlet Temperature

Air inlet temperature is one of the main factors which affect the system COP. Together with air speed they will fix the evaporating temperature T_e , which is one of the most important features of an air source heat pump. For a given condensing temperature T_c a higher T_e means a higher COP and since the compressor work is almost constant, a higher heat output. The effect of air inlet temperature is studied using the heat pump model. The air inlet temperature is varied from 0 to 25 C at an air speed of $0.1 \text{ m}^3 \text{ s}^{-1}$. The water inlet temperature is 12 C and outlet is 45 C. Relative humidity is not an input variable in this model. Because of the use of empirical relationships predictions from the model will only apply to systems having similar humidity regimes to those given in table (5.3).

Figure (7.1) shows that increasing the air inlet temperature will increase the evaporating temperature, which is -6 C at an air inlet temperature of 0 C and 10.5 C at ^{an} air temperature of 25 C. Increasing T_e will increase the freon mass flow rate \dot{M}_r , as shown in figure (7.2). Therefore more heat can be absorbed from the air. This is confirmed by figure (7.3) which shows the plot of heat input against air inlet temperature to be increasing. The water flow rate \dot{M}_w and the heat output (figure (7.2) and (7.3)) show the same form as \dot{M}_r and heat input.

The plots of the three COPs , Carnot, cycle and practical, against air inlet temperature are shown in figure (7.4). All three are seen to increase with higher air temperature. The practical COP includes work done by the air fan in its calculation.

7.2 Air Speed

As has been mention above, apart from the air inlet temperature , air speed is another of the most important parameters in determining the heat pump COP. Using the heat pump model, the air flow is varied from $0.08\text{m}^3\text{s}^{-1}$ to $0.16\text{m}^3\text{s}^{-1}$, with the air temperature at 15 C and water inlet at 12 C and outlet at 45 C.

Figure (7.5) shows that at an air flow of $0.08\text{m}^3\text{s}^{-1}$, T_e is 3.2 C and at $0.16\text{m}^3\text{s}^{-1}$, T_e is 6.2 C. This is simply because at higher speed, more mass of air is passed through the evaporator, and so more energy is available. Since T_e is increased with the air speed, the freon and water mass flow rates \dot{M}_r and \dot{M}_w are also increased (figure (7.6)). As a result the heats input and output are also increased (figure (7.7)). Even though the heat input and output are increased with the air speed the practical COP is not. Figure (7.8) shows that the cycle COP increases with the air speed but not the practical COP. This is because at higher speed the fan will require more electrical power, and so increases the total work supplied to the system; and therefore reduces the practical COP. The plot in figure (7.8) gives an optimum air speed of about $0.11\text{m}^3\text{s}^{-1}$ for this particular evaporator. At this air speed the fan requires about 50W electrical power, which is about 4% of the output (condenser) energy. Figure (7.8) also shows

that practical COP is almost constant for a wide range of air speed A_s , while heat output varies from 1150 to 1350 W (figure (7.7)). Hence A_s can be used as a means of controlling heat output (over a limited range) with no loss of system efficiency.

7.3 Suction Superheat

Another parameter that can change T_e , and so affect the system COP is the suction superheat. The suction superheat is required in the system in the first place to ensure that no liquid freon can enter and damage the compressor. Another advantage of having suction superheat is that the density of freon vapour is lower than the saturated vapour. Tassou (45) has shown that the effect of the vapour density on the compressor input power is higher than the compression ratio. Danfoss (28), the manufacturer of the compressor used in this system allowed the suction temperature to be as high as 32 C (ambient temperature). Therefore it can be concluded that ^ahigh suction temperature is desirable.

There are two ways of increasing suction superheat. One way is by having the line between the evaporator and the compressor heated independently of the evaporator, which is not available in the present system. The other way is by reducing the freon mass flow rate using the expansion valve (note: the one in use is ^athermostatic expansion valve). Increasing the suction superheat in this way will reduce the heat input and output but increases the COP. This is because the work done by the compressor is also reduced.

Using the computer model, the suction superheat is varied for three air inlet temperatures. The other inputs are air speed of $0.1 \text{ m}^3 \text{ s}^{-1}$, water inlet temperature of 12 C and water outlet temperature of 45 C. Figure (7.9) shows the plot of evaporating temperature versus suction superheat at the air inlet temperatures of 23 , 15 , and 10 C. Clearly it can be seen that at the highest air inlet temperature, 23 C, the suction superheat can be as high as 11 deg C, without considerably changing T_e . At the inlet temperature of 15 C the limit is reduced to about 9deg C and at 10 C the limit is about 7 deg C. The limit is obviously set by the impossibility of $T_e + Sh$ exceeding $T_a(i)$.

Figure (7.10) shows that the water and freon mass flow rates fall when the superheat is increased. The same occurs with the heat output (figure (7.11)) and the system COP (figure (7.12)).

From the experimental results (figure (5.5)) a relationship between evaporating temperature T_e and air inlet temperature $T_a(i)$ was found to be $T_e = 0.6 T_a(i) - 5$. The maximum permissible suction superheat Sh is about $(T_a(i) - T_e) - 2$, which equals to $0.4 T_a(i) + 3$. For air temperatures of 23, 15 and 10 C the suction superheats are 12, 9 and 7 deg C respectively, which is in agreement with the predicted values from the model. It can be concluded here that the maximum permissible suction superheat is a variable related to the operating temperature, ($T_a(i)$).

7.4 Hot Water Temperature

The heat pump model is also used to study the variation of heat pump thermodynamic properties at various water outlet temperatures .

The air inlet temperature is kept at 15 C, the air flow at $0.1 \text{ m}^3 \text{ s}^{-1}$, the suction superheat at 8 deg C and the water inlet temperature at 12C. The water outlet temperature is varied from 35 to 60 C.

Figure (7.13) shows that the condensing temperature T_c , increases with the hot water temperature $T_w(o)$; and $T_w(o)$ is always higher than T_c . At $T_w(o)=35\text{C}$, T_c is about 3 degC lower than $T_w(o)$ and 7 degC at $T_w(o)=60\text{C}$. It should be noted that the condenser is designed to produce the hot water temperature a few degrees higher than the refrigerant condensing temperature, T_c by making the condenser length $L \gg D$, the diameter of the condenser tube.

The freon mass flow rate \dot{M}_r is found to be decreasing with increasing hot water temperature as shown in figure (7.14). The plot also shows that to produce hot water at higher temperature, the water flow rate must be reduced (which is done manually using the water regulator). For the above operating conditions, the water mass flow rate \dot{M}_w is 0.014 kgs^{-1} at $T_w(o)=35 \text{ C}$, and 0.006 kgs^{-1} for production of hot water at 60 C. Increasing $T_w(o)$ means increasing T_c , and so the compression ratio Cr is increased. Figure (7.15) shows that to produce a hot water at temperature $T_w(o)$ of 60 C it will require a Cr of about 3.6 , while to produce hot water at 35 C, it only requires a Cr of 2.4 .

It is recommended by the manufacturer that the compressor is cooled by a medium whose temperature is related to T_c . The hot water

discharged from the condenser is used in this work. Figure (7.16) shows how the hot water temperature affects the compressor polytropic index n . The value of n is higher at $T_w(o) = 35$ C compared with ^{the value} at $T_w(o) = 60$ C. This will be discussed in detail in section 7.5 below.

We see that hot water at 35 C can be produced with a practical COP of about 4, and at 60C with the COP of about 2.5(air inlet temperature is 15). The cycle and Carnot COPs also decrease with increasing hot water temperature (figure(7.17)).

7.5 The Compressor Characteristics And Energy Balance

The compressor is the most important component of the heat pump system. Therefore it is felt that a good understanding of its working principles is necessary in order to study the thermodynamics characteristics of the heat pump. The computer model which has been developed can be used to predict the freon discharge temperature, the compressor frequency, the various efficiencies and the energy balance.

The freon discharge temperature T_1 is related to the polytropic index n . The value of n can be varied by the compressor cooling and the operating condition (T_e and T_c).

In the first case cooling the compressor means removing a quantity of heat from the compressor. This will reduce the cylinder wall temperature, and so reduce the effect of direct heating of the freon vapour by the cylinder wall. The discharge temperature T_1 will be

nearer to T_i , the isentropic temperature, and so n will be smaller. Figure (7.18) confirmed this argument. For example when $T_e = -6.17$ C, $\dot{M}_w = 0.005 \text{ kgs}^{-1}$, $T_c = 39.5$ C and $F_c = 34.5$ Hz, n is 1.20. When $T_e = 10.19$ C, $\dot{M}_w = 0.011 \text{ kgs}^{-1}$, $T_c = 40.4$ C and $F_c = 42$ Hz, n is 1.16. In both cases the water inlet temperature is 12 C and outlet is 45 C, and the air flow is $0.1 \text{ m}^3 \text{ s}^{-1}$. The most significant differences from the examples above are T_e and \dot{M}_w . Higher \dot{M}_w means more heat can be removed from the compressor and so reduces n . Higher T_e will reduce the amount of heat that can be transferred to the freon vapour, and so reduces n .

From the example above, the cooler the cooling medium is, the lower n will be; but the compressor must not be overcooled (28).

Overcooling would reduce T_i and the output water temperature. To maintain the same water outlet temperature as the non-overcooled case a higher T_c would be required, so reducing the COP.

Another way of changing the value of n is by varying the condensing temperature, T_c . Figure (7.16) shows that when $T_w(o) = 35$ C, $T_e = 5$ C, $T_c = 32$ C, n is 1.20. While when $T_w(o) = 60$ C, $T_e = 5$ C, and $T_c = 52$ C, n is 1.14. At lower T_c more heat is transferred from the cylinder wall to the freon vapour, and so increasing the value of n . This is because at lower T_c , the temperature difference between the cylinder wall and the freon is higher. In the case of higher T_c , where the temperature difference between the cylinder wall and the freon vapour is lower, less heat can be transferred from the wall to the freon vapour, and this will reduce the value of n .

Figure (7.20) shows the compressor frequency plots against the air inlet temperature, for hot water temperature of 45C, 55C and 65C.

It can be seen that the frequency, F_c' ($=\eta_c F_c$) is high when $T_w(o)=$ is lower and lower when the $T_w(o)$ is higher. For example F_c' is 39 Hz at $T_w(o)=45$ C and 31 Hz at $T_w(o)=65$ C, where air inlet temperature, $T_a(i)$, is 10 C in both cases. The different of 8 Hz is due to the variation in the condenser efficiency, since F_c is almost constant. If F_c is taken as 50 Hz, η_c is about 78% at $T_w(o)=45$ C and 66% at $T_w(o)=65$ C.

The electrical power required by the compressor is also a function of evaporating and condensing temperatures. The power required by the compressor to produce hot water at 45C, 55C and 65C (water inlet temperature is 12 C) is plotted against the air inlet temperatures as shown in figure (7.19). The plot shows that the electrical energy is increasing with the air inlet temperature for constant $T_w(o)$, even though the compression ratio is decreasing. This result is in agreement with Tassou (45), who pointed out that the reduction in energy required because of decreasing compression ratio is outweighed by the increase in the energy required due to the higher vapour density.

As has been mentioned earlier, the total energy transferred to the freon vapour is not only from the compression work of the compressor W_r , but also from the frictional heat Q_r . Equation (6.14) in chapter 6 shows that the work done by the compressor plus Q_r is equal to the total work transferred to the freon vapour. The ideal gas value for Q_r can be derived as follows (see also for examples (27) and (35)).

From the first law of thermodynamics, (see diagram in appendix K),

$$U_2 - U_1 = Q_r + W_c \quad (7.1)$$

where Q_r is heat given to the vapour, and W_c is work done on the vapour in compression.

Q_r can be found if perfect gas assumptions are made. From equation (K.6) ,

$$W_c = \frac{1}{n-1} \dot{M}_r R (T_2 - T_1) \quad (7.2)$$

Joule's hypothesis states that the internal energy of a perfect gas is a function of temperature alone. Thus,

$$U_2 - U_1 = \dot{M}_r C_v (T_2 - T_1) \quad (7.3)$$

$$\text{or} \quad \dot{M}_r C_v (T_2 - T_1) = W_c + Q_r \quad (7.4)$$

Therefore

$$Q_r = \dot{M}_r (T_2 - T_1) \left(C_v - \frac{R}{n-1} \right)$$

Substituting with perfect gas relationships , $C_p - C_v = R$ and $C_p = \gamma C_v$ yields,

$$Q_r = \frac{\gamma - 1}{n-1} \dot{M}_r C_v (T_2 - T_1) \quad (7.5)$$

where $(T_2 - T_1) = \Delta T$ is the temperature difference between the initial and final states of the compression.

In the heat pump model the frictional heat Q_r is calculated from equation (7.5) and the compression work is from equation (6.11) in chapter 6. The energy transferred to the freon vapour is determined

from $\dot{M}r \cdot C_v \Delta T$. Equation (7.4) is then used to check the compressor energy balance. Table (7.1) shows some results on the calculation of the compressor energy balance.

The results show that W_i is about equal to W_{i1} . Therefore the compressor energy balance is satisfied for the isentropic case. For the polytropic case it can be seen that ΔU is about the same as $W_c + Q_r$, and this satisfies equation (7.4). The disagreement of about 10% between ΔU and $W_c + Q_r$ can be accepted considering the errors involved in the process of calculating ΔU , W_c and Q_r . Q_r is the least accurate of the three terms due to the uncertainty in $n-\gamma$ and the assumption of ideal gas behaviour in its determination. Table (7.1) also shows that Pe' which is $W_c + Q_r + Q_c$ is approximately equal to Pe , the electrical energy supplied to the compressor. This result shows that the energies involved with the compressor can be divided as,

$$Pe = W_c + Q_r + Q_c \quad (7.6)$$

If the compressor efficiency is taken as the ratio of the work done on the freon vapour W_c to the work supplied Pe , the efficiency is in the region of 40%, which is very low. Since most of the frictional heat is absorbed by the vapour, The overall efficiency which can be considered as the ratio of energy transferred to the freon vapour to the work supplied is now about 85% (see figure (7.21)), which is reasonable. The other 15% which is the heat removed by the cooling water is utilized in the condenser. Therefore the heat loss in the overall system is very small indeed.

Te	Tc	AU	Wc	Qr	Wc+Qr	W1	W11	Pe'	Pe	Qc
C	C	W	W	W	W	W	W	W	W	W
4.33	39.97	238	117	152	269	140	129	306	294	36
7.46	40.34	243	122	152	274	150	137	315	304	41
10.2	40.43	246	126	151	277	156	139	323	312	46
4.83	43.93	237	121	146	267	148	133	297	308	30
7.66	44.31	244	128	147	275	158	140	310	316	35
10.7	44.67	250	133	147	288	168	146	327	326	39

Table (7.1) The compressor energy distribution

$$AU = \dot{M}_r C_v \Delta T$$

$$Wc : \text{Equation (7.2)}$$

$$W1 : \text{Equation (6.11)}$$

$$Pe' = Wc + Qr + Qc$$

$$: Qc = \dot{M}_w C_{pw} \Delta T_{wc}$$

$$: Qr : \text{Equation (7.5)}$$

$$: W11 = \frac{1}{\gamma - 1} \dot{M}_r R \Delta T_1$$

$$: Pe : \text{Equation (6.9)}$$

ΔT_{wc} : The difference in water temperature across the compressor.

ΔT_1 : is equal to $(T1-T5)$, see figure (5.15) .

ΔT : The difference in freon temperature before and after the compression.

7.6 The Evaporator Effectiveness

The most important characteristic of the evaporator is its effectiveness. The evaporator with higher effectiveness and heat transfer coefficient is desired. Figure (7.23) shows that the effectiveness is increasing with decreasing air speed. While figure (7.24) shows that the heat transfer coefficient of the evaporator is decreasing with decreasing air speed. This suggests that there is an optimum air speed for a certain operating condition. Earlier it has been shown that the optimum air speed is when the fan takes about 4% of the energy output of the heat pump system.

7.6 The Evaporator Effectiveness

The most important characteristic of the evaporator is its effectiveness. The evaporator with higher effectiveness and heat transfer coefficient is desired. Figure (7.23) shows that the effectiveness is increasing with decreasing air speed. While figure (7.24) shows that the heat transfer coefficient of the evaporator is decreasing with decreasing air speed. This suggests that there is an optimum air speed for a certain operating condition. Earlier it has been shown that the optimum air speed is when the fan takes about 4% of the energy output of the heat pump system.

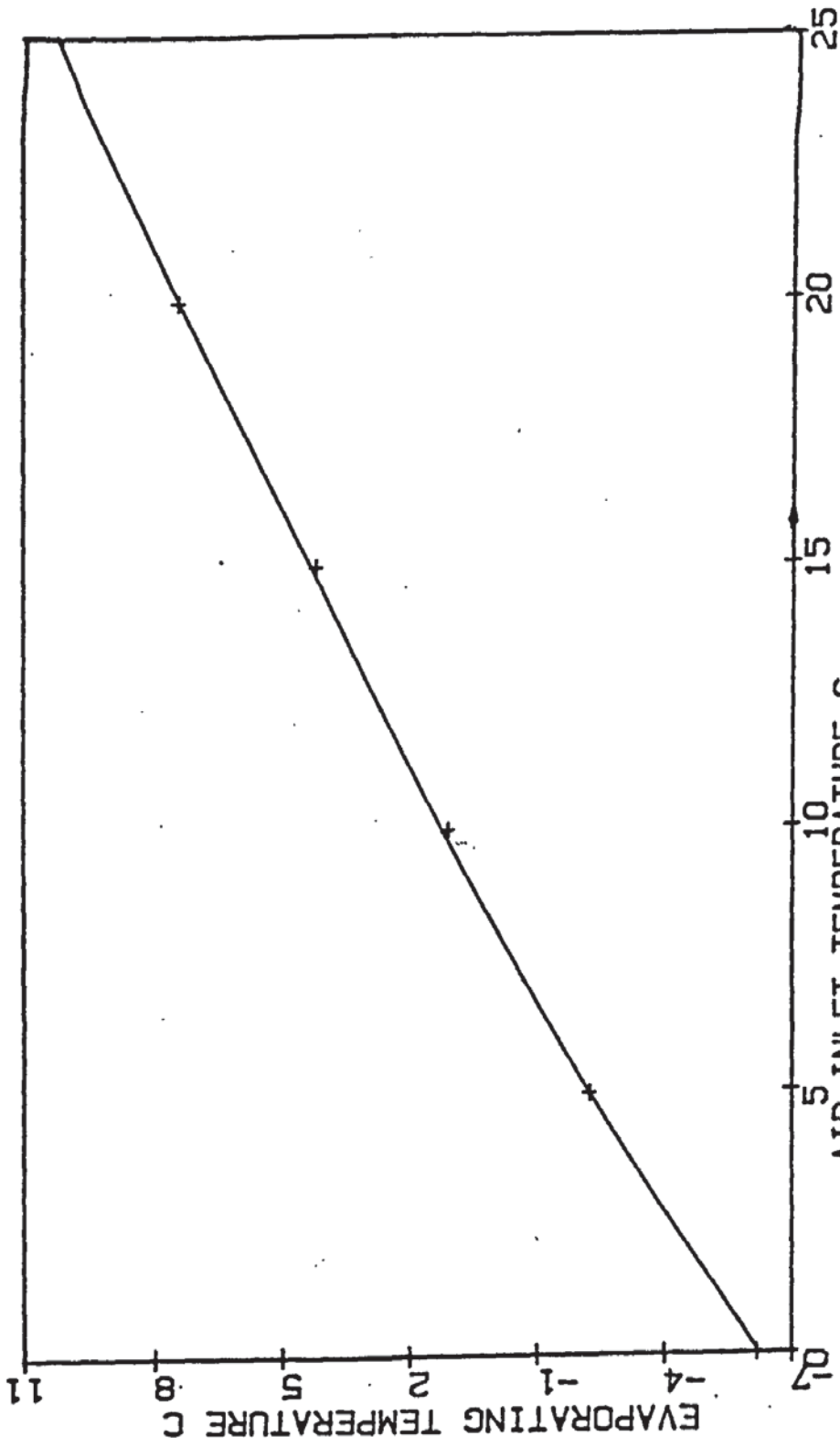


Fig (7.1) T_e is increasing with $T_a(i)$, $A_s = .1 \text{ m}^2/\text{s}$, $T_w(o) = 45 \text{ C}$, $T_w(i) = 12 \text{ C}$

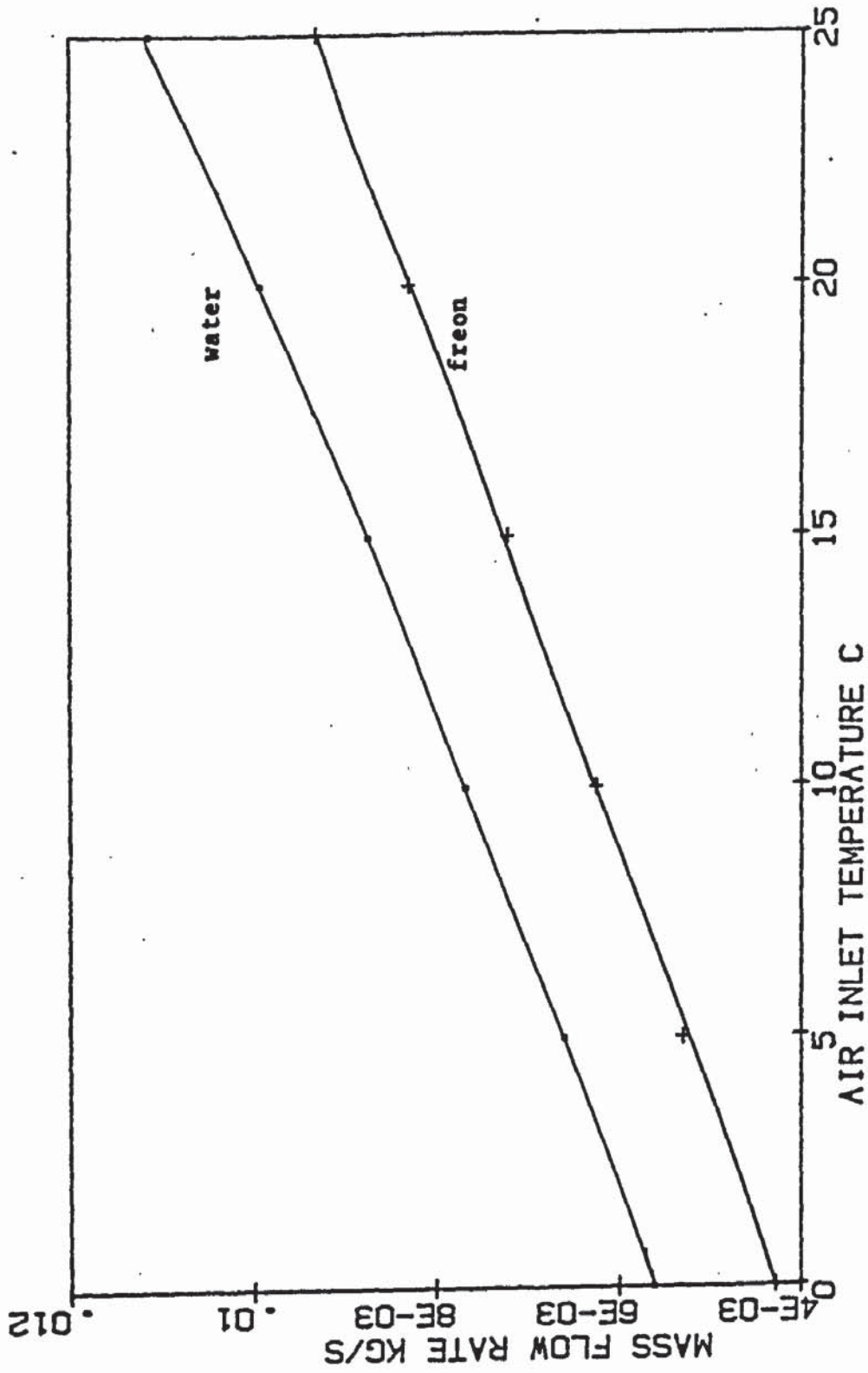


Fig (7.2) The variation of \dot{m}_r and \dot{m}_w with $T_a(1)$, $T_w(o)$, $T_w(1)$ as stated in fig (7.1)

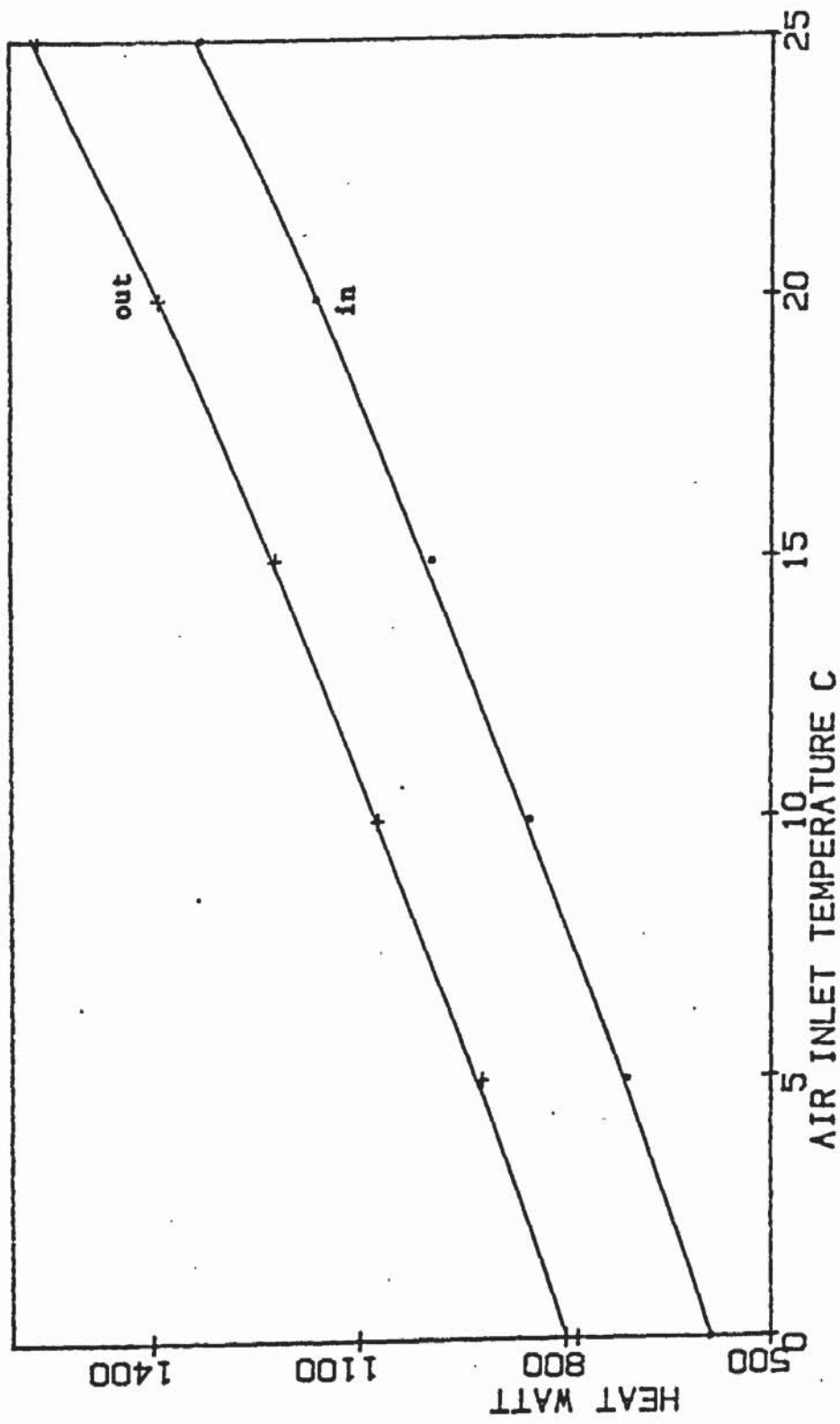


Fig (7.3) Heat input and output at several $T_a(i)$. As, $T_w(o)$, $T_w(i)$ as in fig (7.1)

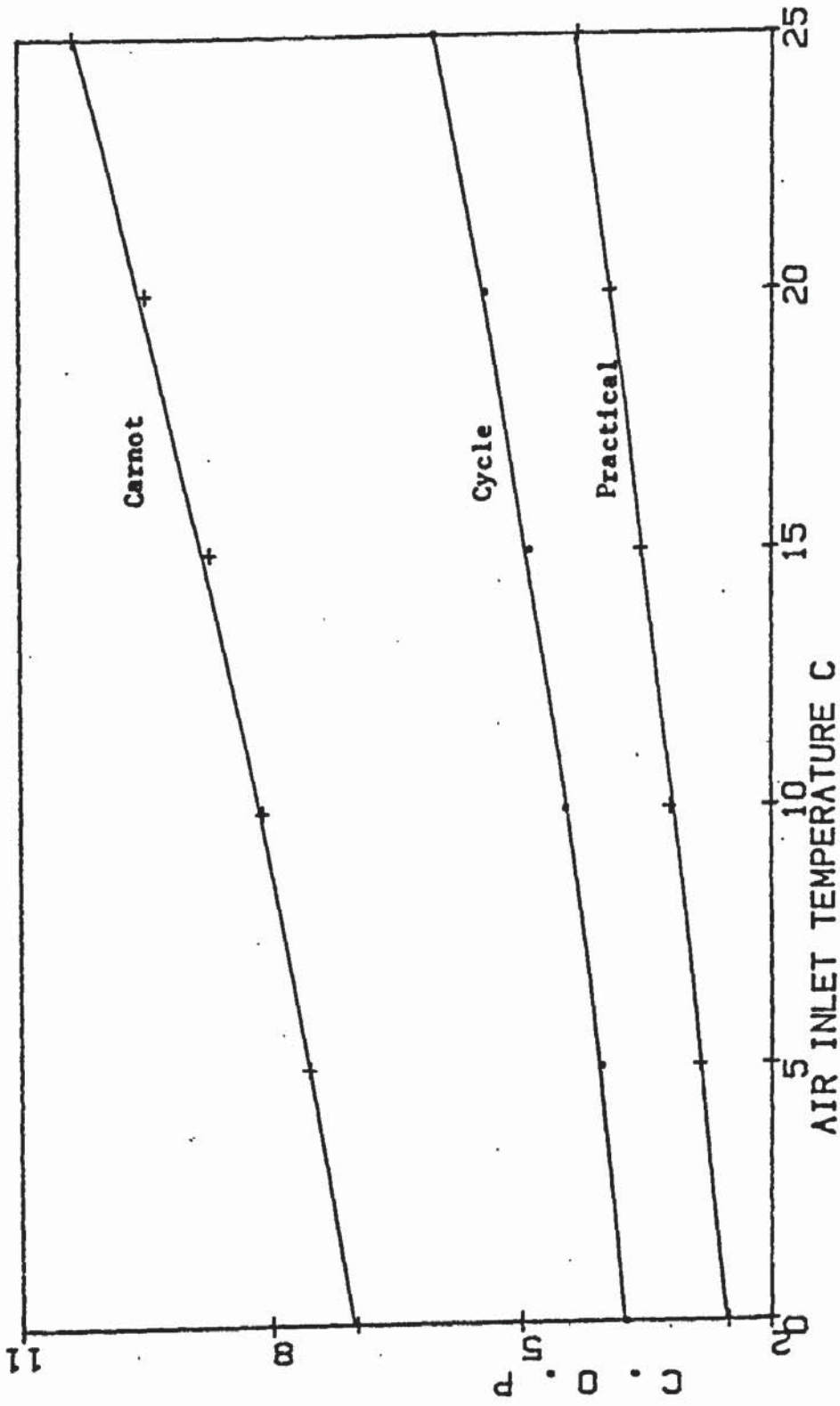


Fig (7.4) COP versus $T_a(i) \cdot A_s, T_w(o) , T_w(i)$ as in fig (7.1)

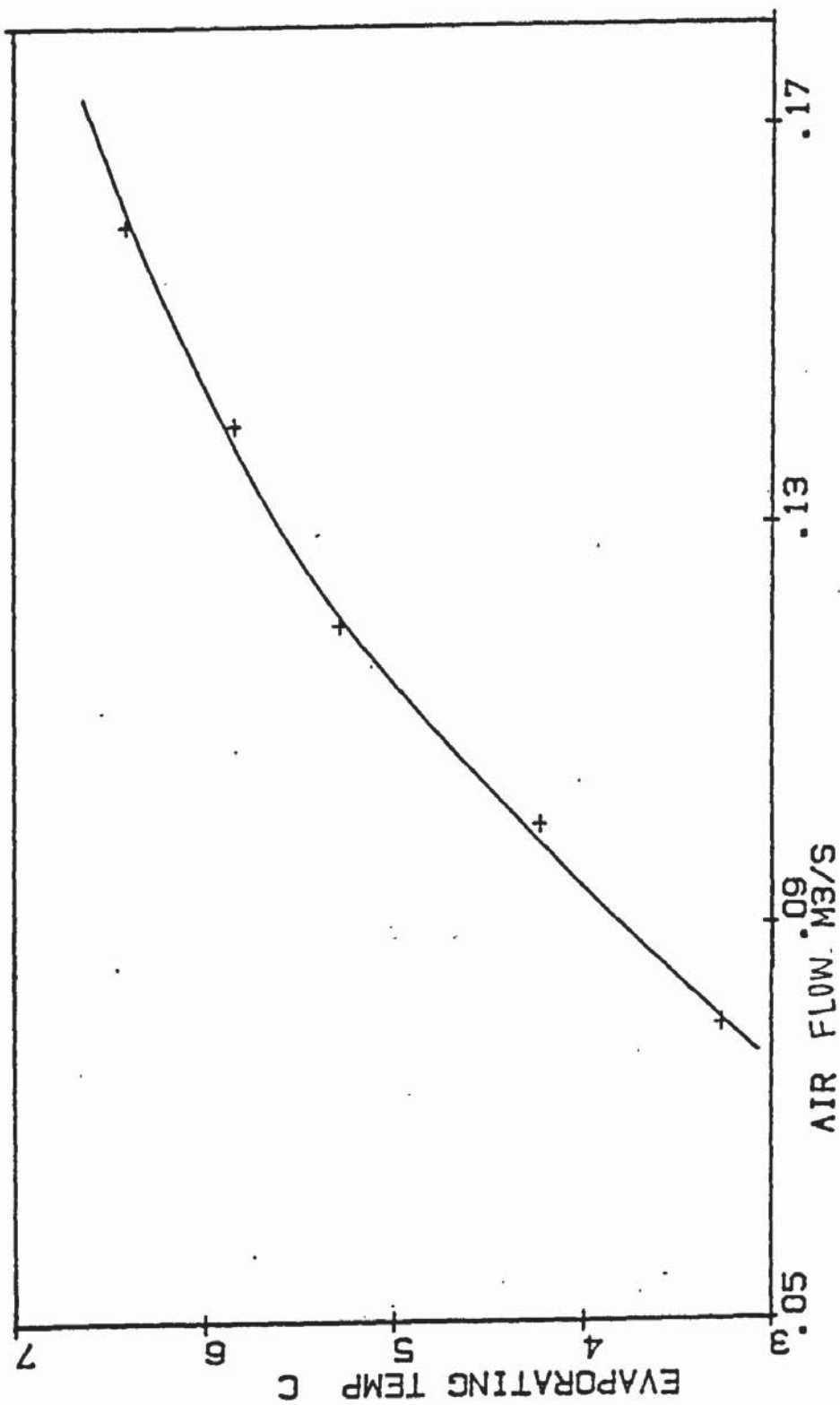


Fig (7.5) T_e at several air flow - As. $T_a(1)=15C$, $T_w(o)=45C$, $T_w(1)=12C$

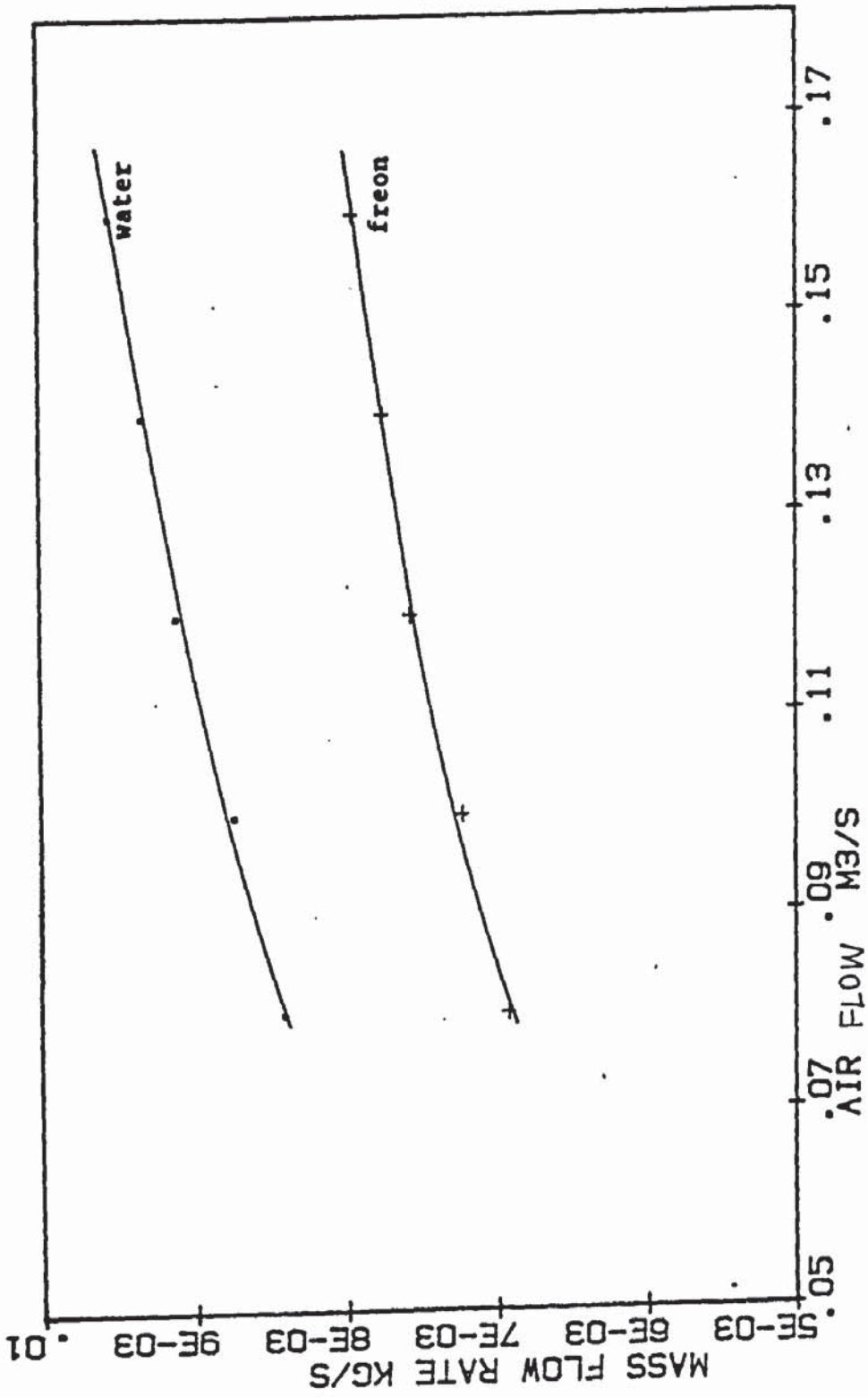


Fig (7.6) The variation of \dot{m}_r and \dot{m}_w with \dot{A}_s . Other operating condition as in fig (7.5)

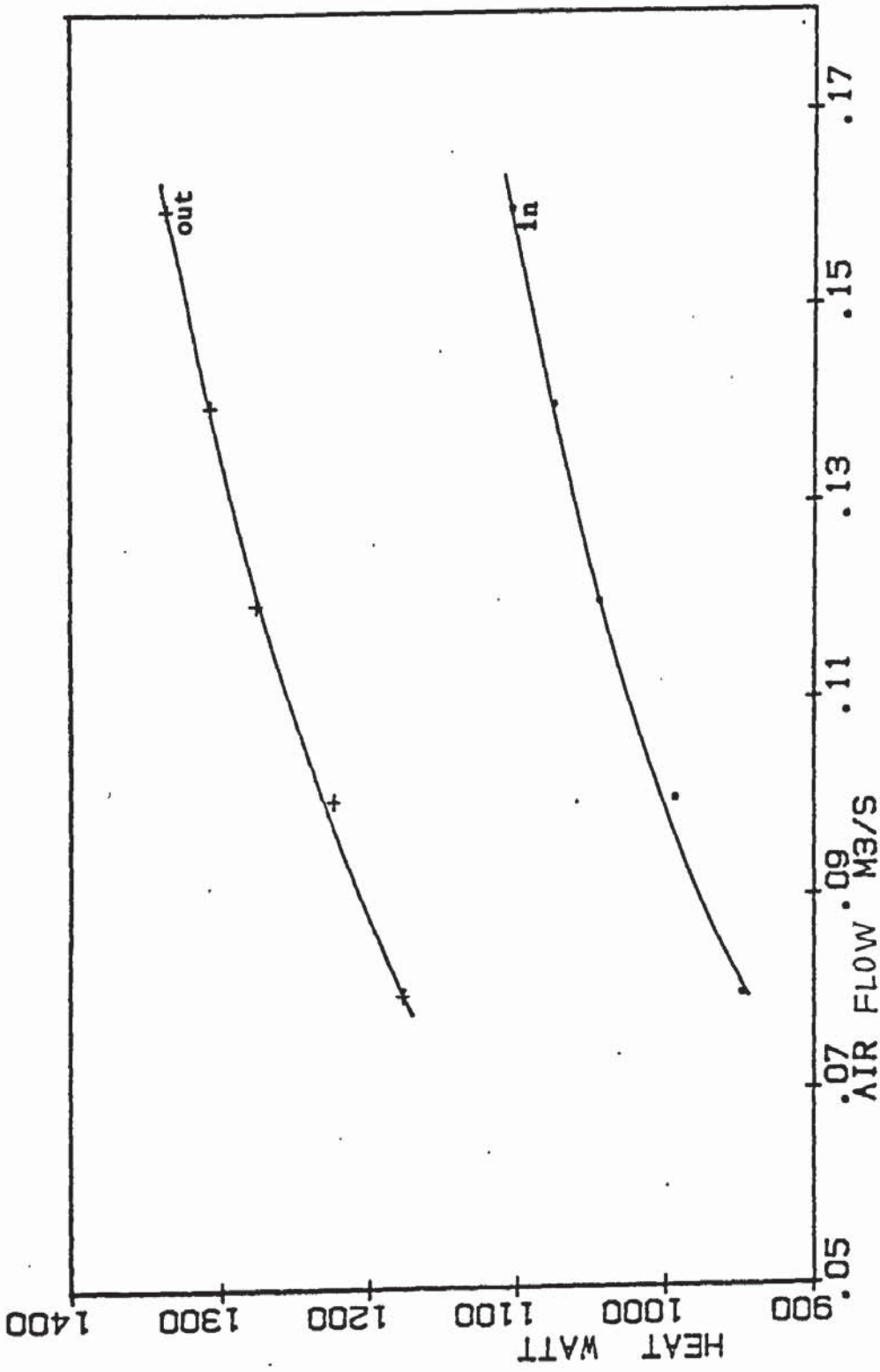


Fig (7.7) Heat Input and output at several As . Operating in the same condition as in fig (7.5)

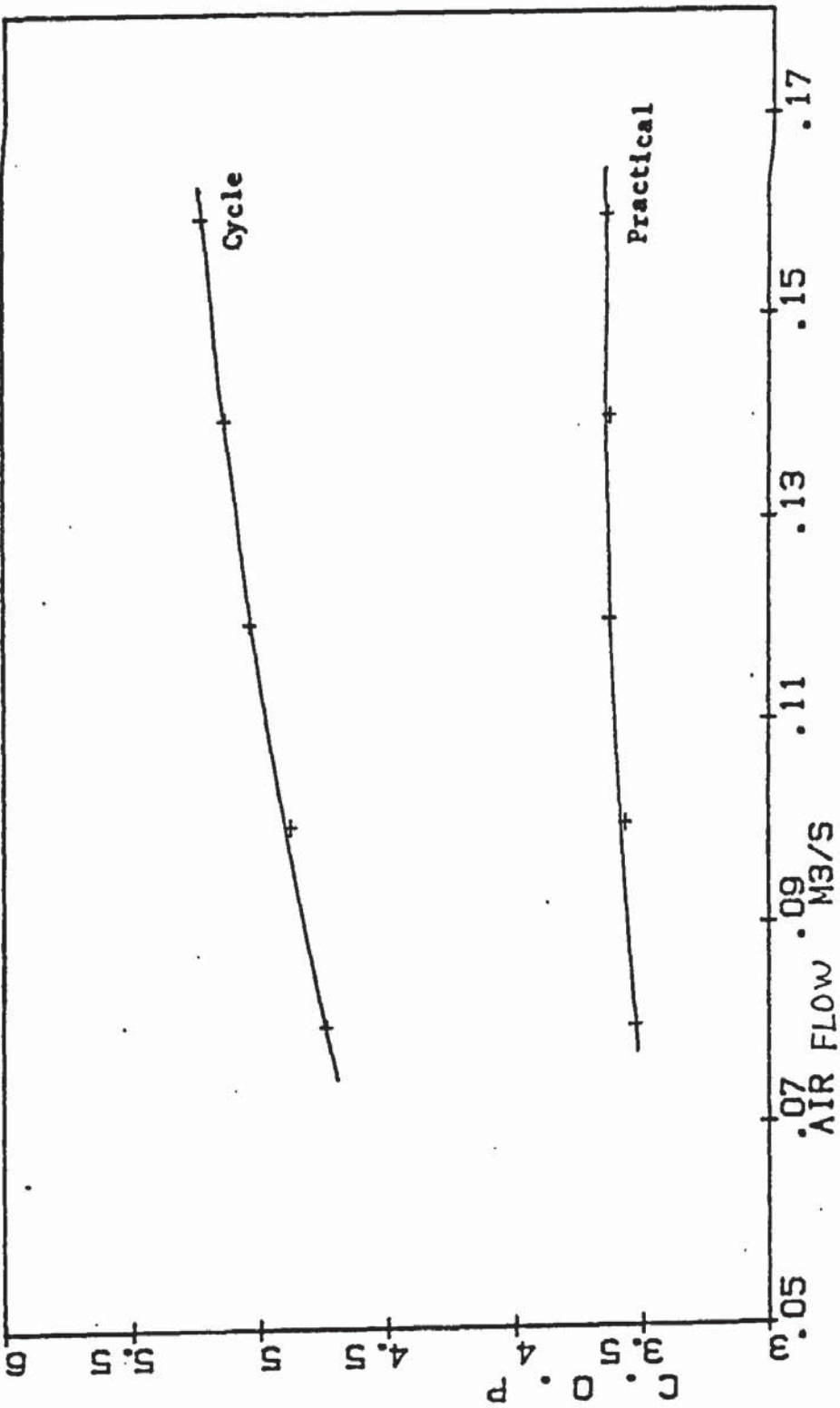


Fig (7.8) COP versus air flow . Operating under the same condition as in figure(7.5).

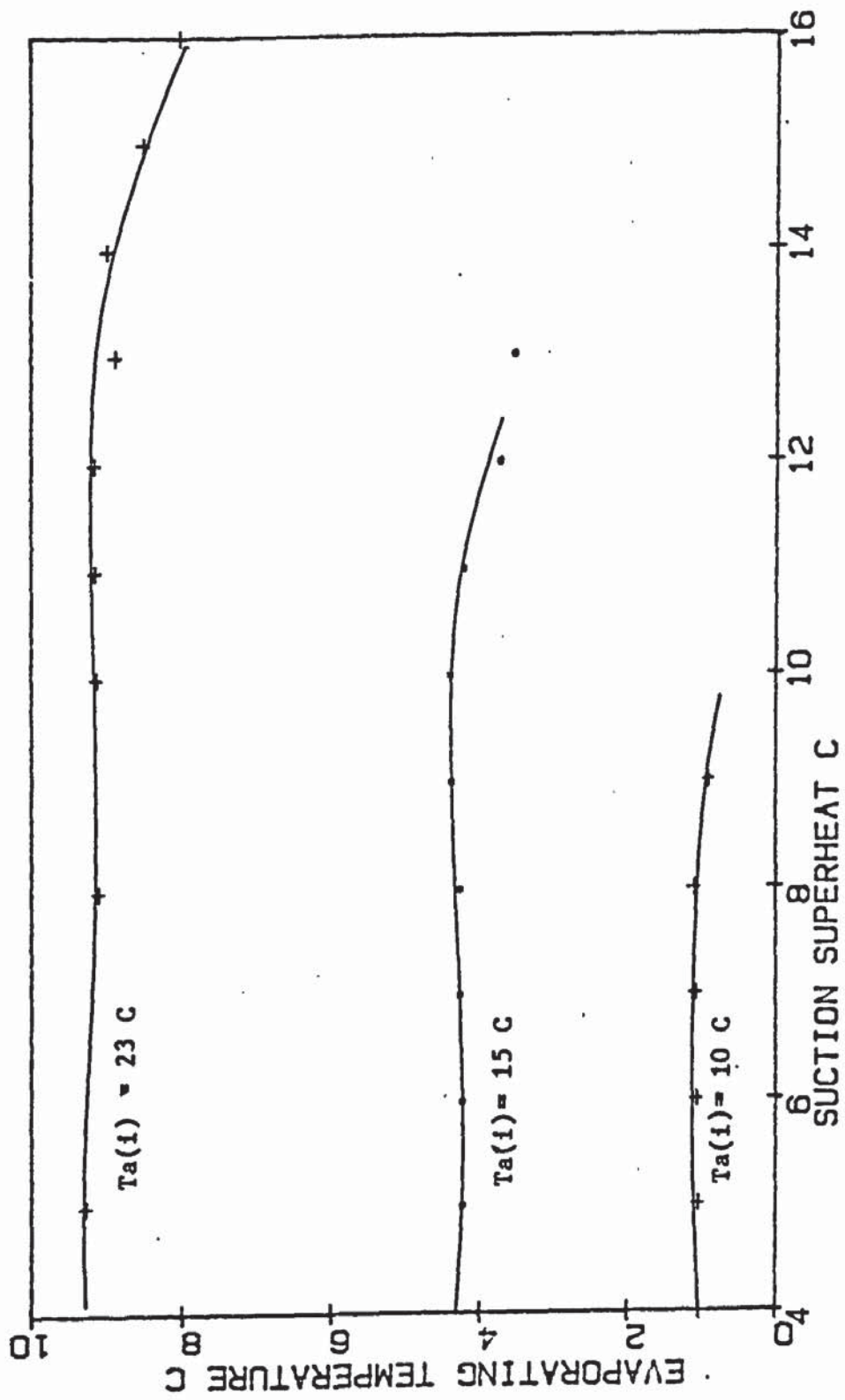


Fig (7.9) T_e at several suction superheat temperature. $A_s = .1m^3/s$, $T_v(o) = 45\text{ C}$ and $T_w(i) = 12\text{ C}$

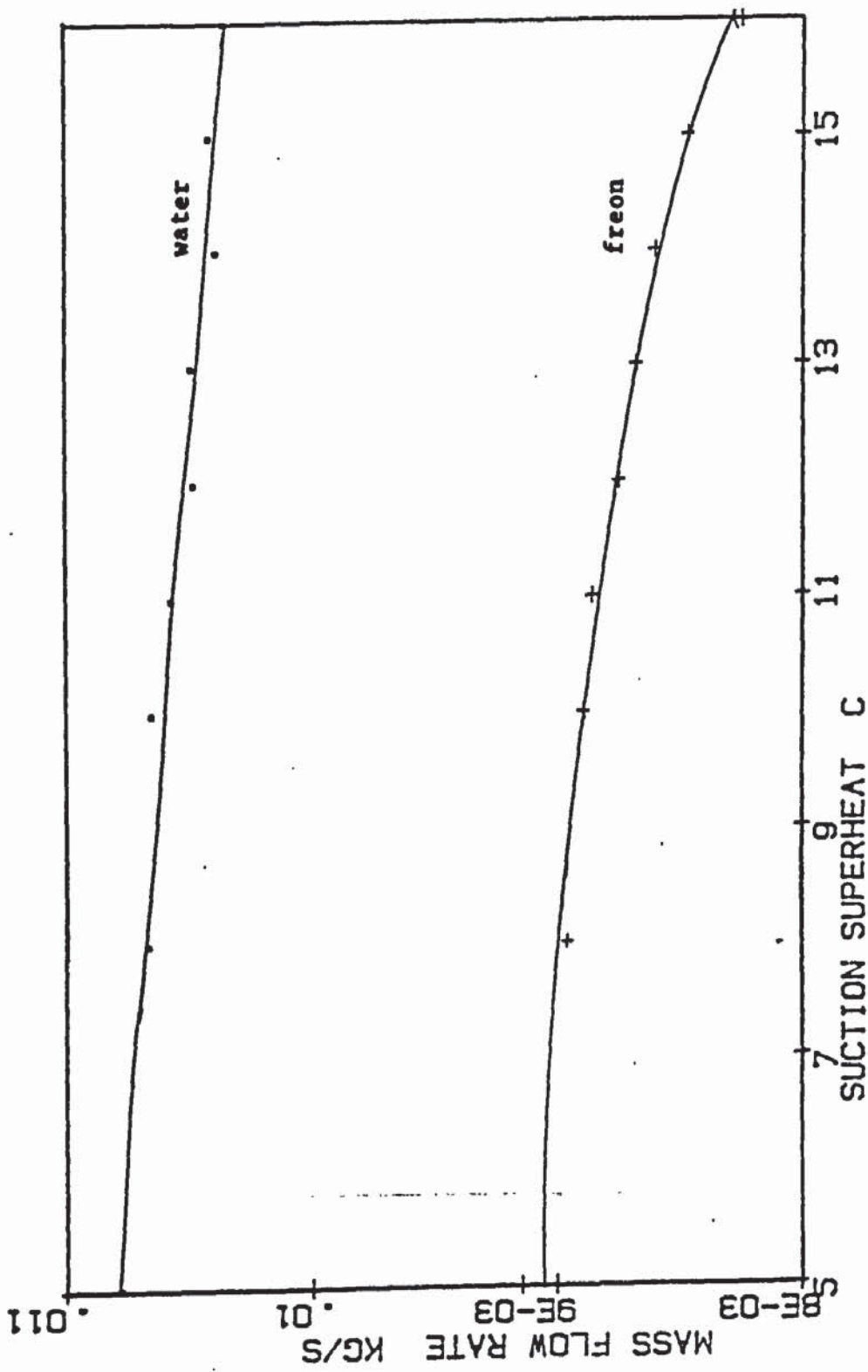


Fig (7.10) \dot{m}_r and \dot{m}_w against Sh. $T_a(1)=23C, A_s=.1 \text{ m}^3/\text{s}, T_w(o)=45 \text{ C}$ and $T_w(1)=12 \text{ C}$

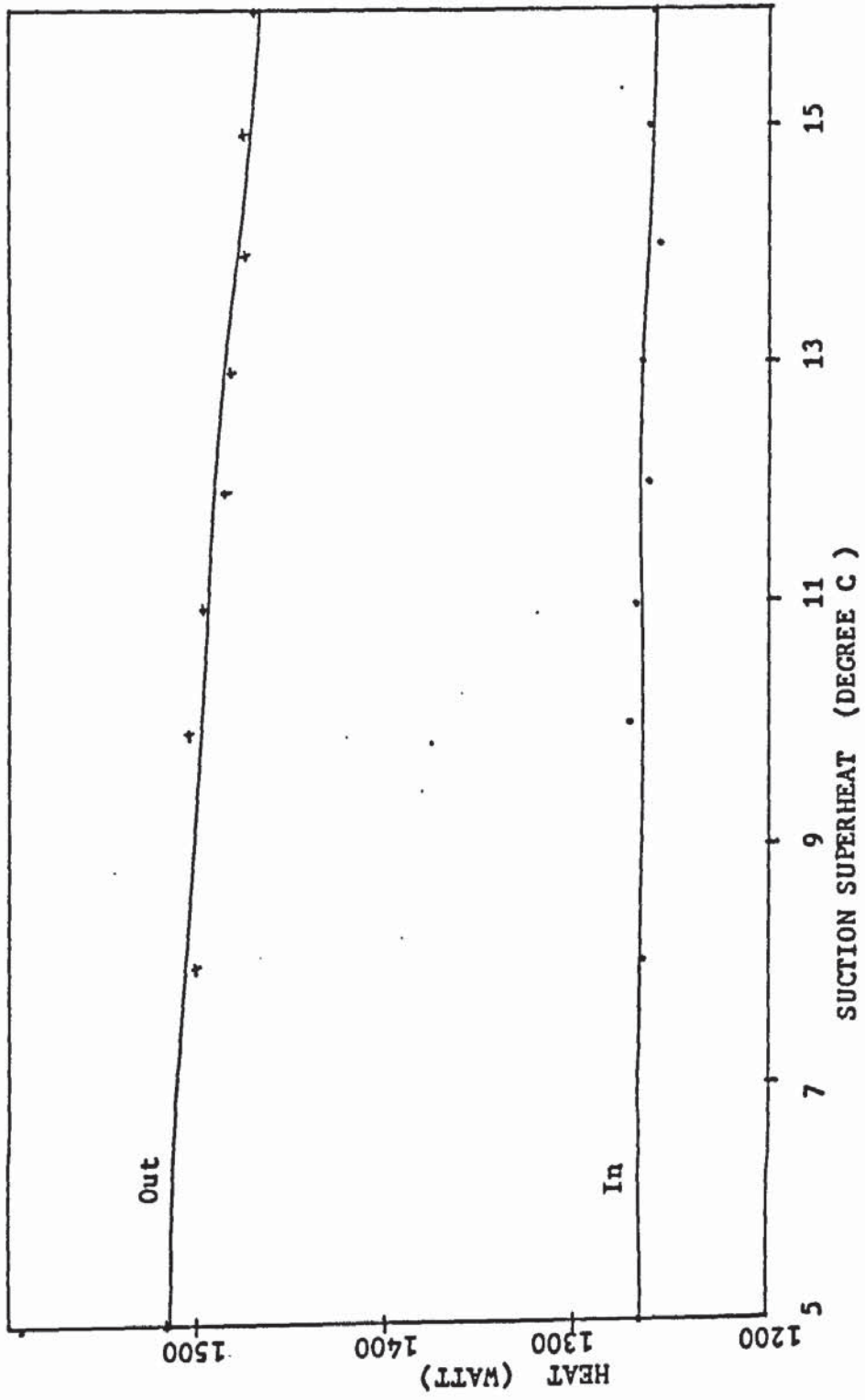


Fig (7.11) Heat output and input versus Sh. Same condition as in figure (7.5).

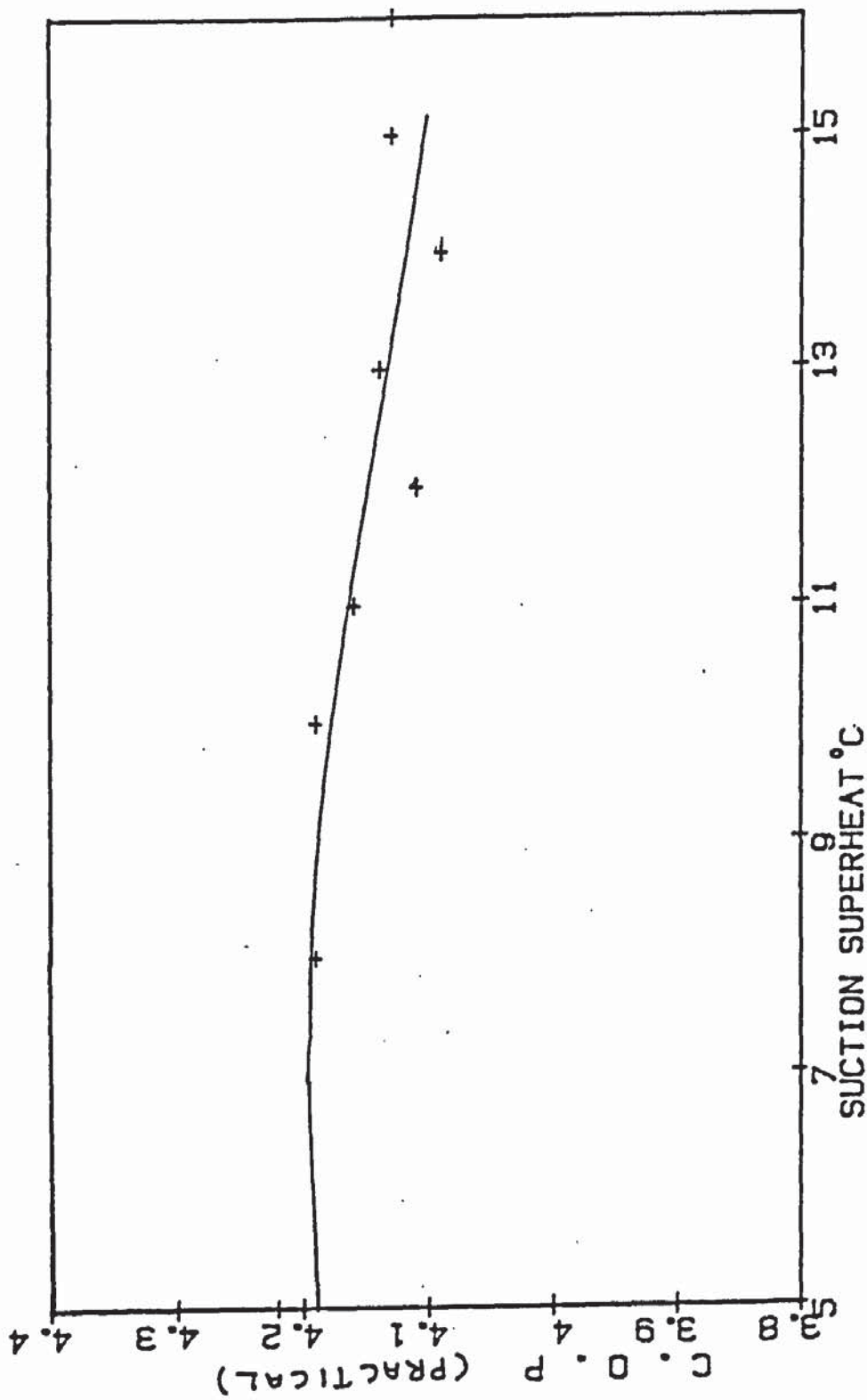


Fig (7.12) Variation of COP with Sh . Same condition as in fig (7.10)

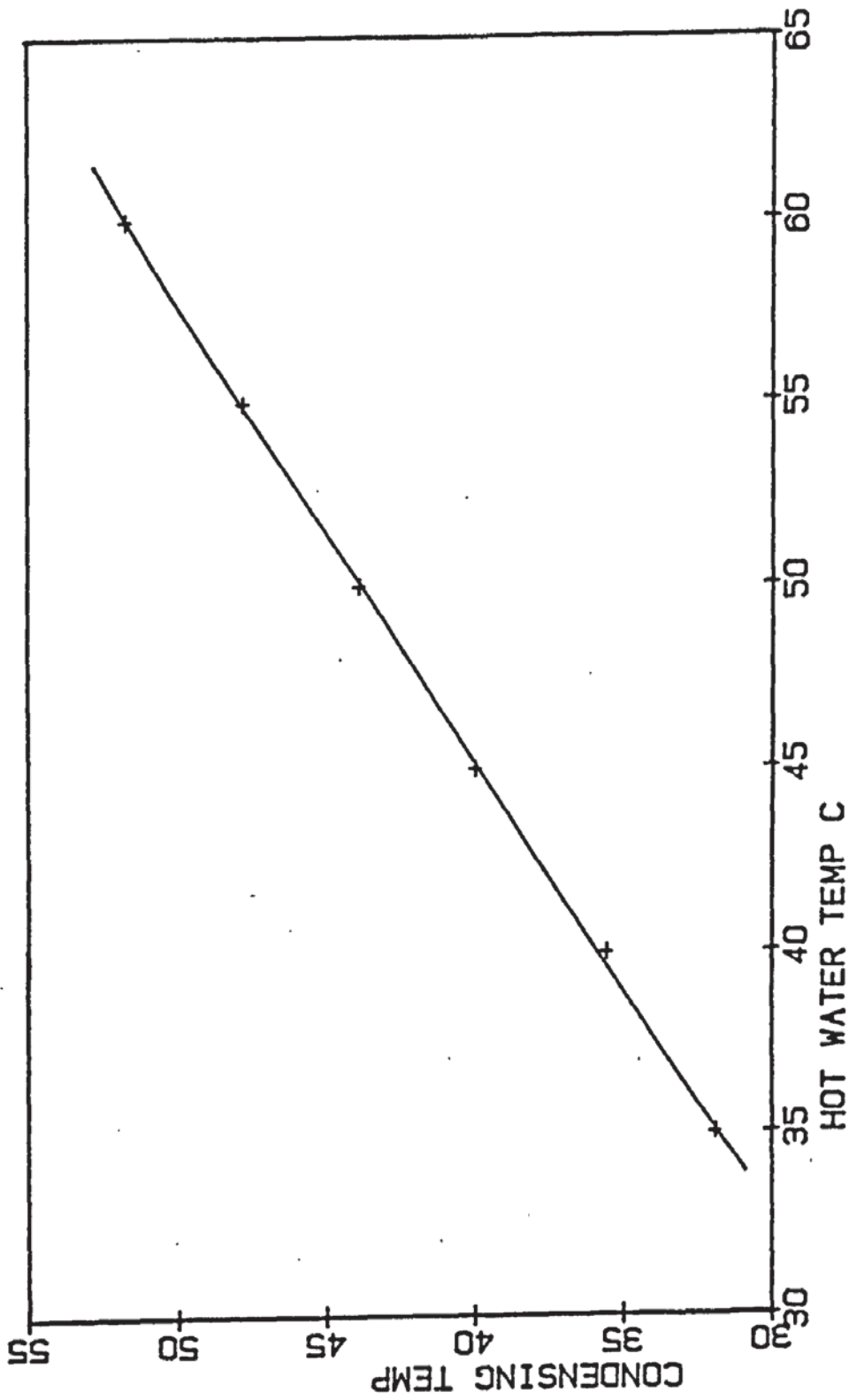


Fig (7.13) T_e at several $T_w(o)$. $T_a(1)=15C$, $A_s = .1 \text{ m}^2 \text{ s}^{-1}$, $T_w(1)=12 \text{ C}$

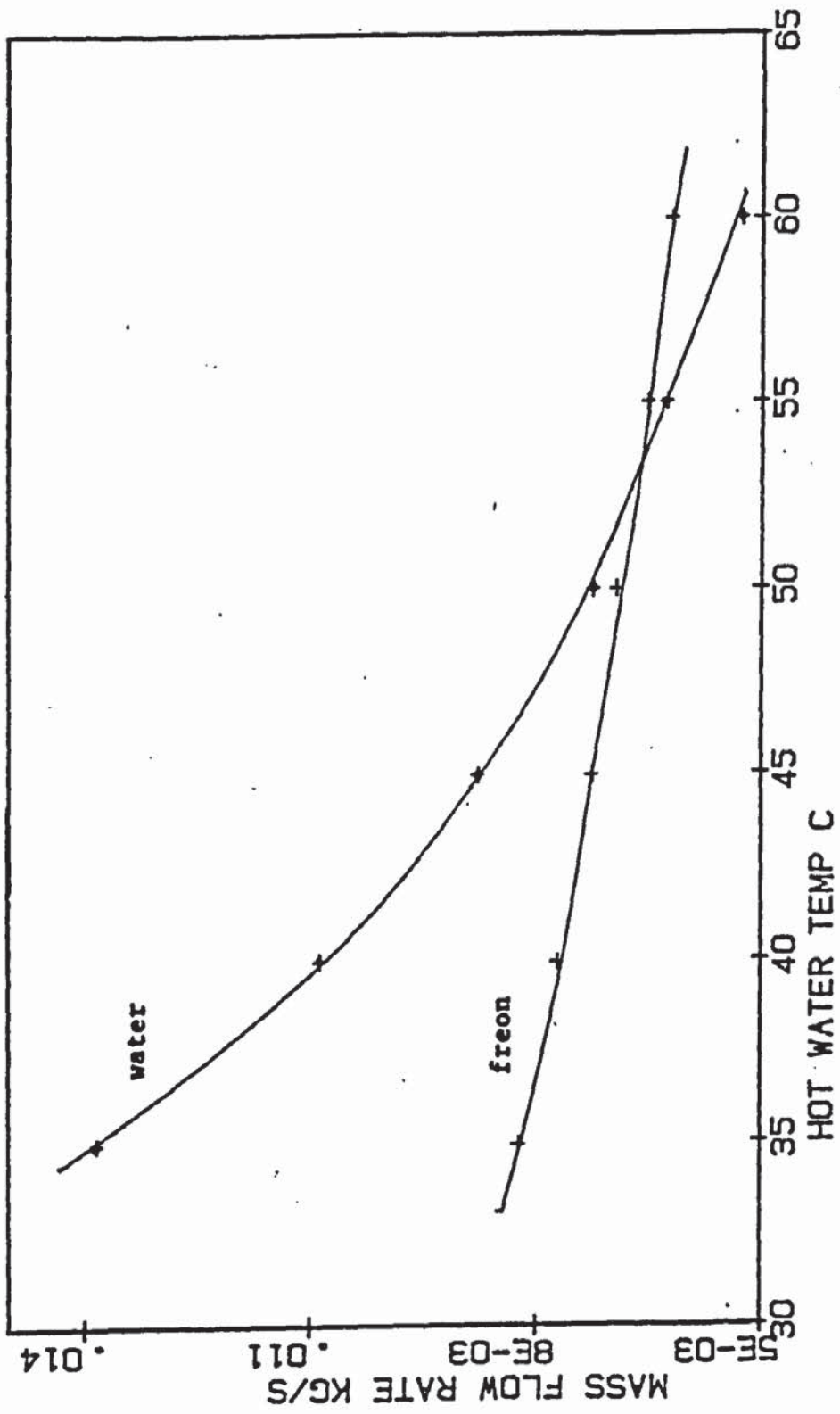


Fig (7.14) \dot{m}_r and \dot{m}_w versus $T_w(o)$. same condition as in fig (7.13)

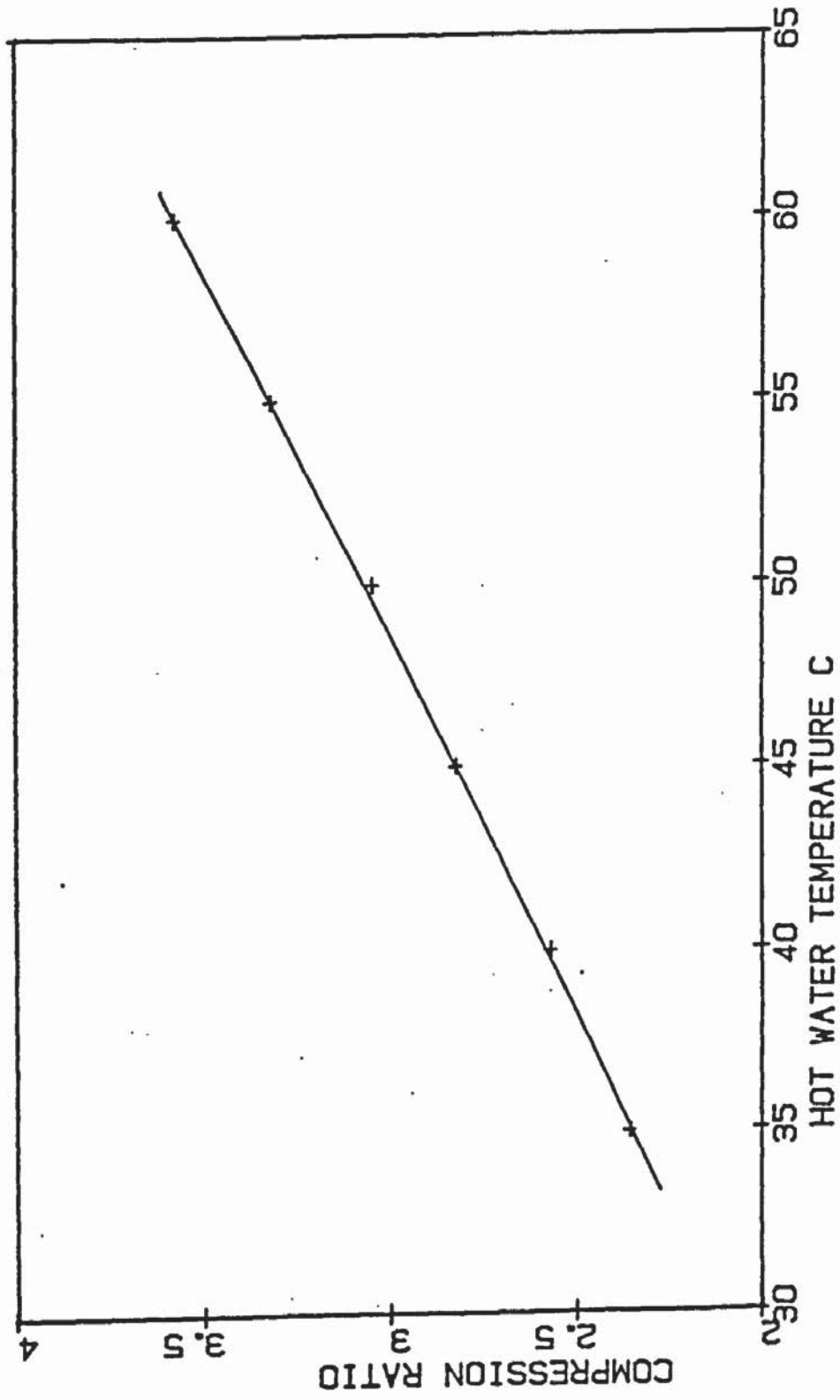


Fig (7.15) Cr versus Tw(o) . Same condition as in fig (7.13)

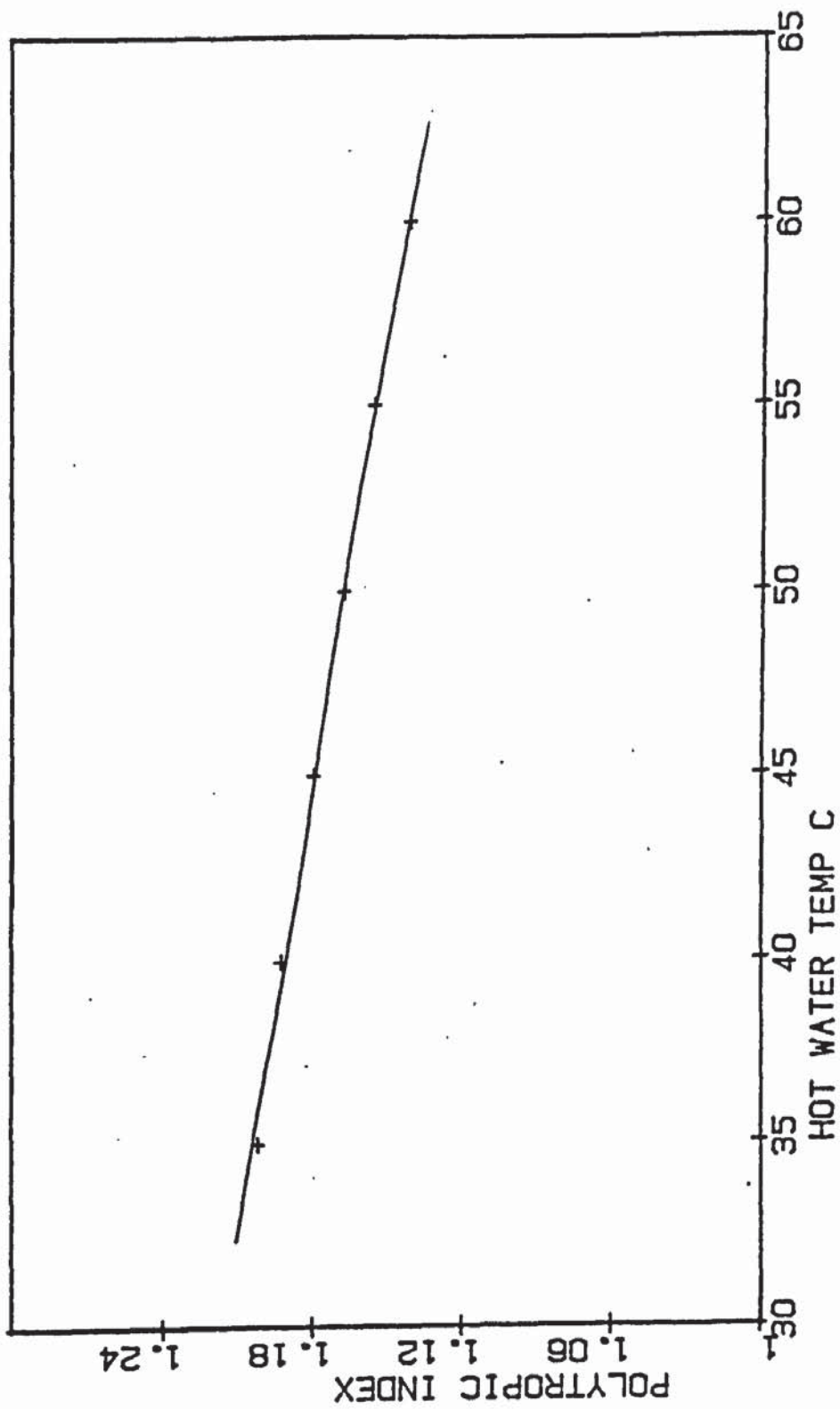


Fig (7.16) n versus $T_w(o)$. Same condition as in fig (7.13)

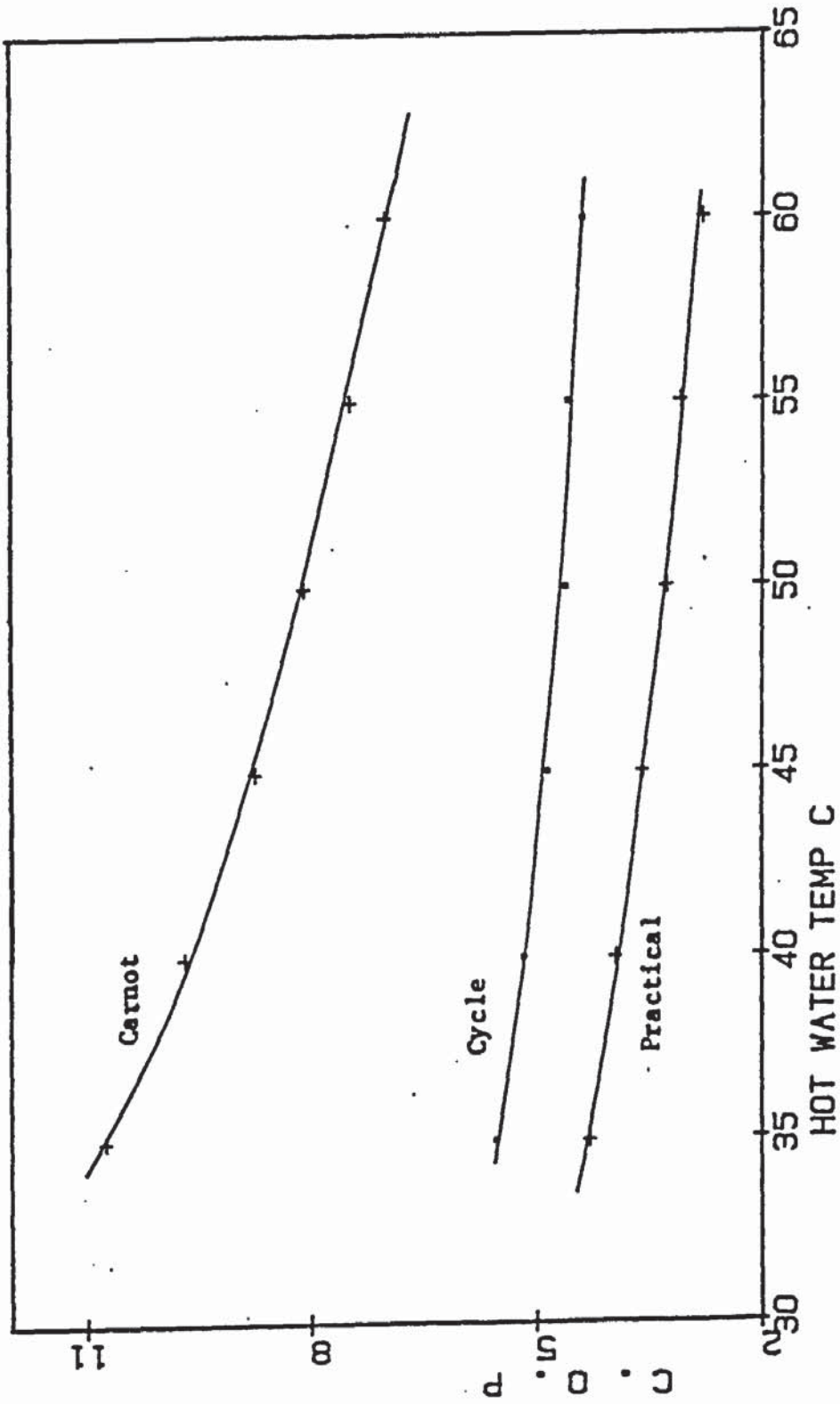


Fig (7.17) COP versus $T_w(o)$. Same condition as in fig (7.13)

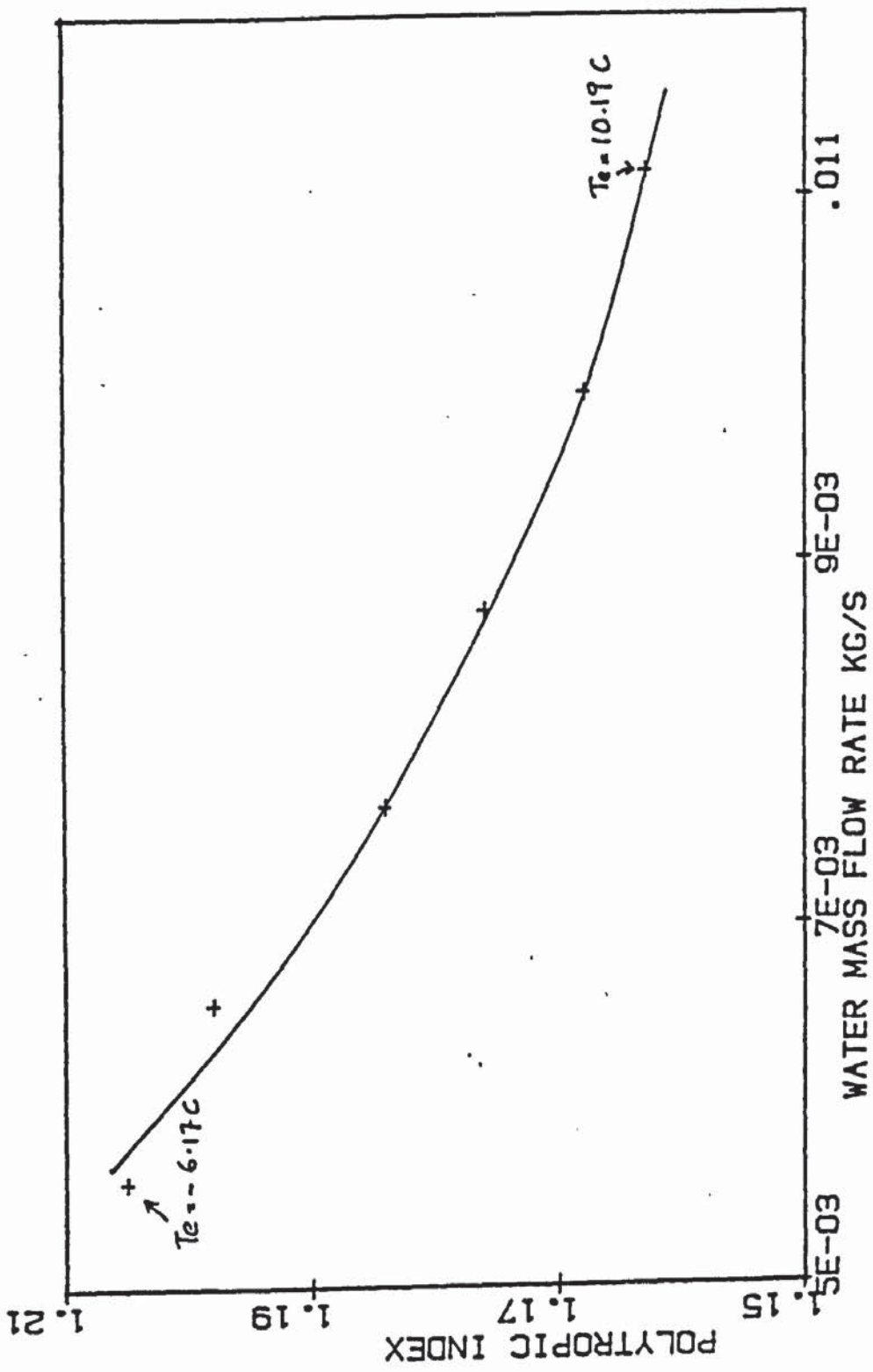


Fig (7.18) n versus \dot{m}_r . $A_s = 0.1 \text{ m}^2$, $T_w(o) = 45 \text{ C}$, $T_w(i) = 12 \text{ C}$

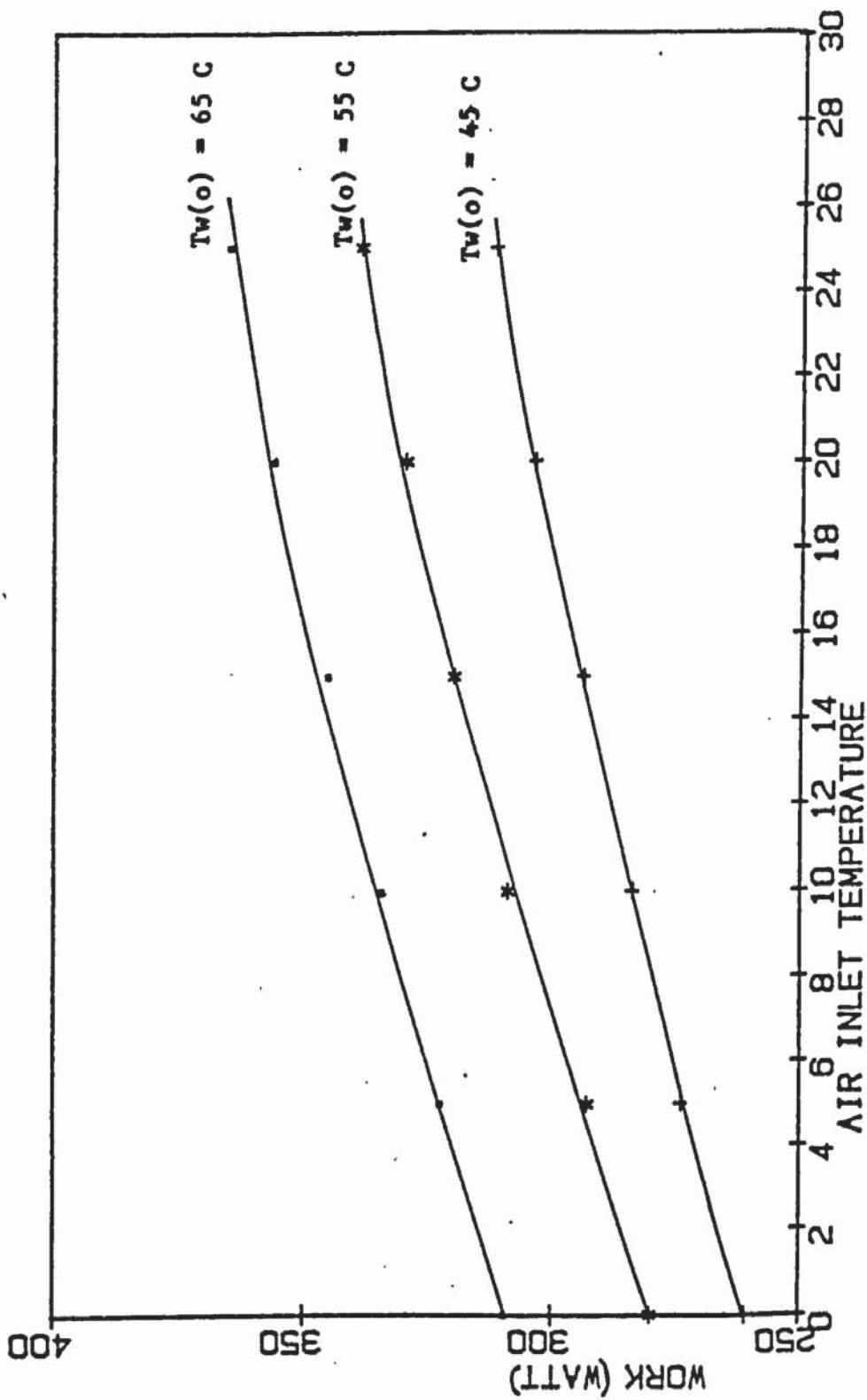


Fig (7.19) Electrical power supplied to the compressor is a function of T_e and T_c . Air speed and water inlet temperature is constant.

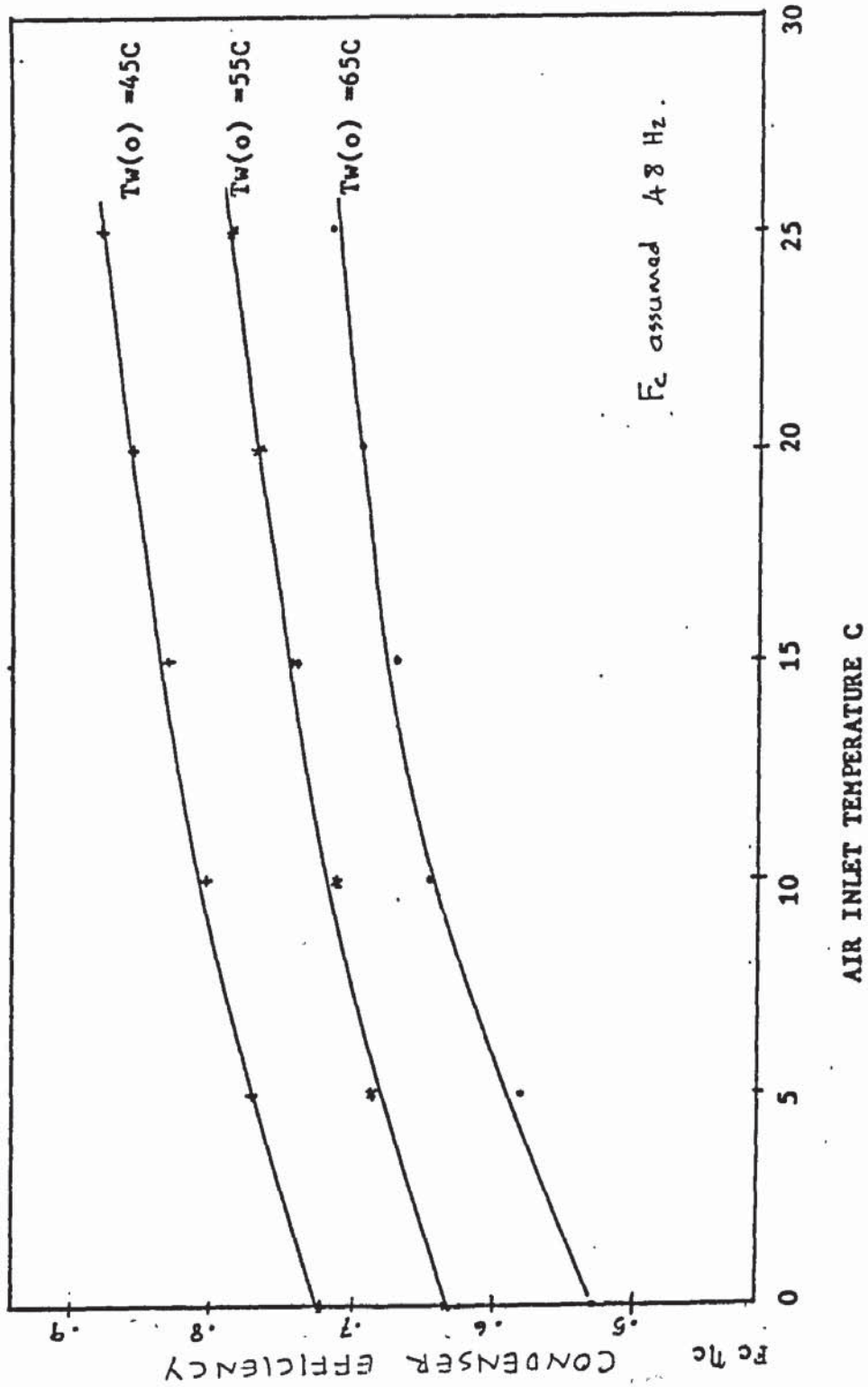


FIG (7.20) Condenser efficiency varies with air and hot water temperatures.

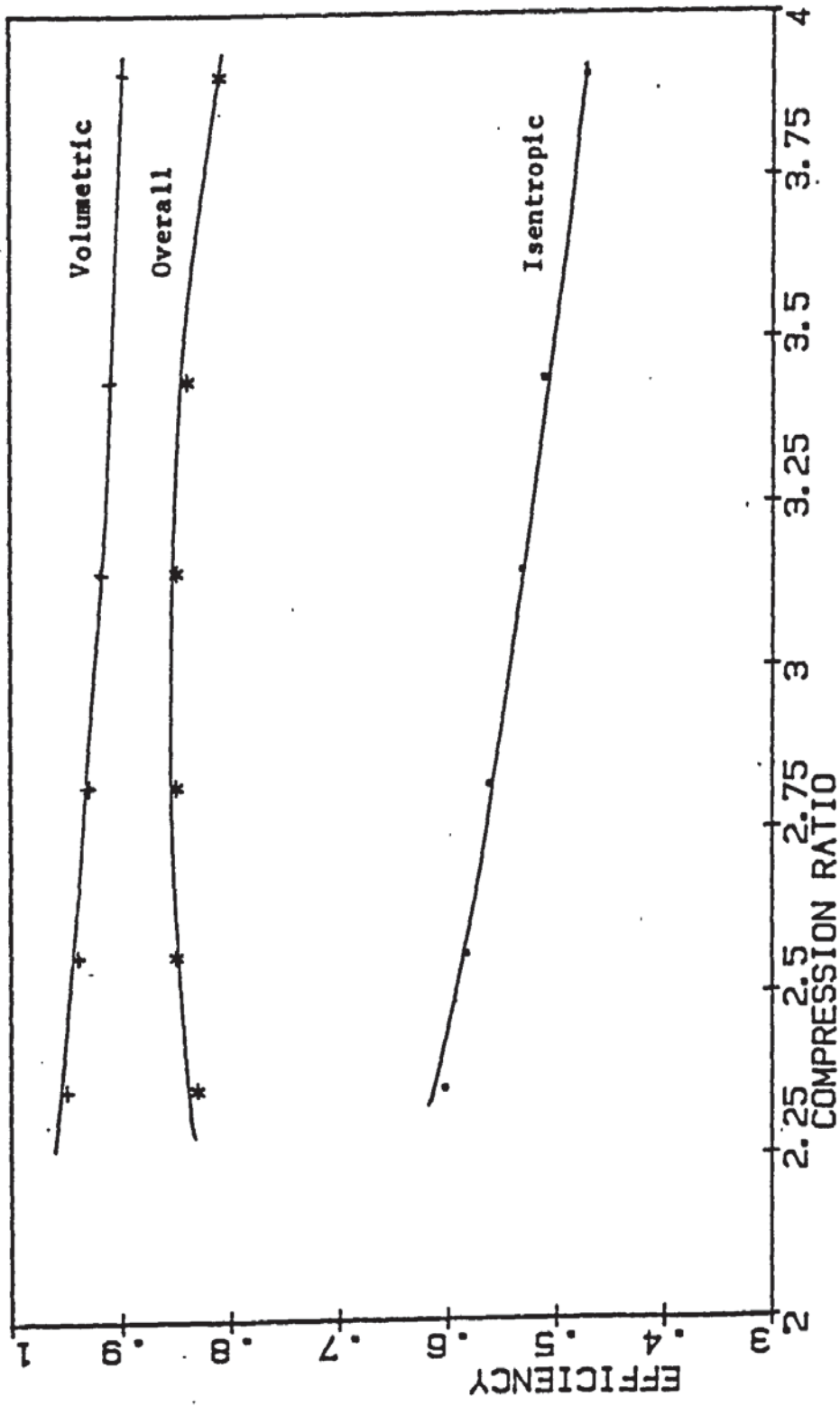


Fig (7.21) The compressor efficiency for several Cr

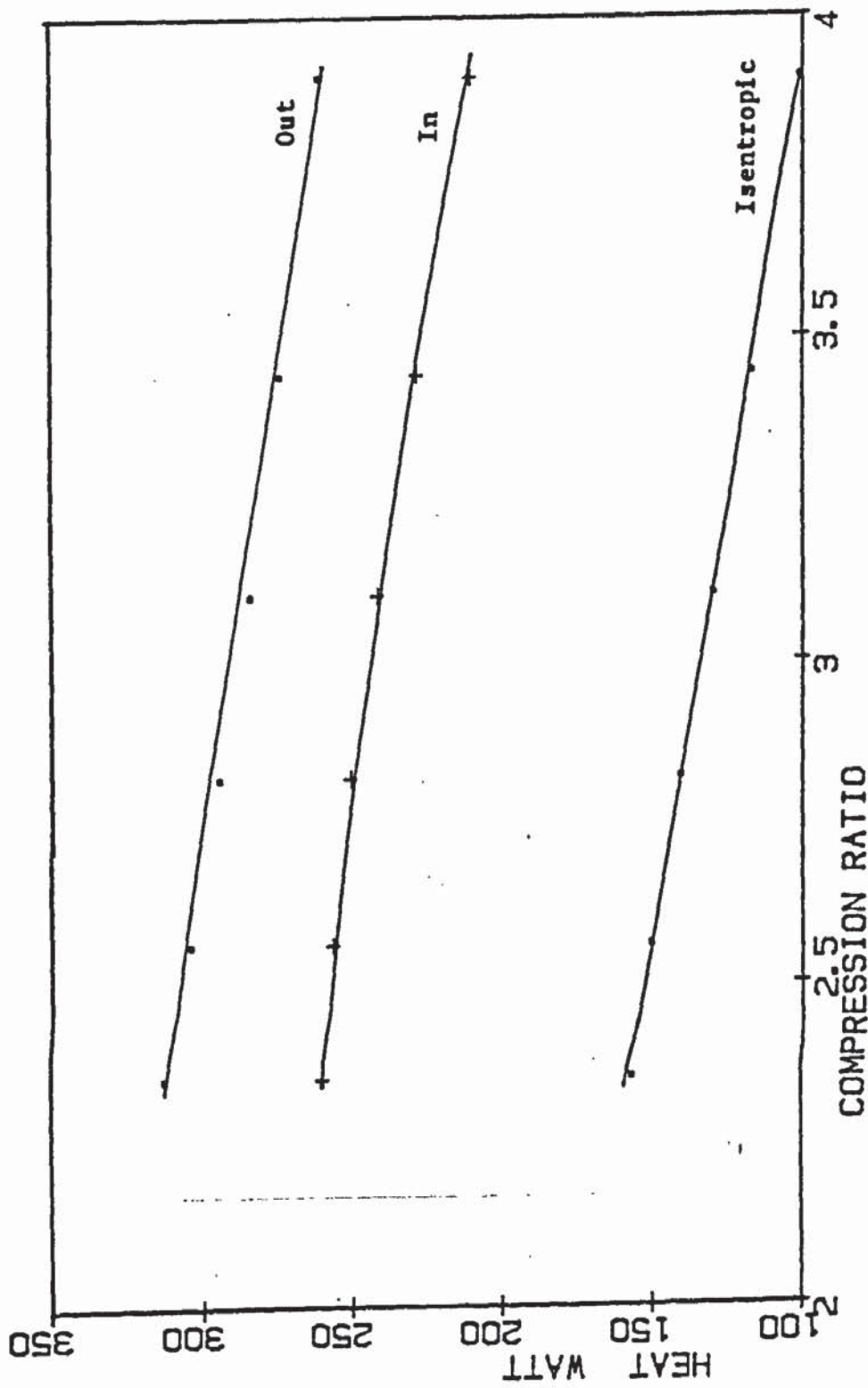


Fig (7.22) A typical values of heat output and input and also isentropic work done.

$A_s = 0.1 \text{ m s}^{-1}$, $T_w(0) = 45 \text{ C}$, $T_w(1) = 12 \text{ C}$

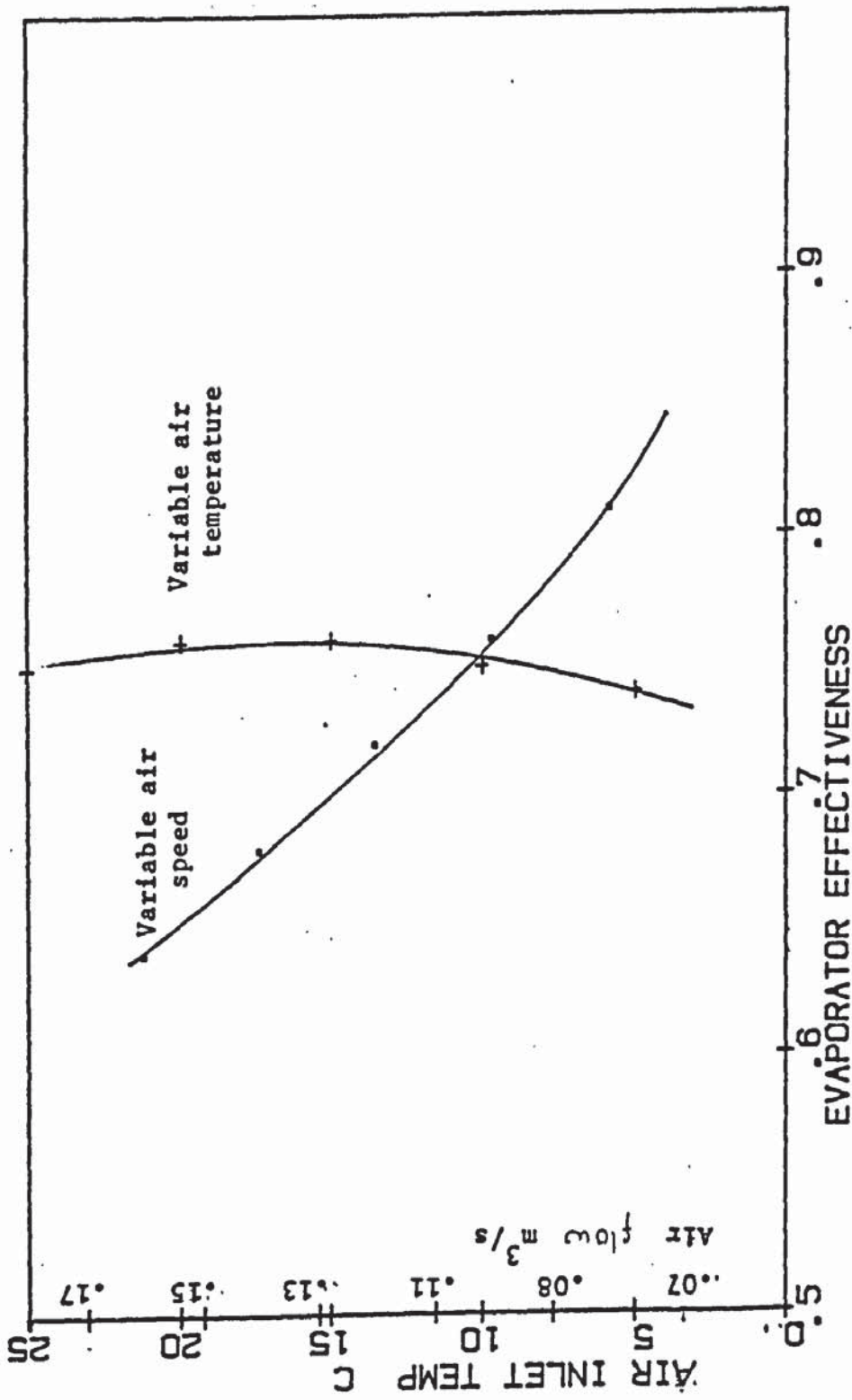


Fig (7.23) Evaporator effectiveness at several air temperatures and flows.

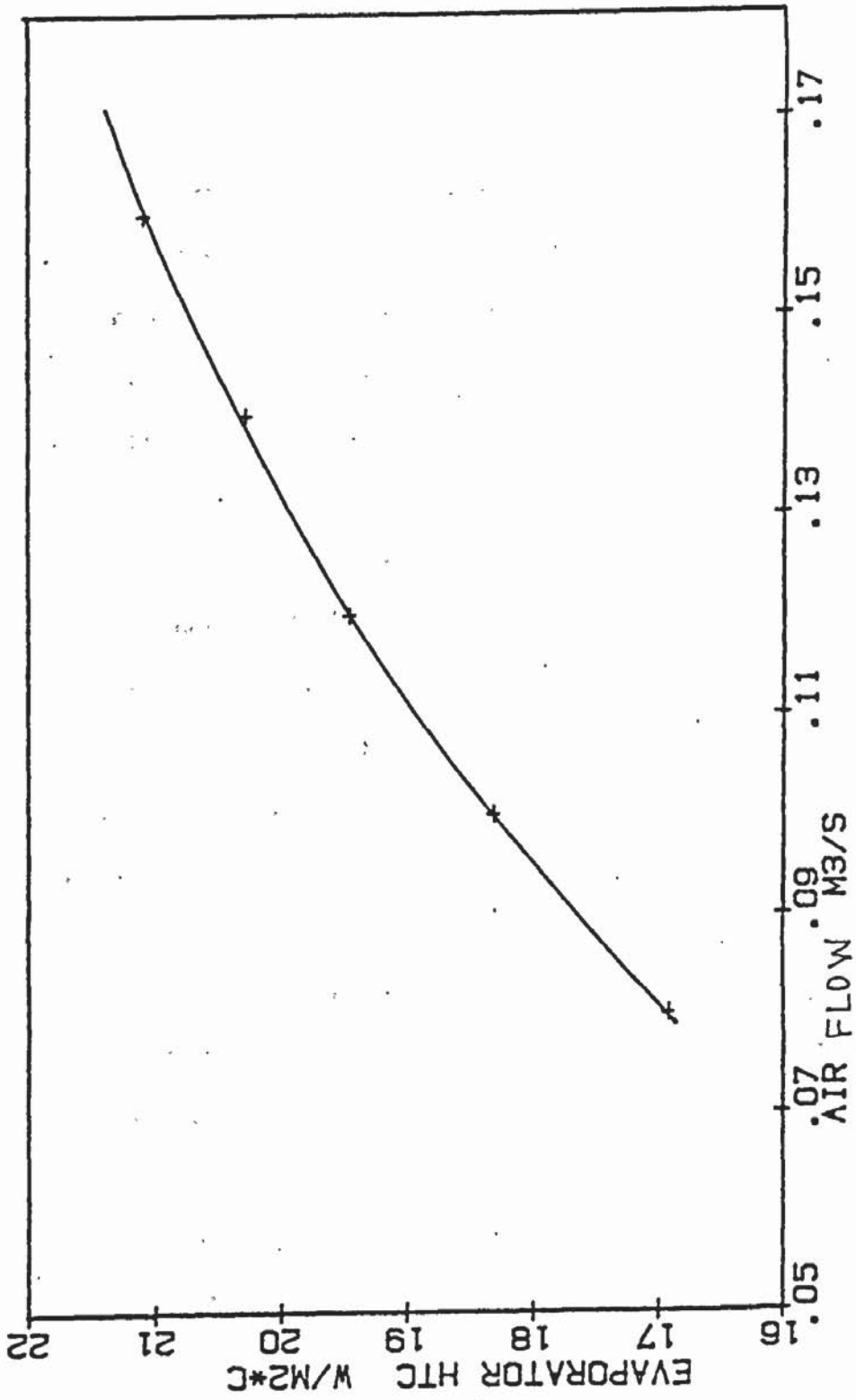


Fig (7. 24) Evaporator HTC at several air flows.

CONCLUSION

8.1 Main Conclusions

1. The design, application and accuracy of the digital data acquisition system developed for the purpose of heat pump monitoring have been described. The data is recorded on the double density 5 $\frac{1}{2}$ " floppy disk . A disk has the capacity of storing about 50 sets of the experimental results. A set of the experimental results consists of 33 data items, and so a disk can be a storage place for about 1650 readings. The advantage of this digital data acquisition system over other types of data recorder, for example chart recorder, is that the data can be transferred directly and quickly into the computer for analysis. Even though a disk system is more expensive than a tape system, because the speed of the data transfer to and from the computer is faster than the tape, it justifies its cost.

It can be concluded here that the digital data acquisition system using floppy disk as a means of storing the data is very important and helpful in monitoring and studying the heat pump system.

2. A computer model for studying the heat pump characteristics has been described. Since some of the equations are empirical, this model is limited to a certain range of operation only. The evaporating temperature T_e must be higher than -6 C and lower than 14 C. This is

because the lowest air temperature in the laboratory is about 5 C to 6C (Te=-2C to -1C) achieved by circulating the outlet air back into the evaporator. This is a suitably low air temperature since it is comparable with the means U.K winter temperature. The upper limit of Te range is 11 C, due to the maximum capacity of the expansion valve. The range of the condensing temperature Tc is from 30C to 60C. This range is chosen because it will give hot water temperature in the range of 33 C to 67 C, which includes the normal domestic hot water temperature.

A detailed model of the condenser is also developed. Since this model is very long and time consuming^{in computer time}, it is not included in the heat pump model. In future it is hoped that this model can be modified and included in the heat pump model.

3. Carrington has shown that^{from modelling} the hot water temperature can be made to be higher than the condensing temperature. This increase in the water temperature is due to the high freon vapour temperature as it exists from the compressor. Here it has been shown that this hot water temperature can be increased further by making use of the heat from the compressor. This is achieved by cooling the compressor with the hot water discharged from the condenser. As a result, the difference between the hot water temperature and the condensing temperature is further increased.

The condenser is also designed to extract heat from the subcooling of the freon liquid. This proved to be very useful. The experiments show that the COP can be increased by about 6% by utilizing this subcooling energy.

4. The experimental results show that only about 40% of the work input to the compressor is transferred to the freon vapour by the process of compression. The remaining 60% generates heat in the compressor, three quarters of this is absorbed by the freon vapour and the rest is removed by the cooling water. Since the heat removed by the cooling water is also utilized, the actual heat loss from the electrical input energy is very small. Thus it is seen that the Danfoss hermetic compressor is well suited to its purpose.

Analysis of the experimental results for the compressor revealed that the polytropic index n could not be regarded as a constant. This is at variance with the assumption of other authors. Reasons are presented in chapter 7, to show that n departs most from the adiabatic value when temperature differences within the compressor between the vapour and cylinder walls are large.

5. The experimental results also show that there is an optimum air speed for a given evaporator. Here it is found that the reasonable air speed occurs when the input power to the fan is about 4% of the output power (at condenser). The results also show that the evaporator is operating with an effectiveness of about 70%. This effectiveness is found to be very sensitive to the air speed. Because of the non-uniform air flow through the evaporator some sections will be operating at a reduced effectiveness. If uniform air flow could be achieved it would be possible to reduce the air flow rate and still obtain the same energy transfer to the freon. Therefore in order to improve the evaporator effectiveness the fan should be properly

designed and placed at a correct position in the system such that a uniform air speed over the evaporator surface is achieved. Further research on the fan design and its integration into the heat pump system should be pursued.

6. Figure (7.7) and (7.8) indicate that a measure of capacity control can be achieved by varying the air speed. Figure (7.8) shows that the practical COP is insensitive to air speed whereas figure (7.7) indicates that the heat output can be made to vary from 1.0 kW to 1.35 kW for the range of available air speeds (0.04 to $0.16 \text{ m}^3 \text{ s}^{-1}$).

8.2 Suggestion For Future Work

1. Since the compressor is one of the most important components in the heat pump system, a detailed of its characteristics is required. At present, since the compressor used is a hermetic type, only the inlet and outlet conditions are measurable. A knowledge of the compressor cylinder wall temperature, suction and discharge valve pressure drops and the temperature increase in the suction line inside the compressor would be most useful in understanding and improving the compressor design. Future research programmes should remove the compressor casing in order to insert sensors to measure these parameters. The compressor frequency should also be measured directly; preliminary observations indicate that it can readily be observed from fluctuations in the compressor discharge pressure.

2. For the side by side tube condenser it is possible to measure the temperatures of freon and water inside the tube. This temperature profiles can be very useful in developing the condenser computer

model. This is because the exact nature of heat transfer in the two phase region is still unclear. The temperature profile and the computer model can be used to estimate the size of the condenser for a particular application.

3. In the present work the relative humidity is not a controlled parameter, therefore the exact effect is not really known. This effect can only be determined by carrying the experiments under controlled environmental conditions. An environmental chamber would be of great assistance to this evaluation.

4. Little is known of the effects of the compressor lubricating oil in the refrigerant line. Some authorities have suggested that the COP may be reduced by as much as 20% in R12 systems. Experiments should be conducted, with variable quantities of oil in the system, to determine the effect on the heat transfer coefficients.

5. The thermostatic expansion valve has been developed for the requirements of the refrigeration industry. It should be experimentally tested at temperatures above its stated design limit. Research could be initiated to design a device or control system that would provide a suitable value of suction superheat for wide variation of input conditions.

6. Two of the sensors are not as accurate as one would wish. The freon flow rate sensor is operating at the bottom end of its range. Though this has an advantage in that the pressure drop across the device is small it would be preferable to use the flow sensor in the range where it is well calibrated. It would be beneficial to purchase a freon

flow sensor of greater sensitivity. The power meter which disc measuring power runs at low frequency. A more accurate output could be obtained if the disc frequency were greater and this could be achieved by modifying the watt meter circuitry.

7. The modelling program could be improved by reducing the number of iterations required. It should be possible to utilise the now determined characteristics to identify more closely how a changing variable should be altered in order to achieve a given condition. For example figure (7.1) shows that a change in the evaporating temperature is about two-thirds of the change in the air inlet temperature. Thus if the initial guess for T_e produces a $T_a(i)$ value 6 deg C higher than the input $T_a(i)$, T_e should be reduced by 4 deg C and not by 1 deg C currently in the program.

APPENDIX A

Thermodynamic Properties Of R12

1. Specific Heat

The R12 specific heat equations below are at atmospheric pressure, but they can be used at other pressures to a very good accuracy because they change very little with pressure. If a precise value of specific heat is required at a certain pressure, it can be determined by calculating the enthalpy difference per one degree change of temperature at that pressure .

a) Specific Heat For Gas

This equation is taken from reference (48), for temperature range between 100K to 600K with accuracy claimed to be better than 1.5%.

$$C_p(\text{gas}) = (0.027882 + 5.6882 \times 10^{-4} T - 7.04559 \times 10^{-7} T^2 + 3.28112 \times 10^{-10} T^3) \cdot 4181 \quad (\text{A-1})$$

where $C_p(\text{gas})$ is the specific heat in $\text{Jkg}^{-1}\text{K}^{-1}$

T is the temperature in K

b) Specific Heat for Liquid

This equation is also taken from the same reference as in (a). The accuracy claimed for the temperature range between 194K to 294K is better than 1% and for temperatures outside the range is better than 1.5% .

$$C_p(\text{liq}) = (0.00963113 + 2.32124 \times 10^{-3} T - 9.7294 \times 10^{-6} T^2 + 1.49532 \times 10^{-8} T^3) 4184 \quad (\text{A} - 2)$$

where $C_p(\text{liq})$ is the specific heat for liquid R12 in $\text{J}(\text{kgK})^{-1}$

T is the temperature in K.

2. Viscosity

a) Viscosity of vapour R12

For R12 in the vapour state , the equation is taken from reference (48) . The error is not stated , but by comparison with data from (19) , it is found to be $\pm 5 \%$ for the temperature range of between 250K to 500K .

$$\begin{aligned} \nu(\text{gas}) = & 3.5071252 \times 10^{-5} - 9.8379394 \times 10^{-3} (1/T) \\ & + 9.291594 \times 10^{-1} (1/T)^2 \end{aligned} \quad (\text{A} - 3)$$

where $\nu(\text{gas})$ is the viscosity of freon gas in Ns m^{-2}

T is temperature in K

b) Viscosity of liquid R12

Using data from reference (48) , an equation for liquid viscosity of R12 is fitted in a polynomial form , with an accuracy of $\pm 5\%$ for temperature range from 200K to 340K .

$$\begin{aligned} \nu(\text{liq}) = & (6.45177299 - 0.05638052 T + 1.72893049 \times 10^{-4} T^2 \\ & - 1.80868046 \times 10^{-7} T^3) \times 10^{-3} \end{aligned} \quad (\text{A} - 4)$$

where $\nu(\text{liq})$ is the freon liquid viscosity in Ns m^{-2}

T is the temperature in K.

3. Conductivity

a) Conductivity of freon gas

The equation for conductivity of R12 gas is taken from (32). The accuracy is better than 1% for temperature range from 240K to 480K.

$$k(\text{gas}) = -4.3497562 \times 10^{-3} + 4.2024094 \times 10^{-5} T + 1.6172318 \times 10^{-8} T^2 \quad (\text{A}-5)$$

where $k(\text{gas})$ is conductivity in $\text{W}(\text{mC})^{-1}$ and T is temperature in C

b) Conductivity of liquid freon

This polynomial equation for conductivity of saturated R12 liquid is fitted from data taken from (48). The accuracy is better than 5% for temperature range between -140K to 230K.

$$k(\text{liq}) = 0.0492558455 - 1.23129085 \times 10^{-4} (T \times 1.8 + 32) - 2.04164148 \times 10^{-7} (T \times 1.8 + 32)^2 + 3.71103703 \times 10^{-9} (T \times 1.8 + 32)^3 - 1.37383454 \times 10^{-11} \times (T \times 1.8 + 32)^4 \quad (\text{A}-6)$$

where $k(\text{liq})$ is the liquid conductivity of R12 in $\text{W}(\text{mC})^{-1}$

T is the temperature in C.

4. Saturation Pressure As A Function Of Temperature

The equation is taken from (47) .

$$\ln P = 79.5288 - 4396.21/T - 12.47152 \ln T + 0.0196059 T \quad (\text{A}-7)$$

where P is pressure in MPa.

T is temperature in K.

APPENDIX B

Thermodynamic Properties of Water

All the equations below are fitted from data taken from reference(48).

a) Viscosity

$$\begin{aligned} \nu_w = & 0.00164323 - 0.393398 \times 10^{-4} (T \times 1.8 + 32) \\ & + 0.43606 \times 10^{-6} (T \times 1.8 + 32)^2 - 0.180044 \times 10^{-8} \\ & \times (T \times 1.8 + 32)^3 \end{aligned} \quad (B-1)$$

where ν_w is the viscosity of water in Ns m^{-2}

T is the temperature in C

b) Conductivity

$$\begin{aligned} k_w = & 1.731 (0.305 + 7.3961 \times 10^{-4} (T \times 1.8 + 32) \\ & - 1.534988 \times 10^{-6} (T \times 1.8 + 32)^2 \end{aligned} \quad (B-2)$$

where k_w is the conductivity of water in W(mC)^{-1}

T is temperature in C.

c) Density

$$\begin{aligned} \rho_w = & 16.019 (62.464 + 1.605602 \times 10^{-3} (T \times 1.8 + 32) \\ & - 6.646718 \times 10^{-5} (T \times 1.8 + 32)^2) \end{aligned} \quad (B-3)$$

where ρ_w is the density of water in kg m^{-3}

T is the temperature in C.

d) Specific Heat

$$\begin{aligned} C_{pw} = & 4.1868 \times 10^3 (1.0144 - 2.85919 \times 10^{-4} (T \times 1.8 + 32) \\ & + 1.174337 \times 10^{-6} (T \times 1.8 + 32)^2) \end{aligned} \quad (B-4)$$

where C_{pw} is the water specific heat in J(kgC)^{-1}

T is temperature in C.

APPENDIX C

Thermodynamic Properties Of Air

All the equations below are taken from (32).

a) Viscosity

$$\begin{aligned} \nu_a = & 2.28797 \times 10^{-6} + 6.25979 \times 10^{-8} T - 3.13196 \times 10^{-11} T^2 \\ & + 8.1503801 \times 10^{-5} T^3 \end{aligned} \quad (C-1)$$

where ν_a is the air viscosity in Nsm^{-2}

T is the temperature in K.

b) Conductivity

$$\begin{aligned} k_a = & 1.30035 \times 10^{-3} + 9.3676581 \times 10^{-5} T - 4.442469 \times 10^{-8} T^2 \\ & + 2.317 \times 10^{-11} T^3 - 6.6 \times 10^{-15} T^4 \end{aligned} \quad (C-2)$$

where k_a is the air conductivity in $\text{Wm}^{-1}\text{K}^{-1}$

T is the temperature in K.

c) Density

$$\rho_a = \frac{352.989}{T} \quad (C-3)$$

where ρ_a is the air density in kgm^{-3}

T is the temperature in K

d) Specific Heat

$$\begin{aligned} C_{pa} = & (0.249679 - 7.55179 \times 10^{-5} T + 1.69194 \times 10^{-7} T^2 \\ & - 6.46128 \times 10^{-11} T^3) \times 4184 \end{aligned} \quad (C-4)$$

where C_{pa} is the air specific heat in $\text{Jkg}^{-1}\text{K}^{-1}$

T is temperature in K.

APPENDIX D

Determination Of Polytropic Index , n

Normally the polytropic index n is calculated by assuming the freon vapour in the region of interest behaves as a perfect gas , and the equation used is ,

$$T_1 = T_5 (P_1/P_5)^{(n-1)/n} \quad (D.-1)$$

On the P-h chart of R12 , several calculations of PV/RT were made in the region of interest as shown by points 1 to 18 in figure (D-1) . It was found that $PV/(RT) = .714$ at 1 and $PV/(RT) = .951$ at point 18 . (for perfect gas $PV/(RT)=1$) . This gives an error of 5 % at point 18 and 30 % at point 1 . The error is too large to assume that freon vapour acts as a perfect gas in the determination of n .

The equation of state of R12 vapour as given by ICI is as follow,

$$P = \frac{R T}{V - b} + \sum_{j=2}^{j=5} \frac{A_j + B_j T + C_j e^{kT}}{(V-b)^j} \quad (D.-2)$$

where P = pressure

T = Temperature

V = Volume

R = Gas constant

$b = .226787$

$k = -5.475$

The values of A_j , B_j and C_j are as follows ,

j	A_j	B_j	C_j
2	-6.93385	2.2478	-115.43
3	4.2679	-0.92326	92.911
4	-1.3545	0.0	0.0
5	0.0	0.20682	-2.11877

The polytropic index n is calculated as follows (see figure(5.15) for reference).

1. From T_5 and P_5 ; V_5 is determined using equation (D-2).
2. From T_1 and P_1 : V_1 is determined using equation (D-2).
3. n is calculated from $P_1 V_1^n = P_5 V_5^n$.

For a given values of n , T_5 , P_5 and P_1 , the discharge temperature of R12 , T_1 is calculated as follows.

1. From T_5 and P_5 ; V_5 is determined using equation (D-2).
2. From n and P_1 ; V_1 is determined using the equation PV^n is constant.
3. T_1 is calculated from the equation of state (D-2) by using the values of V_1 and P_1 .

Appendix E is the computer program for calculating n from T_5 , P_5 , T_1 and P_1 . While appendix F is a program for determining T_1 from n , T_5 , P_5 and P_1 .

point	T (C)	V (m ³ /kg)	PV/(RT)
1	90	.008	.714
2	110	.008	.748
3	70	.012	.775
4	90	.012	.804
5	110	.012	.827
6	50	.02	.840
7	70	.02	.862
8	30	.03	.872
9	90	.02	.879
10	50	.03	.892
11	110	.02	.894
12	70	.03	.907
13	10	.05	.909
14	90	.03	.919
15	30	.05	.924
16	50	.05	.935
17	70	.05	.944
18	90	.05	.951

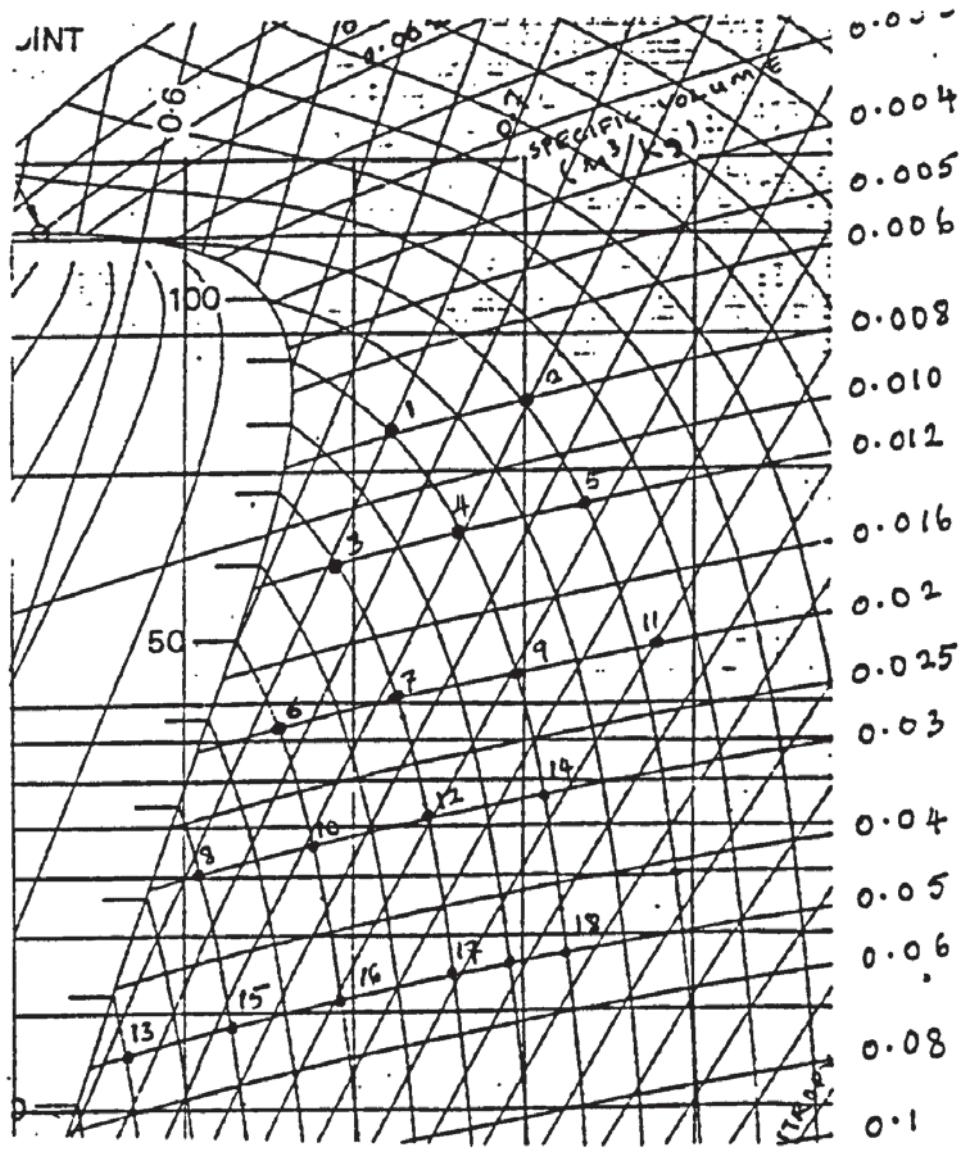


Fig (*D-1) Some values of PV/(RT) for R12 in the region of interest.

APPENDIX E

Computer program for calculating polytropic index n from P1,T1,P5and T5.

```

50 REM "-----"
60 REM THIS PROGRAM IS TO CALCULATE
65 REM THE POLYTROPIC INDEX N FROM
70 REM P1 .T1 .P5 .T5
80 REM "-----"
100 DATA 3.59102,0.226787,-5.475
110 DATA -6.93385,4.2679,-1.3545,0
120 DATA 2.2478,-0.92326,0,0.20682
130 DATA -115.43,92.911,0,-2.11877
140 DATA 4.1155,1.7918E-3,385.17
150 READ R,B,K
160 FOR J=2T05:READ A(J):NEXT
170 FOR J=2T05:READ B(J):NEXT
180 FOR J=2T05:READ C(J):NEXT
190 READ PC,VC,TC
200 Q=PC*145.0377
210 GOT0370
220 INPUT "TEMP.-DEG.CENT.":TE
230 INPUT "PRESSURE-P.S.I.":PI
240 T=(TE+273.15)/TC
250 PR=PI/Q
260 V=R*T/PR
270 C=0
280 FOR J=2T05
290 C=C+(A(J)+B(J)*T+C(J)*EXP(K*T))/(V-B)^J
300 NEXT
310 P=R*T/(V-B)+C
320 P=P*Q
330 D=PI-P
340 IF ABS(D)<.01 THEN 360
350 V=V*(1-D/PI):GOTO270
360 RETURN
370 PRINT "LOW T&P RESULTS"
380 GOSUB 220
390 P1=PI:V1=V:T1=TE
400 PRINT "HIGH T&P RESULTS"
410 GOSUB 220
420 P2=PI:V2=V:T2=TE
430 N=LOG(P2/P1)/LOG(V1/V2)
440 N=INT(N*1000+.5)/1000
450 PRINT "N=":N
460 PRINT "PRESS SPACE TO ENTER MORE RESULTS"
470 GETZ$:IF Z#<>" " THEN 470
480 GOT0370

```


APPENDIX F

A computer program to calculate freon discharge temperature T1 for a given P5,T5,P1 and n.

```

50 REM "-----"
60 REM THIS PROGRAM IS TO CALCULATE
65 REM TEMPERATURE T1 FOR A GIVEN H,
70 REM P5 AND T5
80 REM "-----"
100 DATA 3.59192,0.226787,-5.475
110 DATA -6.93385,4.2679,-1.3545,0
120 DATA 2.2478,-0.92326,0,0.20682
130 DATA -115.43,92.911,0,-2.11877
140 DATA 4.1155,1.7918E-3,385.17
150 READ R,B,K
160 FOR J=2TO5:READ A(J):NEXT
170 FOR J=2TO5:READ B(J):NEXT
180 FOR J=2TO5:READ C(J):NEXT
190 READ PC,VC,TC
200 Q=PC*145.0377
210 PRINT"LOW T&P RESULTS"
220 INPUT"TEMP.-DEG.CENT.":T
230 INPUT"PRESSURE-P.S.I.":PI
240 T=(T+273.15)/TC
250 P1=PI/Q
260 V=R*T/P1
270 C=0
280 FOR J=2TO5
290 C=C+(A(J)+B(J)*T+C(J)*EXP(K*T))/(V-B)^J
300 NEXT
310 P=R*T/(V-B)+C
320 P=P*Q
330 D=PI-P
340 IF ABS(D)<.01 THEN 360
350 V=V*(1-D/PI):PRINTV:GOTO270
360 PRINT"HIGH T&P RESULTS"
370 INPUT"PRESSURE-P.S.I.":PF
380 INPUT"POLYTROPIC INDEX":N
390 V=V*(PI/PF)^(1/N)
400 P2=PF/Q
410 T=P2*V/R
420 C=0:PRINT T
430 FOR J=2TO5
440 C=C+(A(J)+B(J)*T+C(J)*EXP(K*T))/(V-B)^J
450 NEXT
460 P=R*T/(V-B)+C
470 P=P*Q
480 D=PF-P
490 IF ABS(D)<.01 THEN 510
500 T=T*(1+D/PF):GOTO 420
510 PRINT"TEMP. =":T*TC-273.15

```

APPENDIX G

Computer program for calculating thermodynamic properties of R12 (based on McMullan (47)).

1. Saturated pressure at a known temperature:
see line numbers : 2260 - 2330 in appendix H
2. Entropy, enthalpy and specific volume of R12 vapour given pressure and temperature.
see line numbers : 2340 - 2550 in appendix H
3. Entropy, enthalpy and specific volume of R12 liquid given pressure and temperature.
see line numbers : 2560 - 2720 in appendix H
4. Entropy, enthalpy and specific volume at saturation (vapour and liquid) given pressure or temperature.
see line numbers : 2730 - 3080 in appendix H
5. Specific volume at a given temperature.
see line numbers : 3090 - 3430 in appendix H
6. Saturation pressure at a known pressure.
see line numbers : 3440 - 3570 in appendix H

APPENDIX H

Computer program for the heat pump model.

```

100 REM -----
110 REM   HEAT PUMP MODEL
120 REM -----
130 OPEN3,4
140 REM ** COMPRESSOR **
150 INPUT" AIR   INLET  TEMP C";AI
160 INPUT" AIR   SPEED   M3/S";AJ
170 INPUT" REL   HUMID   % ";RH
180 INPUT" SUCT  S-HEAT   C";SH
190 INPUT" HOT   WATER  TEMP C";TU
200 INPUT" COLD  WATER  TEM C";TM
210 FP=19.032+298.459*AJ
220 TE=-3.59530607+.786416131*AI+13.0998402*AJ-.485072472*SH
230 TC=5.23004131+.159133348*TE+.734577654*TU
240 REM
250 REM
260 TV=TC:GOSUB2260:P1=PB*14.5
270 TV=TE:GOSUB2260:P4=PB*14.5
280 T5=TE+SH:P5=P4-2
290 XN=1.27308274-7.92672924E-4*P1+1.35560865E-3*P5-4.36587376E-3*T5
300 N=XN
310 XN=INT(1000*XN+.5)/1000
320 GOSUB4930:REM FOR T1
330 T1=PT
340 YN=(XN-1)/XN
350 TV=T1*1.8+32:PS=P1:GOSUB2340
360 H1=HP/.4299:S1V=SV*.0624
370 TV=TC*1.8+32:PS=P1:GOSUB2730
380 H2=HG/.4299:HK=HF/.4299
390 TV=T5*1.8+32:PS=P5:GOSUB2340
400 H5=HP/.4299:S5V=SV*.0624:U5=SP/.2388
410 CP=(H1-H5)*1000/(T1-T5):REM SPC HEAT
420 R1=P1*1E5*S1V/(14.5*(T1+273.15)):REM GAS CONST AT DISCH
430 R5=P5*1E5*S5V/(14.5*(T5+273.15)):REM GAS CONST AT SUCTION
440 RC=(R1+R5)/2:REM AVE GAS CONST
450 VC=CP-RC ;REM SPC HEAT  CONST VOL
460 IFZZ=1THEN510
470 GOTO590
480 XS=U5:GOSUB5310
490 GN=LOG(P1/P5)/LOG(S5V/S6V)
500 REM T6,H6,S6V ----AT ISEN
510 GN=1.056
520 N=6N:GOSUB4930:T6=PT
530 TV=T6*1.8+32:PS=P1:GOSUB2340
540 H6=HP/.4299:S6V=SV*.0624
550 GY=(6N-1)/6N
560 CJ=P1/P5
570 WH=XN*P5*1E5*10.3E-6*(CJ^YN-1)*(1-.05*(CJ^(1/XN)))/(14.5*(XN-1))
580 WI=6N*P5*1E5*10.3E-6*(CJ^GY-1)*(1-.05*(CJ^(1/6N)))/(14.5*(6N-1))
590 FC=31.2563+1289.88*S1V-372.138*S5V
600 CB=.05 ;REMRATIO OF CLEARANCE VOL TO SWEEP VOL
610 FR=FC*10.3E-6*((1+CB)/S5V-CB/S1V)
620 IFZZ=0THEN720

```



```

630 VE=1+CB-CB*S5V/S1V
640 W1=(H1-H5)*FR*1000
650 W6=(H6-H5)*FR*1000
660 W6=INT(W6+.5)
670 SJ=W6/W1 :REM ISEN EFF
680 W8=WH*FC
690 W9=WI*FC
700 QR=VC*(XN-6N)*FR*(T1-T5)/(XN-1)
710 PE=162.119048+2.71428572*TE+3.01428572*TC
720 TC=INT(TC*100+.5)/100:TE=INT(TE*100+.5)/100
730 PRINT" COND TC :";TC;" EVAP TE: ";TE
740 PRINT" R12 MASS FR KG/S: ";FR
750 REM
760 WR=XN*FR*RC*(T1-T5)/(XN-1)
770 REM
780 FC=INT(FC*100+.5)/100
790 PRINT" FREQUENCY HZ: ";FC
800 IFTB=0THEN1030
810 REM ESTIMATE WATER F/RATE
820 WF=.97*FR*(H1-H3)*1000/(4186*(TU-TM))
830 PRINT" WATER F/R KG/S: ";WF
840 QC=WF*4186*(1.0)
850 GOTO1460
860 GOSUB63999
870 IFVT<>TCTHEN260
880 Q9=Q5+W1
890 T9=TU-(TU-TC)*(H1-HK)/(H1-H2)
900 PRINTT9
910 PX=P1-223.360881*14.5*FR^1.07917658:REM LIQUID PRESSURE
920 IFT9<TM)THENT9=TM+3:TC=TU-(TU-T9)*(H1-H2)/(H1-HK):TB=0:GOTO240
930 PRINTT9
940 H3=(HK*(TU-TM)-H1*(T9-TM))/(TU-T9)
950 GX=H3*.4299
960 WL=-39.8047638+4.70226517*6X-2.34409608E-03*GX^2-1.3864116E-04*GX^3
970 WL=(WL-32)*5/9
980 PRINTH3;WL;T9
990 ZN=1
1000 GOTO1140
1010 REM
1020 REM
1030 WL=TM+5
1040 PX=P1-223.360881*14.5*FR^1.07917658:REM LIQUID PRESSURE
1050 ZM=0
1060 TV=WL*1.8+32:PS=PX:GOSUB2560
1070 PRINTZM,WL
1080 IFZM=1THEN1040
1090 PRINT"**** HA";HA
1100 IFWL<TM+2THENTC=TC+1:GOTO240
1110 H3=HA/.4299
1120 PRINT"*** H3=";H3
1130 REM
1140 ED=(H1-H3)*1000*FR
1150 EI=(H5-H3)*1000*FR:REM INPUT ENERGY(WATT)
1160 REM CAL QUALITY R-12
1170 TV=TE*1.8+32:PS=P4:GOSUB2730
1180 HM=HF/.4299:HN=HG/.4299

```



```

1190 XQ=(H3-HM)/(HN-HM)
1200 DH=1/(VF*.0624);DG=1/(VG*.0624)
1210 REM CALCULATE EVAP HTC & EFFECTIVE
1220 TA=AI;GOSUB4550
1230 GOSUB4820
1240 DC=(1+WJ)/(1+1.607*WJ);DA=DC*DA
1250 CC=(1+1.915*WJ)/(1+WJ);CA=CC*CA
1260 AF=AJ*DA
1270 GOSUB4150
1280 PRINT"AIR TEMP INPUT : "AI;" CALCULATED:";TB
1290 IFZN=1THEN1400
1300 IFAI-TB>2.1THENTE=TE+.5;TB=0;GOTO240
1310 IFAI-TB>1.0THENTE=TE+.3;TB=0;GOTO240
1320 REMIFTE+SH>AITHENPRINT" SUCTION SUPERHEAT IS TO HIGH":STOP
1330 IFAI-TB>.4THENB90
1340 IFTB-AI>2.1THENTE=TE-.5;TB=0;GOTO240
1350 IFTB-AI>1.0THENTE=TE-.3;TB=0;GOTO240
1360 IFTB-AI>.4THENB90
1370 Q5=EI
1380 REM
1390 REM
1400 REM
1410 IFAI-TB>.6THENWL=WL-4;GOTO1040
1420 IFTB-AI>.6THENWL=WL+4;GOTO1040
1430 IFAI-TB>.25THENWL=WL-1;GOTO1040
1440 IFTB-AI>.25THENWL=WL+1;GOTO1040
1450 ZZ=1;GOTO240
1460 Q7=WF*4186*(TU+.5-TM)
1470 CN=Q7/(1000*FR*(H1-H5));REM CYCLE COP
1480 CM=Q7/(PE+FP) ;REM COP- PRACTICAL
1490 CS=(TC+273.15)/(TC-TE)
1500 FR=INT(FR*1E6+.5)/1E6;WF=INT(WF*1E6+.5)/1E6
1510 W1=INT(W1+.5);W8=INT(W8+.5);PE=INT(PE+.5);Q7=INT(Q7+.5)
1520 EI=INT(EI+.5)
1530 CS=INT(CS*100+.5)/100;CN=INT(CN*100+.5)/100;CM=INT(CM*100+.5)/100
1540 HA=INT(HA*100+.5)/100;HR=INT(HR*100+.5)/100;UY=INT(UY*100+.5)/100
1550 EZ=INT(EZ*100+.5)/100;VE=INT(VE*100+.5)/100;SJ=INT(SJ*100+.5)/100
1560 REM PRINT
1570 PRINT£3," HEAT PUMP MODEL-- RESULT"
1580 PRINT£3," -----"
1590 PRINT£3," ---INPUT "
1600 PRINT£3," AIR INLET TEM C: ";AI
1610 PRINT£3," AIR SPEED M3/S: ";AJ
1620 PRINT£3," AIR REL HUM Z: ";RH
1630 PRINT£3," SUCT S-HEA C: ";SH
1640 PRINT£3," HOT WATER T C: ";TU
1650 PRINT£3," COLD WATER T C: ";TM
1660 PRINT£3," -----"
1670 PRINT£3," ---OUTPUT"
1680 PRINT£3," EVAP TEMP C: ";TE
1690 PRINT£3," COND TEMP C: ";TC
1700 PRINT£3," COMP SPEED HZ: ";FC
1710 PRINT£3," FREON F-R KG/S: ";FR
1720 PRINT£3," WATER F-R KG/S: ";WF
1730 PRINT£3," COMP WORK W: ";W1
1740 PRINT£3," COMP WORK (EQ) W: ";W8

```



```

2870 REM CAL HV BY CLAUDIUS CLAPEYRON
2880 HV=(VG-VF)*PS*2.3025851*(3436.632/T-5.41631329+.4730442E-2*T)*.185
2890 SX=HV/T
2900 REM CAL HG&SG
2910 TX=T*T:TY=TX*T:TZ=TY*T
2920 VR=VG-.65093886E-2:V2=2*VR*VR
2930 V3=1.5*V2*VR:V4=V2*V2
2940 KC=7.897E-3*T:EK=EXP(-KC):EV=EXP(0)
2950 E1=.80945E-2*T+.332662E-3*TX/2-.2413896E-6*TY/3+.672363E-10*TZ/4
2960 E2=.185053*PS*VG
2970 E3=-3.40972713/VR+.0602394465/V2-.54873701E-3/V3
2980 E4=-56.7627671/VR+1.31139908/V2-.254390678E-4/V4
2990 SB=.80945E-2*LOG(T)+.332662E-3*T-.2413896E-6*TX/2+.672363E-10*TY/3
3000 SC=.185053*.088734*LOG(VR)
3010 S8=.159434848E-2/VR-.187961843E-4/V2+.3468834E-8/V4
3020 S9=E4
3030 HG=E1+E2+.185053*E3+.185053*EK*(1+KC)*E4+39.55655
3040 SG=SB+SC-.185053*S8+.185053*EK*7.89E-3*S9-.0165374
3050 REM CAL HF&SF
3060 HF=HG-HV
3070 SF=SG-SX
3080 RETURN
3090 REM      SUB SPVOL
3100 REM "88888888888888888888"
3110 REM CONVERT TV FROM F TO R &CHECK
3120 TD=TV+459.7
3130 IFTD<0THENPRINT"*#ERROR:T<0":STOP
3140 REM FIND TSAT & CHECK
3150 GOSUB3440
3160 IFTV<TTTHENTD=TT+459.7
3170 IFTV=TTTHENTD=TT+459.7
3180 IFP<1E-20THENPRINT"*#ERROR:P<0":STOP
3190 REM CALCULATE CONSTANTS
3200 E0=EXP(-7.897E-3*TD)
3210 E7=P:EB=.088734*TD:E9=-3.40972713+.159434848E-2*TD-56.7627671*E0
3220 EW=.0602394465-.187961843E-4*TD+1.31139908*E0
3230 E6=-.54873701E-3:E6=.3468834E-8*TD-.2543390678E-4*E0
3240 EA=2*E9:EB=3*EW:EC=4*E6
3250 ED=5*E6
3260 REM INI. VL OF V FRM GAS LAW
3270 VN=.088734*TD/P
3280 REM COMP V TO WTH 1E-8/V
3290 L=1
3300 V=VN:V2=V*V:V3=V2*V
3310 V4=V3*V:V5=V4*V:V6=V5*V
3320 EV=EXP(-34.84*(V+.65093886E-2))
3330 F=E7-EB/V-E9/V2-EW/V3-EG/V4-E6/V5
3340 FV=EB/V2+EA/V3+EB/V4+EC/V5+ED/V6
3350 FF=F/FV
3360 IFABS(FF)>VNTHENFF=FF/5
3370 VN=V-FF
3380 IFABS((VN-V)/V)<1E-8THEN3410
3390 L=L+1:GOTO3300
3400 PRINT"NOT CONVERGED"
3410 SV=VN+.65093886E-2
3420 SV=INT(1E4*SV+.5)/1E4

```



```

5110 IF ABS(D)<.01 THEN 5130
5120 V=V*(1-D/P5):GOTO5040
5130 REM P1 FINAL PRESS
5140 REM N POLY INDEX
5150 V=V*(P5/P1)^(1/N)
5160 P2=P1/Q
5170 PT=P2*V/3.59102
5180 C=0
5190 FOR J=2T05
5200 C=C+(A(J)+B(J)*PT+C(J)*EXP(-5.475*PT))/(V-.226787)^J
5210 NEXT
5220 P=3.59102*PT/(V-.226787)+C
5230 P=P*Q
5240 D=P1-P
5250 IF ABS(D)<.01 THEN 5270
5260 PT=PT*(1+D/P1):GOTO 5180
5270 PRINT"TEMP. =";PT*385.17-273.15
5280 PT=PT*385.17-273.15
5290 PT=INT(PT*100+.5)/100
5300 RETURN
5310 REM ** R12--- P & ENTROPY
5320 YA=XS*.2388 :REM IN BHTU
5330 PS=P1:GOSUB3440
5340 TA=TT:REM IN FEH !
5350 FORI=1T020
5360 TS=TA+.00001
5370 TV=TA:PS=P1:GOSUB2340
5380 H9=HP:V9=SV:SZ=SP
5390 TV=TS:PS=P1:GOSUB2340
5400 H8=HP:V8=SV:SY=SP
5410 YB=SZ:YC=SY :REM IN BTH UNIT
5420 IFABS(YA-YB)<.0001THEN5450
5430 BT=TA+.00001*(YA-YB)/(YC-YB):TA=BT
5440 NEXT
5450 T6=(TA-32)*5/9 :REM IN CENT
5460 H6=H9/.4299:S6V=V9*.0623
5470 RETURN

```


APPENDIX I

Computer program for the detail model of the condenser , where the temperature profiles of R12 and water are the output.

```
100 REM-----
110 REM      CONDENSER MODEL
120 REM-----
130 PRINT""
140 DIMPF(50),PW(50),TF(50),TW(50)
150 DIMUL(50),UW(50),UF(50)
160 DIMEF(50),EW(50),TB(50)
170 DIMQF(50),QW(50),X(50)
180 DIMHX(50),LX(50)
190 OPEN3,4
200 REM----- INPUT -----
210 INPUT" T1 & P1";T1,P1
220 INPUT" COLD & HOT WATER ";TM,TU
230 INPUT" WATER FLOW RATE ";WF
240 INPUT" R12 FLOW RATE ";FR
250 REM ----- BASIC CYCLE -----
260 TV=T1*1.8+32:PS=P1:GOSUB410
270 H1=HP/.4299:TC=(TT-32)*5/9
280 FR=.0078
290 PRINT"R12 MAS FLOW RATE";FR
300 PRINT"CONDENSING TEMP ";TC
310 GOSUB2220
320 STOP
330 REM      PSAT(T)
340 REM -----
350 TF=TV*1.8+32
360 T=TF+459.7
370 XZ=10^(39.8838-3436.6322/T-12.4715223*LOG(T)/LOG(10)+.4733044E-2*T)
380 PB=XZ/14.5
390 REM PB IS IN BAR
400 RETURN
410 REM      SUB VAPOUR
420 REM -----
430 TN=TV+459.7:REM F TO R
440 GOSUB1510
450 GOSUB1160
460 TX=TN^2:TY=TX*TN:TZ=TY*TN
470 VR=SV-.65093886E-2
480 V2=2*VR^2:V3=1.5*V2*VR
490 V4=V2^2
500 KC=5.475*TN/693.3:EK=EXP(-KC)
```

```

510 EV=EXP(0)
520 E1=.80945E-2*TN+.332662E-3*TX/2-.2413896E-6*TY/3+.672363E-10*TZ/4
530 E2=.185053*PS*SV
540 E3=-3.40972713/VR+.0602394465/V2--.54873701E-3/V3
550 E4=-56.7627671/VR+1.31139908/V2-.254390678E-4/V4
560 SB=.80945E-2*LOG(TN)+.332662E-3*TN-.2413896E-6*TX/2+.672363E-10*TY/3
570 SC=.185053*.088734*LOG(VR)
580 SB=.159434848E-2/VR-.187961843E-4/V2+.3468834E-8/V4
590 S9=E4
600 HP=E1+E2+.185053*E3+.185053*EK*(1+KC)*E4+39.55655
610 SP=SB+SC-.185053*SB+.185053*EK*5.475/693.3*S9-.01653794
620 RETURN
630 REM          SUB  SUBCOOL
640 REM -----
650 REM HA(SP H):SA(SP S)
660 GOSUB1510:GOSUB800
670 DT=TT-TV
680 IFDT<-.0001THENWL=WL-2:ZM=1:RETURN
690 VA=VF
700 IFABS(TT+40)<1E-6THEN730
710 HA=HF*(1-DT/(TT+40))
720 GOTO740
730 HA=HF
740 IFABS(TV+40)<1E-6THEN770
750 SA=SF+(HF/(TV+40))*LOG((TV+459.7)/(TT+459.7))
760 GOTO780
770 SA=SF
780 S=SA:H=HA
790 RETURN
800 REM          SUB  SATPRP
810 REM -----
820 REM TV(TEMP),PS(ABS PRESS)
830 REM VF(SPC VL SAT LQ),VG(SV S G)
840 REM HF(S H S L),HV(L HEAT VP)
850 REM HG(S H S V),SF(S S S L)
860 REM SG(S S S V)
870 REM CALCULATE PRESSURE
880 GOSUB1160
890 VG=SV
900 REM CAL VF
910 T=TT+459.7:REM F TO R
920 TJ=1-T/693.3
930 VF=1/(34.84+53.3412*TJ^(1/3)+18.6914*TJ+21.984*TJ^.5-3.151*TJ*TJ)
940 REM CAL HV BY CLAUSIUS CLAPEYRON
950 HV=(VG-VF)*PS*2.3025851*(3436.632/T-5.41631329+.4730442E-2*T)*.185053
960 SX=HV/T
970 REM CAL HG&SG
980 TX=T*T:TY=TX*T:TZ=TY*T
990 VR=VG-.65093886E-2:V2=2*VR*VR
1000 V3=1.5*V2*VR:V4=V2*V2

```



```

1010 KC=7.897E-3*T;EK=EXP(-KC);EV=EXP(0)
1020 E1=.80945E-2*T+.332662E-3*TX/2-.2413896E-6*TY/3+.672363E-10*TZ/4
1030 E2=.185053*PS*VG
1040 E3=-3.40972713/VR+.0602394465/V2-.54873701E-3/V3
1050 E4=-56.7627671/VR+1.31139908/V2-.254390678E-4/V4
1060 SB=.80945E-2*LOG(T)+.332662E-3*T-.2413896E-6*TX/2+.672363E-10*TY/3
1070 SC=.185053+.088734*LOG(VR)
1080 SB=.159434848E-2/VR-.187961843E-4/V2+.3468834E-8/V4
1090 S9=E4
1100 HG=E1+E2+.185053*E3+.185053*EK*(1+KC)*E4+39.55655
1110 SG=SB+SC-.185053*SB+.185053*EK*7.89E-3*S9-.0165374
1120 REM CAL HF&SF
1130 HF=HG-HV
1140 SF=SG-SX
1150 RETURN
1160 REM          SUB SPVOL
1170 REM -----
1180 REM CONVERT TV FROM F TO R & CHECK
1190 TD=TV+459.7
1200 IFTD<0THENPRINT**ERROR:T<0*:STOP
1210 REM FIND TSAT & CHECK
1220 GOSUB1310
1230 IFTV<TTTHENTD=TT+459.7
1240 IFTV=TTTHENTD=TT+459.7
1250 IFP<1E-20THENPRINT**ERROR:P<0*:STOP
1260 REM CALCULATE CONSTANTS
1270 E0=EXP(-7.897E-3*TD)
1280 E7=P;E8=.088734*TD;E9=-3.40972713+.159434848E-2*TD-56.7627671*E0
1290 EW=.0602394465-.187961843E-4*TD+1.31139908*E0
1300 EG=-.54873701E-3;E6=.3468834E-8*TD-.2543390678E-4*E0
1310 EA=2+E9;EB=3*EW;EC=4*EG
1320 ED=5*E6
1330 REM INI. VL OF V FRM GAS LAW
1340 VN=.088734*TD/P
1350 REM COMP V TO WITH 1E-8/V
1360 L=1
1370 V=VN;V2=V*V;V3=V2*V
1380 V4=V3*V;V5=V4*V;V6=V5*V
1390 EV=EXP(-34.84*(V+.65093886E-2))
1400 F=E7-EB/V-E9/V2-EW/V3-EG/V4-E6/V5
1410 FV=EB/V2*EA/V3+EB/V4+EC/V5+ED/V6
1420 FF=F/FV
1430 IFABS(FF)>VNTHENFF=FF/3
1440 VN=V-FF
1450 IFABS((VN-V)/V)<1E-8THEN1480
1460 L=L+1;GOTO1370
1470 PRINT*NOT CONVERGED*
1480 SV=VN+.65093886E-2
1490 SV=INT(1E4*SV+.5)/1E4
1500 RETURN

```

```

1510 REM      SUB TSAT
1520 REM -----
1530 P=PS
1540 PG=LOG(P)/LOG(10)
1550 TR=120*PG+323.1
1560 T0=TR
1570 F=39.8838-3436.6322/T0-12.4715*(LOG(T0)/LOG(10))+.47304E-2*T0-PG
1580 FQ=3436.6322/T0^2-12.4715/(2.3026*T0)+.47304E-2
1590 TR=T0-F/FQ
1600 IFABS(TR-T0)<.0001THEN1620
1610 GOTO1560
1620 TT=TR-459.7:REM TT IN FEH
1630 TT=INT(100*TT+.5)/100
1640 RETURN
1650 REM      VISCOSITY OF WATER
1660 REM -----
1670 TL=TL:REM TL IN CENT
1680 WV=.00164323-.393398E-4*TL+.43606E-6*TL^2-.180044E-8*TL^3
1690 RETURN
1700 REM CONDUT. OF WATER
1710 TL=32+TL*9/5:REM TL IN CENT
1720 WK=1.731*(.305+7.3961E-4*TL-1.534988E-6*TL^2)
1730 RETURN
1740 REM DENSITY OF WATER
1750 TL=32+9*TL/5:REMTL IN CENT
1760 WD=16.019*(62.464+1.605602E-3*TL-6.646718E-5*TL^2)
1770 RETURN
1780 REM CP OF WATER
1790 TL=32+9*TL/5:REM TL IN CENT
1800 WC=4.1868E3*(1.0144-2.85919E-4*TL+1.174337E-6*TL^2)
1810 RETURN
1820 REM      THD. PROPERTIES OF R-12
1830 REM -----
1840 REM      SPECIFIC HEAT
1850 T=TV+273.15
1860 REMCG:SPC HEAT OF GAS
1870 CG=(.040567612+4.52415E-4*T-3.60905E-7*T^2)*4184
1880 CG=INT(100*CG+.5)/100
1890 REMCL:SPC HEAT OF LIQUID
1900 CL=(.00963113+2.32124E-3*T-9.7294E-6*T^2+1.49532E-8*T^3)*4184
1910 CL=INT(100*CL+.5)/100
1920 CX=.143683799+2.52426014E-4*TF+1.74152945E-6*TF^2+1.68742687E-8*TF^3
1930 CY=-3.43625649E-10*TF^4+1.60509031E-12*TF^5
1940 CV=CX+CY:REM SPC HEAT OF SAT VAPOUR
1950 CV=CV*4184
1960 CV=INT(100*CV+.5)/100
1970 RETURN
1980 REM      VISCOSITY OF R-12
1990 REM -----
2000 REM****TV IS INPUT TEMP IN CENT

```



```

2010 T=TV+273.15
2020 REM UT:VIS OF R12 GAS
2030 UG=3.5072152E-5-9.8379394E-3*(1/T)+.9291594*(1/T)^2
2040 REM UV:VIS OF R12 SAT VAPOUR
2050 UV=(-6.93423653+.0796469152*T-2.73627695E-4*T^2+3.31833E-7*T^3)*1E-5
2060 REM UL:VIS OF LIQUID R12
2070 UL=(6.45177299-.0563805196*T+1.72893049E-4*T^2-1.80868046E-7*T^3)*1E-3
2080 RETURN
2090 REM CONDUCTIVITY OF R-12
2100 REM -----
2110 REM*****TV IS INPUT TEMP IN CENT
2120 T=TV+273.15
2130 REM GK:CONDUCTIVITY OF R12 GAS
2140 GK=-4.3497562E-3+4.2024094E-5*T+1.6172318E-8*T^2
2150 REM FK:CONDUCTIVITY OF R12 LIQUID
2160 TF=TV*9/5+32
2170 F1=.0492558455-1.23129085E-4*TF-2.04164148E-7*TF^2+3.71103703E-9*TF^3
2180 FK=(F1-1.37383454E-11*TF^4)*1.7296
2190 GK=INT(1E6*GK+.5)/1E6
2200 FK=INT(1E5*FK+.5)/1E5
2210 RETURN
2220 REM CONDENSOR
2230 REM -----
2240 DF=.0045:REM INTR DIA OF FREON TUBE
2250 LX(1)=0:LE=2.15:REM LENGTH INCREMENT
2260 DW=.0065:REM INT DIA OF WATER TUBE
2270 BO=500:REM LEAD COND W/MC
2280 TW(1)=TU:REM WATER TEMP OUT
2290 PF(1)=P1:PW(1)=0
2300 TF(1)=T1
2310 TP=TC :REM SAT TEMP STARTING
2320 LE=1
2330 TF(1)=T1:TW(1)=TU:PF(1)=P1
2340 I=1
2350 REM----- VAPOUR -----
2360 REM GAS PROP OF FREON
2370 TV=TF(I)*1.8+32:PS=PF(I)
2380 GOSUB410:RK=1/(SV*.0624):HX(I)=HP/.4299
2390 TB(I)=(TF(I)+TW(I))/2:REM WALL TEMP
2400 GR=1.273*FR/(DF^2)
2410 TV=TF(I)
2420 GOSUB1980:UX=UG
2430 RY=GR*DF/UX:RY=INT(RY+.5)
2440 REM CAL CP
2450 TV=TF(I):GOSUB1820
2460 TV=TF(I):GOSUB2090
2470 PR=UX*CG/GK:PR=INT(1E3*PR+.5)/1E3
2480 TV=TB(I):GOSUB1980:UD=UG
2490 RV=UX/UD
2500 GOSUB5160:REM GAS HEAT TRNS

```

```

2510 REM LIQUID PROP OF WATER
2520 GW=1.273*WF/(DW^2)
2530 TL=TW(I):GOSUB1650:VX=WV
2540 TL=TB(I):GOSUB1650:RM=VX/WV
2550 TL=TW(I):GOSUB1740:WT=WD
2560 TL=TW(I):GOSUB1700
2570 TL=TW(I):GOSUB1780
2580 PW=VX*WC/WK:REM PRANDL NO
2590 RW=GW*DW/VX:REM REYNOLD NO
2600 GOSUB4870
2610 UL(I)=1/((1/BO)+(1/(3.142*DW*QW(I)))+(1/(3.142*DF*QF(I))))
2620 CW=WF*WC
2630 CR=FR*CG
2640 UW(I)=LE*UL(I)/CW
2650 UF(I)=LE*UL(I)/CR
2660 A=UW(I)/UF(I)
2670 B=EXP(-UF(I)+UW(I))
2680 EF(I)=(1-B)/(1-B*A)
2690 EW(I)=A*EF(I)
2700 TW(I+1)=(TW(I)-EW(I)*TF(I))/(1-EW(I))
2710 TF(I+1)=TF(I)+EF(I)*(TW(I+1)-TF(I))
2720 PF(I+1)=PF(I)
2730 PW(I+1)=PW(I)+LE*PJ*14.5
2740 TB(I+1)=TF(I+1)-(TF(I+1)-TW(I+1))*UL(I)/(3.142*DF*QF(I))
2750 TF(I)=INT(TF(I)*100+.5)/100:TW(I)=INT(TW(I)*100+.5)/100
2760 WF=INT(WF*1E5+.5)/1E5
2770 Y1=(I-1)*LE:Y2=TF(I):Y3=TW(I):Y4=WF:Y5=X(I):Y6=PF(I)
2780 Y1$=LEFT$(STR$(Y1)+"          ",6)
2790 Y2$=LEFT$(STR$(Y2)+"          ",10)
2800 Y3$=LEFT$(STR$(Y3)+"          ",10)
2810 Y5$=LEFT$(STR$(Y5)+"          ",6)
2820 Y6$=LEFT$(STR$(Y6)+"          ",6)
2830 Y4$=LEFT$(STR$(Y4)+"          ",12)
2840 PRINT(I-1)*LE:TF(I):TW(I):WF
2850 PRINT£3,Y1$:Y2$:Y3$:Y5$:Y4$:Y6$
2860 REMPRINT£3,(I-1)*LE:PF(I):TF(I):TW(I):100*X(I):RY:RW:EF(I):EW(I)
2870 JI=I
2880 REMIFLX(I)>2.5THEN4770
2890 IFTW(I)=>TF(I)THENWF=WF-.01*WF:GOTO2320
2900 REMIFTF(I)-TW(I)<.5THENWF=WF-.008*WF:GOTO4160
2910 IFTP-TF(I+1)>3THENTC=TC+2.5:VT=0:RETURN
2920 IFTP>TF(I)THEN3010
2930 IFLX(I)=>5THEN2980
2940 LX(I+1)=LX(I)+LE
2950 I=I+1:GOTO2360
2960 IFTW(I)>TPTHENPRINT"TW(I)>TC":STOP
2970 REM
2980 FR=FR+.01*FR:GOTO2320
2990 REM
3000 REM CONTINUE

```

```

3010 REM
3020 REM
3030 REM          TWO-PHASE REGION
3040 REM -----
3050 REM DET ENTH AT SAT (GAS)
3060 TF(JI)=TP:TW(JI)=TW(I)
3070 REM CALCULATE QUALITY X(I)
3080 TV=TF(JI)*1.8+32:PS=PF(I):GOSUB800
3090 HL=HV/.4299:REM LATENT HEAT
3100 HJ=HF/.4299:REM LIQ SAT ENTH
3110 X(JI)=.98:REM TO START WITH
3120 HX(JI)=HJ+X(JI)*HL
3130 XB=X(JI)
3140 REM FLUID PROPERTIES
3150 GR=1.273*FR/(DF^2)
3160 LX=12-I*LE
3170 IFLX<=0THENSTOP
3180 REMPX=.7*(P1-P3)/LX
3190 I=JI
3200 PS=PF(I)
3210 GOSUB1510:GOSUB800
3220 HL=HV/.4299:REM LATENT HEAT
3230 RG=1/(VG*.0624):RF=1/(VF*.0624)
3240 TV=TF(I):GOSUB1980
3250 MG=UG:MF=UL
3260 TV=TB(I):GOSUB1980:MW=UL
3270 RV=MF/MW
3280 TV=TF(I):GOSUB1820
3290 TV=TF(I):GOSUB2090
3300 PR=MF*CL/FK:PR=INT(1E3*PR+.5)/1E3
3310 RY=(1-X(I))*GR*DF/MF
3320 REM IF(1-X(I))<.015 ; 1-PHASE
3330 IF(1-X(I))>.015THEN3360
3340 GOSUB5160:REM GAS HEAT TRNS
3350 GOTO3540:REM TO WATER PROP
3360 IFRY>50THEN3390
3370 F2=.707*PR*RY^.5
3380 GOTO3430
3390 IFRY>1125THEN3420
3400 F2=5*PR+5*LOG(1+PR*(.09636*RY^.585-1))
3410 GOTO3430
3420 F2=5*PR+5*LOG(1+5*PR)+2.5*LOG(.0031*RY^.812)
3430 B1=MF/MG
3440 B2=RG/RF
3450 IFX(I)<0THENJK=I+1:GOTO4260
3460 XT=B1^.1*B2^.5*((1-X(I))/X(I))^.9
3470 FJ=.15*(1/XT+2.85/(XT^.446))
3480 IFFJ>1THEN3500
3490 NU=PR*RY^.9*FJ/F2:GOTO3530
3500 IFFJ<20THEN3510

```



```

3510 NU=PR*RY^.9*FJ^1.15/F2
3520 TV=TF(I):GOSUB2090
3530 QF(I)=NU*FK/DF
3540 REM WATER PROPERTIES
3550 TL=TW(I):GOSUB1740:WT=WD
3560 TL=TW(I):GOSUB1650:VX=WV
3570 TL=TB(I):GOSUB1650:RM=VX/WV
3580 TL=TW(I):GOSUB1700
3590 TL=TW(I):GOSUB1780
3600 PW=VX*WC/WK:REM PRANDL NO
3610 RW=GW*DW/VX:REM REYNOLD NO
3620 GOSUB4870
3630 UL(I)=1/((1/BO)+(1/(3.142*DW*QW(I)))+(1/(3.142*DF*QF(I))))
3640 CW=WF*WC
3650 UF(I)=0.0
3660 EF(I)=0.0
3670 UW(I)=LE*UL(I)/CW
3680 EW(I)=1-EXP(-UW(I))
3690 TW(I+1)=(TW(I)-EW(I)*TF(I))/(1-EW(I))
3700 X(I+1)=XB-CW*EW(I)*(TF(I)-TW(I))/((1-EW(I))*FR*HL*1000)
3710 REM 1560 TO1650 TO CAL PRS DROP
3720 A1=X(I)^1.8
3730 A2=5.7*B1^.0523*(1-X(I))^.47*X(I)^1.33*B2^.261
3740 A3=8.11*B1^.105*(1-X(I))^.94*X(I)^.86*B2^.522
3750 A4=GR^1.90/(RG*DF)
3760 A5=.09*(MG/(GR*DF))^2
3770 A6=2*X(I)+(1-2*X(I))*B2^.333+(1-2*X(I))*B2^.667-2*(1-X(I))*B2
3780 A7=DF*(X(I+1)-X(I))/LE
3790 PD=A4*(A5*(A1+A2+A3)+A6*A7)
3800 PF(I+1)=PF(I)-LE*(PD*14.5*1E-5)
3810 PW(I+1)=PW(I)+LE*PJ
3820 REMPF(I+1)=PF(I)-PX*LE
3830 PS=PF(I+1):GOSUB1510:GOSUB800
3840 TF(I+1)=(TT-32)*5/9:HL=HV/.4299:HY=HF/.4299
3850 HX(I+1)=HX(I)-CW*1E-3*(TW(I)-TW(I+1))/(FR)
3860 X(I+1)=(HX(I+1)-HY)/HL
3870 TB(I+1)=TF(I+1)-(TF(I+1)-TW(I+1))*UL(I)/(3.1416*DF*QF(I))
3880 TW(I)=INT(100*TW(I)+.5)/100
3890 PF(I)=INT(100*PF(I)+.5)/100
3900 TF(I)=INT(100*TF(I)+.5)/100
3910 X(I)=INT(100*X(I)+.5)/100
3920 TF(I)=INT(TF(I)*100+.5)/100:TW(I)=INT(TW(I)*100+.5)/100
3930 TF(I)=INT(TF(I)*100+.5)/100:TW(I)=INT(TW(I)*100+.5)/100
3940 Y1=LX(I):Y2=TF(I):Y3=TW(I):Y4=WF:Y5=X(I):Y6=PF(I)
3950 Y1$=LEFT$(STR$(Y1)+"      ".6)
3960 Y2$=LEFT$(STR$(Y2)+"      ".10)
3970 Y3$=LEFT$(STR$(Y3)+"      ".10)
3980 Y5$=LEFT$(STR$(Y5)+"      ".6)
3990 Y6$=LEFT$(STR$(Y6)+"      ".12)
4000 Y4$=LEFT$(STR$(Y4)+"      ".12)

```



```

4010 PRINTLX(I);TF(I);TW(I);WF
4020 PRINT£3,Y1£:Y2£:Y3£:Y5£:Y4£:Y6£
4030 REMPRINT£3,(I-1)*LE;PF(I);TF(I);TW(I);100*X(I);RY;RW;EF(I);EW(I)
4040 IFTW(I)=>TF(I)THENWF=WF-.003*WF;GOTO2320
4050 REMIFLX(I)=>14.5THENWF=WF+.001*WF;GOTO4160
4060 JK=I
4070 IFLX(I)>14THEN4820
4080 IFX(I)<0THENLX(JK)=LX(I)+LE;GOTO4260
4090 IFX(I)<.14THEN4160
4100 LX(I+1)=LX(I)+LE
4110 IFX(I+1)<0THENX(I+1)=.01
4120 I=I+1;GOTO3200
4130 REM
4140 REM
4150 REM
4160 REM END OF 2-PHASE REGION
4170 REM
4180 GOTO4260
4190 X(JK)=X(I+1)
4200 REM
4210 REM IFX(I)>.4THENTC=TC+.5;VT=0;RETURN
4220 REM IFX(I)>.2THENTC=TC+.3;VT=0;RETURN
4230 REM IFX(I)>.1THENTC=TC+.05;VT=0;RETURN
4240 GOTO4090
4250 TF(JK)=TF(I);TW(JK)=TW(I);PF(JK)=PF(I);LX(JK)=LX(I)+LE
4260 REM-----SUBCOOLING -----
4270 IFTF(I)-TM<5THENPRINT"TF(I)<WATER INLET TEMPERATURE":STOP
4280 LE=1
4290 GR=1.273*FR/(DF^2)
4300 I=JK
4310 REM R12 LIQUID PROP
4320 PS=PF(I)
4330 GOSUB1510;GOSUB800
4340 HL=HV/.4299;REM LATENT HEAT
4350 RF=1/(VF*.0624)
4360 TV=TF(I);GOSUB1980
4370 MF=UL
4380 TV=TB(I);GOSUB1980;MW=UL
4390 RV=MF/MW
4400 TV=TF(I);GOSUB1820
4410 TV=TF(I);GOSUB2090
4420 PR=MF*CL/FK;PR=INT(1E3*PR+.5)/1E3
4430 RY=GR*DF/MF
4440 GOSUB5270
4450 REM WATER PROPERTIES
4460 TL=TW(I);GOSUB1740;WT=WD
4470 TL=TW(I);GOSUB1650;VX=WV
4480 TL=TB(I);GOSUB1650;RM=VX/WV
4490 TL=TW(I);GOSUB1700
4500 TL=TW(I);GOSUB1780

```

```

4510 PW=VX*WC/WK:REM PRANDL NO
4520 GW=1.273*WF/(DW^2):RW=GW*DW/VX:REM REYNOLD NO
4530 GDSUB4870
4540 UL(I)=1/((1/BO)+(1/(3.142*DW*QW(I)))+(1/(3.142*DF*QF(I))))
4550 CW=WF*WC
4560 UW(I)=LE*UL(I)/CW
4570 CR=FR*CL
4580 UF(I)=LE*UL(I)/CR
4590 A=CR/CW:REM CW>CR
4600 B=EXP(-UF(I)+UW(I))
4610 EF(I)=(1-B)/(1-A*B)
4620 EW(I)=A*EF(I)
4630 TW(I+1)=(TW(I)-EW(I)*TF(I))/(1-EW(I))
4640 TF(I+1)=TF(I)-EF(I)*(TF(I)-TW(I+1))
4650 TB(I+1)=TF(I+1)-(TF(I+1)-TW(I+1))*UL(I)/(3.1416*DF*QF(I))
4660 X(I)=0
4670 TF(I)=INT(TF(I)*100+.5)/100:TW(I)=INT(TW(I)*100+.5)/100
4680 TF(I)=INT(TF(I)*100+.5)/100:TW(I)=INT(TW(I)*100+.5)/100
4690 Y1=LX(I):Y2=TF(I):Y3=TW(I):Y4=WF:Y5=X(I):Y6=PF(I)
4700 Y1$=LEFT$(STR$(Y1)+"          ",6)
4710 Y2$=LEFT$(STR$(Y2)+"          ",10)
4720 Y3$=LEFT$(STR$(Y3)+"          ",10)
4730 Y5$=LEFT$(STR$(Y5)+"          ",6)
4740 Y6$=LEFT$(STR$(Y6)+"          ",6)
4750 Y4$=LEFT$(STR$(Y4)+"          ",12)
4760 PRINTLX(I);TF(I);TW(I);WF
4770 PRINT$3,Y1$;Y2$;Y3$;Y5$;Y4$
4780 REMPRINT$3,(I-1)*LE;PF(I);TF(I);TW(I);100*X(I);RY;RW;EF(I);EW(I)
4790 PF(I+1)=PF(I)-1
4800 IFLX(I)>14THEN4820
4810 LX(I+1)=LX(I)+LE:I=I+1:GOTO4360
4820 IFX(I)>.50THENTC=TC+.5:VT=0:RETURN
4830 IFX(I)>.10THENTC=TC+.3:VT=0:RETURN
4840 RETURN
4850 STOP
4860 REM-----
4870 REM CAL OF HEAT TRN FOR LIQUID
4880 REM-----
4890 REM GW:MASS-RATE,RW:REYN NO
4900 REM PW:PRAND NO, DW:TUBE IN DI
4910 REM LE:LENGTH,CD:CONDUCT.
4920 REM WT:DENSITY,RM:VIS RATIO
4930 XA=RW*PW*DW/LE
4940 NL=(3.66+.057*XA/(1+.04*XA^(.8)))
4950 FL=16/RW
4960 NS=NL
4970 FW=FL
4980 IFRW<2100THEN5120
4990 FT=1/(.687*LOG(RW)-3.28)^2
5000 IFRM>1THEN5040

```

```

5010 AN=.25
5020 FU=FT/RM^.24
5030 GOTO5060
5040 AN=.08
5050 FU=FT*.167*(7-RM)
5060 NT=RW*PW*(FT/2)*(RM^AN)/(1+13.6*FT+9*FT^.5*(PW^.667-1))
5070 NS=NT
5080 FW=FU
5090 IFRW>7100THEN5120
5100 NS=(7100-RW)*NL/5000+(RW-2100)*NT/5000
5110 FW=(7100-RW)*FL/5000+(RW-2100)*FU/5000
5120 QW(I)=NS*WK/DW
5130 REMPJ=(2*FW*GW^2/(WD*DW))*1E-5
5140 RETURN
5150 REM-----
5160 REM GAS HEAT TRN IN TUBE
5170 REM-----
5180 REM NU:NUSSELT NO,QH:HEAT TRN CO
5190 REM FF:FRICTION FACT,PD:PRESS GRD
5200 NU=.0203*(1+(DF/(I*LE))^.8)*RY^.8*PR^.3
5210 QF(I)=NU*GK/DF
5220 FI=1/((1.581*(LOG(RY))-3.28)^2*RV^.24)
5230 PD=(2*FI*GR^2/(DF*RK))*1E-5
5240 NU=INT(NU*100+.5)/100
5250 RETURN
5260 REM-----
5270 REM LIQ R12 HTC
5280 REM-----
5290 XA=RY*PR*DF/LE
5300 NL=(3.66+.057*XA/(1+.04*XA^(.8)))
5310 FL=16/RY
5320 NS=NL
5330 FW=FL
5340 IFRY<2100THEN5480
5350 FT=1/((.687*(LOG(RY))-3.28)^2
5360 IFRV>1THEN5400
5370 AN=.25
5380 FU=FT/RV^.24
5390 GOTO5420
5400 AN=.08
5410 FU=FT*.167*(7-RV)
5420 NT=RY*PR*(FT/2)*(RV^AN)/(1+13.6*FT+9*FT^.5*(PR^.667-1))
5430 NS=NT
5440 FW=FU
5450 IFRY>7100THEN5480
5460 NS=(7100-RY)*NL/5000+(RY-2100)*NT/5000
5470 FW=(7100-RY)*FL/5000+(RY-2100)*FU/5000
5480 QF(I)=NS*FK/DF
5490 REM PD=(2*FW*GR^2/(WD*DF))*1E-5
5500 RETURN

```

APPENDIX J

Computer program for the data acquisition system and online analysis
of the data.

```
10 REM -----
12 REM DATA ACQUITION SYSTEM
15 REM -----
50 OPEN15,8,15
55 INPUT£15,A$,B$,C$,D$
60 IFVAL(A$)<>0THENPRINTA$,B$,C$,D$
70 PRINT£15,"I1"
100 PRINT""
300 DIM A(32)
320 DIMT(30)
330 DIMB(32):DIMG(5,32)
340 V1=-4.4151247E-3;V2=25.8296676
360 V3=-.605540752 :V4=-.0271947738
380 V5=.0123705268;V6=-9.81733203E-4
400 Y1=-4.895E-3;Y2=1.804E-5
420 Y3=-4.943E-8;Y4=7.612E-11
440 Y4=-4.723E-14
568 DB=-5.23805618E-4;DL=340.549683
569 OV=311.818359;OW=-625.23291
570 OY=545.860352;OZ=-165.802002
610 X=1
620 PRINT"";
640 INPUT"HOW MANY SAMPLE?";SP
680 INPUT"TIME BETWEEN SAMPLES SECS";DZ
700 INPUT"NO OF AVERAGE";AR
720 PRINT""
740 Y8=TI
760 Z$="FILE"
780 W$=Z$+STR$(X)
800 F$="@1:"+W$+",S,W"
860 OPEN6,8,Z,F$
870 IFSP<10THENSY=1;GOTO900
880 FORG=1TO10
900 FORM=1TOAR
920 PRINT"***READING NO:";G+SY;F$
940 PRINT"#####2#####2#####2#####"
960 A=9:REM DEVICE NO
980 IF A<40RA>14THEN960
1000 FORB=0TO15
1020 GOSUB1920
1050 G(M,B)=A(B)
1060 NEXT
1280 A=10 :REM DEVICE NO
1300 IFA<40RA>14THEN1280
1320 FORB=0TO15
1340 GOSUB1920
1390 G(M,B+16)=A(B)
1400 NEXT
1410 NEXTM
1420 FORL=0TO31:FORM=1TOAR
1425 BX=BX+G(M,L)
```



```

1430 NEXT
1432 A(L)=BX/AR
1434 PRINT£6,A(L);CHR$(13);
1436 INPUT£15,A$,B$,C$,D$
1437 IFVAL(A$)<>OTHENPRINTA$,B$,C$,D$:CLOSE6:STOP
1440 BX=0
1442 NEXT
1450 GOSUB2240
1500 ZI=(T(0)+T(1)+T(2))/3
1520 DY=1.293+Y1*ZI+Y2*ZI^2+Y3*ZI^3+Y4*ZI^4+Y5*ZI^5
1580 PRINT" JTI:MJ";YT
1590 Y9=TI:YT=(Y9-Y8)/(60*60)
1595 YT=INT(100*YT+.5)/100
1600 PRINT"@@@@@@@@@@@@1000000000100001000000000"
1620 PRINT£6,YT;CHR$(13);
1625 INPUT£15,A$,B$,C$,D$
1627 IFVAL(A$)<>OTHENPRINTA$,B$,C$,D$:CLOSE6:STOP
1680 REM***** N GIVES TIME DELAY BETWEEN SAMPLES *****
1700 REM***** 1000=ABOUT 1.2SECONDS *****
1720 FORN=1TO800*DZ:NEXT
1730 IFSY=0THEN1760
1740 IFSP-SY<=0THENCLOSE6:GOTO1880
1745 SY=SY+1
1750 GOTO900
1760 NEXTG
1780 CLOSE6
1800 SP=SP-10
1820 X=X+1
1840 IFSP>0THEN780
1880 PRINT" LAST FILE IS ";X
1885 PRINT"TO CONTINUE PRESS C"
1886 GETA$:IFA$=""THEN1886
1887 IFA$="C"THEN1910
1900 END
1910 PRINT"TO OPEN A NEW FILE PRESS F"
1911 GETF$:IFF$=""THEN1911
1912 IFF$="F"THENX=X+1
1915 GOTO620
1920 REM SUBROUTINE TO GET DATA FROM INTERFACE
1940 REM A IS DEVICE NO B IS CHANNEL NO
1960 OPEN1,A,B
1980 GET£1,J$,K$
2000 K=ASC(K$)-224
2020 IF K<0 THEN D=(K+32)*-1
2040 IF K>=0 THEN D=K
2060 D=D*256
2080 IF J$="" THEN J=0:GOTO2140
2100 J=ASC(J$)
2140 IF K<0 THEN J=J*-1
2160 A(B)=(J+D)/4000
2180 CLOSE1
2200 RETURN
2220 END
2240 REM SUB: TEMP CONVERSION
2245 FORB=0TO21
2260 A(B)=A(B)/219*1000

```

```

2280 T(B)=V1+V2*A(B)+V3*(A(B)^2)+V4*(A(B)^3)+V5*(A(B)^4)+V6*(A(B)^5)
2300 T(B)=INT(100*T(B)+.5)/100
2320 NEXT
3210 ZI=(T(16)+T(17)+T(18))/3
3215 DY=1.293+Y1*ZI+Y2*ZI^2+Y3*ZI^3+Y4*ZI^4+Y5*ZI^5
3220 ZU=T(4)-T(3):ZT=T(6)-T(5)
3225 TP=(T(15)+T(14)+T(12)+T(11))/4
3230 TM=(T(13)+T(14)+T(10)+T(11))/4
3235 TY=(T(14)+T(11))/2
3240 TF=(T(15)+T(12))/2
3245 TV=(T(13)+T(10))/2
3250 ZO=(T(13)+T(14)+T(15))/3
3260 DT=INT(100*(T(4)-T(3))+.5)/100
3380 REM PRESSURE CONVERSION
3430 P6=A(22)*996.231+14.7
3432 P6$=LEFT$(STR$(P6)+"      ",6)
3460 P2=A(23)*2473.78+14.7
3480 P2$=LEFT$(STR$(P2)+"      ",6)
3520 P3=A(24)*996.56+14.7
3540 P3$=LEFT$(STR$(P3)+"      ",6)
3580 P4=A(25)*998.85+14.7
3600 P4$=LEFT$(STR$(P4)+"      ",6)
3640 P5=A(26)*993.39+14.7
3660 P5$=LEFT$(STR$(P5)+"      ",6)
3700 FC=0.009E-3+33.37E-3*A(27)
3705 FC=(CV+CZ)/1000
3720 FC=INT(1E5*FC+.5)/1E5
3730 DR=1.4-3.823E-3*T(3)+1.5*T(3)^2-2.635E-7*T(3)^3
3760 FF=(-2.458E-4+.0147*A(28))*DR
3780 FF =INT(10E5*FF+.5)/10E5
3808 FS=A(29)
3969 AS=(2.64*FS-.71)*0.18
3970 AF$=LEFT$(STR$(AF)+"      ",5)
3974 PL=1.1560320E-3+109.63921*FS-252.787323*FS^2+505.469406*FS^3
3975 PN=-272.154892*FS^4
3977 FP=PL+PN
3978 FP$=LEFT$(STR$(FP)+"      ",5)
4000 PC=406.25*A(30)-3.12
4020 PC$=LEFT$(STR$(PC)+"      ",6)
4060 ED=ZT*4181.6*FC
4080 ED$=LEFT$(STR$(ED)+"      ",8)
4130 EX=DY*1000*AX*(ZI-TF)
4132 EQ=DY*1000*XL*(ZI-TP)
4134 WX=DY*1000*QX*(ZI-TP)
4136 EY=DY*1000*AZ*(ZI-TY)
4138 WY=DY*1000*QZ*(ZI-TM)
4140 EZ=DY*1000*AY*(ZI-TM)
4142 WZ=DY*1000*QY*(ZI-TV)
4145 EI=EX+EY+EZ+PC+WX+WY+WZ+EQ
4160 EI$=LEFT$(STR$(EI)+"      ",8)
4180 P1=A(31)*2451.46+14.7
4182 P1$=LEFT$(STR$(P1)+"      ",6)
4200 EF=FF*(146338.4+966*ZU)+PC
4220 EF$=LEFT$(STR$(EF)+"      ",8)
4290 COP=EO/(FP+PC)
4292 COP$=LEFT$(STR$(COP)+"      ",8)

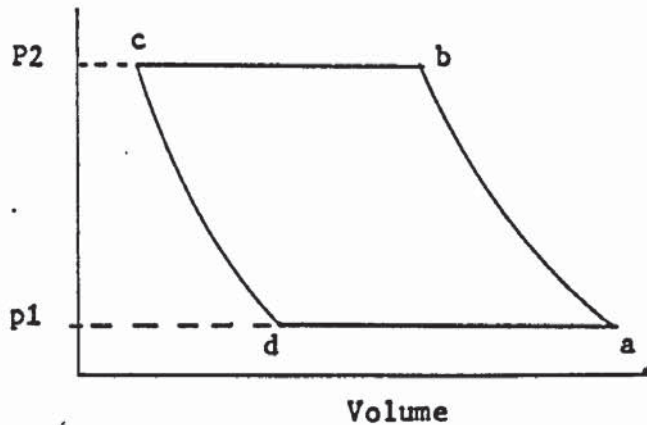
```

```

4300 AO=(T(10)+T(11)+T(12)+T(13)+T(14)+T(15))/6
4310 AI=(T(16)+T(17)+T(18))/3
4320 AO=INT(100*AO+.5)/100
4322 AI=INT(100*AI+.5)/100
4350 FORI=1T02
4352 IFI=1THENWB=T(7):DB=AO:GOTO4360
4354 IFI=2THENWB=T(21):DB=AI
4360 GOSUB4500
4362 NEXT
4365 DH=ABS(HA(1)-HA(2))
4366 EK=DH*AF*DY*1000
4367 EL=(EI+EK)/2
4369 EL=INT((10*EL+.5)/10)
4370 EK=INT((10*EK+.5)/10)
4375 PS=P1:REM CAL COND TEMP
4377 PG=LOG(PS)/LOG(10)
4379 TR=120*PG+323.1
4381 T0=TR
4383 FV=39.8838-3436.6322/T0-12.4715*(LOG(T0)/LOG(10))+.47304E-2*T0-PG
4385 FQ=3436.6322/T0^2-12.4715/(2.3026*T0)+.47304E-2
4387 TR=T0-FV/FQ
4389 IFABS(TR-T0)<.0001THEN4393
4391 GOTO4381
4393 TT=TR-459.7
4395 TT=INT(100*TT+.5)/100
4397 TE=(TT-32)*5/9
4399 TE=INT(100*TE+.5)/100
4410 PRINT"R12 TEMPJ";TAB(11)T(0);TAB(19)"J";T(1);TAB(27)"J";T(2)
4412 PRINT" J";TAB(11)T(3);TAB(19)"J";T(4);TAB(27)"J";"DT
4415 PRINT"WATER TEMPJ";TAB(11)T(5);TAB(19)"J";T(9);TAB(27)"J";T(6)
4418 PRINT"WET B: OUTJ";TAB(11);T(7);TAB(19);"J IN";TAB(27);":";T(21)
4419 PRINT"R HUM: OUTJ";TAB(11);RH(1);TAB(19);"J IN";TAB(27);":";RH(2)
4420 PRINT"AIR T :OUTJ";TAB(11)AO;TAB(19)"J";" IN";TAB(27)":";AI
4426 PRINT"R12 COND J";TAB(11)TE;TAB(19)"J";"OUTS T: ";T(20)
4428 PRINT"#####2#####"
4430 PRINT"PRES PSI J";P1$;TAB(19)"J";P6$;TAB(27)"J";P2$
4432 PRINT"PRES PSI J";P3$;TAB(19)"J";P4$;TAB(27)"J";P5$
4434 PRINT"#####102#####1#####1#####"
4436 PRINT"FR KG/S:CONDJ";FC;TAB(19)":";"R12: ";FF
4438 PRINT"AIR M3/S J";AF$
4440 PRINT"ELC J/S:COMPJ";PC$;": FAN: ";FP$
4445 PRINT"#####2#####2#####"
4450 PRINT"HEAT J/S:OUTJ";EO$;": J IN J";EK
4452 PRINT"#####2#####"
4454 PRINT" COP ";COP$;
4480 RETURN
4500 REM MOIST AIR PROPERTIES
4510 C1=-5800.2206:C2=1.3914993:C3=-.04860239:C4=.41764768E-4
4520 C5=-.14452093E-7:C6=6.5459673
4540 TW=WB+273.15:TD=DB+273.15
4550 PK=C1/TW+C2+C3*TW+C4*TW^2+C5*TW^3+C6*LOG(TW)
4560 PW=2.7183^PK
4570 WS=.62198*PW/(101325-PW)
4580 W=((2501-2.381*WB)*WS-(DB-WB))/(2501+1.805*DB-4.186*WB)
4590 HA=DB+W*(2501+1.805*DB)
4600 PX=C1/TD+C2+C3*TD+C4*TD^2+C5*TD^3+C6*LOG(TD)

```

```
4610 PD=2.7183^PX
4620 WD=.62198*PD/(101325-PD)
4630 UR=W/WD
4640 RH=(UR/(1-(1-UR)*(PD/101325)))*100
4650 WP=101325*W/(.62198+W)
4660 DW=-35.957-1.8726*LOG(WP)+1.1689*LOG(WP)^2
4670 PW=INT(100*PW+.5)/100
4680 WS=INT(1E5*WS+.5)/1E5
4690 W=INT(1E5*W+.5)/1E5
4700 HA=INT(100*HA+.5)/100
4710 RH=INT(100*RH+.5)/100
4720 DW=INT(100*DW+.5)/100
4800 HA(I)=HA:RH(I)=RH:DW(I)=DW
5000 RETURN
```

a - b and c - d are polytropic processes obeying the relationship $PV^n = \text{Constant}$ where n is the polytropic index.

V_a is the maximum cylinder volume and V_c is the clearance volume. The work done per cycle by the compressor on the vapour is equal to the area enclosed by the cycle.

$$W_r = \frac{1}{n-1} (P_2 V_b - P_1 V_a) + P_2(V_b - V_c) - \frac{1}{n-1} (P_2 V_c - P_1 V_d) - P_1 (V_a - V_d)$$

$$= \frac{n}{n-1} (P_2 (V_b - V_c) - P_1 (V_a - V_d)) \tag{K.1}$$

since $V_b = V_a \left(\frac{P_1}{P_2}\right)^{1/n}$ and $V_c = V_d \left(\frac{P_1}{P_2}\right)^{1/n}$

$$W_r = \frac{n}{n-1} P_1 (V_a - V_d) \left(\left(\frac{P_1}{P_2}\right)^{(n-1)/n} - 1 \right) \tag{K.2}$$

$(V_a - V_d)$ can either be expressed in terms of other cycle volumes, i.e $V_a - V_d = V_a - V_c \left(\frac{P_2}{P_1}\right)^{1/n} = V_a \left(1 - \left(\frac{V_c}{V_a}\right) \left(\frac{P_2}{P_1}\right)^{1/n} \right)$ to yield

$$W_r = \frac{n}{n-1} P_1 V_a \left(1 - \left(\frac{V_c}{V_a}\right) \left(\frac{P_2}{P_1}\right)^{1/n} \right) \left(\left(\frac{P_2}{P_1}\right)^{(n-1)/n} - 1 \right) \tag{k.3}$$

or in terms of the volumetric efficiency,

$$\eta_v = \frac{V_a - V_d}{V_a - V_c}$$

the denominator, $V_a - V_c$, is the swept volume V_s , therefore

$$W_r = \frac{n}{n-1} P_1 V_s \left(\left(\frac{P_2}{P_1}\right)^{(n-1)/n} - 1 \right) \eta_v \tag{k.4}$$

The volumetric efficiency may be expressed in terms of the compression ratio and cylinder volumes.

$$\begin{aligned}\eta_v &= \frac{1}{V_s} (V_a - V_d) = \frac{1}{V_s} (V_s + V_c - V_c \left(\frac{P_2}{P_1}\right)^{1/n}) \\ &= 1 + \frac{V_c}{V_s} - \frac{V_c}{V_s} \left(\frac{P_2}{P_1}\right)^{1/n}\end{aligned}\quad (K.5)$$

By assuming perfect gas behaviour the work equations can be simplified. If M_c is the mass of vapour that remains in the clearance volume, V_c , and M_m is the maximum mass of vapour contained by the cylinder then the mass transferred per cycle $M_r = M_m - M_c$.

Equation (K.1) becomes $W_r = \frac{n}{n-1} M_r R (T_2 - T_1)$

and (k.2) becomes $W_r = \frac{n}{n-1} M_r R T_1 \left(\left(\frac{P_2}{P_1}\right)^{(n-1)/n} - 1\right)$

where T_1 and T_2 are the inlet and exhaust temperatures.

The net work done by the compressor on the vapour from a to b is equal to the area under the curve ab less the area under the curve cd.

$$W_c = \frac{1}{n-1} (P_2 V_b - P_1 V_a) - \frac{1}{n-1} (P_2 V_c - P_1 V_d)$$

By assuming perfect gas behaviour,

$$W_c = \frac{1}{n-1} M_r R (T_2 - T_1) \quad (K.6)$$

REFERENCES

1. Cooper K.W , Saving energy with refrigeration, ASHRAE Journal, vol 20, pp23-27 , 1978
2. Thomson W , Glasgow Phil. Soc. Proc. vol 111 , 1852
3. Sandfort J.F , Thermodynamic criteria for heat pump ,Transaction Americans Society Of Heating And Ventilating Engineers, vol 56, pp75-86 , 1950 .
4. The world market for heat pump . The Heating And Ventilating Engineer , vol 57 (Oct), pp 20-21 , 1983
5. Realism about heat pump . The Heating And Ventilating Engineer , vol 57 (oct) , pp18-19, 1983
6. Relay, Midland Research Station Of British Gas, pp14,Sept.1983
7. Hunt J.S , Heat recovery in leisure centers, The Heating And Ventilating Engineer, vol 57 ,pp10-13 ,1983
8. Heat pumps , Energy Digest , vol 10, No1, pp4-8 , 1981
9. Carrington C.G, Use of controlled water circulation in tap water heat heat pump, International Journal Of Energy Research, vol 6, pp 233-240 , 1982.
10. Carrington C.G, Sandle W.J, Warrington D.M, and Bradford R.A , Demonstration of a hot water heat pump system, New Zealand Energy Research And Development Committee , Contract 3105, 1983
11. Heap R.D, Heat Pumps: Encouraging results from a domestic installation , Electrical Review, vol 196 (March/April) , pp393-395 , 1975 .
12. Leach S.J, Heat pump application in houses' , Elektrowarme International Edition A, Bd 35 ,pp A277-A283 , 1977
13. Weber H, Integrating heat pump into heating system, Sulzer Technical Review 1, vol 63, pp14-20 , 1981

14. New heat pumps for U.K , Energy Digest , vol 10, no 1,pp9-10,1981
15. Sumner J.A , Domestic Heat Pumps, Prism Press, London ,1976
16. Neal W.E.J, Pabon Diaz M, Solar energy for refrigeration and air conditioning, Refrigeration And Air Conditioning ,vol 81, pp59-76 , 1978
17. Reay D.A, Macmichael D.B.A , Heat Pumps: Design and application, Pergamon Press, U.K. , 1979
18. Thomas T.F, The air cycle heat pump, Proceedings Of The Institute Of Mechanical Engineer , vol 157, pp30-38, 1948
19. ASHRAE Handbook Of Fundamentals, American Society Of Heating, Refrigeration And Air Conditioning Engineers, Inc, U.S.A ,1981
20. Heat pump for domestic use. Building Research Establishment Digest (Digest 253) , Sept , 1981
21. Pabon-Diaz M , A study in the application of domestic solar assisted heat pumps for heating and cooling , PhD Thesis, Aston University, 1982 .
22. Ogbeide S.E, An experimental evaluation of R11 as a heat pump working fluid in comparison with some other fluids , International Journal Of Energy Research, vol7, pp129-135 , 1983
23. Morgan R.G , Solar assisted heat pump, Solar Energy, vol 28, no 2, pp129-135 , 1982
24. Tleimat B.W, and Howe E.D, Solar assisted heat pump system for heating and cooling residences, Solar Energy , vol 21, pp45-54,1978
25. Freund P, and Cattell R.K , The development and testing of a heat pump for heating a single room , International Journal Of Energy Research, vol 4, pp 353-362 , 1980
26. Tai K.W, Zyla R, Devotta S, Diggory P.J, Watson F.A, Holland F.A, The potential for heat pumps in drying and dehumidification system 11: An experimental assesment of the heat pump.

- characteristics of a heat pump dehumidification system using R114, International Journal Of Energy Research, vol 6, pp323-331, 1982
27. Sneed J.B.O, and Keer S.V, Applied heat for engineer, Blackie And Son LTD, London , 1969
 28. Danfoss specification leaflet on reciprocating compressor SC10H
 29. Pitts D.R, and Sissom L.E, Schaum's Outline of theory and problems of heat transfer , McGraw Hill, London, 1977
 30. Carrington C.G, Computer program on tube side by side counter flow heat pump condenser, Unpublished, Aston University, 1982
 31. Ozisik M.N, Basic heat transfer , McGraw Hill, London, 1977
 32. Heat transfer and fluid flow data book, General Electric , New York, 1982
 33. Blundell C.J, Optimising heat exchangers for air-air space heating heat pump in the U.K, International Journal Of Energy Research, vol 1, pp69-94, 1977
 34. Chilson D , Development in heat exchanger 1 , Applied Science Publisher , London , 1980
 35. Thomas T.H, Hunt R, Applied Heat , Heineman Educational Books , London , 1979
 36. RS Data Sheet: Reflective and slotted opto switches , R.S Components Ltd. U.K, 1981
 37. Seippel R.g, and Nelson, R.L, Designing circuit with IC operational amplifiers, American Technical Society, Chicago, 1975
 38. Norton, H.N, Sensor and Analyser handbook, Prentice Hall Inc, U.S.A, 1982
 39. Tassou, S.A, Marquand C.J, Wilson D.R, Modelling of variable speed air to water heat pump systems, Journal Of Institute Of Energy, vol 55, pp 59-64 , 1982

40. Ahrens F.W, Heat pump modelling , simulation and design,
Fundamental Of Heat Pump, ASI of NATO No 53, M. Nijhoft ,pp155-
191 , 1983
41. James R.W, and Marshall S.A , The heat pump as a means of
utilizing low grade heat energy, Building Service Establishment,
vol 43, pp201-207 , 1976
42. Properties of R12, Imperial Chemical Industry, U.K.
43. Tong L.S ,Boiling heat transfer and two phase flow, John Wiley
and Sons ,pp118-126 , 1965
44. Stoeker W.F, and Jones J.W, Refrigeration and air conditioning,
McGraw Hill, 2nd Edition , 1982.
45. Tassou S.A, Green R.k, Wilson D.R, and Searle M , Energy
conservation through the use of capacity control in heat pump,
Journal Of The Institute Of Energy, vol54, pp30-35, 1981
46. Butterworth D , Engineering design guides: Introduction to heat
transfer , Oxford University Press,1977
47. McMullan J.T, Morgan R,and Lipman N.H, Heat Pump, Pergamon Press,
London, 1981
48. Thermophysical properties of matter - The TFR Data Series,
IFI/plenum , New York , 1976.
49. Rosell J, Morgan R, Hughes D.W, and McMullan J.T, Improvement in
controlled-environment facilities for testing domestic air- water
heat pumps, International Journal Of Energy Research , vol 7,
pp 35-48, 1983.